THE ROLE OF CHLR1 IN DNA REPLICATION, DNA DAMAGE REPAIR AND COHESION ESTABLISHMENT

Christopher Wasson

A Thesis Submitted for the Degree of PhD
at the
University of St Andrews

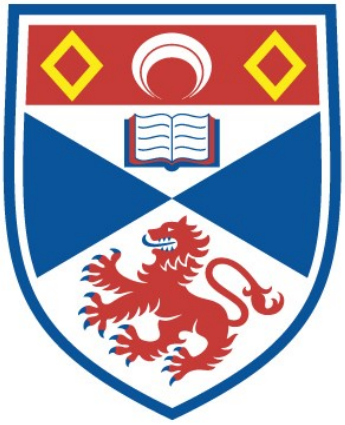

2011

The role of ChlR1 in DNA replication, DNA damage repair and cohesion establishment

Christopher Wasson
070013753

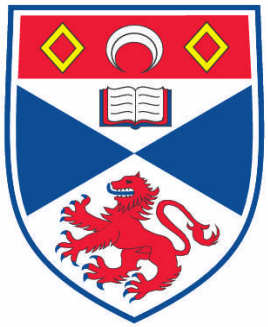

This thesis is submitted in partial fulfilment for the degree of
PhD
at the
University of St Andrews

Date of Submission
21/06/2011

1. Candidate's declarations:

I, Christopher Wasson, hereby certify that this thesis, which is approximately 43,558 words in length, has been written by me, that it is the record of work carried out by me and that it has not been submitted in any previous application for a higher degree.

I was admitted as a research student in October, 2007 and as a candidate for the degree of Medical Research in October, 2007; the higher study for which this is a record was carried out in the University of St Andrews between 2007 and 2011.

(If you received assistance in writing from anyone other than your supervisor/s):
I, …..., received assistance in the writing of this thesis in respect of [language, grammar, spelling or syntax], which was provided by ……

Date signature of candidate

2. Supervisor's declaration:

I hereby certify that the candidate has fulfilled the conditions of the Resolution and Regulations appropriate for the degree of Medical Research in the University of St Andrews and that the candidate is qualified to submit this thesis in application for that degree.

Date signature of supervisor

3. Permission for electronic publication: (to be signed by both candidate and supervisor)

In submitting this thesis to the University of St Andrews I understand that I am giving permission for it to be made available for use in accordance with the regulations of the University Library for the time being in force, subject to any copyright vested in the work not being affected thereby. I also understand that the title and the abstract will be published, and that a copy of the work may be made and supplied to any bona fide library or research worker, that my thesis will be electronically accessible for personal or research use unless exempt by award of an embargo as requested below, and that the library has the right to migrate my thesis into new electronic forms as required to ensure continued access to the thesis. I have obtained any third-party copyright permissions that may be required in order to allow such access and migration, or have requested the appropriate embargo below.

The following is an agreed request by candidate and supervisor regarding the electronic publication of this thesis:

Add one of the following options:

(i) Access to printed copy and electronic publication of thesis through the University of St Andrews.

Date signature of candidate
signature of supervisor

A supporting statement for a request for an embargo must be included with the submission of the draft copy of the thesis. Where part of a thesis is to be embargoed, please specify the part and the reasons.

Phd1c.doc - PhD Candidate' Report Form – 2009/2010 version

UNIVERSITY OF ST ANDREWS

REGISTRY – STUDENT OFFICE

EXAMINATION FOR THE DEGREE OF Ph.D, D.Lang, Eng.D or M.D
(by research thesis)

Special Circumstances Form

(to be completed by the candidate)

Name of Candidate: Christopher Wasson

ID Number: 070013753

Department / School: Medicine

Are there Special Circumstances? NO

Student's Signature:

Date:

N.B. The form should state any special circumstances that have affected the progress of the thesis or its final presentation e.g. ill health, bereavement or other temporary incapacity, and which should be brought to the attention of the examining committee and the Faculty Officer before the thesis is examined. Failure to report any special circumstances without good reason may affect any subsequent appeal. This form must be submitted with the thesis. It is expected that the form will normally be blank.

Details of Special Circumstances:-

Acknowledgements

First of all I would like to thank my supervisor Joanna for the opportunity to study for a PhD and for the invaluable advice and support throughout my studies (including the nagging about controls).

I would like to thank Katherine for the advice and the time spent training me up in lab. Sorry for the annoying questions.

I would like to thank the rest of the Parish lab for the advice and support throughout my studies.

I would like to thank my family for the support provided during my studies. Thank you, mum, dad and Laura for the encouragement.

Enough with the serious stuff, Katherine sorry for all the innuendoes at work, I'm sure you loved it, Katherine you have made the time spent in the lab an enjoyable experience.

I would like to offer an apology to Mary, the abuse would justify a sexually harassment complaint. So thank you for not filing a complaint. Mary you have made the time spent in the lab an enjoyable experience and I'm sure I won't meet another person like you, p.s you, Feeney and Young got me a peach in your office with that prank.

Sorry to the rest of the folk in the Bute Medical School research labs (Keeley, Parks, Eva, Laura, Christian, Lotte, Vita and Sarah) for my inappropriate behaviour. I'm sure you all loved it.

To the St Andy's lads (Adam, Keeks, Neil, Debar, Sam, Feezer) cheers for the nickname that will stick with me for life (c c c unit). More importantly cheers for the great laughs.

To my EK brothers (Mick, Steve and Alan) love you lads, we'll always remain bros.

To the Bobby Jones Place lads (Scott, Alan and Andy) cheers boys for the banter and sorry for the loud calls on the white telephone (Hope I made up for it with the wingman duties).

Finally, big hugh thanks for providing the wine that kick started many a good night in St Andrews.

Table of contents

Table of Figures

Abstract

Sister chromatid cohesion is essential for the equal distribution of genetic material in mitosis. The cohesin complex plays a central role in the establishment of sister chromatid cohesion. The cohesin complex is a ring shaped structure that encircles sister chromatids prior to the onset of anaphase ensuring equal distribution of genetic material. The DEAD/H DNA helicase ChlR1 is important in the establishment of sister chromatid cohesion. ChlR1 interacts with the cohesin complex and is required for the loading of cohesin onto DNA. Cohesin is loaded onto the DNA during DNA replication.

Here I identified a novel interacting partner of ChlR1. The multifunctional DNA binding protein FHL2 was shown to interact with ChlR1 and FHL2 was shown to have a role in sister chromatid cohesion since depletion of FHL2 resulted in abnormal metaphase spreads and reduced centromeric cohesion. These sister chromatid cohesion defects also result in a G_2/M delay.

Here I show an additional function of ChlR1 in the repair of DNA damage. ChlR1 was required for the repair of DNA double strand breaks and ChlR1 was recruited to DNA double strand breaks. Furthermore the function of ChlR1 in DNA double strand break repair is S phase specific. This suggests that ChlR1 is important in the homology recombination repair pathway.

I also show that ChlR1 is important in DNA replication. Depletion of ChlR1 results in inefficient DNA replication. In addition depletion of ChlR1 results in defects in DNA replication after hydroxyurea treatment.

The results in this thesis shed light on novel functions of the DNA helicase ChlR1 in DNA replication and DNA damage repair and the multifunctional DNA binding protein FHL2 in cohesion establishment.

Introduction

Genetic integrity is important for all species. Organisms have evolved to protect the integrity of their genomes in a number of ways including assault from DNA damage reagents (UV radiation, reactive oxygen species, replication errors and viruses) and the co-ordinated segregation of the genome into daughter cells.

The genome is protected from DNA damage reagents by a number of DNA damage repair pathways including homologous recombination, non-homologous end joining and nucleotide excision repair. These pathways will be explained in detail later. The majority of DNA damage repair occurs during DNA replication. Defects in the DNA damage repair pathways can cause increased cancer susceptibility, progeria (accelerated aging disease), growth and mental retardation.

Co-ordinated segregation of the genome occurs during mitosis. Sister chromosomes are paired together during mitosis by the cohesin complex. The cohesin complex is a ring shaped structure that encircles the sister chromatids and holds them together (termed sister chromatid cohesion) until segregation occurs. At this stage the cohesin ring is cleaved by the enzyme separase to releases the sister chromatids (discussed later). The accurate separation of the chromosomes is controlled by the spindle assembly checkpoint. The spindle assembly checkpoint and the cohesin complex will be explained in detail later. Defects in mitosis that result in disruption of chromosome segregation can cause aneuploidy (where there is an abnormal number of chromosomes in daughter cells) and translocations (when a portion of one chromosome is transferred to another chromosome). Aneuploidy and translocations can result in birth defects and cancer.

Work completed in this thesis looks at the role of the DEAD/H DNA helicase ChlR1 in the protecting the integrity of the genome. ChlR1 is important in the establishment of sister chromatid cohesion. ChlR1 interacts with the cohesin complex and plays a role in loading the cohesin complex onto the chromosomes (explained in detail later). ChlR1 has recently been linked to the Warsaw breakage syndrome. Patients with mutations in ChlR1 have a phenotype of microcephaly, growth retardation, aneuploidy and abnormal skin pigmentation. Results in this thesis help explain the phenotype in Warsaw breakage syndrome. The results suggest that ChlR1 has a role in DNA double strand break repair and in DNA replication. Therefore the phenotype associated with Warsaw breakage syndrome may be a result of DNA damage repair defects due to mutations in the gene encoding ChlR1.

1.1 The Cell Cycle

ChlR1 and the cohesin complex are important in a number of phases of the cell cycle. The cell cycle is divided into 4 main phases G_1, S, G_2 and mitosis. G_1 phase (also known as the gap phase) is marked with an increase in the biosynthetic activity of the cells. Proteins required for S phase such as the replication machinery proteins are synthesised in G_1. S phase starts when DNA replication (explained in detail below) begins, and ends when all the chromosomes are replicated. Rates of protein synthesis are very low in S phase. In G_2 the level of protein synthesis increases again and proteins important for mitosis are synthesised. In mitosis the replicated sister chromosomes in the nuclei are separated into two daughter nuclei (explained in detail below).

1.2 DNA Replication during S phase

DNA replication occurs in S phase and begins at specific sites in the DNA called origins of replication complexes

Origin recognition complex

The origin recognition complex (ORC) binds to the origins of replication. The ORC was identified in *S.cerevisiae* as a heterohexameric complex of proteins Orc1-6 that binds to origins of DNA replication [1]. Orc 1-6 were shown by chromatin immunoprecipitation (ChIP) to localise to 70 of the 96 replication origins in *S.cerevisiae* [2]. Cell division cycle 6 (Cdc6) is a replication factor in mammalian cells that is involved in the loading of the MCM complex has strong similarities to Orc1 in *S.cerevisiae* suggesting it is a member of the ORC in mammalian cells [3]. Orc 1-6 as well as Cdc6 have conserved AAA+ (ATPase Associated Activity) folds including walker A and B ATP binding domains that are characteristic of ATP dependent clamp loading proteins, which allow ring shaped protein complexes to encircle DNA [4].

ATP binding by Orc1 promotes its association to DNA in *S.cerevisiae* [5]. The other Orc proteins are believed to bind to the DNA through AT hooks [6]. Origin of replication sequences are AT rich and Orc4 protein in *S.pombe* has been shown to have an AT hook domain that allows it to bind to the replication origins [6]. In the human embryonic kidney cell line HEK293 a High Mobility Group A protein (HMGA1) protein that contains an AT hook, acts as a mediator for the ORC recruitment to origins [7]. HMGA1 also localises to AT rich sequences and co-immunoprecipitation assays showed an interaction of HMGA1 with Orc1, 2, 4 and 6 [7]. Furthermore, immunofluorescence analysis showed that

HMGA1 and the Orc proteins co-localise at AT rich regions [7]. From these data it is hypothesised that Cdc6 binds ATP and associates with the Orc1-6 proteins causing a conformational change in the complex that results in increased specificity for origin DNA [8].

When the ORC and Cdc6 bind to replication origins, Cdc6 interacts with Cdt1 (chromatin licensing and DNA replication factor 1) of the pre-replication complex to promote association of the replicative helicase, the MCM (minichromosome maintenance) complex with the origin DNA in *S.cerevisiae* [9]. Depletion of Orc6 in late G1 results in displacement of the MCM complex from the chromatin [9]. ATP hydrolysis by Orc6 is thought to result in increased binding affinity of MCM complex to the origins and recruitment of additional MCM complexes to the origins [8]. The ORC complex is required to maintain the MCM complex at the origins until S phase [9].

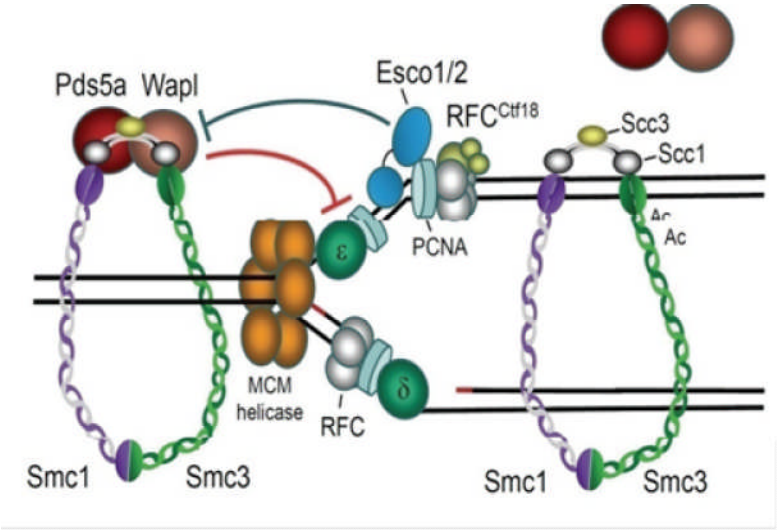

Figure 1: **The replication fork complex**. *The MCM helicase unwinds the DNA. The clamp loading complex RFC ctf18 loads PCNA onto the DNA. The Polymerases δ and ε are then loaded to the PCNA-primer-template complex. Esco1 (Eco1) is involved in the establishment of cohesion during DNA replication. Esco1 acetylates the cohesin complex and this is thought to allow for the progression of the replication complex through the cohesin complex [10]. Image taken with permission from the Nature Publishing Group*

MCM Replicative Helicase

The canonical MCM complex consists of 6 subunits, Mcm2 to 7 that together form a heterohexameric helicase. Electron microscopy images of the MCM complex from *methanobacterium thermoautotrophicum* shows a ring shaped structure [11]. Mutations of each subunit in *S.cerevisiae* and *S.pombe* resulted in a variety of replication defects [12].

The Mcm2-7 complex is transported to the origin of replication in an active state by Cdt1 [13]. This occurs during G1. At the replication origins it forms the pre-replication complex (pre-RC) with the AAA+ proteins Cdc6 and the ORC [14]. The loading of the MCM complex to the origin of replication requires the hydrolysis of ATP by Orc1-6 and Cdc6 [9]. Once the MCM complex is loaded then Cdc6 and Orc1-6 are removed from the origin [9]. The MCM complex is then activated at the onset of S phase by activated cyclin

dependent kinases (CDKs) and Cdc7 [13]. Upon activation the MCM complex unwinds the DNA resulting in the formation of the replication fork [13].

All six Mcm proteins have DNA dependent ATPase motifs in the central domains of the complex suggesting that the helicase activity of complex is dependent on ATP hydrolysis. These motifs are conserved from yeast to mammals [15]. The MCM complex was purified from HeLa cells and this purified complex was able to displace oligonucleotides annealed to single stranded circular DNA [16]. Furthermore the complex had a preference to displace oligonucleotides annealed to the single stranded DNA in a 3'-5' direction [16]. The helicase activity of the complex was only seen in the presence of hydrolysable ATP [16]. The role of ATP in the helicase activity of MCM was further analysed in *Xenopus* egg extracts [17]. Recombinant Mcm2-7 complexes with mutations in the walker A motif of Mcm6 that abolishes ATP binding and hydrolysis of the complex was added to *Xenopus* egg extracts with endogenous MCM complexes depleted [17]. This assay showed that ATP hydrolysis was not required for chromatin loading and pre-RC assembly but was required for origin unwinding and DNA replication [17].

Cdc45 and GINS (from the Japanese go-ichi-ni-san meaning 5-1-2-3, after the four related subunits of the complex Sld5, Psf1, Psf2 and Psf3) proteins were shown to activate the helicase activity of the MCM complex purified from *Drosophila* [18]. The helicase activity of the MCM complex was enhanced when associated with either Cdc45 or GINS *in vitro* [19]. The ATP hydrolysis rates of the MCM complex increased two fold upon association with these proteins and the binding of these proteins to the MCM complex resulted in the complex having an increased affinity to DNA. These two proteins were shown to interact with Mcm4 [18].

GINS proteins (Sld5, Psf1, Psf2 and Psf3 in *S.pombe*) have an important function in DNA replication that is linked to stimulating the activity of the MCM complex [20]. In *S.pombe*

deletion of any of the GINS proteins results in cell cycle arrest and the yeast are unable to undergo DNA replication [20]. DNA replication is also blocked in *Xenopus* egg extracts where GINS protein Sld5 is immunodepleted [20].

In the event of DNA damage during S phase the replication fork stops and stabilises. This stabilisation involves the strengthening of the association of the MCM complex with the replication fork [21]. This stabilisation of the fork requires the phosphorylation of the MCM complex by Cds1 (Checking DNA synthesis 1 (a checkpoint kinase)). In the absence of this protein the MCM complex continues to unwind the DNA in the presence of DNA damage which results in collapsed replication forks [21]. Furthermore in metazoans the MCM subunits are phosphorylated by the ATM (Ataxia telangiectasia mutated) kinases promoting the interaction of the MCM complex with Rad51 (involved in homologous recombination) in mammalian cells [21]. These results suggest that DNA damage repair pathways target the MCM complex to stabilise the replication forks until the DNA damage has been repaired.

The removal of the MCM complex after DNA replication involves the MCM binding protein (McmBP) [22]. This protein interacts with Mcm7 and accumulates in the nuclei in late S phase. Immunodepletion of McmBP in *Xenopus* egg extracts inhibits MCM dissociation from DNA. Furthermore the addition of recombinant McmBP to *Xenopus* egg extracts results in the release of the MCM complex from chromatin isolated in late S phase [22].

Replication licensing

The pre-replication complex (pre-RC) can only be assembled from late mitosis to G1 phase [23]. CDKs inhibit the assembly of the pre-RC for the remainder of the cell cycle [23]. In this manner CDKs regulate replication licensing [23]. In *S.cerevisiae* temperature

sensitive mutants of Cdk1 cause pre-RC re-assembly in S phase [24]. CDKs inhibit pre-RC assembly by inhibiting each component of the complex [25]. In *S.cerevisiae,* phosphorylation of Cdc6 by CDKs results in ubiquitin-mediated proteolysis of Cdc6 by SCF^{cdc4} (Skp1–Cdc53/cullin–F box) [25]. This proteolysis occurs in late G1 through S phase [25] and is important as it stops the ORC from assembling therefore preventing re-replication.

Mcm2-7 enters the nucleus at the end of mitosis and remains in the nucleus during G1 phase [13]. After which it is transported to the cytoplasm. Inactivation of Cdk1 in *S.cerevisiae* results in the nuclear accumulation of Mcm2-7 [26]. This suggests that CDKs are involved in the transporting of the MCM complex to the cytoplasm in S phase. Furthermore expression of a stable mitotic CDK (Clb2) results in the re-distribution of the MCM complex to the cytoplasm [27].

Regulation of Cdt1 in *S.cerevisiae* is connected to that of Mcm2-7 [13]. Cdt1 protein levels remain constant through the cell cycle but are localised in the nucleus in G1 and the cytoplasm later in the cycle [13]. Cdt1 binds to free Mcm2-7 and in the absence of Cdt1, Mcm2-7 do not localise in the nucleus during G1 [13].

In mammalian cells CDKs play an important role in the regulation of replication licensing. Depletion of Cdk1 results in multiple rounds of replication [28]. Inhibition of Cdk1 in G2 causes Mcm2-7 binding to the DNA and re-licensing of replication [29]. Cdk2 also plays an important role in the regulation of replication licensing. Cyclin A-Cdk2 targets Cdc6 for proteolysis in mammalian cells [30]. Cdk2 phosphorylates Cdt1 and this targets Cdt1 for proteolysis by SCF^{cdc4} [31]. Orc1 is phosphorylated by Cdk2 and results in the proteolysis of the protein by SCF^{cdc4} [32].

In mammalian cells a further protein called Geminin is involved in the regulation of replication licensing. Geminin protein levels fluctuate during the cell cycle. The protein is

absent in G1 but accumulates in the nucleus in S phase through to mitosis [33, 34]. Geminin binds to Cdt1, thereby preventing Cdt1 association with Mcm2-7 and thus preventing the formation of pre-RC during S phase [34]. Geminin is degraded in late mitosis by the anaphase promoting complex/cyclosome (APC/C) and it has been shown that inhibition of ubiquitination by APC/C results in stabilization of Geminin during mitosis [33].

CDKs may also have a positive role in licensing of replication. Cyclin E deficient cells result in replication defects. These cells are unable to load Mcm2-7 onto DNA [35]. Furthermore cyclin E activates the E2F transcription factor. Cdc6, Cdt1 and Orc1 are transcribed throughout this pathway [36].

PCNA

Proliferating cell nuclear antigen (PCNA) is a member of the DNA sliding β clamp family. These sliding clamps form ring shaped complexes (homotrimers in eukaryotes and heterotrimers in archaea) that encircle the DNA and are able to slide along the DNA in both directions [37]. PCNA monomers have two similar globular domains linked by a long flexible loop called the interdomain connecting loop [37]. The head to tail arrangement of the three monomers forms the ring structure [37].

PCNA is loaded onto the DNA by the replication factor C (RFC) complex which recognises the template primer 3’ ends of the fork and loads PCNA at these sites [38]. The binding of RFC to PCNA is dependent on ATP binding, as well as the loading of this complex onto DNA [39]. The binding of RFC to DNA results in the activation of the complexes ATP hydrolysis activity which causes it to dissociate with the loading clamp

and DNA [39]. The RFC complex binds to the C terminus of PCNA resulting in positioning of this end of PCNA toward the 3' end of the elongating DNA [40]. This ensures that the polymerase is oriented towards the elongating DNA as the polymerase binds to the C terminus of PCNA. Dissociation of RFC from the DNA upon loading of PCNA suggests that PCNA alone is required for the loading of the DNA polymerases to the DNA [41]. Indeed, PCNA was shown to be required for the loading of DNA polymerases *in vitro*, DNA polymerases δ and ε are unable to bind to DNA in the absence of PCNA [42].

Studies have shown that PCNA stimulates the activity of the DNA polymerases as well as loading the polymerases onto the DNA. The archaeal *Pyrococcus furiosus* (*Pfu*) PCNA stimulates the activity of DNA polymerases [43]. *Pfu* PCNA protein has a similar amino acid sequence to eukaryotic PCNA and the three dimensional structure is highly conserved. The incorporation of radio-labelled nucleotides by DNA polymerases I and II increased 3.6 fold when *Pfu* PCNA was added [43]. In this study the addition of high salt to create physiological conditions inhibited the activity of polymerase I but the activity was restored after the addition of *Pfu* PCNA [43]. *Pfu* PCNA was also able to stimulate the activity of the eukaryotic DNA polymerase δ [43].

PCNA also has a function in lagging strand processing as both flap endonuclease 1 (Fen1) and DNA ligase 1, which are both important in lagging strand processing are specifically recruited to PCNA. Both proteins have PCNA interacting protein (PIP) box motifs [44]. It has been shown that PCNA stimulates the activity of Fen1. In this study *in vitro* biochemical assays were used to analyse the flap endonuclease activity of Fen1 and it was shown that the addition of PCNA resulted in a 7 fold increase in the activity of the protein [44]. The addition of a mutated PCNA that no longer binds to Fen1 resulted in only a 1.7 fold increase in the flap endonuclease activity of Fen1 suggesting that the stimulation of

Fen1 activity by PCNA is dependent on physical association of these proteins [44]. PCNA has also been shown to increase the activity of the *S.cerevisiae* Fen1 protein by 50-fold [44].

PCNA is also involved in the prevention of re-replication by the destruction of Cdt1 [45]. Cdt1 also contains a PIP box and it is thought that PCNA remains on DNA after the completion of replication and this may recruit free Cdt1 and subsequently promote its destruction by DDB1-Cul4 (DNA damage binding- Cullin 4) ubiquitin ligase [45].

Fen1 Endonuclease

The lagging strand of the replication fork is synthesised discontinuously. These series of short segments of DNA are known as Okazaki fragments. In eukaryotic cells these Okazaki fragments are usually of 100-150 nucleotides in length [46]. The synthesis of an Okazaki fragment is initiated by the DNA polymerase α-primase complex (pol α). The primase domain of the complex produces an 8–12 oligoribonucleotide primer, and then the polymerase extends the primer by adding another 20 deoxyribonucleotides (dNTPs) [47].

When the synthesis of one fragment encounters the following fragment, the elongating DNA strand displaces the 5'end of the preceding strand [48]. This creates a 5' unannealed flap that has to be removed before ligation of the fragments. These 5' unannealed flaps are removed by Fen1 [48]. Fen1 is a structure specific 5' endo/exonuclease that specifically recognises double stranded DNA with a 5'-unannealed flap [49]. On encountering this flap Fen1 makes an endonucleolytic cleavage at the base of the flap [49].

Interestingly, ChlR1 may have a role in lagging strand processing as it is an interacting partner of Fen1 [50]. ChlR1 was shown to stimulate the endonuclease activity of Fen1 [50]. In the presence of low levels of Fen1 (5 fmol), increasing concentrations of hChlR1stimulated the cleavage reaction approximately 3-fold.

DNA Polymerases

Eukaryotes contain 5 distinct families of DNA polymerases and in humans there have been 15 DNA polymerases characterised [51]. The large number of polymerases is required to perform a wide range of actions ranging from DNA replication to DNA repair. All the DNA polymerase families share a common core catalytic structure with 'palm', 'finger' and 'thumb' domains [51].

DNA polymerases require a single stranded DNA template to begin the synthesis of the complementary strand [52]. Therefore the activity of the polymerase is dependent on the unwinding of the DNA by the Cdc45, MCM and GINS complex (CMG complex) [18]. This complex associates with polymerase α-primase and recruits it to the single stranded DNA [53]. Polymerase α-primase is a tetrameric complex that consists of two pol α subunits and two primase subunits [54]. The complex initiates replication through the synthesis of a short RNA primer (10 nucleotides) by the primase. The 3' end of this primer translocates from the primase active site to the polymerase active site to allow for the synthesis of 20 nucleotides of DNA. After this initiation event the clamp loading complex RFC loads PCNA onto the double stranded DNA [54]. Polymerase δ or ε is then loaded to the PCNA-primer-template complex [54]. Polymerase δ is involved in lagging strand progression and polymerase ε is involved in leading strand synthesis [52]. These enzymes were shown to synthesis opposite strands of the DNA by genetic experiments in *S.pombe*

[55]. Mutations in the active sites of the polymerases were created. This resulted in an increase in DNA mutation rates. A reporter gene was placed in different orientations on opposite sides of a replication origin. For polymerase ε a higher rate of mutation was present in the leading strand suggesting a role in leading strand synthesis [55]. The opposite was observed for polymerase δ suggesting a role in lagging strand synthesis [55]. In agreement with this conclusion polymerase δ has been shown to interact with Fen1 in *S. pombe* suggesting a role in lagging strand synthesis [56].

Replication Protein A

Replication protein A (RPA) is a heterotrimeric single stranded DNA binding complex [57]. It consists of a large (70kDa), middle (32kDa) and small (14kDa) subunits [57]. RPA was initially discovered to have a role in DNA replication using an *in vitro* assay to study simian virus 40 (SV40) replication [58]. RPA accumulates along stretches of single stranded DNA generated during DNA replication [59] and is required for the activation of the pre-RC complex to form the initiation complex [58]. It is also believed that RPA has a role in the ordered loading of essential initiators such as DNA polymerase α primase [60]. RPA is an important factor in the DNA repair process nucleotide excision repair (NER) [61]. During strand elongation RPA stimulates DNA polymerase α, λ, κ and ε [62]. RPA interacts with Xeroderma pigmentosum A (XPA) at sites of DNA damage and stimulates the recruitment of Excision repair cross-complementing 1/ Xeroderma pigmentosum F (ERCC1/XPF) [63]. Finally RPA interacts with the Blooms and Werner syndrome DNA helicases (WRN and BLM, respectively) [61]. These helicases are closely related to ChlR1.

TopBP1

Topoisomerase 2-binding protein 1 (TopBP1) was initially shown to function in DNA replication when it was shown to interact with DNA polymerase ε [64]. This polymerase has proof-reading ability and associates with origins of replication and progresses along with the replication forks [65]. A role in pre-initiation for TopBP1 was suggested as TopBP1 depleted cells were unable to enter S phase [66]. The depletion resulted in down regulation of cyclin E/Cdk2 [66] both of which are thought to be involved in the initiation of replication [67]. Depletion of TopBP1 also results in increased levels of p21 and p27 [66] both of which inhibit Cdk2 [68]. The *S.cerevisiae* homologue of TopBP1, Dbp11 also forms a complex with polymerase ε, GINS complex and Sld2 [69]. This complex is known as the preloading complex. Cdk2 regulates the formation of this complex and this complex is involved in the initiation of replication [69].

TopBP1/Dbp11 also has a role in re-initiation of replication at stalled replication forks. It has been shown that TopBP1 is involved in the recruitment of the 9-1-1 clamp (Rad 9, Rad 1 and Hus 1) to stalled replication forks [70]. Depletion of TopBP1 in *Xenopus* egg extracts resulted in the inability of the 9-1-1 clamp to be recruited to stalled replication forks [70]. The three proteins of the 9-1-1 complex interact to form a heterotrimeric complex similar to the PCNA sliding clamp [71]. Upon replication stress the complex assembles around the damaged DNA and activates the protein kinase Checkpoint kinase 1 (Chk1) through the ataxia telangiectasia and Rad3-related (ATR) pathway [72, 73]. This results in the stabilisation of the replication forks. In addition, in *S.pombe* the 9-1-1 complex regulates the use of the translesion polymerases instead of high fidelity polymerases [74]. These translesion polymerases specialise in the insertion of nucleotides

into bulky lesions [75]. When the 9-1-1 complex is knocked out in *S.cerevisae*, ATM checkpoint activation is defective [76].

1.3 Sister Chromatid Cohesion

The structure of the cohesin complex

The structural maintenance of chromosomes (SMC) proteins are members of a family of highly related proteins that function in numerous areas of DNA maintenance. Smc1 and 3 function in sister chromatid cohesion, Smc2 and 4 in chromatin condensation, Smc5 and 6 in homologous recombination and Rad50 functions in DNA damage repair. These proteins are large polypeptides of 1000-1300 amino acids in size [77]. They contain two canonical nucleotide binding Walker A and B motifs that are situated at the N- and C- termini of the protein, respectively [78]. Two coiled-coil motifs that are folded in an antiparallel conformation connect the Walker motifs (shown in figure 2). This antiparallel conformation was first shown by electron microscopy [79]. The Smc monomer folds back on itself which leads to the Walker motifs situated at close proximity to each other and the creation of hinge domain [80, 81]. Smc1 and Smc3 associate with each other at the hinge domain resulting in the formation of a heterodimer [79] (shown in Figure 2).

The Walker A motif head domain of the Smc proteins is an ATPase domain. The C-terminal Walker B domain of Smc contains the conserved sequence LSGG (E/Q)(K/R) [78]. This sequence is found in the ATP binding cassettes (ABC) of ATPases [82] (discussed later). The Walker motifs of Smc that are situated in close proximity form a pocket that binds ATP [83]. ATP binding is important for head-head engagement and mutations in the Walker motifs that abolish ATP binding disrupt this [83].

The structure of the hinge region of Smc was first defined by the crystal structure of the bacterium *Thermotoga maritime* Smc hinge domain [80]. The hinge monomers are composed of two domains that display pseudo-two fold symmetry. The N-terminal region of one monomer associates with the C-terminal region of the same monomer. This leads to the formation of the antiparallel coiled-coil formation. Dimerization of the monomers occurs through ß-sheet interactions between the monomers [80]. The interaction between the Smc1 and 3 is independent of ATP binding [83].

Scc1 is a member of the Kleisin superfamily of proteins [84]. This family of proteins is known to form complexes with Smc proteins [84]. The *S.cerevisae* Scc1 protein contains three domains. The N-terminal domain of Scc1 interacts with the Smc3 ATPase domain and the C-terminal domain of Scc1 interacts with the Smc1 ATPase domain [85]. The third domain is situated in the middle of the polypeptide chain and contains the separase cleavage site. This domain is 180 amino acids in length and connects the N and C-terminal domains of Scc1 [80], acting as a bridge between the two Smc subunits (shown in figure 2). Mutations in Smc1 that abolish ATP binding also disrupt the binding of Scc1 and sister chrmatid cohesion suggesting that the binding of ATP is important in binding of Scc1 and the function of cohesin [86]. Mutations in Smc3 that disrupt ATP binding do not abolish Scc1 binding but also result in inactivation of cohesin function [87]. This suggests that Scc1 binds to Smc1 first. The binding interface between the C-terminus of Scc1 and the ATPase domain of Smc1 has been solved by X-ray crystallography [88]. The structure shows that the two Walker domains of Smc1 bind to Scc1 and two ATP molecules are sandwiched in between [88]. Scc1 binds to Smc1 via its winged helix motif [88]. A winged helix motif is a compact α/β structure consisting of two wings three α-helixes and three β-sheets [89]. The N-terminus of the motif is largely helical whereas the C-terminus

is largely formed from β-sheets [89]. Two β sheets in the winged helix domain of Scc1 bind to the ATPase head of Smc1 [88].

Expression of a version of Scc1 that separase (a cysteine protease that cleavages Scc1 and destroys the cohesion ring releasing the chromatids) cannot cleave shows little exchange of cohesin or its subunits [88]. This suggests Scc1 completes the ring structure of cohesin and locks the other components in the ring (figure 2). Electron microscopy studies on the *S.cerevisiae* cohesion complex confirmed the ring shaped structure. The ring structures consists the two Smc subunits folded up individually into rod shaped molecules of 45nm in length that are connected at their hinge domains. This forms a V-shaped heterodimer. The ATPase heads are then connected by Scc1 closing the ring [80] [90].

Another protein that has been shown to associate with the cohesin complex is the Scc3 protein. In vertebrate cells Scc3 exists as two closely related homologues SA1 and 2 (stromal antigen 1 and 2) [91]. These proteins associate with the cohesin complex and the complex contains either SA1 or SA2 at one time [91]. In *S.cerevisiae* Scc3 was shown to interact with Scc1 at the C-terminus but does not interact with either Smc1 or Smc3 [80]. In human cells cohesin associated with SA1 is required for telomere cohesion and cohesin associated with SA2 is required for centromere cohesion [92]. Cells deficient in SA1 are unable to establish or maintain cohesion between sister telomeres after DNA replication. In SA2 depleted cells, telomere cohesion is normal but centromeric cohesion is prematurely lost [92].

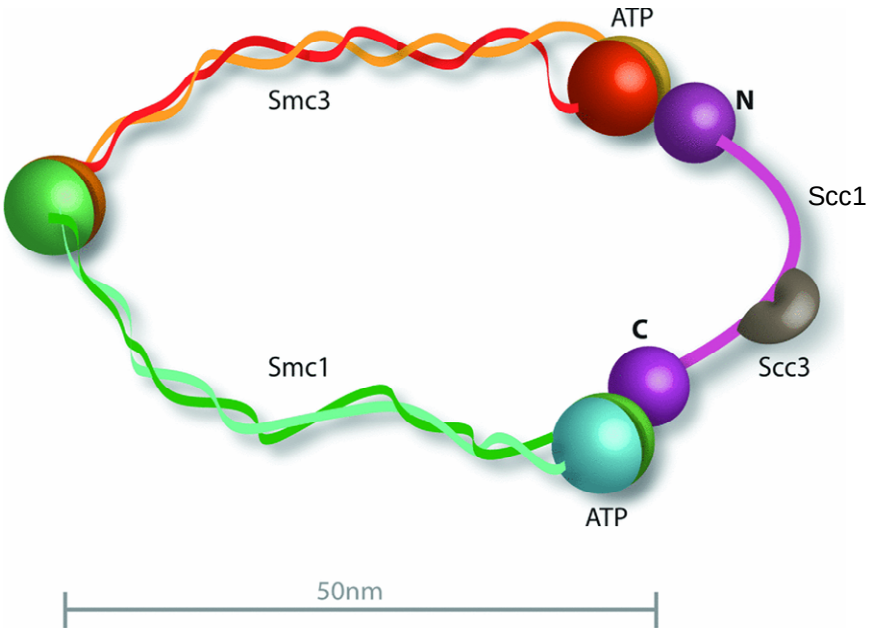

Figure 2**: The structure of the cohesin complex.** *The complex consists of 4 proteins Smc1, Smc3, Scc1 and Scc3. These proteins create a ring structure. The Smc proteins interact with each other via their hinge region and Scc1 acts as a bridge linking the ATPase head domains of the Smc proteins [93].*

Loading of cohesin

The loading of cohesin onto DNA occurs at different points of the cell cycle in different species. In lower eukaryotes cohesin is loaded onto the DNA at the end of G_1 [94]. However in mammalian cells cohesin is loaded at telophase [95]. This suggest that cohesin has other functions apart from sister chromatid cohesion (discussed later) and these additional functions vary amongst species. In both lower and higher eukaryotes association of cohesin and DNA becomes more stable as the cell progresses from G_1 to S phase [96]. The loading of cohesin requires ATP hydrolysis and the Scc2-Scc4 protein complex [97]. Scc2 is believed to interact with the cohesin complex and promote ATP hydrolysis at the Smc heads [86]. This results in the hinge opening or Scc1 dissociation that would allow for DNA to enter the cohesin ring.

Cohesin was initially believed to bind to the DNA and act as an intermolecular bridge between the DNA [98]. This theory was changed following the structural analysis of the cohesin complex that suggested a ring shaped structure [80]. The current theory is that the cohesin ring encircles and therefore entraps the DNA strands (Figure 3). This theory is possible because the Smc heterodimers are 50-60nm in length and along with Scc1 is able to encircle the DNA strand that is 10nm in diameter (Figure 2)[80]. Further evidence supporting this theory is that disruption of the ring results in dissociation of the DNA [85, 99]. Cleavage of Scc1 by separase at the end of mitosis results in dissociation of the DNA [85]. A further study showed that cleavage of Smc3 containing TEV cleavage sequences in both coils of the coil-coiled domain expressed in *S.cerevisiae* resulted in dissociation of the DNA from the cohesin complex [99]. This confirms that the cohesin complex encircles the DNA instead of acting as an inter-molecular bridge. Finally, linearization of a circular minichromosome by restriction enzyme digestion in *S.cerevisiae* resulted in dissociation of the cohesin ring from the DNA [100], suggesting the cohesin complex encircles the DNA and does not associate with the DNA.

There are two models to explain how the cohesin complex encircles the DNA. The ring model, where one cohesin ring encircles two DNA strands and the handcuff model where two cohesin complexes are required each encircling one DNA strand and the two complexes associate with each other (shown in Figure 3). The evidence to corroborate with the ring model comes from data showing that interactions between multiple cohesin complexes are undetectable by FRET analysis in *S.cerevisiae* [101]. Site specific cross-linking at the three interfaces of the cohesin ring that creates a convalently closed ring was used to show that one cohesin ring is required to encircle the DNA. Protein denaturation did not disrupt the cohesin-minichromosome DNA structure *in vitro* [102].

Evidence to corroborate with the handcuff model includes data suggesting Scc1 interacts with itself in a yeast-two hybrid system, which was confirmed by co-immunoprecipitation in mammalian cells [103]. Cohesin rings are only able to encircle one strand of DNA at silent heterochromatin regions where the DNA has a larger diameter which also suggests that cohesin rings may multimerise to facilitate cohesion [104]. Finally the four cohesin complex subunits have been shown to interact with themselves in a Scc3 dependent manner. Depletion of Scc3 abolished the ability of the other three cohesin subunits to interact with themselves [103]. This suggests Scc3 is important in creating a link between two cohesin rings.

Cohesion establishment

Cohesion establishment is believed to occur during DNA replication and does not require additional cohesin complexes to be loaded onto DNA [105]. Eco1 (Esco1 in humans) is a lysine acetyltransferase and it is required for cohesion establishment [106]. Eco1 associates with numerous members of the DNA replication complex including the clamp loader proteins Ctf18 and Elg1[107, 108]. Both of these proteins play a role in cohesion establishment. PCNA also associates with Eco1 [109]. Therefore it is believed cohesion establishment is linked to PCNA-dependent DNA replication. Eco1 may allow for the dissociation and re-association of the cohesin ring as the replication fork passes, thus facilitating cohesion establishment during DNA replication [93].

Recent evidence suggests that acetylation of cohesin is important for replication fork processivity. Smc3 has been shown to be acetylated *in vivo* at two conserved lysines by Eco1 during S phase [105, 110]. The Ctf18 subunit of the alternative RFC complex RFC-Ctf18 has also been shown to been involved in the regulation of acetylation of cohesin

[10]. When Ctf18 is depleted in mammalian cells replication and cohesin acetylation is impaired [10]. Ctf18 does not acetylate Smc3 but is believed to be important in regulating Eco1 activity [111]. Furthermore, cohesin associated proteins Wpl1 and Pds5 also regulate cohesion establishment [112, 113]. Wpl1 and Pds5 remove cohesin from the chromosomes during mitosis. Depletion of these proteins in mammalian cells blocks the removal of cohesin in prophase and increases the residence time of cohesin on the chromosomes in interphase [113]. These proteins interact with Smc3 and are removed from the complex when it is acetylated [114].

Interestingly fork progression through the cohesin complex is necessary for establishment as it leads to entrapment of the nascent DNA strand within the ring [105]. Therefore the acetylation of cohesin by Eco1 may cause conformation changes to the complex that allow for replication fork passage. The conformational change may result from the removal of Wpl1 or Pds5 from cohesin upon acetylation [10]. It may be possible that acetylation of Smc3 may cause dissociation of Scc1 to allow the replication fork to pass through [10].

Acetylation of Smc3 by Eco1 is important for the establishment of cohesion because deletion of Eco1 in *S.cerevisiae* causes premature chromosome separation when Esp1p (yeast homologue of separase) proteolysis is inhibited [106]. Deletion of Eco1 did not affect the loading of Scc1 and 3 onto the chromosomes which suggests it is not required for the loading of cohesin onto DNA but for the establishment of cohesion [106].

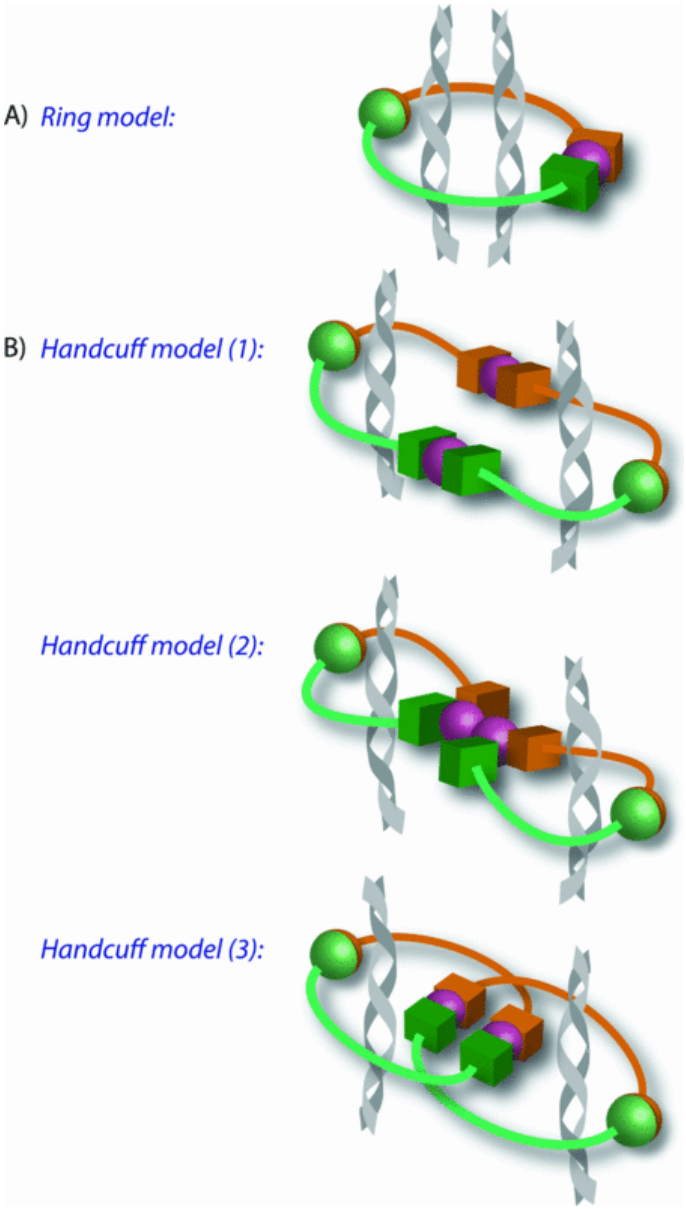

Figure 3**: Models of sister chromatid cohesion.** *The four proposed models of sister chromatid cohesion are shown. The ring model involves one cohesin ring encircling two DNA strands. The handcuff model involves the interaction between two cohesin rings with each ring encircling one DNA strand [93]. Image taken with permission from Portland Press.*

1.4 Mitosis

ChlR1 and cohesin are important in the pairing of sister chromatids, which allows for the equal distribution of genetic material in mitosis. Mitosis is divided into 4 main stages prometaphase, metaphase, anaphase and telophase.

In the prometaphase stage the nucleus dissolves and the mitotic spindle microtubules attach to the kinetochores at the centromeres (located near the centre of the chromosomes and is the region where the sister chromatids come in close contact) of the chromosomes. The kinetochore is a structure that containing a number protein complexes, that form around the centromeres. The simplest kinetochore structure is found in *S.cerevisiae* and contains 60 proteins in 7 complexes [115]. The complexes of the kinetochore are conserved from yeast to humans. Two of these complexes Ndc80 and Dam1 (Duo1 And Mps1 interacting) complexes have an important function in interacting with the microtubules [116]. Another kinetochore protein Centromere protein A (CENP-A) a centromeric specific conserved histone H3, is important in the recruitment and assembly of the kinetochore complexes at the centromeres [115].

The mitotic spindle microtubules consist of polarized filaments composed of α/ß- tubulin heterodimers arranged in a head to tail configuration within protofilaments [117]. The microtubule polarity is due to the asymmetric arrangement of the tubulin subunits. The minus and plus ends of the microtubule have different dynamic properties [118]. This polarity is important in the transport of the chromosomes along the microtubule to the poles.

The microtubules undergo repeated growth and shrinkage in various directions, searching for kinetochores [119]. The growth and shrinkage of the microtubules is a result of the addition and loss of tubulin dimers at the end of the polymers [118]. This searching for

kinetochores is not a random process in vertebrate cells as the microtubules are guided to the kinetochores by a concentration gradient of Ran-GTP around the chromosomes [120]. Interestingly microtubules are generated by the kinetochores and these microtubules interact with and guide spindle microtubules to the kinetochores [121]. At this stage of mitosis the cohesin encircling the arms of the chromosomes is removed through phosphorylation of the cohesion subunits by Polo-like kinase 1 (Plk1) [122] which will be discussed later.

In metaphase the chromosomes are aligned on the mitotic spindles. Alignment of the chromosomes on the spindles requires bi-orientation of the kinetochore and microtubules. Bi-orientation is control by two mechanisms; kinetochore geometry and error correction. Kinetochore geometry relies on a back to back position of sister kinetochores [123]. When one kinetochore attaches to the microtubules from one spindle pole, the constraints in geometry requires the other kinetochore faces the opposite direction and attach to the microtubule from the opposite pole [123]. If aberrant attachments are made between the kinetochore and microtubules the geometry mechanism cannot correct the mistake. Tension created by correctly bi-orientated kinetochore and microtubules stabilises the interaction between the two structures. If this tension is not present then the two structures dissociate and a new interaction is created. This mechanism of control is termed error correction and requires the spindle assembly checkpoint protein Aurora B kinase [124]. Defects in Aurora B or its yeast homologue Ipl1 results in the kinetochores being unable to interact with the microtubules [125]. Aurora B localises at the centromeres in metaphase and phosphorylates kinetochore components [126]. This weakens the interaction between the kinetochores and microtubules [127]. This is believed to be important in the turnover of kinetochore and microtubule interactions during bi-orientation. Once bi-orientation and tension between the kinetochores and microtubules is achieved then a number of

kinetochore components including Dam1 and Knl1 are dephosphorylated [128]. This stabilises the interaction between the kinetochores and the microtubules and the cells can progress into anaphase.

During anaphase the cohesin that encircles the chromosomes at the centromeres is cleaved by a cysteine protease called separase, which is inhibited by the spindle assembly checkpoint upon alignment of the chromosomes [129]. The separated sister chromosomes are transported along the spindle microtubule to the poles. The movement of the chromosomes towards the spindle poles is achieved by microtubule depolymerization along with the activity of molecular motor proteins such as dynein and kinesin proteins. Dynein associates with the kinetochores and has poleward minus end directed motility [130]. Inhibition of dynein in drosophila embryos causes a reduction in chromatid movement towards the poles [131]. Kinesin proteins are microtubule depolymerising enzymes localised at the kinetochores [132]. Disruption of these proteins in vertebrate cells causes lagging chromosomes in anaphase [133].

After the chromosomes are transported to the spindle poles during anaphase, the cell progresses to telophase where the microtubules disappear and new nuclear envelopes form from fragments from the parent cells nuclear envelope and portions of the endomembrane system. The compacted chromosomes decondense back into chromatin.

1.5 Spindle assembly checkpoint

The accurate segregation of chromosomes in mitosis is controlled by the spindle assembly checkpoint (SAC). The SAC was identified by a mutation screen in *S.cerevisiae* in which cells were isolated that were able to progress through mitosis in the presence of a spindle

poison. The screen identified a number of genes including Mad (mitotic arrest defects) 1, 2, and 3 (BubR1 in humans) and Bub (budding uninhibited by benzmidazole) 1 and 3 [134]. These genes are conserved in all eukaryotes. They are activated in prometaphase and form the basis of the spindle assembly checkpoint (SAC) [135].

The SAC targets Cdc20, which is a co-factor of the anaphase promoting complex/cyclosome (APC/C) [136]. The SAC negatively regulates the ability of Cdc20 to activate the APC/C mediated poly-ubiquitination of cyclin B and securin. Hence progression through the SAC results in proteasome-mediated degradation of cyclin B and securin and progression to anaphase. Activation of the SAC prolongs prometaphase until all the chromosomes have become bi-orientated between the spindle poles [136]. The SAC monitors the interactions between the kinetochores and the spindle microtubules. Mutations in kinetochore proteins which impair the function of the kinetochores results in the activation of the SAC in *S.cerevisiae* [137]. The vertebrate homologues of the SAC proteins were shown to accumulate at unattached kinetochores and disperse upon microtubule attachment [138].

In humans Bub1 is present at the kinetochores from prometaphase until kinetochore microtubule attachment in humans [139]. Bub1 is believed to recruit a number of the SAC proteins to the kinetochores including Mad1, Mad2, BubR1, Bub3 and Cdc20 in *Xenopus* egg extracts [140]. Bub1 also phosphorylates Cdc20 and this inhibits Cdc20 [141]. Replacement of wild type Cdc20 with a mutant that Bub1 is unable to phosphorylate results in mitotic exit despite spindle damage in HeLa cells [141].

The main function of the protein kinase BubR1 in regulating the SAC is to interact with and phosphorylate the microtubule plus end directed motor CENP-E [142]. In *X. laevis* the depletion of CENP-E disrupts the SAC suggesting it directly functions in the SAC [143]. In mammalian cells, depletion of CENP-E results in some unattached kinetochores [144].

CENP-E binds to BubR1 and activates the kinase in vitro [145]. This activation is repressed when CENP-E binds to the microtubules [145] suggesting that BubR1 is inactivated upon kinetochore microtubule attachment. Replacement of the wildtype CENP-E with a truncated CENP-E that lacks the microtubule binding domain results in continued activation of the SAC in mammalian cells [145].

The kinase Aurora B/Ipl1 is also involved in the SAC. It detects and destabilizes faulty microtubule-kinetochore attachments [146]. This generates unattached kinetochores and results in SAC activation [146]. There is evidence that suggests Aurora B recruits BubR1 and Mad2 to the kinetochores. Inhibition of Aurora B in mammalian cells reduces Mad2 and BubR1 localisation to the kinetochores in nocodazole treated cells [147].

There are a number of mechanisms for the inactivation of the SAC after kinetochore attachment. Mad1 and 2 are stripped from the kinetochores by dynein that is present on microtubules [148]. This is dependent on dynein motility along the microtubules [148]. The activated APC/C is believed to target a number of the SAC proteins for degradation. Mps1 is a kinase involved in the SAC that localises to the kinetochores [124]. In *S.cerevisiae* Mps1 is degraded at anaphase in a Cdc20 dependent manner [149]. Overexpression of Mps1 or removal of Cdc20 during anaphase results in SAC reactivation [149].

1.6 The removal of cohesin in mitosis

At the onset of anaphase, cohesion is dissolved by the proteolytic cleavage of Scc1 by the activated cysteine protease separase [85, 129]. Separase is activated by the degradation of its inhibitory binding partner securin by the 26S proteasome [150]. Securin is targeted for degradation by polyubiquitination by activated APC/C which is a large 1.5MDa ubiquitin

ligase [151]. Cdc20 act as co-activator and allows APC/C to recognise securin as a target [151]. It is believed that Cdc20 delivers securin to APC/C [152]. Cdc20 is activated following satisfaction of the spindle assembly checkpoint (discussed above). Securin binds to separase at the protease active site therefore blocking the function of separase [153].

When securin is knocked out in mice, the embryonic cells are viable and undergo normal anaphase progression [154]. This suggests there is another pathway of separase inhibition and it has been shown that phosphorylation of serine 1226 of separase results in inhibition of separase during metaphase [150].

Before cleavage of Scc1 by separase in anaphase, the majority of cohesin dissociates with the chromosomes in prometaphase [122]. Polo-like kinase 1 (Plk1) is involved in this process [122]. Plk1 is a key regulator of mitotic division [122] and a member of a family of four related serine/threonine kinases. When Plk1 is depleted in mammalian cells the cells fail to establish bipolar spindles [122]. Plk1 can phosphorylate Scc1 and Scc3 *in vitro* [155] and is required for their phosphorylation in *Xenopus* egg extracts [156]. Phosphorylation of Scc1 and 3 subunits results in cohesin being unable to bind to the chromatin in the extracts [156]. Evidence suggests that the phosphorylation of Scc1 by Plk1 can enhance the cleavage of Scc1 by separase [157]. In human cells phosphorylation of Scc3 is important for cohesin dissociation [158] and mutations at the phosphorylation site on Scc3 results in an inability to remove cohesin from the chromosome arms during prometaphase [158]. This phenotype is similar in cells depleted of Plk1 [159]. Therefore Plk1 is important for the removal of cohesin from the chromosome arms during prophase and prometaphase.

Cohesin located at the centromeric regions of sister chromatids are protected from phosphorylation by a protein called Shugoshin (Sgo1). Sgo1 starts to accumulate at the centromeres during prophase [160] and at anaphase the protein is found at the leading

edges of the chromosomes moving towards the spindle poles [161]. Sgo1 was first shown to be involved in the process of sister chromatid cohesion in *S.cerevisiae* where Sgo1 deletion resulted in sensitivity to spindle destabilizing drugs and premature sister chromatid separation [162, 163]. Depletion of Sgo1 in HeLa cells resulted in mitotic arrest and chromosome mis-segregation [160]. Depletion of Sgo1 results in the loss of Scc1 at the centromeres. Therefore, Sgo1 was shown to protect centromeric cohesion from dissociation at the centromeres during prophase [160].

The serine/threonine protein phosphatase 2A (PP2A) has been shown to interact with Sgo1 [164]. This protein is important for sister chromatid cohesion as depletion of the protein causes cohesion defects in HeLa cells [164] and premature centromere segregation in *S.cerevisiae* [165]. It is believed to protect centromeric cohesin from the prophase pathway by preventing phosphorylation of the Scc3 subunit of cohesin [166]. *In vitro* analysis showed that PP2A is able to dephosphorylate the peptides of the Scc3 that are targeted by Plk1 [166]. Furthermore PP2A is required for the recruitment of Sgo1 to the centromeric regions [164].

The function of PP2A and Sgo1 is controlled by the kinetochore associated protein Bub1 [167]. Depletion of Bub1 prevents localisation of both PP2A and Sgo1 to the centromere [162]. Furthermore, it has been demonstrated that the kinase activity of Bub1 restricts the localisation of PP2A and Sgo1 to the centromere [168].

1.7 The role of ChlR1 in sister chromatid cohesion

Chl1 (Chromosome loss 1; Chl-Related1 (ChlR1) in humans) was initially discovered in a screen for mutants of *S.cerevisiae* that exhibited decreased chromosome transmission fidelity in mitosis [169]. Analysis of *Chl1* mutant strains showed a 200-fold increase in

chromosome missegregation at the MATά locus on chromosome III and mutants exhibited both loss and gain of chromosomes fragments [169]. The loss of chromosomes and chromosome non-disjunction was 100-fold above wildtype rates [169]. In addition, the mutant cells showed signs of cell cycle checkpoint activation leading to G_2/M delay [170]. The Chl1 protein has been shown to have sequence homology to the Rad3 protein, which is involved in nucleotide excision repair of DNA damage. The two proteins are 23% identical and 48% similar [170]. Interestingly, regions of high homology include the ATP binding site domain of Rad3 [170]. Mutations in Chl1 that prevent ATP binding result in the inactivation of its function in chromosome segregation and overexpression of this mutant interferes with chromosome transmission [171].

ChlR1 is a member of the DEAD/H family of DNA and RNA helicases. ChlR1 mRNA and protein is expressed in dividing cells but not terminally differentiated cells or cells in growth arrest suggesting that ChlR1 has a similar role to Chl1 in cell proliferation [172]. ChlR1 and Chl1 are 32% identical and 55% similar [173]. The expression of ChlR1 was not present until 16 hours after the addition of serum to fibroblasts [172]. This coincides with the entry of these cells in S phase. The expression levels increased over the next 12 hours [172]. This suggests that ChlR1 is required for S phase and mitosis. Using *in vitro* transcribed and translated ChlR1 protein it has also been shown that ChlR1 binds to both double and single stranded DNA [172].

The helicase activity of ChlR1 has been investigated using purified ChlR1 expressed in insect cells using the baculovirus expression system [174]. The protein possesses both ATPase and DNA helicase activities that are dependent on DNA, divalent cations and ATP [174]. The helicase activity is abolished by a single amino acid substitution of lysine to arginine at position 50 in the ATP binding domain of the protein [174]. ChlR1 can unwind DNA/DNA and RNA/DNA duplexes. It has a preference to unwind in the 5-3’ direction on

short single stranded DNA templates of 19 nucleotides in length [174]. Unlike other DNA helicases, ChlR1 can translocate along single stranded DNA in both directions when the substrates have a very long single stranded DNA region [174].

Depletion of ChlR1 resulted in pro-metaphase delay and mitotic failure. There are a higher percentage of cells in mitosis 24 hours after depletion and there are a higher percentage of cells with chromosome dispersed over the entire spindle [175]. This is a phenotype associated with pro-metaphase delay. Depletion of ChlR1 also results in chromosome mis-segregation [175]. Depletion of ChlR1 for 96 hours results in hTERT-RPE1 cells with enlarged and fragmented nuclei indicting the cells failed to correctly segregate sister chromatids following the delay in pro-metaphase [175]. Depletion of ChlR1 in HeLa cells causes failure to form tight metaphase plates and after the pro-metaphase delay the DNA decondenses without mitotic segregation [175].

ChlR1 associates with the cohesin complex and when ChlR1 is depleted the cells show signs of abnormal sister chromatid cohesion [175]. Sister chromatid pairing was analysed through metaphase spreads. Measurement of the distance between chromatid pairs revealed that sister chromatids were further apart at the centromeric regions in ChlR1 depleted cells indicating abnormalities in sister chromatid cohesion [175]. These results suggest a role for ChlR1 in chromatin condensation and organization of the DNA through the correct assembly of cohesin onto DNA during replication [175].

There is evidence suggesting ChlR1 has a role in the spindle assembly. ChlR1 has been shown to accumulate at the spindle poles in early mitosis where it remains until telophase [175]. The cohesin subunits Smc1 and SA1 have also been shown to localise to the spindle poles during mitosis [175]. This localisation is mediated by NuMA a protein required for mitotic spindle organization and inhibition of these cohesin subunits inhibited mitotic aster

assembly [176]. The localisation of ChlR1 at the spindle poles and the evidence that ChlR1 associates with cohesin may indicate a role for ChlR1 in mitotic aster assembly [175].

The knockout of the mouse ChlR1 gene DDX11 resulted in lethality at the embryonic stage of the mouse development [177]. Lethality was a result of accumulation of aneuploid cells and placental malformation [177]. Mutant embryos were smaller in size, malformed and exhibited sparse cellularity compared to normal or heterozygous litter mates [177]. Cells isolated from the $Ddx11^{-/-}$ embryos displayed a G_2/M delay, increased chromosome missegregation, decreased chromosome cohesion and increased aneuploidy [177]. These cellular defects are displayed in mammalian cells depleted of ChlR1 with siRNA.

1.8 The role of cohesin in gene expression

Cohesin re-associates with chromosomes at the end of mitosis [95]. This re-association occurs long before sister chromatid cohesion is established suggesting additional functions for cohesin.

There is evidence that cohesin has a role in the control of gene expression in S.*cerevisae.* The positioning of cohesin was shown to be affected by transcription with cohesin accumulating at convergent transcripts [178]. This suggests that as the transcription machinery moves along the DNA any cohesin it encounters is pushed along until transcription termination. This accumulated cohesin was shown to have a role in transcription termination in *S.pombe*. The cohesin is thought to act as a barrier between coding regions to aid efficient transcriptional termination [179].

Cohesin binding sites have been discovered at heterochromatin regions, which are silent loci with several functions from gene regulation to the protection of the integrity of chromosomes [180]. Heterochromatin regions remain transcriptionally silent through the

function of Sirtuins (SIR) proteins [181]. Cohesin therefore is thought to play an important function in chromatin silencing. Cohesin is recruited to heterochromatin regions in a SIR dependent manner [104]. Heterochromatin regions contain a number of repeated sequences that are unstable due to recombination therefore it is believed that cohesin is recruited to act with the SIR proteins to prevent unwanted recombination [182]. Cohesin subunits Smc1 and 3 have been found at the boundary regions of the heterochromatin and mutations of these proteins results in disruption of the boundaries [183] (shown in Figure 4). It is believed that cohesin helps create boundaries at the end of the heterochromatin regions to prevent unwanted spread of the silent chromatin.

There is evidence that suggests cohesin inhibits the formation of silent chromatin. Silencing of the heterochromatin regions is unable to take place in the presence of Scc1 in G_2/M even in the presence of SIR proteins. When Scc1 is cleaved or repressed the heterochromatin becomes silent [184] (shown in Figure 4). This suggests that the cohesin subunits prevent silencing of the region until the boundaries have been established.

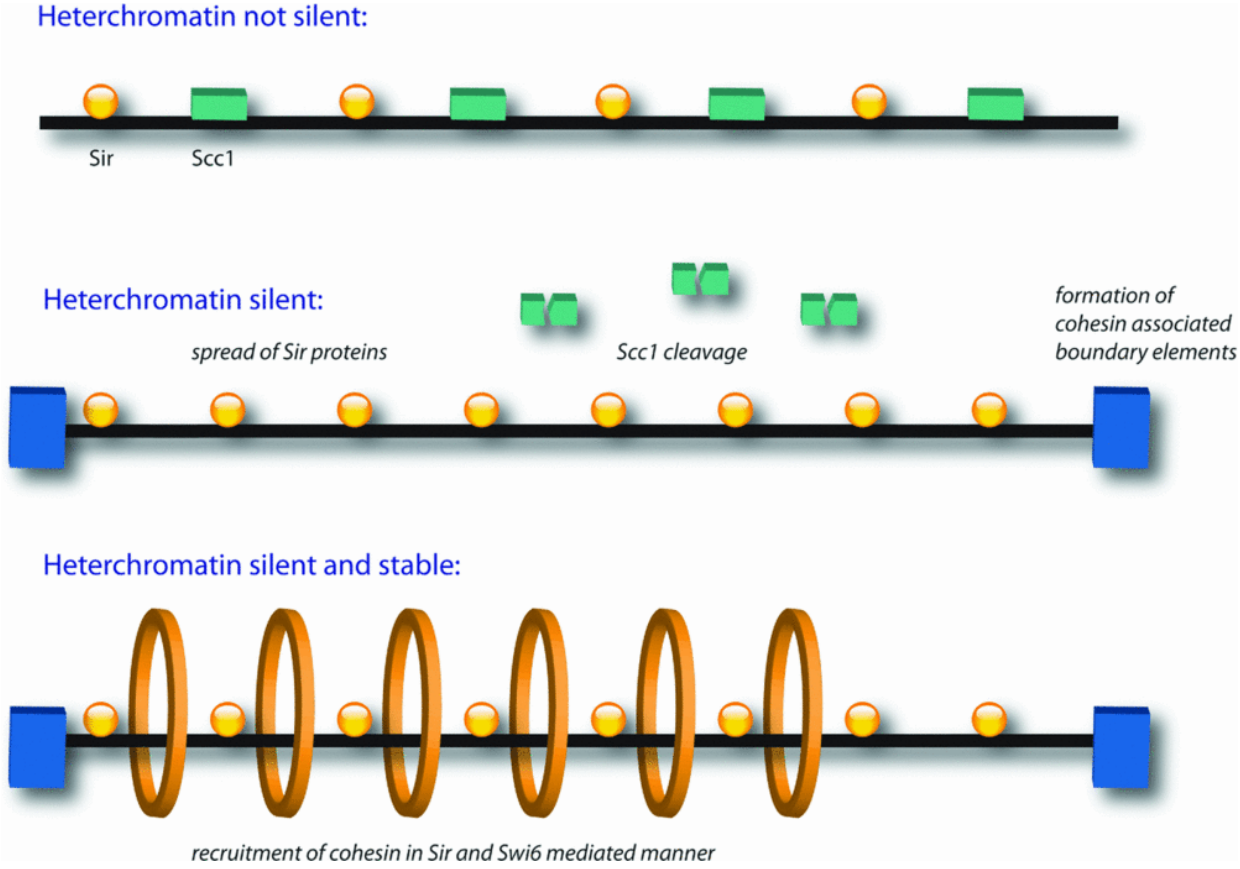

Figure 4**: The model for the role of cohesin at silent domains**. *Top panel: Scc1 associates with the silent domain preventing the establishment of silencing until the creation of cohesin-associated boundary elements. This prevents the unwanted spread of silent heterochromatin. Middle panel: following establishment of the boundary elements, Scc1 is cleaved and the spread of Sir proteins can occur. Bottom panel: once silent heterochromatin is developed, cohesin (orange rings) re-associates to stabilize the domain, preventing unwanted recombination [93]. Image taken with permission from Portland Press.*

In mammalian cells cohesin does not accumulate at convergent transcripts but at CTCF consensus binding sites, which have the general sequence CCCTC. Depletion of CTCF disrupts the positioning of cohesin at these sites suggesting that CTCF is involved in the recruitment of cohesin to DNA [185]. CTCF is an 11 zinc finger domain protein and its expression is cell cycle specific from S to G_2 phase [186]. The major function of CTCF is in the insulation of groups of genes that are transcriptionally co-regulated. CTCF often flanks these genes. It is thought that CTCF prevents communication between genes and

enhancer elements of flanking genes [187] and it has been suggested that cohesin has a role in this function CTCF. Mammalian cells were depleted of CTCF or the cohesin subunit Scc1 and transcriptional changes were measured by DNA-chip. Similar transcriptional changes were observed after down-regulation of CTCF or Scc1 and genes within 25kb of cohesin rich sites had a higher tendency to be up regulated, consistent with the conclusion that cohesin mediates CTCF insulator function [188].

The β-globin gene locus has been shown to be insulated by CTCF. This locus contains CTCF binding sites at the 5’ and 3’ boundaries of the locus [189], insulating inappropriate interactions between the genes of the locus and the enhancer elements of neighbouring genes (Figure 5) . Cohesin binds to these boundaries aiding the barrier and creates an active hub for the active β-globin genes through looping of the locus [190] . Disruption of CTCF or cohesin binding results in destabilization of the loop. CTCF and cohesin have been shown to be involved in the insulation of a number of other loci through looping. These include the H19/IGF locus [191] and the IFN-gamma cytokine locus [192].

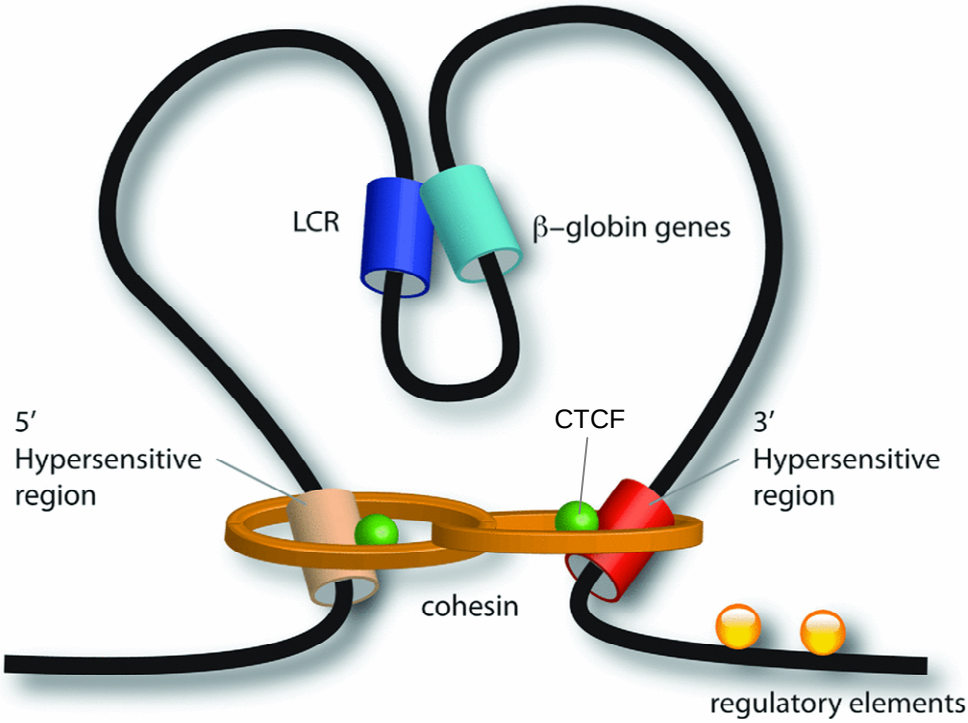

Figure 5**: The structure of the β-globin locus**. *Looping in the β-globin locus involves the interaction of CTCF and cohesin to the 5' and 3' hypersensitive regions. This looping insulates the genes within the locus from regulatory elements of neighbouring genes [30]. Image taken with permission from Portland Press*

1.9 DNA damage responses

DNA damage occurs during all stages of the cell cycle, during DNA replication and through exposure to DNA damage reagents such as sunlight and radiation. Cells have to maintain the integrity of their genomes, so have evolved numerous pathways to repair DNA damage. These pathways are discussed below.

Non homologous end joining

Non Homologous End Joining (NHEJ) is considered the major pathway for the repair of DNA double strand breaks in mammalian cells. NHEJ can be activated to repair DNA double strand breaks throughout the cell cycle [193]. NHEJ requires a number of proteins including Ku70 and 80, DNA-PKcs, XRCC4, DNA ligase IV, Artemis and XLF (Figure 6). Deletion of any of these proteins results in sensitivity to DNA damaging reagents [194].

Detection of the break involves Ku70 and 80 which is recruited to the break seconds after induction [195]. The Ku proteins may assist in tethering the ends together [196]. Atomic force microscopy images showed that DNA forms loops in the presence of purified Ku70 protein. Looping of the DNA around the break may result in tethering of the DNA ends [196]. Ku interacts with and is phosphorylated by DNA-PKcs. The recruitment of DNA-PKcs to the sites of breaks requires Ku80 [197] (shown in figure 6). DNA-PKcs does not accumulate at sites of DNA double strand breaks in Ku80 deficient cells [197]. In the absence of Ku, purified DNA-PKcs is unable to bind to DNA *in vitro* [197]. This suggests that Ku has a role in the loading of DNA-PKcs onto DNA around the DNA double strand break.

DNA-PKcs is a member of the PIKKs (phosphoinositide 3 kinase like family of protein kinases) and cells defective of the protein are highly radiosensitive [194]. The interaction between Ku and DNA-PKcs stimulates the phosphorylation of DNA-PKcs around the DNA double strand break [198]. Autophosphorylation at two clusters within the DNA-PKcs protein results in the activation of the kinase activity of the protein [198]. The autophosphorylation results in the DNA ends becoming accessible to DNA end processing factors such as Artemis [198]. The autophosphorylation may result in a conformation

change in DNA-PKcs that alters the DNA ends allowing for access from the end processing factors. Mutations within the autophosphorylation clusters results in NHEJ repair defects [198].

Once the DNA double strand break has been detected and stabilised then the next step of the NHEJ process is the processing of the DNA ends. The processing involves the removal of non-ligatable end groups by endonucleases such as Artemis. Artemis possesses 5'-3' exonuclease activity and in the presence in DNA-PKcs has endonuclease activity [199]. Artemis is phosphorylated by DNA-PKcs [200] and DNA-PKcs is required for its recruitment to DNA double strand break [201]. The removal of nucleotide at the break can create gaps that require DNA polymerases μ and λ. Both these polymerases interact with Ku [202]. After the ends have been processed they are ligated together. This process requires DNA ligase IV, which is found in a complex with XRCC4 (X-ray repair cross-complementing protein 4). XRCC4 acts as a scaffold and stabilises DNA ligase IV and stimulates it's activity [203]. XRCC4 interacts with Ku and is also phosphorylated by DNA PKcs [204].

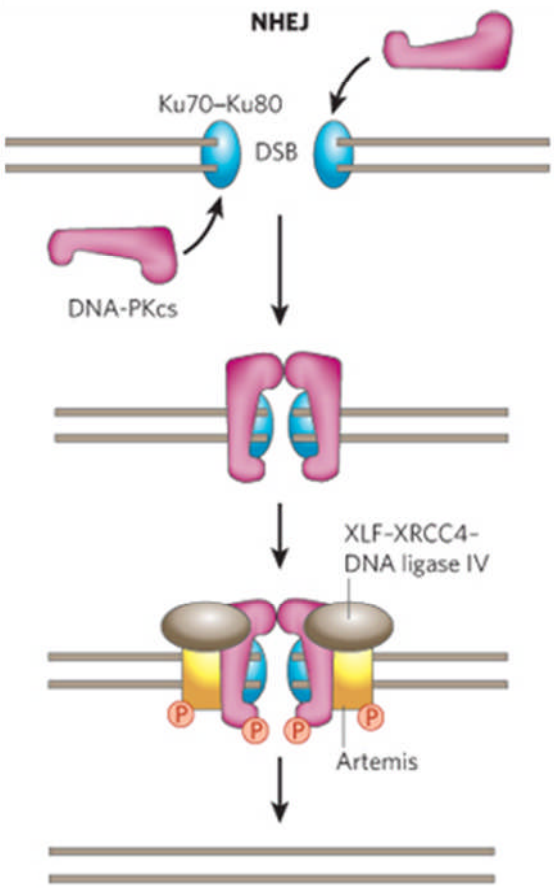

Figure 6**: Non-homologous end joining pathway of DNA double strand break repair**. *The DNA double strand break is detected and stabilised by Ku and DNA-PKcs. The endonuclease Artemis is recruited to break by DNA-PKcs and processes the ends of the breaks. The ends are ligated together by DNA ligase IV. XRCC4 acts as a scaffold for DNA ligase IV [205]. Image taken with permission from Nature Publishing Group*

Homologous Recombination

Homologous Recombination (HR) is an error free repair process of DNA double strand breaks which involves a homologous template such as the sister chromatid [205]. HR requires the MRN (Mre11, Rad50, NBS1) complex to recognise the DNA double strand break [205] (discussed later). The MRN complex then recruits the cohesin complex to the break [206] (discussed later). This step ensures the homologous template remains in close

proximity for recombination. The MRN complex also recruits and activates the ATM protein kinase [207].

The early step in processing the break involves the creation of an ssDNA containing a 3'-hydroxyl overhang. This process involves the MRN complex. In yeast deletion of the complex slows down the rate of the 5'-3' exonuclease that creates the 3'-hydroxyl end [208]. In *S.cerevisiae* the Sae2 endonuclease interacts with the MRN complex to create an intermediate DNA end [209]. The DNA double strand break is then processed by the 5'-3' exonuclease activity of Exo1 [210]. This creates the processed ends that are required for the process in yeast. In mammalian cells there are Exo1 and Sae2 homologues suggesting the process is similar in mammalian cells [210].

The ssDNA created in the processing is bound to RPA (Figure 7). This occurs to remove secondary structures from the DNA [211]. Rad51 is involved in the searching of homologous sequences and the resolution of the break. The RPA bound to the ssDNA recruits the Rad51 nucleoprotein [212]. It is believed the search for homologous sequences involves random collisions. The movement of the ssDNA Rad51 filaments may be driven by the constant association and disassociation of Rad51 from the strand [213]. It is thought that a Rad51 nucleofilament of at least 100 basepairs is required for strand exchange [214]. The chromatin remodelling complex Rad54 has been shown to be involved in strand exchange. It may move nucleosomes to allow for strand invasion [215].

The homologous DNA strand invasion involves the displacement of one strand of the homologous duplex by the invasive strand and pairing of the invasive strand with the other. This leads to the creation of a heteroduplex DNA complex called the displacement loop (D loop) (Figure 7). The D loop is extended until it finds and captures the non-invasive strand of the broken DNA. This process is called double strand break recombination (DSBR) [216]. It is unclear which polymerase is involved in the extension

of the D loop *in vivo* but Pol η can perform this function *in vitro* [217]. This process results in the formation of Holliday junctions (Figure 7). Gap filling ligation and cleavage then results in the crossover of DNA and repair of the DNA double strand breaks [216].

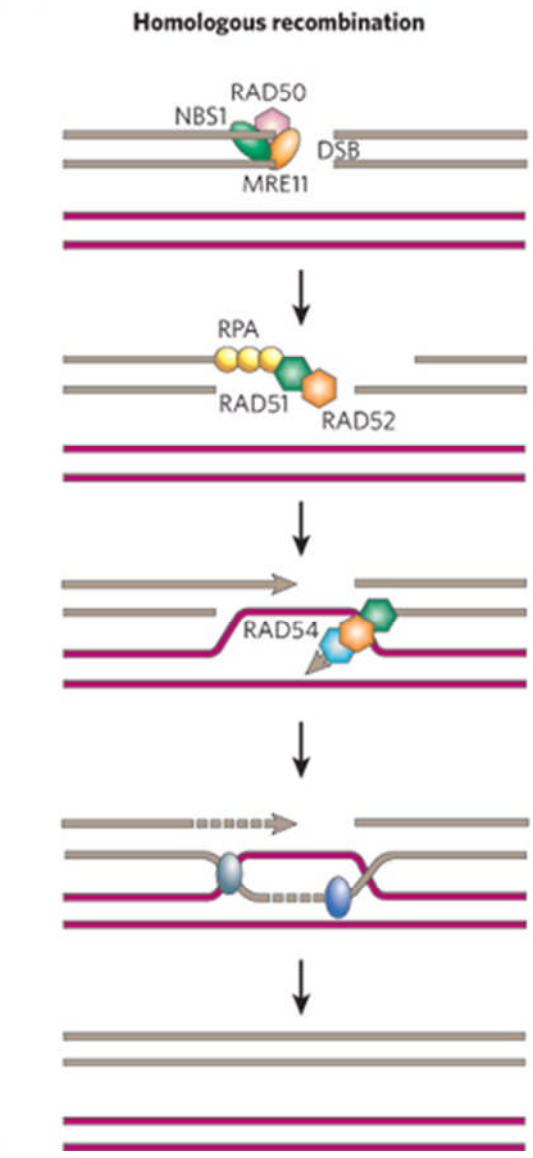

Figure 7**: Homologous recombination pathway of DNA double strand break repair.** *The DNA double strand break is recognised by the MRN complex. The early step in processing the break involves the creation of ssDNA containing a 3'-hydroxyl overhang. This process involves RPA, Rad51 and Rad52. The ssDNA then searches for homologous sequences usually from the sister chromatid. Upon discovery of the homologous sequence strand exchange occurs which involves Rad54 [205]. Image taken with permission from Nature Publishing Group.*

Nucleotide excision repair

Nucleotide Excision Repair (NER) is the process involved in the removal of DNA lesions such as minor DNA distortions produced by photoproducts and bulky adducts formed by chemical reactions with endogenous and environmental compounds. In eukaryotic cells the XPC (Xeroderma pigmentosum, complementation group C) protein acts as an initial sensor for unpaired bases [218] (Figure 8). XPC forms a heterotrimeric complex with HR23B the human homologue of Rad23 and centrin 2 [219]. The XPC-HR23B complex specifically binds to DNA with small bubble structures with or without damaged bases [219]. This suggests that XPC recognises distorted DNA and not the damaged nucleotides. The crystal structure of the *S.cerevisiae* XPC homologue Rad4 bound to DNA containing a lesion showed that Rad4 did not associate with the damaged nucleotide but recognised local destabilisation of the Watson-Crick basepairing through the insertion of a β-hairpin domain through the helix [220].

After the DNA lesion is sensed then the transcription factor II H (TFIIH) complex is recruited to the lesion [221] (Figure 8). TFIIH consists of a number of proteins including XPB, XPD, p34, p52 and p63. The crystal structure of the TFIIH shows a ring shaped structure, which encircles the DNA. As well as playing a role in NER, TFIIH is an essential factor for the synthesis of mRNA by RNA polymerase II [221]. The TFIIH complex contains two DNA helicases XPB and XPD. XPB unwinds the DNA in the 3'-5' direction and XPD unwinds in the opposite direction [222]. Strand opening around the damaged site is further stabilized by the subsequent binding of the XPA repair proteins and the single-strand DNA binding protein, RPA. XPA is a 32kDa Zinc finger protein that interacts with the TFIIH complex and it is believed that XPA is involved in the recruitment

of RNA polymerase II and RPA to the DNA lesion [223, 224]. Structural analysis of the XPA protein revealed the protein interacts with DNA that contains sharp bends [225]. This suggests that XPA binds to the DNA at the ends of the bubble and stabilises the bubble. RPA is a complex of 3 subunits (70, 32 and 14kDa) and is thought to recruit replication factors to the lesion for DNA repair synthesis [226].

This leads to the formation of a large bubble DNA structure that is excised by the endonucleases XPG and ERCC1-XPF [227]. The endonucleases are recruited to the lesion by XPA protein [228]. RPA is involved in the correct positioning of ERCC1-XPF onto the strand [229]. The XPG protein creates the incision on the 3' of the lesion and ERCC1-XPF creates an incision at the 5' end of the opening [230] (shown in Figure 8). This leads to the removal of the lesion-containing oligonucleotide of about 30 nucleotides. Using catalytically inactive mutants of both endonucleases, the XPF incision occurs first and the XPG incision is not required for the initiation of repair synthesis. This suggests the XPF incision is repaired first and this prevents the formation of single stranded DNA gaps that can disrupt genome integrity [230]. After the incisions are made two DNA polymerases Pol ε and Pol δ, and RPA are required for the gap filling DNA synthesis [231].

In bacteria the DNA lesion is recognised by UvrA and UvrB, which form a heterodimeric complex. UvrA is a homologue of XPC. UvrA probes for the presence of damage. Upon recognition of the DNA lesion UvrA disassociates with the lesion and UvrB unwinds the lesion with its limited helicase activity that is stimulated by UvrA [232]. After the unwinding of the lesion UvrB associates with UvrC which induces 3' and 5' incisions of the unpaired DNA [233].

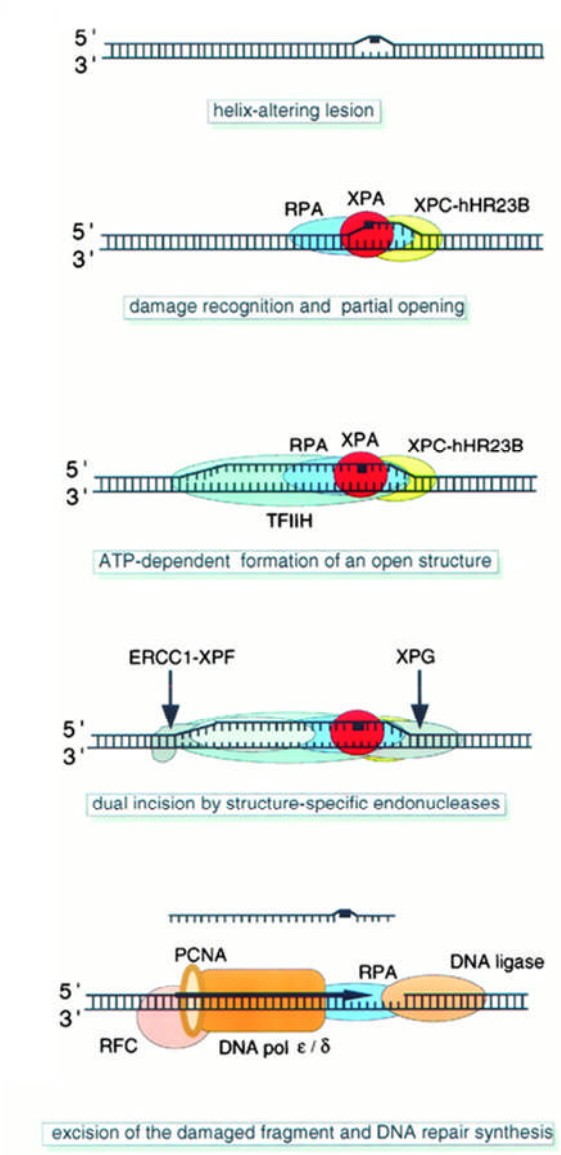

Figure 8**: Nucleotide excision repair pathway**. *The lesion is initially detected by XPC and RPA. After detection of the lesion the TFIIH complex is recruited and unwinds the DNA around the lesion. This leads to the formation of a bubble complex that is excised by the nucleases XPG and ERCC1-XPF. The gap created is filled by the DNA polymerases Pol ε and Pol δ [234]. Image taken with permission from the American Society for Biochemistry and Molecular Biology.*

The structure and function of the MRN complex

The MRN complex consists of the proteins Mre11, Rad50 and NBS1. The complex is an important factor in the response to DNA double strand breaks. It acts as a sensor of DNA

double strand breaks and activator of the repair pathway. It is believed to be involved in the HR and NHEJ repair pathways. The complex was first discovered in *S.cerevisiae*. The three proteins Mre11, Rad50 and Xrs2 (*S.cerevisiae* homologue of NBS1) were identified in a screen for genes involved in resistance to UV and X-ray induced DNA damage [235]. They were shown to associate with one other [236].

Mre11 is 70-90kDa in size and consists of an N-terminally Mg^{2+}-dependent phosphoesterase domain [237] and two DNA binding domains at the C-terminus [238]. The protein has been shown to form dimers that have DNA binding activity specifically for the synapses of DNA double strand break termini [239]. Recently the protein has been shown to have endo- and exonuclease activity to ssDNA and dsDNA [240]. This nuclease activity may have a role in the processing of the break in HR and NHEJ.

Rad50 is a 150kDa protein with structural homology to Smc proteins. The N-terminal Walker A and C-terminal Walker B nucleotide binding motifs stably associate with one another to form a bipartite ATP-binding cassette (ABC)-type ATPase domain that binds and partially unwinds dsDNA termini [82]. The intervening 575 amino acids form an anti-parallel coiled-coil that spans 500 angstroms and terminates with a zinc hook (CxxC) motif [241]. Scanning force microscopy shows that the globular heads of Rad50 associate with Mre11 at the DNA double strand breaks and the coiled-coil domains face outwards from the DNA acting as flexible arms [241]. The coiled-coil arms act to mediate interactions between sister chromatids. The zinc hooks motifs at the ends of the coiled-coil domains are important in this DNA tethering. Mutations of the zinc coordinating cysteines in Rad50 results in DNA double strand break repair defects in *S.cerevisiae* and a reduction in damage induced recombination between sister chromatids [242].

NBS1 (Nijmegen breakage syndrome 1) is a 65-85kDa protein that consists of a FHA domain (forkhead associated domain) and two BRCT domains (BRCA1 C-Terminus

binding) at the N-terminus and has an Mre11 binding domain at its C-terminus [243]. The FHA domain binds phosphorylated threonine residues present in DNA damage repair proteins such as Mdc1 (DNA damage checkpoint protein involved in ATM signalling) and Ctp1 (yeast homologue Sae2, a DNA-end processing factor) [244]. NBS1 has a role in the translocation of the MRN complex into the nucleus. Disruption of the binding between NBS1 and Mre11 results in cytoplasmic retention of Mre11 and Rad50 [245].

Recently the MRN complex has been shown to have a role in ATM signalling. Deregulation of the MRN components leads to defects in ATM signalling [246, 247] and ATM is recruited to the DNA double strand breaks through the C-terminus of NBS1 [248]. ATM is autophosphorylated after interacting with the C-terminus of NBS [248]. This autophosphorylation of ATM is essential in the activation of ATM. Depletion of NBS in *Xenopus* egg extracts results in the inactivation of ATM and the addition of the C-terminus of NBS activates ATM in NBS depleted extracts [248]. The MRN complex is also involved in ATR (ATM-Rad3 related) signalling. The nuclease activity of Mre11 contributes to the activation of ATR [249, 250].

The MRN complex has a role in early responses to DNA double strand breaks. The Mre11 dimer is thought to act as a bridge across the DNA double strand breaks, which stabilises the break. Structural analysis of the Mre11 dimer from *pyrococcus furiosus* shows that two opposed DNA ends bind within the DNA binding cleft [239]. This provides evidence that the dimer acts as a bridge between the DNA double strand break. The endonuclease activity of Mre11 may have a role in processing of the ends of the break for HR. Mutations in Mre11 that abolish the exonuclease activity causes mild repair defects in *S.pombe [239]*. Mutations that abolish the endonuclease activity however result in a severe defect in repair in *S.pombe.* The endonuclease activity of Mre11 produces a 5’-3’ excision that creates 3’ ssDNA for RPA loading and strand invasion in the HR repair pathway [239].

Rad50 has a role in stabilising the break through tethering the sister chromatid of the broken DNA that would be important in the HR repair pathway [251]. The endonuclease activity of Mre11 would create the long 3' ssDNA overhangs required for strand invasion in HR [240]. These functions of the MRN complex suggest it is involved in the repair of DNA damage through the HR repair pathways.

1.10 The role of cohesin in DNA damage responses

A role for cohesin in the DNA damage response was initially shown in *S.cerevisiae* and chicken cells. In *S.cerevisiae* repair of damage was impaired in cells with Scc1 depleted and Smc1 mutated [252]. Interestingly mutations in the cohesin establishment factors Scc2 and Pds5 caused a similar defect in DNA damage repair [252]. To confirm cohesin was required for the repair of DNA damage a Scc1 inducible system was used in *S.cerevisiae*. Scc1 expression was delayed until after S phase in *S.cerevisiae* resulting in repair defects similar to cells with depleted Scc1 protein. This suggests that sister chromatid cohesion is important in the repair process because sister chromatid cohesion is established in S phase. This idea was confirmed in cells with defects in Eco1, these cells have defects in sister chormatid cohesion in S phase but cohesin still associates with the chromosomes. These cells have defects in DNA damage repair [252]. In chicken DT40 cells the level of chromosome breaks increased in Scc1 depleted cells [253]. Scc1 was shown to promote cohesion in interphase [253] and the fact that HR plays an important role in damage induced by IR in the S/G2 phases [254] provides evidence that cohesin's role in the DNA damage response is to establish sister chromatid cohesion for the HR pathway.

The theory suggested above requires that cohesin accumulates at sites of DNA damage (Figure 9). Cohesin has been shown to be recruited to laser induced DNA damage [206]

and to gamma H2AX foci in HeLa cells and nontransformed human fibroblasts. Mre11, Rad50 and BRCA1 were all shown by immunofluorescence to be recruited to the induced damage suggesting that the cells deal with the laser induced damage *de novo*. Interestingly, cohesin was not recruited to the damage in ATLD2 cells that have mutated Mre11 suggesting that Mre11 is involved in recruitment of cohesin to sites of damage although Rad50 is also down regulated in these cells. Cohesin is still recruited to NBS deficient cells along with Mre11 and Rad50 [206]. Rad50 in the MRN complex was shown to specifically interact with cohesin subunit Smc1 and the interaction occurs in S and G_2 phase of the cell cycle [255].

The recruitment of cohesin to DNA double strand breaks was also observed in *S.cerevisiae* using ChIP [256]. The DNA double strand breaks in this assay were created using a HO endonuclease (HOmothallic switching). In this study, a region on chromosome V was analysed that Smc1 and Scc1 do not normally bind. An HO endonuclease recognition site was inserted into the genome and when the DNA double strand break was induced. Smc1 and Scc1 were recruited to the region. Smc1 and Scc1 were shown to accumulate in a region of 50kb around the DNA double strand breaks. Scc2 (required for the loading of cohesin in *S.cerevisiae*) was shown to be required for the accumulation of Smc1 as Scc2 deficient cells were unable to recruit Smc1 to the DNA double strand break created by the HO endonuclease.

The recruitment of cohesin to DNA damage requires H2AX phosphorylation [257]. In *S.cerevisiae* wild type H2AX was substituted with a mutant version of that cannot be phosphorylated. There was no accumulation of the cohesin subunit Mcd1p at sites of damage. This is a similar phenotype to that seen in *S.cerevisiae* that have Mec1 and Tel1 mutations [257]. These two kinases are needed for the DNA double strand break checkpoint response and have been shown to phosphorylate H2AX. The DNA double

strand break induced cohesin binding region correlates with the size of H2AX phosphorylation region (shown in Figure 9). Until recently, it was unclear why H2AX was phosphorylated over a large distance either side of a DNA double strand breaks but it may be phosphorylated over this large distance to recruit cohesin [257]. A recent study has shown that a phosphorylated version of cohesin is recruited to DNA double strand breaks [258]. A phosphorylated Smc1 subunit was shown to be recruited to gamma H2AX foci by immunofluorescence [258], suggesting that the cohesion complex is recruited to DNA double strand breaks through phosphorylation by kinases such as Mec1 and Tel1.

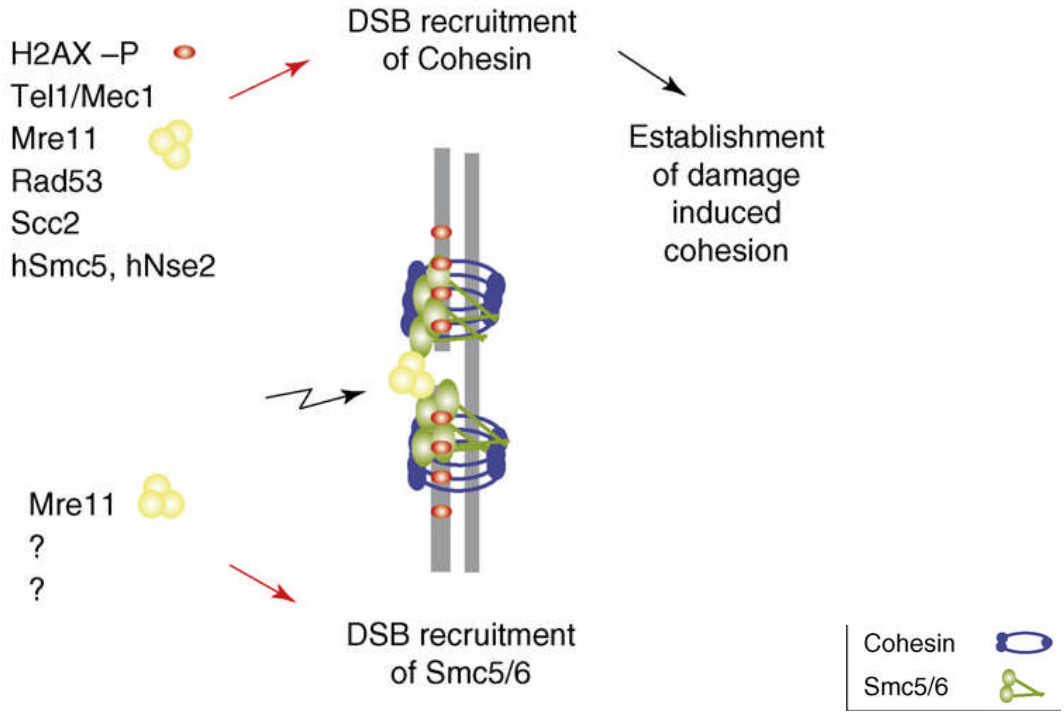

Figure 9: **Recruitment of cohesin to DNA double strand breaks** [259]. *The figure shows the recruitment of cohesin to 50kilobase regions either side of the DNA double strand break. H2AX is also shown to accumulate to 50kilobase regions around the break and is involved in the recruitment of cohesin to double strand breaks. Image taken with permission from Elsevier Ltd.*

The theory that cohesin is recruited to DNA double strand breaks to promote sister chromatid cohesion was confirmed by measuring the inter-sister chromatid distances at DNA double strand break in DT40 and U20S cells with an Sce1 restriction enzyme recognition sequence inserted into the genome. A 112 repeat tetracycline operator is positioned upstream of the recognition sequence. An expression vector encoding a tetracycline repressor-GFP was transfected into these cells and used to localise the inserted recognition sequence. Addition of the Sce1 restriction enzyme resulted in the creation of a DNA double strand break [260]. Gamma H2AX was recruited to the sites after the addition of the enzyme confirming a DNA double strand break had been created [260]. Using this assay they induced a DNA double strand break and measured the distance between the TetR-GFP spots on opposite sister chromatids in mitotic cells [260]. Creation of the DNA double strand break resulted in a reduction of the inter-sister chromatid distance around the break which suggests that cohesion is important in the repair of double strand breaks [260]. The cohesin complex is important in the creation of the damage induced cohesion because the inter-sister chromosome distance around the break was significantly larger in ATM knockdown cells compared to wildtype cells [260]. Cohesin is an ATM target in the DNA damage response and phosphorylation of cohesin is important in it’s recruitment to DNA double strand breaks [261]. The inter-sister distance between wild type and ATM knockdown cells was similar before the induction of the break.

Smc1 has been shown to be a downstream target of the ATM/NBS1 dependent S phase checkpoint pathway [261, 262]. Smc1 is phosphorylated in response to ionising radiation (IR) but this phosphorylation is disrupted in ATM deficient cells. Interestingly NBS1 and BRCA1 are required for optimal phosphorylation of Smc1 [261]. In NBS1 deficient cells Smc1 phosphorylation is defective [262]. Phosphorylation of NBS1 by ATM is required for the phosphorylation of Smc1 suggesting that NBS1 is an adaptor in this process [262].

The phosphorylation of Smc1 by ATM/NBS1 is required for the activation of the S phase checkpoint in response to IR. Phosphorylated Smc1 may act in slowing down S phase progression by associating with elongating chromosomes and thus slowing down replication fork progression [262].

Recent evidence in *C.elegans* suggests that the cohesin subunit Smc1 has a role in NER in response to UV damage. *C.elegans* with mutations in the Smc1 gene resulted in UV sensitivity [263]. Cohesin has been shown in human cells to associate with the ATP dependent chromatin remodelling complexes SWI/SNF, ISW1 and NuRD families [264]. These ATPase dependent chromatin remodelling complexes have been shown to have a role in NER. The SWI/SNF complex enhances the activity of NER at lesions located in nucleosome core regions in humans [265]. The remodelling of these regions in *S.cerevisiae* by the SWI/SNF complex is dependent on the presence of XPC, XPA and RPA. Two subunits of this complex, snf5 and 6, are co-purified with the yeast homologue of XPC [266]. ISW1 is a DEXD/H box helicase which is involved in moving the nucleosome along the DNA generating internucleosomal spaces of 50 to 60 base pairs [267]. This nucleosomal sliding enhances NER activity [268]. Mutations of these ATPase dependent chromatin remodelling complexes in *C.elegans* results in UV sensitivity [263]. These chromatin remodelling complexes may have a role in creating more accessible DNA around the lesion for the NER complex. Cohesin may act as a stabilizer for the DNA around this unstable area of DNA.

1.11 Diseases associated with mutations in cohesin and ChlR1

ChlR1 and the cohesin complex play an important role in chromosome segregation DNA damage repair and DNA replication. Mutations in the cohesin complex account for two severe syndromes Cornelia de Lange syndrome and Robert's syndrome. Mutations in ChlR1 accounts for Warsaw breakage syndrome. These syndromes are discussed below.

Cornelia de Lange Syndrome

Cornelia de Lange syndrome is a dominant genetic disorder that is characterised by growth and mental retardation, upper limb defects and microcephaly [269]. Cohesion establishment and sister chromatid cohesion are disrupted in the syndrome. The disruption in cohesion establishment and sister chromatid cohesion is mild suggesting other functions of cohesin for example the control of gene expression, are disrupted in the syndrome [269].

Around 60% of Cornelia de Lange syndrome patients have a heterozygous mutation in Nipped B homology (NIPBL) [269]. NIPBL is involved in the loading of cohesin complex onto DNA during S phase [270]. In *drosophila* Nipped B has been shown to alleviate cohesin-mediated blocking of enhancer-promoter communication. Cohesin and Nipped B co-localised to the active transcription sites [271]. Binding of cohesin to these active transcription sites is reduced in Cornelia de Lange syndrome patient and NIPBL mutant cells, resulting in the upregulation of the genes downstream of the enhancers [272]. This suggests that the phenotype seen in Cornelia de Lange syndrome patients is a result of deregulation of genes controlled by cohesin. As discussed earlier, cohesin along with

CTCF in mammalian cells contribute to the insulation of genes. This function may be defective in the patients.

Mutations in Smc1 and 3 account for 5% of the cases of Cornelia de Lange syndrome [269]. The common mutations of the Smc found in the patients were mapped onto the molecular model of these proteins. The mutations are located in the hinge domain of the protein and the coiled-coil region [273] and are believed to cause a conformation change resulting in a reduction in the proximity of the head domains that disrupts the binding of the accessory proteins such as Scc2. These effects would result in the abolishment of loading of cohesin onto chromatin [273].

Robert's Syndrome

Robert's syndrome has a number of similar characteristics to Cornelia de Lange syndrome but has quite distinct genetic differences to Cornelia de Lange syndrome. Roberts syndrome is autosomal recessive disorder in which all patients have homozygous or heterozygous mutations of Esco2 [274]. Esco2 is the human homologue of Eco1. Like Cornelia de Lange syndrome patients, Robert's syndrome patients show signs of sister chromatid cohesion defects. This is characterised by heterochromatin repulsion [275]. This suggests that Esco2 is involved in the establishment of cohesion at heterochromatin regions. The mutations in Esco2 found in Roberts syndrome patients are associated with the loss of the acetyltransferase activity of the protein [276]. Interestingly replication fork progression in Robert's syndrome cells is also disrupted. The acetylation of cohesin is important to allow for the progression of the replication fork through the complex. If the replication forks progress slower in Roberts syndrome cells then there could be an accumulation of DNA damage that may contribute to the phenotype [10].

The interesting feature of these diseases associated with the cohesin complex is that sister chromatid cohesion defects are limited. This suggests that the phenotype of these conditions is caused by the disruption of other functions of cohesin. It is hypothesised is that the role of cohesin in gene expression is disrupted in some way. This hypothesis is supported by a study in *S.cerevisae* in which the mutations in the cohesin complex and associated proteins in these diseases were reproduced. The mutations showed not effect on sister chromatid cohesion but there were defects in transcriptional control, gene silencing and sub-nuclear organization of chromatin [277].

Association of ChlR1 with Warsaw Breakage Syndrome

Warsaw breakage syndrome was defined in a male patient with severe microcephaly, pre- and post-natal growth retardation and abnormal skin pigmentation [278]. Molecular studies discovered the patient had a high level of chromosomal breaks which would have suggested Fanconi anaemia but the patient also showed abnormal cohesion of sister chromatids where chromosomes had centromeric cohesion defects and premature chromatid separation [278]. Cohesion defects are not seen in Fanconi anaemia, but are typical of Robert's syndrome as stated above. As this patient showed traits associated with both Fanconi anaemia and Robert's syndrome, candidate genes were investigated including Esco2, cohesin complex subunits and cohesion establishment factors. None of these proteins were affected in this individual. However, ChlR1 protein was barely detectable by western blot in the fibroblasts of the individual. Sequence analysis showed two mutations in the gene; a splice site mutation in intron 22 of the maternal allele and a 3 basepair deletion in exon 26 of the paternal allele. The splice mutation causes the loss of the last 10 basepair of exon 22 from the cDNA resulting in premature termination of the

polypeptide, and the 3 basepair deletion results in deletion of a highly conserved lysine residue at the extreme C-terminus of the protein for which no function has been ascribed [278]. Introduction of DDX11 cDNA into lymphoblasts rescued the abnormal phenotypes [278], confirming that the phenotypes observed in WBS cells were directly due to loss of functional ChlR1 protein.

1.12 Hypothesis and Aims

1) Interaction of ChlR1 with FHL2, a novel binding protein.

FHL2 was identified as an interacting partner of ChlR1 in a yeast two-hybrid screen. I hypothesise that ChlR1 interacts with FHL2 in mammalian cells and the transcriptional activity of FHL2 is required for the loading of cohesin and establishment of cohesion. Somewhat supporting this hypothesis, there is evidence to suggest that the loading of cohesin is linked to gene expression. In *S.cerevisiae* the cohesin complex accumulates at sites of convergent transcripts. In mammalian cells cohesin accumulates at CTCF consensus sequences. The major function of CTCF is in insulation of groups of genes that are transcriptionally co-regulated. This suggests that the loading of cohesion onto DNA is linked to gene expression and transcription.

The work in this thesis aims to confirm the interaction between ChlR1 and FHL2 in mammalian cells by co-immunoprecipitation experiments with exogenously and endogenously expressed ChlR1 and FHL2. To confirm the interaction between ChlR1 and FHL2 I aim to perform *in-vitro* binding assays with *in-vitro* transcribed radio-labelled ChlR1 and bacterially expressed FHL2. Using *in-vitro* binding assays, I also aim to define the regions of each protein involved in the interaction.

To confirm the hypothesis that FHL2 is required for the loading and establishment of cohesion I will use siRNA oligonucleotides to depleted FHL2 RNA and protein. Metaphase spreads from FHL2 depleted cells would be analysed for cohesion defects.

In addition to metaphase spread analysis of FHL2 depleted cells, ChIP analysis of a cohesin rich region of the genome would be performed in FHL2 depleted cells to confirm the hypothesis. The H19/IGF region of the genome would be used to confirm if FHL2 is involved in the loading of cohesin.

2) Elucidate the role of ChlR1 in DNA damage repair

The *S.cerevisiae* homologue of ChlR1, Chl1 has previously been shown to have a role in DNA damage repair responses. I hypothesise that ChlR1 is involved in DNA damage repair by recruiting cohesin to sites of DNA double strand breaks. Cohesin subunits are recruited to double strand breaks and depletion of these subunits results in repair defects.

I aim to confirm that ChlR1 functions in the repair of DNA damage using siRNA specific for ChlR1 to deplete ChlR1. The comet assay would be used to analyse the repair of DNA damage in cells depleted of ChlR1.

To confirm that ChlR1 is recruited to sites of DNA double strand breaks I will use immunofluorescence with an antibody specific for gamma-H2AX. This allows for visualisation of the DNA double strand breaks and using a mCherry-ChlR1 fusion protein, I will investigate the recruitment of ChlR1 to DNA double strand breaks.

In addition to immunofluorescent analysis of ChlR1 localisation, a ChIP assay to detect the presence of ChlR1 on the DNA surrounding a DNA double strand break will be used to investigate my hypothesis. A U20S derived cell line with an SceI restriction endonucloease recognition sequence inserted into the genome will be used in the ChIP assay. There are no

SceI recognition sequences found in the human genome therefore the inserted recognition sequence is unique. This means that the restriction enzyme would only create one DNA double strand break. Primers will be designed to anneal to the DNA upstream of the SceI restriction site. If this upstream region of DNA is immunoprecipitated with a ChlR1 specific antibody, then it can be concluded ChlR1 associates with the regions of DNA around a DNA double strand break.

This cell line will also be used to confirm the recruitment of cohesin subunits to the DNA double strand breaks by ChIP assay. If this upstream region of DNA is immunoprecipitated with a cohesin subunit antibody, then I could conclude that cohesin associates with the regions around the DNA double strand break.

Furthermore, the U20S/SceI cell line described above will be used to confirm the hypothesis that ChlR1 is required for the recruitment of cohesin to double strand breaks. If ChlR1 is depleted in the cell line, does this result in the disruption of the recruitment of cohesin to DNA double strand breaks?

3) The function role of ChlR1 in DNA replication

There is evidence in the literature that suggests a role for ChlR1 in DNA replication. ChlR1 interacts with a number of replication fork proteins (Mcm7, PCNA, Fen1 and TopBP1). Furthermore a number of other cohesin establishment factors (Esco1/2 and Ctf18) have been previously shown to be located at replication forks. A number of DNA helicases that are highly related to ChlR1 (FANCJ and RecF) also have roles in DNA replication.

The loading of cohesin onto DNA occurs after telophase. This means that replication forks must pass through at least one cohesin associated region during S phase during the next

cell cycle. Therefore I hypothesise is that ChlR1 is required for the passage of the replication fork through cohesin complexes.

I aims are to confirm that ChlR1 is involved in DNA replication using siRNA oligonucleotides to deplete ChlR1. The DNA combing assay will then be used to analyse the replication of DNA in cells depleted of ChlR1.

To confirm that ChlR1 associates with newly replicated DNA I will use a reverse ChIP assay. This involves the immunoprecipitation of BrdU incorporated DNA and the detection of associated proteins (PCNA and ChlR1) by western blot using specific antibodies for the proteins.

Materials and Methods

2.1 Transformation of *E.coli* with plasmid DNA

2µl of ß-mecaptoethanol was added to 50µl of chemically component *E.coli* (Stratagene XL-10 ultra) and incubated for 10 minutes. The required amount of plasmid DNA was added to the *E.coli* and incubated on ice for 30 minutes. The *E.coli* were heat shocked at 42ºC for 30 seconds and incubated on ice for 2 minutes. 950µl of Luria Broth (LB) was added to the *E.coli* and incubated at 37ºC shaking at 220 rpm for 1 hour. 100µl of this culture was spread on an LB agar plate with 100µg/ml of required antibiotic. The plates were incubated overnight at 37ºC to allow the colonies to grow.

2.2.Purification of plasmid DNA from *E.coli*

Colonies of transformed *E.coli* were picked and incubated overnight in 5ml of LB containing 100µg/ml of required antibiotic at 37ºC shaking at 220 rpm. The *E.coli* were harvested by centrifugation at 14000 rpm for 1 minute in a bench top centrifuge (Eppendorf 5415c). Following the protocol for the Qiagen mini/maxi preparation kit the plasmids were purified from the *E.coli*. The plasmid DNA purity and concentration was then analysed using the NanoVue spectrophotometer (GE healthcare).

2.3 Proteins Expression in *E.coli*

Colonies of BL21 (DE3) *E.coli* were grown up in 5ml of Luria Broth (LB) containing 100µg/ml of required antibiotic overnight at 37ºC shaking at 220 rpm. 10ml of LB was inoculated with 0.5ml of the overnight culture and grown at 37ºC shaking at 220rpm until the optical density (OD) of the culture read 0.5 at a wavelength of 600nm. A 1ml aliquot taken from the culture was centrifuged at 14000 rpm for 1 minute in a bench top centrifuge (Eppendorf 5415c) and the pellet frozen at -20ºC for future analysis. The remainder of culture was induced with 1mM of IPTG. The cultures were grown for a further 4 hours at 37°C. 1ml aliquots were taken from the culture, centrifuged at 14000 rpm for 1 minute in a bench top centrifuge (Eppendorf 5415c) and the pellet frozen at -20ºC. The collected pellets were lysed in 100µl of 2x SDS loading buffer (100mM Tris pH 6.8, 4% SDS, 0.2% bromophenol blue, 20% glycerol and 200mM DTT) and the proteins separated on an SDS-PAGE gel to analyse the expression of the recombinant protein.

2.4 Nickel Affinity Protein Purification

BL21 (DE3) *E.coli* were grown up in 75ml of Luria Broth (LB) containing 100µg/ml of required antibiotic overnight at 37ºC shaking at 220 rpm. 250ml of LB was inoculated with 15ml of the overnight culture and grown at 37ºC shaking at 220rpm until the optical density (OD) of the culture read 0.5 at a wavelength of 600nm. A 1ml aliquot taken from the culture was centrifuged at 14000 rpm for 1 minute in a bench top centrifuge (Eppendorf 5415c) and the pellet frozen at -20ºC for future analysis. The remainder of the culture was induced with 1mM IPTG and grown at 37ºC for 4 hours as described above. A

1ml aliquot taken from the culture was centrifuged at 14000 rpm for 1 minute in a bench top centrifuge (Eppendorf 5415c) and the pellet frozen at -20ºC for future analysis.

The culture was harvested by centrifugation at 6000 rpm for 15 minutes in a Beckman J-21B centrifuge using the JA-10 rotor. The cell pellet was re-suspended in 20ml of ice cold Nickel A buffer (25mM Tris-HCl pH 8.0, 500mM NaCl, 5mM DTT plus protease inhibitors (Sigma)). 1ml of re-suspended solution was removed for analysis by SDS PAGE. The re-suspended cells were sonicated (60% amplitude. 3x 1 minute bursts) and centrifuged for 30 minutes at 18500 rpm in a Beckman J2-MC centrifuge using the JA-20 rotor. 1ml of supernatant was taken for analysis by SDS PAGE. 0.5ml of Nickel beads previously equilibrated in Nickel A buffer was added to the supernatant and incubated on a roller for 1 hour at room temperature. The beads were centrifuged at 2000 rpm for 5 minutes in an Eppendorf 5403 bench top centrifuge and collected. 1ml of supernatant was taken for analysis by SDS PAGE. The beads were washed twice in 30ml 95% Nickel A buffer plus 5% Nickel B buffer (Nickel A plus 500mM imidazole). 1ml of each wash was removed for analysis by SDS PAGE. The proteins were eluted with 6x 1ml fractions of 80% Nickel A buffer and 20% Nickel B buffer. Analysis of fractions was performed by SDS PAGE.

2.5 GST Affinity Protein Purification

BL21 (DE3) *E.coli* were grown up in 75ml of Luria Broth (LB) containing 100µg/ml of required antibiotic overnight at 37ºC shaking at 220 rpm. 250ml of LB was inoculated with 15ml of the overnight culture and grown at 37ºC shaking at 220rpm until the optical density (OD) of the culture read 0.5 at a wavelength of 600nm. A 1ml aliquot taken from the culture was centrifuged at 14000 rpm for 1 minute in a bench top centrifuge

(Eppendorf 5415c) and the pellet frozen at -20ºC for future analysis. The remainder of the culture was induced with 500mM IPTG and grown at 37ºC for 4 hours as described above. A 1ml aliquot taken from the culture was centrifuged at 14000 rpm for 1 minute in a bench top centrifuge (Eppendorf 5415c) and the pellet frozen at -20ºC for future analysis.

The culture was harvested by centrifugation at 6000 rpm for 15 minutes using the Beckman J-21B centrifuge and the pellet re-suspended in NETN buffer (100mM NaCl, 20mM Tris-HCl pH 8.0, 1mM PMSF, 1mM $ZnCl_2$, 0.1% NP40 AND 0.1% ß-mercaptoethanol). The re-suspended cells were sonicated (60% amplitude 3x 1 minute). 1ml of re-suspended solution was removed for analysis by SDS PAGE. The remaining solution was centrifuged for 30 minutes at 18500rpm in a Beckman J2-MC centrifuge using the JA-20 rotor. 1ml of supernatant was taken for analysis by SDS PAGE and the remaining supernatant was discarded. The cell pellet was re-suspended in 4ml of 8M urea containing 1% triton. This mixture was sonicated (60% amplitude 3x1 minute) and 30mls of NETN buffer was added and centrifuged at 18500rpm for 30 minutes in a Beckman J2-MC centrifuge using the JA-20 rotor. 1ml of supernatant was taken for analysis by SDS PAGE and 0.5ml glutathione agarose beads (previously equilibrated in NETN buffer) was added to the remaining supernatant. The beads and supernatant were incubated on the roller for 1 hour at room temperature. The beads were then harvested by centrifugation at 2000 rpm for 5 minutes in an Eppendorf 5403 bench top centrifuge and washed twice with 30ml of NETN buffer. The beads were then re-suspended in 1ml NETN buffer and the presence of bound protein analysed by SDS PAGE.

2.6 GST Affinity Protein Purification- 'Double Lysis' Method

Rosetta DE3 *E.coli* (Novagen) were grown up in 75ml of Luria Broth (LB) containing 100µg/ml of required antibiotic overnight at 37ºC shaking at 220 rpm. 250ml of LB was inoculated with 15ml of the overnight culture and grown at 37ºC shaking at 220rpm for 8 hours. The *E.coli* were induced with 1mM IPTG and grown at 30ºC shaking at 220rpm overnight.

The culture was harvested by centrifugation at 6000 rpm for 15 minutes in the Beckman J-21B centrifuge using the JA-10 rotor and the pellet re-suspended in lysis buffer (50mM Tris-HCl pH 8, 25mM NaCl, 2mM EDTA, 0.2mM DTT and 10µg/ml PMSF). The re-suspended cells were frozen in liquid nitrogen and thawed at 37ºC in a water bath. Lysosyme (4000 unit re-suspended in water) was added and incubated for 1 hour at 30ºC in the water bath. The solution was sonicated (60% amplitude. 2x 30 second bursts) and 0.5% streptomycin (re-suspended in 70% ethanol) added. This solution was centrifuged at 4°C for 15 minutes at 5000 rpm (Eppendorf 5403 bench top centrifuge). The supernatant was retained for SDS-PAGE analysis. The cell pellet was re-suspended in lysis buffer. The re-suspended cells were frozen in liquid nitrogen and thawed at 37ºC in a water bath. Lysosyme was added and incubated for 1 hour at 30ºC in a water bath. The solution was sonicated (60% amplitude. 2x 30 second burst) and 0.5% streptomycin added. The solution was centrifuged for 15 minutes at 5000 rpm (Eppendorf 5403 bench top centrifuge). 1ml of supernatant was taken for analysis by SDS PAGE and 0.5ml glutathione agarose beads (previously equilibrated in lysis buffer) was added to the remaining supernatant and incubated on the roller for 1 hour at room temperature. The beads were then harvested by centrifugation at 2000 rpm for 15 minutes in an Eppendorf 5403 bench top centrifuge and washed twice with 30ml lysis buffer. A small sample of the beads was collected for

analysis on the SDS PAGE. 50mM glutathione (resuspended in lysis buffer) was added to the remaining beads and incubated for 30 minutes to remove the protein from the beads. The beads were centrifuged for 15 minutes at 5000rpm (Eppendorf 5403 bench top centrifuge) and the supernatant collected. This supernatant was analysed by SDS PAGE.

2.7 PCR Reactions

DNA was amplified in a PCR reaction containing DNA template (50ng), Taq reaction buffer (Sigma), dNTP (1mM), Forward primer (10pmol), Reverse Primer (10pmol) (Primers listed in table), 2.5% DMSO and 10 units of Taq polymerase (Sigma). The thermal cycle profile of the reaction included an initial denaturing step of 95ºC for 1 minute followed by 30-40 amplification cycles that included 95ºC for 30 seconds, 52-57ºC annealing for 30 seconds and 72ºC elongation for 1 minute. Following these cycles there was a final 10 minute 72ºC elongation step.

Primer Name	Primer Sequence
Sce1 cut site	5'-cattaccctgttatccctaggatc-3'
Sce1 ChIP forward	5'-ataggccgaaatcggca-3'
Sce1 ChIP reverse	5'-gagctccaattcgccctatag-3'
HA FHL2	5'-cgggatccatgtatccatatgacgtcccagactacgccatgactgagcgct-3'
FHL2 Forward	5'-cgggatccatgactgagctttgactac-3'
FHL2 Reverse	5'-cggaattctcagatgtctttcccacagtcggg-3'
ChlR1 RT PCR forward	5'-gtgctagggggggaacattaagcaa-3'
ChlR1 RT PCR reverse	5'-gcgacccacctcgtccatcatctga-3'
Actin Ex 3 Forward	5'-caggaaggaaggctggaaga-3'
Actin Ex 3 Reverse	5'-gctgtgctatccctgtacgc-3'
ChlR1 mCherry Forward	5'-ggcctcgaggcatggctaatgaaacagaagg-3'
ChlR1 mCherry Reverse	5'-gcgaagctttcaggaagaggccgacttctc-3'

Table 1: *Shows the sequences of primers used in PCR reactions*

2.8 Restriction Digestion

Digestion of 1µg of DNA in a 20µl reaction required 16µl of sterile deionized water, 2µl of 10X restriction enzyme buffer (Promega), compatible for the restriction enzyme, 0.5µl of 10µg/µl acetylated BSA and 0.5µl of 10 units/µl restriction enzyme (Promega). This reaction is then incubated at 37°C for 2 hours.

2.9 Ligation of DNA

Ligation of DNA fragments into DNA vector backbones was performed at a ratio of 3:1 vector to insert. The conversion of molar ratio to mass ratio was performed using the calculation below.

$$\frac{\text{ng of vector} \times \text{kb size of insert}}{\text{kb size of vector}} \times \text{molar ratio of } \frac{\text{insert}}{\text{vector}} = \text{ng of insert}$$

To the calculated amounts of insert and vector DNA 2µl of 10X ligase buffer (Promega), 1 unit of T4 DNA ligase enzyme and nuclease free water was added to a final volume of 20µl. The reaction was then incubated at 4°C for 16-18 hours.

2.10 DNA Electrophoresis

1% agarose was added to 1x TBE (Sigma T3913) and boiled until the agarose was melted into the solution. Ethidium bromide (Sigma E1510) at a concentration of 0.5µg/ml was added to the agarose solution and the solution poured into the casting apparatus (50ml into Agagel mini electrophoresis apparatus (Biometra 02-000)). The appropriate comb was

inserted into the molten solution. The solution was left at room temperature for 30 minutes to solidify.

DNA samples were prepared for loading by adding 1x DNA loading dye (Bioline BIO-37045). The comb was removed from the set gel and the gel was then placed into the electrophoresis tank. 1x TBE buffer was added to a level just covering the gel (200mls for the Agagel mini). 5µl of molecular weight ladder (Hyperladder IV (Bioline)) was loaded into one of the wells to visualise the separation of the DNA. The DNA samples including loading dye were loaded into the remaining wells. The gel was run at 30mA for 1 hour. After this period the gel was removed and the DNA imaged under UV light (GeneGenius (Syngene)).

2.11 Reverse Transcriptase-PCR

The RNA required for this method was extracted following the Qiagen RNeasy extraction kit protocol. Extracted RNA was quantified using the NanoVue spectrophotometer.

The synthesis of the cDNA was carried out using an AffinityScript qPCR cDNA synthesis kit. Following the instructions the following reactions were set up; 45ng random primers, 1 unit of AffinityScript RT/RNase block enzyme, 1x mastermix (containing $MgCl_2$ and dNTPs), 0.5µg RNA and ultra pure water to 20µl.

The thermal cycle for the cDNA synthesis included a 25ºC primer annealing step for 5 minutes, a 42ºC cDNA synthesis step for 15 minutes and a 95ºC termination step for 5 minutes. The cDNA was then added to a standard PCR reaction as described above.

2.12 Antibody Purification

Initially 150µl of peptide was diluted in 3ml of coupling buffer (0.1M Na_2CO_3, 0.5M NaCl, Tris-HCl pH 8.3). Then 3ml of gel solution was equilibrated in 8ml coupling buffer and centrifuged at 2000 rpm in a bench top centrifuge (Eppendorf 5403) for 5 minutes. The supernatant was removed and the diluted peptide was added to the gel solution in a 1.5ml Falcon tube. This solution was incubated for 15 minutes at room temperature on a roller. The solution was then transferred to a column and incubated for 30 minutes at room temperature to allow the resin to settle.

After the incubation the liquid was allowed to drain through the column slowly, without allowing the column to dry out. The column was then washed with 6ml of coupling buffer. 2ml of 50mM cysteine dissolved in coupling buffer was then added to the column and incubated on the roller at room temperature for 15 minutes. The column was again placed in an upright position for 30 minutes. The cysteine solution was then drained from the column. The column was washed with 12ml of 1M NaCl. Finally the column was washed with 4ml PBS containing 0.05% sodium azide.

The column was stored overnight at 4ºC. The column was equilibrated to room temperature then washed with 6ml of PBS. 2ml of clarified rabbit serum (containing antibodies) was diluted in 8ml of PBS and added to the column. The solution was allowed to drain slowly from the column, 3 times. The column was washed in 12ml PBS. The antibody was eluted with 8ml of 150mM glycine pH 2.5, which was added to the column and collected in 1ml fractions. These fractions were neutralised with 200µl 1M Tris pH 8.8. The fractions were then analysed by SDS-PAGE.

2.13 Routine Cell Culturing

Cell lines were grown at 37ºC in a humid environment of 5% CO_2 (within a HERA Cell incubator (Thermo)). The different cell lines and growth mediums are shown in the table 2. The cells were passaged by the removal of the growth medium, washing with PBS and detaching the cells by incubating with trypsin at 37ºC for 5 minutes. Growth medium was added to stop the reaction and an appropriate amount of cells seeded into a fresh dish.

Cell Lines	Growth Medium	Provider
HeLa	DMEM [+]L-Glutamine, Glucose (Invitrogen 41965-039) 10% Foetal Bovine Serum 1% penicillin/streptomycin	
HEK 293	DMEM [+]L-Glutamine, Glucose 10% Foetal Bovine Serum 1% penicillin/streptomycin	Dr Simon Powis University of St Andrews
hTERT-RPE1	DMEM F-12 [+] L-Glutamine (Invitrogen 11320-074) 10% Foetal Bovine Serum 1% penicillin/streptomycin	
U20S TET O/R Clones	DMEM [+]L-Glutamine, Glucose 10% Foetal Bovine Serum 1% penicillin/streptomycin 0.4mg/ml G418 (Roche 04727878001)	Dr Ciaran Morrison University of Galloway

Table 2: *Shows the human cell lines used in the study and the growth media used.*

2.14 Cell Counting

Cells were counted using a haemocytometer (Bright line counting chamber (Hausser Scientific). An 10µl aliquot of cells suspended in growth medium was applied under the haemocytometer coverslip. The number of cells within the central 1mm x 1mm square grid

was counted using a phase contrast light microscope. The cell count in the grid was multiplied by 10^4 to represent the number of cells per ml.

2.15 Cryopreservation and thawing

Logarithmically growing cells were harvested by trypsination as described above. $1x10^6$ cells were resuspended in 1ml of growth medium containing 10% DMSO. This solution was added to freezing vials which were placed in a 'Mr Freezy' box containing isopropanol at -80ºC overnight. The vials were then transferred to liquid nitrogen for long-term storage.

The cells were thawed rapidly at 37ºC in a water bath and the 1 ml cell suspension was added to a 10cm dish. 9mls of growth medium was added to the dish. The growth medium was changed after 24 hours.

2.16 Cell Synchronisation

Cells were synchronised in S phase by double thymidine block. Cells were plated and incubated at 37ºC 5% CO_2 for 8 hours. 2mM thymidine (final concentration) was added to the growth medium and the cells were incubated at 37ºC, 5% CO2 for 16 hours. The thymidine was then removed with 2 washes of PBS and the cells incubated in growth medium at 37ºC 5% CO2 for 8 hours. 2mM thymidine was then added to the growth medium and the cells were incubated again at 37ºC, 5% CO2 for 16 hours. The thymidine was removed with 2 washes of PBS and the cells collected for flow cytometry analysis.

Cells were synchronised in G_1 phase by serum starvation. Cells were plated and incubated at 37ºC, 5% CO2 for 8 hours. The growth medium was removed and replaced with growth

medium containing no serum. The cells were then incubated at 37ºC, 5% CO2 for 16 hours. After serum starvation the cells were collected for flow cytometry analysis.

2.17 Calcium Phosphate Transfection

To make the calcium phosphate precipitate, 10μg of DNA was mixed with 250μl of 0.25M $CaCl_2$. Then 250μl of 2xBBS (50mM BES, 280mM NaCl and 1.5mM $NaHPO_4$) was added drop wise whilst bubbling air through the mixture. The precipitate was incubated for 20 minutes at room temperature. The precipitate was added to $1x10^6$ cells plated in a 10 cm tissue culture dish the previous evening. The cells were incubated overnight at 37ºC, 5% CO_2. The growth medium was then removed and the cells washed twice with PBS. Fresh growth medium was added and the cells were incubated at 37ºC, 5% CO_2 for 24 hours before harvesting.

2.18 Fugene Transfection

A ratio of 3μl of Fugene (Roche) reagent to 1μg of DNA was required for efficient transfection. 21μl of Fugene was added to 79μl serum free growth medium and the mixture vortexed for 1 second. The mixture was incubated at room temperature for 5 minutes. 7μg of DNA was then added to the mixture, which was then incubated for a further 20 minutes at room temperature. The mixture was added to $0.5\text{-}1x10^6$ cells plated in 10cm tissue culture dishes the previous evening. The cells were incubated for 24 hours at 37°C, 5% CO_2 before harvesting.

2.19 siRNA Transfection

$1x10^5$ cells were plated in each well of a 6 well plate. The cells were incubated at 37ºC, 5% CO_2 for 4 hours. For each transfection 5µl of Dharmafect transfection reagent (ThermoSci) was added to serum free growth medium (to make a total volume of each reaction to 200µl) and an appropriate volume of siRNA (siRNA sequences in table 3) added to a final volume of 100µl of serum free growth medium. These solutions were incubated at room temperature for 5 minutes and then mixed. The mixtures were incubated at room temperature for 20 minutes. The cells were washed twice with medium containing serum and 1.7ml of medium added to each well. The siRNA mixtures were added to the growth medium. The cells were incubated at 37ºC 5% CO_2 for 24 hours.

Description of siRNA	DNA Target Sequence (5'-3')
ChlR1 nt212 siRNA	AAGACTTCATGGCAGAGCTGT
5' ChlR1 siRNA	GGAAGGGCAGACTGGTGAATT
3' ChlR1 siRNA	AGTCACTCCTTCAGTAGAATT
FHL2 siRNA	GAAACTCACTGGTGGACAATT

Table 3: *Shows the sequences of the siRNA oligonucleotides used.*

2.20 Immunoprecipitation

Cells were harvested by trypsinisation and re-suspended in 300µl of freshly prepared lysis buffer (50mM Tris-HCl pH 7.4, 100mM NaCl, 20mM NaF, 10mM KH_2PO_4, 1% Triton X-100, 0.1mM DTT, 10% Glycerol, 1% Protease Inhibitors) and vortexed. The lysed cells were incubated on ice for 30 minutes and sonicated (50% amplitude. 2x 10 second bursts). The lysates were then centrifuged at 14000 rpm at 4ºC for 15 minutes in an Eppendorf 5415c bench top centrifuge. Protein G sepharose beads (Sigma P3296) were prepared by washing twice in 1ml of binding buffer (50mM Tris-HCl pH 7.4, 100mM KCl, 0.1mM

EDTA, 0.2% NP40, 0.1% BSA, 2.5% Glycerol, 2mM DTT, 1% Protease Inhibitors). The clarified cell lysates were then mixed 1:1 with binding buffer, 5µl of antibody (list of antibodies used in table 4) and 10µl of Protein G slurry. The reactions were incubated overnight on roller at 4ºC. The beads were washed 3 times with 1ml wash buffer (100mM Tris-HCl pH 7.4, 100mM NaCl, 0.5% NP40, 2mM DTT, 1% Protease Inhibitors). The beads were prepared for analysis by adding 1x SDS loading buffer and boiling for 5 minutes. The protein complexes were separated by SDS PAGE and the presence of bound protein detected by western blot.

Antibody (Source)	Use
ChlR1 2774 (Rabbit)	Precipitate endogenous ChlR1
FLAG (Mouse, Sigma)	Precipitate FLAG tagged FHL2
Smc1 (Rabbit, Abcam)	Precipitate endogenous Smc1
HA (Mouse, 12CA5 cells, ATCC)	Negative control

Table 4: *Shows the antibodies used in the immunoprecipitation assays and their purpose in these experiments.*

2.21 Western Blotting

Electrophoresis

The gel casting apparatus was assembled and the separating gel (1.5M Tris-HCl pH 8.8, 10% Acrylamide-bis, 1% SDS, 1% ammonium persulphate and 0.1% TEMED) was poured to within 1cm of the gel comb. 70% ethanol was added on top of the gel to remove air bubbles and the gel incubated at room temp for 30 minutes to polymerise. After polymerisation the ethanol was poured off and the stacking gel (1M Tris-HCl pH 6.8, 5% Acrylamide-bis, 1% SDS, 1% ammonium persulphate and 0.1% TEMED) added and incubated at room temperature for 20 minutes. After the stacking gel had polymerised the comb was removed and the wells washed with water. The gel cassette was then placed in

the electrophoresis chamber. The chamber was filled with running buffer (125mM Tris-HCl pH 8.3, 1.25M glycine and 0.1% SDS).

30µg of protein sample with SDS loading buffer (300mM Tris-HCl pH 6.8, 12% SDS, 0.2% bromophenol blue, 60% glycerol and 600mM DTT) added at a ratio of 6:1 was heated to 100ºC for 5 minutes and then loaded into the appropriate wells. A prestained protein marker (peqGOLD Protein Marker V (Peqlab)) was loaded to visualise the separation of the proteins. The lid was attached to the electrodes and the whole rig then connected to a power supply. Electrophoresis was then carried out at 30mA until sufficient protein separation was achieved.

Blotting

The PVDF membrane (Roche 03 010 040 001) was activated in methanol for 10 seconds. The gel, PVDF membrane, filter paper and filter pads were equilibrated for 10 minutes in transfer buffer (125mM Tris-HCl pH 8.3, 1.25M glycine and 5% methanol). The gel sandwich was prepared on the black panel of the cassette in the following sequence: filter pad, filter paper, inverted gel with ladder on right hand side, PVDF membrane, filter paper and filter pad. The cassette was placed into the transfer tank and immersed in transfer buffer. The blotting rig was connected to a power supply and blotted at 400mA for 1 hour.

Immunodetection

After blotting the membrane was rinsed in water and stained with Ponceau S solution to ensure correct protein transfer. A rocking platform was used for the remaining steps. The stain was removed by washing the membrane with TBS/T (10mM Tris pH 7.6, 150mM

$NaCl_2$ and 1% Tween 20). The membrane was blocked in blocking buffer (5% non-fat dry milk in TBS/T) overnight at 4ºC. After blocking the membrane was incubated in primary antibody solution (antibody diluted in blocking buffer) for 1-3 hours at room temperature. The membrane was washed 4x15 minutes in TBS/T and then incubated with blocking buffer containing horseradish peroxidise conjugated secondary antibody for 1 hour at room temperature. The membrane was washed 4x15 minutes in TBS/T and detected using ECL chemiluminescent reagent (Pierce) and the Fujifilm LAS-3000 digital detection system.

2.22 Alkaline Comet Assay

Fully frosted microscope slides (Surgipath 00280) were covered with 300µl of molten 1% normal melting point agarose (Thistle Scientific) and covered with 22x50mm coverslips. The agarose was allowed to solidify and then the coverslips were removed. $5x10^3$ cells were re-suspended in 75µl of 0.75% low melting point agarose (Sigma) and spread onto the first agarose layer with a 22x50mm coverslip. This was then left to solidify on ice. The coverslips were removed and the slides irradiated on ice with gamma radiation in a ^{137}Cs gamma – irradiator. The slides were incubated in growth medium at 37°C, 5% CO_2 for an appropriate time to allow for the cells to repair the damaged DNA. The slides were immersed in freshly prepared neutral lysis buffer (2.5M LiCl, 10mM Tris-HCl pH 8, 0.03% EDTA, 0.1% LiDS; heated at 37ºC to dissolve, 0.003mg/ml fresh Proteinase K added before use) and incubated overnight at 37ºC. The slides were removed from neutral lysing solution and immersed in freshly prepared cold alkaline lysing buffer (2.5M NaCl, 100mM EDTA, 10mM Tris-HCl pH 10, 1% fresh Triton X-100 added before use) and incubated at 4ºC for 1 hour. The slides were removed from the alkaline lysing buffer, drained and placed in a horizontal electrophoresis tank (BDH maxi horizontal

electrophoresis unit) side by side with the gaps filled with blank slides. The tank was filled with fresh electrophoresis buffer (0.3M NaOH, 1mM EDTA) to a level just covering the slides. The slides were left in the solution for 40 minutes to allow the unwinding of the DNA before electrophoresis 20 minutes at 300mA. After electrophoresis the slides were drained, placed on a tray and washed with three changes of neutralisation buffer (0.4M Tris-HCl pH 7.4) for 5 minutes each wash. The slides were washed with PBS for 5 minutes. The DNA was stained with 40µl of 1µg/ml propidium iodine in PBS (Invitrogen), covered with a 22x22mm coverslip and incubated for two hours at 4°C. The comets were viewed using a Zeiss Axiovision 2 epifluorescence microscope fitted with a TRITC filter set and analysed with Comet IV software.

2.23 Neutral Comet Assay

Fully frosted microscope slides were covered with 300µl of molten 1% normal melting point agarose and covered with a 22x50mm coverslips. The agarose was allowed to solidify and then the coverslips removed. $5x10^3$ cells were re-suspended in 75µl of 0.75% low melting point agarose (Sigma) and spread onto the first agarose layer with a coverslip. These were then left to solidify on ice. The coverslips were then removed and the slides irradiated on ice with gamma radiation in a ^{137}Cs gamma – irradiator. The slides were incubated in growth medium at 37°C, 5% CO_2 for an appropriate time to allow for the cells to repair the damaged DNA. The slides were immersed in freshly prepared neutral lysis buffer (2.5M LiCl, 10mM Tris-HCl pH 8, 0.03% EDTA, 0.1% LiDS, 0.003mg/ml Proteinase K, 5µg/ml RNase A) and incubated overnight at 37ºC. The slides were removed from neutral lysis buffer and immersed in freshly prepared cold alkaline lysis buffer (2.5M NaCl, 100mM EDTA, 10mM Tris-HCl pH 10, 1% Triton X-100) and incubated at 4ºC for

1 hour. The slides were removed from the alkaline lysis buffer, drained and placed in a horizontal electrophoresis tank side by side with the gaps filled with blank slides. The tank was filled with fresh neutral electrophoresis buffer (300mM sodium acetate, 100mM Tris-HCl, pH 8.3) to a level just covering the slides. The slides were left in the solution for 40 minutes before electrophoresis for 30 minutes at 200mA. After electrophoresis the slides were drained and washed with PBS twice. The DNA was stained with 40µl of 1µg/ml Propidium Iodide in PBS, covered with a 22x22mm coverslip and incubated for two hours at 4°C. The comets were viewed using a Zeiss Axiovision 2 epifluorescence microscope fitted with a TRITC filter set and analysed using Comet IV software

2.24 Immunocytochemistry

Cells were grown on 22x22mm coverslips (VWR 631-0124). The cells were pre-extracted with PBS (containing 80mM PIPES pH 6.8, 5mM EGTA, 1mM $MgCl_2$ and 0.1% Trition-X-100) for 30 seconds then incubated in fixing buffer PBS (containing 80mM PIPES pH 6.8, 5mM EGTA, 1mM $MgCl_2$, 4% Formaldehyde) for 1 minute. The cells were rinsed with PBS and then fixed in 4% formaldehyde (Sigma) for 10 minutes at room temperature. The cells were rinsed twice in PBS and permeabilised in 0.2% Trition-X-100 (Sigma) for 10 minutes at room temperature. After which the cells were rinsed twice in PBS. The cells were blocked in PBS (containing 1% BSA and 0.2M glycine) rocking at 20 rpm for 1 hour. After blocking the cells were incubated with 50µl of PBS (containing 0.5% BSA) containing primary antibodies at a dilution of 1:50 for $1^1/_2$ hours at room temperature. The cells were washed with PBS (containing 0.5% BSA) rocking at 20 rpm for 1 hour. Secondary antibodies were applied at a dilution of 1:150 in 50µl of PBS (containing 0.5% BSA) and incubated at room temperature for $1^1/_2$ hours in the dark. The cells were then

washed 4 x with PBS rocking at 20 rpm for 1 hour in the dark and stained with Hoechst 33342 at a dilution of 1:1000 in PBS for 20 minutes in the dark. The coverslips were washed in PBS twice and then mounted onto slides (VWR 631-0112) with Prolong Gold (Invitrogen) and stored at 4ºC. Cells were imaged using a Leica TCS SP2 confocal microscope.

2.25 Chromosomal Spreads

Cells were incubated with 100ng/ml colcemid (Gibco 15210-057) diluted in growth medium for 2 hours. Cells were then harvested and swelled in 7mls of hypotonic buffer (0.8% sodium citrate) for 10 minutes at room temperature. Cells were fixed in 7mls of Carnoy's fixative (75% methanol, 25% glacial acetic acid) for 10 minutes at 4ºC. The cells were centrifuged at 2000 rpm for 5 minutes in an Eppendorf 5403 bench top centrifuge. The Carnoy's fixative step was repeated and the cell pellet resuspended in 300µl of the Carnoy's fixative reagent. Spreads were prepared by dropping (from a height of 20cm) suspended cells onto slides tilted at an angle of 20º and allowed to air dry at room temperature. Slides were then stained with 1mg/ml propidium iodide in PBS for 30 minutes in the dark. The slides were washed twice with PBS and mounted with Prolong Gold (Invitrogen) and stored at 4ºC.

2.26 PI/Phospho-H3 staining for flow cytometry

Cells were harvested and centrifuged at 1000 rpm for 5 minutes in an Eppendorf 5403 bench top centrifuge. The cell pellets were then resuspended in 3mls of 1% formaldehyde in PBS while vortexing and incubated at room temp for 20 minutes. The cells were

centrifuged at 1000 rpm for 5 minutes in an Eppendorf 5403 bench top centrifuge and the pelleted cells were re-suspended in 3mls of 70% ethanol while vortexing and stored at 4ºC overnight. The ethanol was removed after centrifugation of the cells at 1000rpm for 5 minutes. 3mls of incubation buffer (PBS containing 0.5% BSA) was added to the cell pellets and then centrifuged at 1000 rpm for 5 minutes. The supernatant was removed and 98µl of incubation buffer including 2µl of H3 Alexa 488 conjugated antibody (Cell Signaling #9708) was added to the incubation buffer and incubated at room temperature in the dark for 1 hour. After the incubation 3mls of incubation buffer was added to the cells and centrifuged at 1000 rpm for 5 minutes. The supernatant was removed and the cells were resuspended in 0.5ml staining solution (PBS containing 0.5% BSA, 50µg/ml propidium iodide (Sigma) and 5µg/ml RNase (Sigma)). The cells were incubated in this solution for 30 minutess at room temperature and analysed using a FACSscan flow cytometer (Becton-Dickinson).

2.27 DNA Combing

Cells were grown in 6cm dishes and treated with 50µM IdU (Sigma I7125-5G resuspended in 1N ammonium hydroxide at 50mg/ml stock concentration) diluted in growth medium for 30 minutes at 37ºC, 5% CO_2. The plates were washed twice with HBSS (Invitrogen). Hydroxyurea (HU) (Sigma) at a concentration of 10µM was added to the growth medium and incubated for 2 hours at 37ºC, 5% CO_2. The plates were washed twice with HBSS. The cells were then treated with 50µM CIdU (Sigma C6891-100MG resuspended in 1N ammonium hydroxide at 20mg/ml stock concentration) for 30 minutes at 37ºC, 5% CO_2. The plates were washed twice with HBSS and the cells harvested and centrifuged at 1000rpm for 5mins in an Eppendorf 5403 bench top centrifuge. The cell pellets were

resuspended with 0.5ml of PBS. 5µl of the cell suspension was pipetted onto a glass slide (pre-washed with 70% ethanol). 10µl of spreading buffer (0.5% SDS in 200mM Tris-HCl pH 7.4 and 50mM EDTA) was added to the droplet of cells and incubated at room temperature for 10 minutes. The solution was allowed to run along the slides by tilting the slide at a 15° angle for 30 seconds. The slides were air dried at room temperature before being fixed in 3:1 methanol/acetic acid solution (stored at -20ºC) at room temperature for 2 minutes. The slides were air dried before being stored overnight at 4ºC.

The slides were then incubated in 2.5M HCl for 30 minutes at room temperature and rinsed with PBS 3 times followed by incubation in PBS-T (0.1% Trition-X-100 and 1% BSA in PBS) for 1 hour. After blocking the slides were incubated with rat anti-BrdU at 1/100 (Abcam ab6326; recognizes CIdU) and mouse anti-BrdU at 1/100 (Becton Dickinson 347580; recognizes IdU) diluted in PBS-T for $1^1/_2$ hour and then rinsed 3 times in PBS. The slides were then incubated with goat anti-mouse FITC conjugated antibody (Invitrogen) at 1/300 and goat anti-rat Alexa Fluor 594 conjugated antibody (Invitrogen) at 1/300 in PBS-T for $1^1/_2$ hour in the dark. The slides were rinsed 3 times with PBS and air dried being before mounted with Prolong Gold (Invitrogen P36930) and viewed with a Leica TCS SP2 confocal microscope.

2.28 Chromatin Immunoprecipitation

Cells growing in 10cm tissue culture dishes were fixed with 1% formaldehyde (Sigma F8775) diluted in the growth medium for 10 minutes at room temperature. The cells were then washed and then 125mM glycine was added to the growth medium for 5 minutes at room temperature to quench any residual formaldehyde. The cells were then washed twice with ice cold PBS and harvested by adding 1 ml of lysis buffer (50mM Tris-HCl pH 8,

10mM EDTA, 1% SDS, 1µg/µl BSA and 100µg/ml salmon sperm DNA (Invitrogen AM9680)) to the plate and scraped into 1.5ml tubes. The cells were incubated in the lysis buffer for 1 hour at room temperature. The cells were centrifuged at 13000 rpm for 5 minutes at room temperature in an Eppendorf 5415c bench top centrifuge. The supernatant was removed and 1ml of sonication buffer (200mM NaCl, 50mM Tris-HCl pH 8, 10mM EDTA, 0.1% SDS, 1µg/µl BSA and 100µg/ml salmon sperm DNA) was added to the extracts. The extracts were incubated in sonication buffer for 1 hour at room temperature. The samples were sonicated (40% amplitude, 3x 30 second bursts) and then centrifuged at 13000 rpm for 5 minutes at room temperature in an Eppendorf 5415 bench top centrifuge. 300µl of the supernatant was added to 15µl of Dynabeads ((Invitrogen 14311D) equilibrated in DBP (350mM NaCl, 50mM Tris-HCl pH 8, 5mM EDTA, 0.5% NP40 and 100µg/ml salmon sperm DNA)) and incubated with the appropriate antibody in 0.5ml DBP overnight at 4ºC. The beads were washed with 0.5ml low salt buffer (20mM Tris-HCl pH 8, 150mM NaCl, 0.1% SDS, 2mM EDTA, 0.5% Trition-X-100) then high salt buffer (20mM Tris-HCl pH 8, 500mM NaCl, 0.1% SDS, 2mM EDTA, 0.5% Trition-X-100) and finally LiCl wash buffer (10mM Tris-HCl pH 8, 250mM LiCl, 1mM EDTA, 0.5% NP-40). The beads were washed with TE buffer (10mM Tris-HCl pH 8, 1mM EDTA) twice. The protein-DNA complexes were eluted from the beads with 100µl elution buffer (1% SDS, 100mM $NaHCO_3$) incubated at room temperature for 30 minutes. The beads were centrifuged at 2000rpm for 1 minute and the supernatant collected. 0.2M NaCl was added to the supernatant and incubated at 65ºC overnight to reverse the cross-links. The samples were allowed to cool to room temperature before 10mM EDTA, 40mM Tris-HCl pH 6 and an appropriate volume of H_2O was added to each sample. RNase was added to the samples and incubated for 1hour at 37ºC. Proteinase K was then added to the samples and incubated for 1 hour at 50ºC.

To precipitate the DNA 200µl of TE and 400µl of phenol-chloroform was added to each sample. The samples were vortexed and then spun at 13000 rpm for 5 minutes at 4ºC in an Eppendorf 5415 bench top centrifuge. The top layer of the phenol extract was collected. The remaining phenolic layer (bottom) of the extract was used for back extraction. 200µl of TE was added and the sample was vortexed and centrifuged at 13000rpm for 5 minutes at 4ºC. The top layer was again removed and added to the first extract. To the extracted aqueous layer, 2µl of glycogen, $1/10^{th}$ the volume of 3M sodium acetate and 1 volume of isopropanol was added. This solution was incubated at -80ºC for 1 hour and centrifuged at 13000rpm for 15 minutes in an Eppendorf 5415 bench top centrifuge. The supernatant was removed and the DNA pellet washed with 70% ethanol followed by a 100% ethanol wash. The pellet was allowed to dry at room temperature and resuspended in 20µl of ultra pure H_2O.

2.29 Reverse Chromatin Immunoprecipitation

Cells growing in 10cm tissue culture dishes were fixed with 1% formaldehyde (Sigma F8775) diluted in the growth medium for 10 minutes at room temperature. The cells were then washed with PBS and then 125mM glycine was added to the growth medium for 5 minutes at room temperature to quench the residual formaldehyde. The cells were then washed twice with cold PBS. The cells were harvested by adding 1 ml of lysis buffer (50mM Tris-HCl pH 8, 10mM EDTA, 1% SDS, 1µg/µl BSA and 100µg/ml salmon sperm DNA (Invitrogen AM9680)) to the plate and the cells scraped into 1.5ml tubes. The cells were incubated in the lysis buffer for 1 hour at room temperature. The cells were centrifuged at 13000 rpm for 5 minutes at room temperature in an eppendorf 5415c bench top centrifuge. The supernatant was removed and 1ml of sonication buffer (200mM NaCl,

50mM Tris-HCl pH 8, 10mM EDTA, 0.1% SDS, 1µg/µl BSA and 100µg/ml salmon sperm DNA) was added to the extracts. The extracts were incubated in sonication buffer for 1 hour at room temperature. The samples were sonicated (40% amplitude, 3x 30 second bursts). The samples were centrifuged at 13000 rpm for 5 minutes at room temperature in an Eppendorf 5415 bench top centrifuge. 300µl of the supernatant was added to 15µl of Dynabeads ((Invitrogen 14311D) equilibrated in DBP (350mM NaCl, 50mM Tris-HCl pH 8, 5mM EDTA, 0.5% NP40 and 100µg/ml salmon sperm DNA)) and incubated with the appropriate antibody in 0.5ml DBP overnight at 4ºC. The beads were washed with 0.5ml low salt buffer (20mM Tris-HCl pH 8, 150mM NaCl, 0.1% SDS, 2mM EDTA, 0.5% Trition-X-100) then high salt buffer (20mM Tris-HCl pH 8, 500mM NaCl, 0.1% SDS, 2mM EDTA, 0.5% Trition-X-100) and finally LiCl wash buffer (10mM Tris-HCl pH 8, 250mM LiCl, 1mM EDTA, 0.5% NP40). The beads were washed with TE buffer (10mM Tris-HCl pH 8, 1mM EDTA) twice. The protein-DNA complexes were eluted from the beads with 100µl elution buffer (1% SDS, 100mM $NaHCO_3$) incubated at room temperature for 30 minutes. The beads were centrifuged at 2000 rpm for 1 minute in an Eppendorf 5415 bench top centrifuge and the supernatant collected. 0.2M NaCl was added to the supernatant and incubated at 65ºC overnight to reverse the cross-links.

The proteins in the sample were concentrated by TCA precipitation. $1/5^{th}$ the volume of 40 % trichloroacetic acid was added to the protein samples and incubated for 1 hour at 4ºC. The samples were centrifuged at 13000 rpm for 5 minutes in an Eppendorf 5415c bench top centrifuge. The supernatant was removed and 200µl of cold acetone was added to the protein pellets. The samples were centrifuged at 13000 rpm for 5 minutes. The acetone wash was repeated twice. The pellets were dried at 95ºC for 10 minutes. Sample buffer was added to the protein pellets, which were then boiled for 20 minutes and analysed by SDS-PAGE.

Results

Chapter 3: A Novel Interacting Partner of ChlR1

The identification of novel protein interactions can provide invaluable information about protein functions. A yeast two-hybrid screen was used to indentify ChlR1 interacting partners. FHL2 was isolated as an interacting partner in the screen. FHL2 accounted for 6 independent clones out of 15 postive hits (Parish, unpublished). This suggests that the interaction between ChLR1 and FHL2 was not a false positive result.

FHL2 is a protein of 279 amino acids in length and consists of four and a half LIM domains [279]. LIM domains are protein structural domains that consist of two zinc finger domains separated by two amino acid residues [279]. LIM domains mediate protein protein interactions. FHL2 has no enzymatic activity but acts as a scaffold protein mediating protein-protein interactions [279].

3.1 The Functions of FHL2

Transcription regulation

FHL2 has been shown to stimulate transcription through the β-catenin pathway. Beta-catenin is a binding partner of E-cadherin in cell-cell adherens junctions and is a key effector in the Wnt signalling pathway involved in embryogenesis and oncogenesis [280]. β-catenin is a transcriptional activator it binds to the transcriptional factors T-cell factor and lymphoid enhancer factor and is thought to regulate gene expression in response to Wnt signalling [281]. The activation of transcription of Wnt responsive genes is achieved

through the formation of a transcriptional complex in which TCF provides the DNA binding domain and beta catenin provides the transcriptional activation domain [282]. β catenin recruits CBP/p300 to the Wnt responsive genes and it acts as a protein scaffold for the assembly of a transcriptional complex [283]. CBP/p300 possess acetyltransferase activity and acetylates transcription factors including ß-catenin [284]. FHL2 increases acetylation of β-catenin by interacting with CBP/p300 which in turn increases the binding of β-catenein to TCF [280]. FHL2 interacts with a number of other proteins that are involved in protein acteylation and deacetylation including SIRT1 and FOXO [279]. This maybe important in protein function regulation (eg regulation of the function of ChlR1).

There are a number of downstream targets of β-catenin including c-myc, cyclin D and interleukin-8 (IL-8) [285]. β-catenin has been shown to interact with FHL2 *in vitro* and *in vivo* [286]. FHL2 was shown to co-operate with β-catenin to activate T-cell factor and lymphoid enhancer factor transcription as well activate the promoters of cyclin D and IL-8 [286].

Another transcription pathway stimulated by FHL2 is the cAMP response element-binding protein (CREB) pathway. The CREB protein is a well characterized transcription factor within the basic leucine zipper (bZIP) family [287]. In response to various stimuli such as growth factors, neurotransmitters, stress signals and other agents that elevate intracellular cAMP or Ca^{2+} levels, CREB is activated through phosphorylation at Ser133 and/or nuclear translocation of transducer of regulated CREB activity (TORC) coactivators [288]. The activation of CREB turns on the transcription of more than 5000 target genes, including proto-oncogenes such as c-*fos* and cell cycle regulatory genes such as cyclin A1 and cyclin D2 [289, 290]. FHL2 has also been shown to act as an direct activator of the CREB transcription pathway upon binding to CREB [291].

Cell Cycle Regulation

FHL2 associates with the cyclin D1 promoter. This suggests that cyclin D is a direct target of FHL2 [292]. FHL2 deficient mouse embryonic fibroblasts were found to express half the normal amount of cyclin D1 [280]. Interestingly a number of other G_1/S regulators were down regulated in FHL2 deficient fibroblasts including cyclin E and E2F transcription factors [292]. Proteins involved in the G_2/M transition are also down regulated including cyclin B1 and Cdc25A. Consistent with the lower rate of proliferation in these FHL2 deficient cells there is also a down regulation of components of the replication machinery MCM, RPA subunits, and Cdc45L [292]. An *in vitro* interaction between FHL2 and Mcm7 has also been demonstrated [293].

DNA damage responses

There is a possible role for FHL2 in the cellular responses to DNA damage. FHL2 expression increases in human peripheral blood lymphocytes after the induction of DNA damage through irradiation in a linear dose-expression relationship [294]. Furthermore the increased expression of FHL2 in response to radiation is stimulated by p53 [295]. It is suggested that FHL2 is a direct transcriptional target of p53 because five potential p53 target sites were identified in the promoter region of the DRAL gene, which encodes the FHL2 protein. In support of this, over-expression of wild type p53 in Rhabdomyosarcoma (RMS) cells increased the transcription of DRAL and the increase in FHL2 expression after the induction of DNA damage only occurs in cells with wild type p53 present [295]. Finally in U2OS cells it has been shown that FHL2 translocates to the nucleus after UV radiation treatment in a complex with E4F1 which is a ubiquitin ligase [296]. E4F1

associates with p53 and stimulates the ubiquitylation of p53 [297]. This results in post-transcriptional modification of p53.

A further link to a role of FHL2 in DNA damage repair and cancer development is the association of FHL2 with BRCA1 [298]. Mutations in BRCA1 account for 40-50% of hereditary breast cancers [299]. BRCA1 is shown to have functions in DNA damage repair. BRCA1 deficient cells are sensitive to IR due to defects in oxidative DNA damage and double strand break repair through HR [300]. BRCA1 also interacts with a number of DNA damage repair proteins including RAD51 [301] and the MRN complex [302]. DNA damage repair kinases such as ATR and ATM have been shown to phosphorylate BRCA1 [303]. The interaction between FHL2 and BRCA1 was confirmed by yeast two-hybrid, *in-vitro* GST pull down and *in vivo* co-immunoprecipitation. BRCA1 was shown to enhance the transcriptional activity of FHL2 suggesting that FHL2 is a downstream effector of BRCA1 [298]. When the BRCA1 binding sites in FHL2 were abolished by site directed mutagensis, the transcriptional activity of FHL2 was reduced. The same effects were seen in BRCA1 defective cells [298]. Furhtermore, FHL2 mRNA levels are down regulated in many breast cancer cell lines and this may be due to mutated BRCA1 [298]. Interestingly as discussed above FHL2 has a role in the induction of apoptosis therefore FHL2 along with BRCA1 may be involved in regulation of cancer cell growth. However the functional significance of the interaction between FHL2 and BRCA1 is not understood.

Possible Functions of the Interaction Between ChlR1 and FHL2

The interaction between FHL2 and ChlR1 was first shown in a yeast two-hybrid screen (Parish, unpublished). There are a number of possible roles for this interaction. One

possible function of this protein interaction is to facilitate the establishment of cohesion during DNA replication. ChlR1 has been shown to function in the establishment of cohesion during DNA replication. FHL2 is important in the transcriptional regulation of cell cycle genes involved in replication and the progression of cells into mitosis. Therefore FHL2 may have a role in the regulation of cohesion establishment and mitosis. In addition FHL2 may have a role in the regulation of the de/acetylation of ChlR1 through its association with FOXO, CBP/p300 and SIRT1

3.2 Aims and Hypotheses

Hypothesis

FHL2 interacts with ChlR1 in mammalian cells and this interaction is important in the establishment of cohesion and subsequent progression through mitosis.

Aims

To confirm this hypothesis I aimed to:

1) Confirm the interaction between ChlR1 and FHL2 in mammalian cells by co-immunoprecipitation and *in vitro* by GST-pull down assay with purified ChlR1 and FHL2.
2) Assay the effect of FHL2 depletion on sister chromatid cohesion by analysis of metaphase spreads.

3.3 *In Vivo* Analysis of ChlR1 interaction with FHL2

To confirm the interaction between ChlR1 and FHL2 *in vivo*, co-immunoprecipitation experiments were performed. An antibody specific for endogenous ChlR1 was required for

these experiments. Therefore the first step was to purify ChlR1 antibodies from serum extracted from rabbits inoculated with a ChlR1 peptide (amino acids 120-136). Antibody purification was performed as described in the materials and methods.

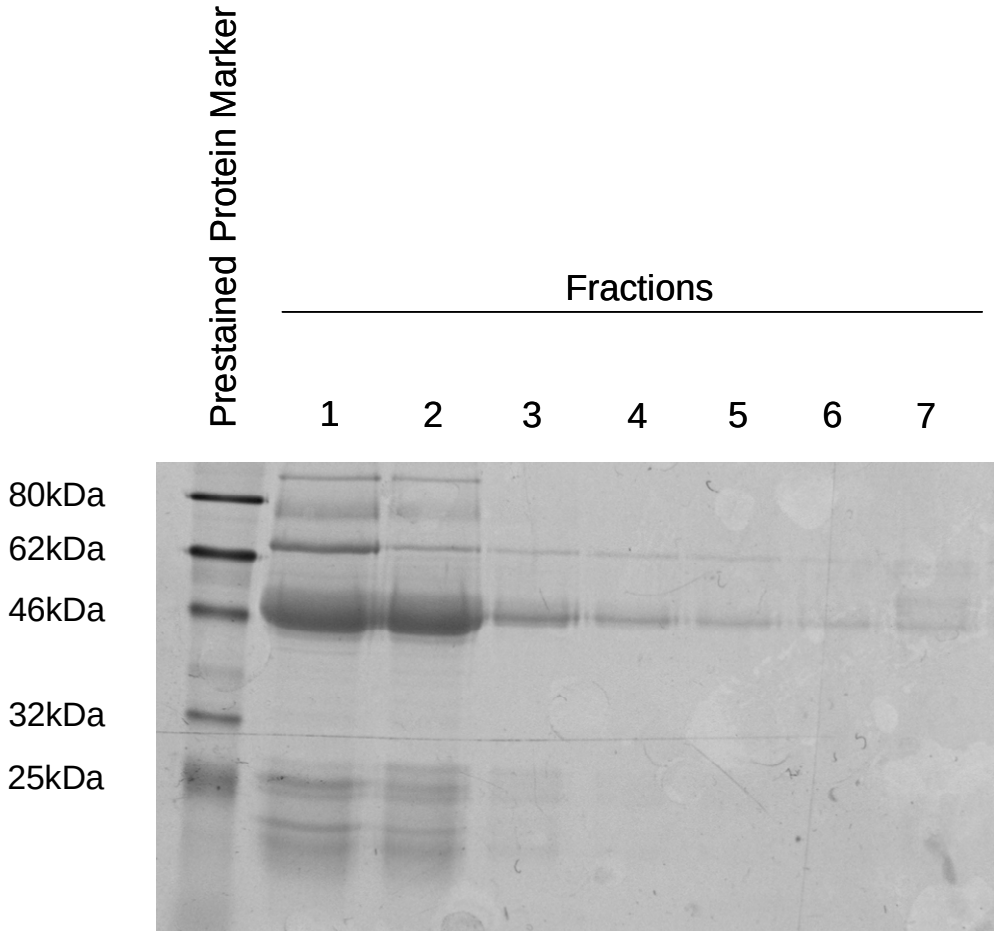

Figure 10: **Elution fractions following affinity purification of rabbit anti-ChlR1 serum**. *Serum from rabbits inoculated with ChlR1 peptide (amino acids 120-136) was passed through a column coupled with the same peptide. The bound antibody was then eluted with 150mM glycine pH 2.5. Eluted 1ml fractions were collected, and 10µl aliquots of each fraction were separated by SDS PAGE and stained with Coomassie. Bands of 55KDa corresponding to the heavy chains of the antibody are present in all the fractions. Bands of 20KDa corresponding to the light chains of the antibody are present in fractions 1 and 2.*

The majority of the antibody was eluted in fractions 1 and 2, and these fractions contain both the light (25kDa) and heavy (50kDa) chains. Therefore these fractions were tested for

their ability to detect endogenous and exogenously expressed ChlR1 by western blot. Lysates from HeLa cells transfected with FLAG-ChlR1 and ChlR1 specific siRNA were separated by SDS PAGE and proteins detected by western blot using affinity purified ChlR1 antibody at increasing dilutions (Figure 11).

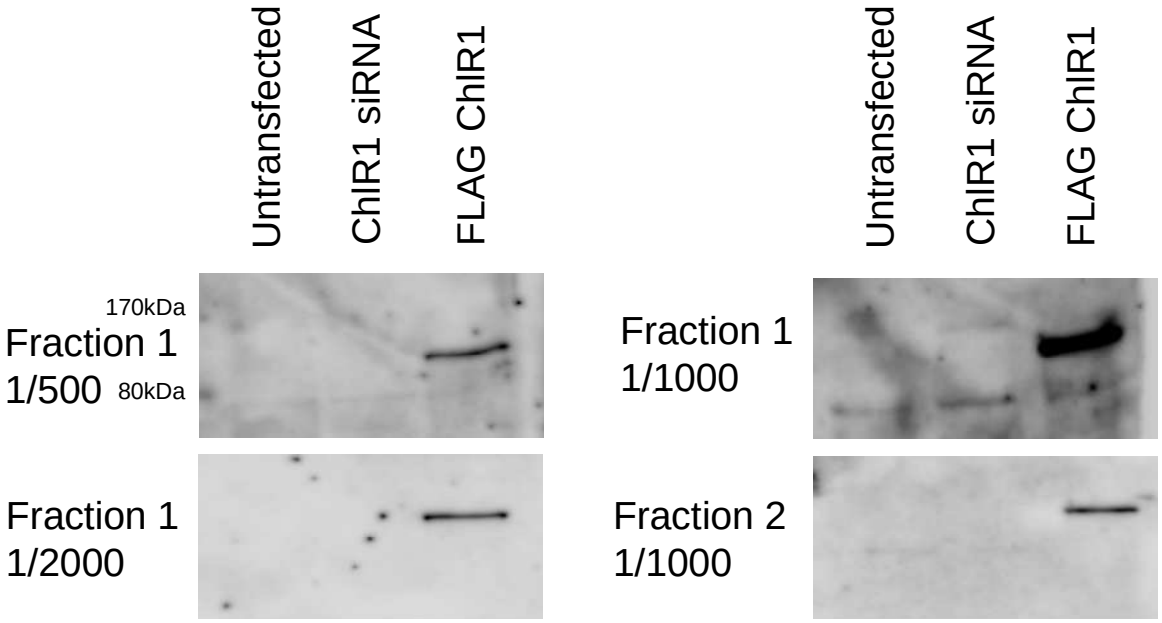

Figure 11: **Characterisation of affinity purified rabbit anti-ChlR1 antibody**. *HeLa cells were transfected with 10µg of FLAG-ChlR1 or 50nM of siRNA specific for ChlR1. Lysates from these transfected cells were separated by SDS PAGE and proteins detected by western blot using fractions 1 and 2 of the affinity purified rabbit anti-ChlR1 antibody at different concentration. A band of 110KDa corresponding to the predicted molecular mass of FLAG-ChlR1 is detected in the all of the FLAG-ChlR1 transfected samples using both antibody fractions. Bands corresponding to endogenous ChlR1 are seen in the untransfected, siRNA transfected and FLAG transfected samples in the 1/1000 dilution of fraction 1.*

Fraction 1 of the affinity purified antibody appears to detect both endogenous ChlR1 and FLAG-ChlR1 at a concentration of 1/1000 (Figure 11). However, since ChlR1 protein is still detectable in the siRNA transfected cell lysate it was not possible to confirm that the band of 100 kDa in the 1/1000 fraction 1 blot corresponds to endogenous ChlR1. This could be due to inefficient depletion of ChlR1 in this experiment. However, since the

affinity purified antibody in fraction 1 recognised FLAG-ChlR1 with high affinity, this fraction was used in the subsequent immunoprecipitation experiments.

The next step in optimising the immunoprecipitation experiments was to test the expression levels of exogenously expressed FLAG-FHL2 in transiently transfected cells. Two expression vectors that express either N-terminally (NF) or C-terminally (CF) FLAG tagged-FHL2 from the pCDNA3 vector backbone were transfected into HEK 293 cells using the calcium phosphate transfection method. HEK 293 cells were used in these experiments because of their high levels of endogenous ChlR1 [172]. Cells were transfected with 10µg of each FHL2 expression plasmid as described in the materials and methods. Figure 3 shows that both constructs express well in the cell line using this transfection method.

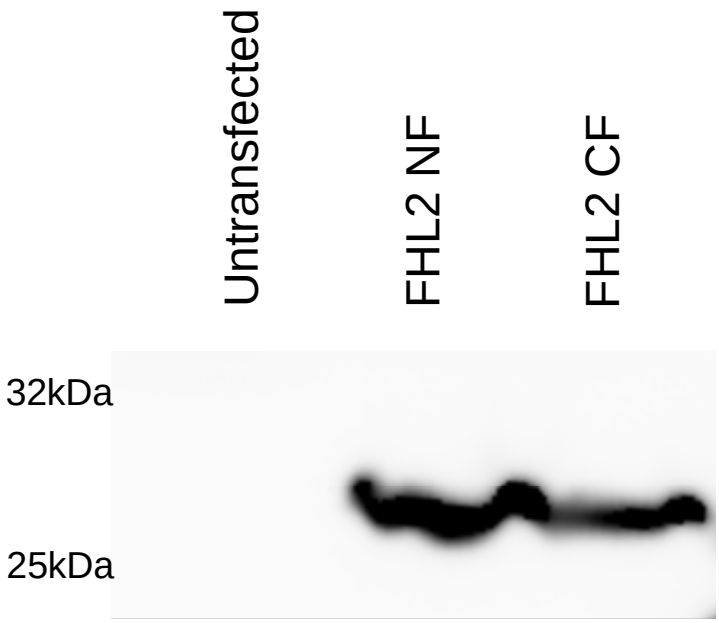

Figure 12: **Calcium phosphate precipitation transfection of FHL2 NF and CF in HEK 293 cells**. *HEK 293 cells were transfected with 10µg of FHL2 NF or CF expression vector and incubated for 48 hours. Mouse anti-FLAG antibody diluted 1:5000 was used to detect FHL2 expression by western blot. A band of 32 kDa corresponding to the predicted molecular mass of FLAG-FHL2 was expressed in the FHL2 NF and CF lanes.*

Both the FHL2-NF and -CF expression constructs efficiently expressed FHL2 in HEK 293 cells, therefore I continued with the co-immunoprecipitation experiments (Figure 12). N- and C-terminally FLAG-tagged FHL2 were used in the experiment to eliminate the possibility that the FLAG epitope in a specific region of the protein may disrupt the interaction with ChlR1. The first co-immunoprecipitation experiment involved the immunoprecipitation of endogenous ChlR1 and subsequent detection of exogenously expressed FLAG-FHL2 by western blot.

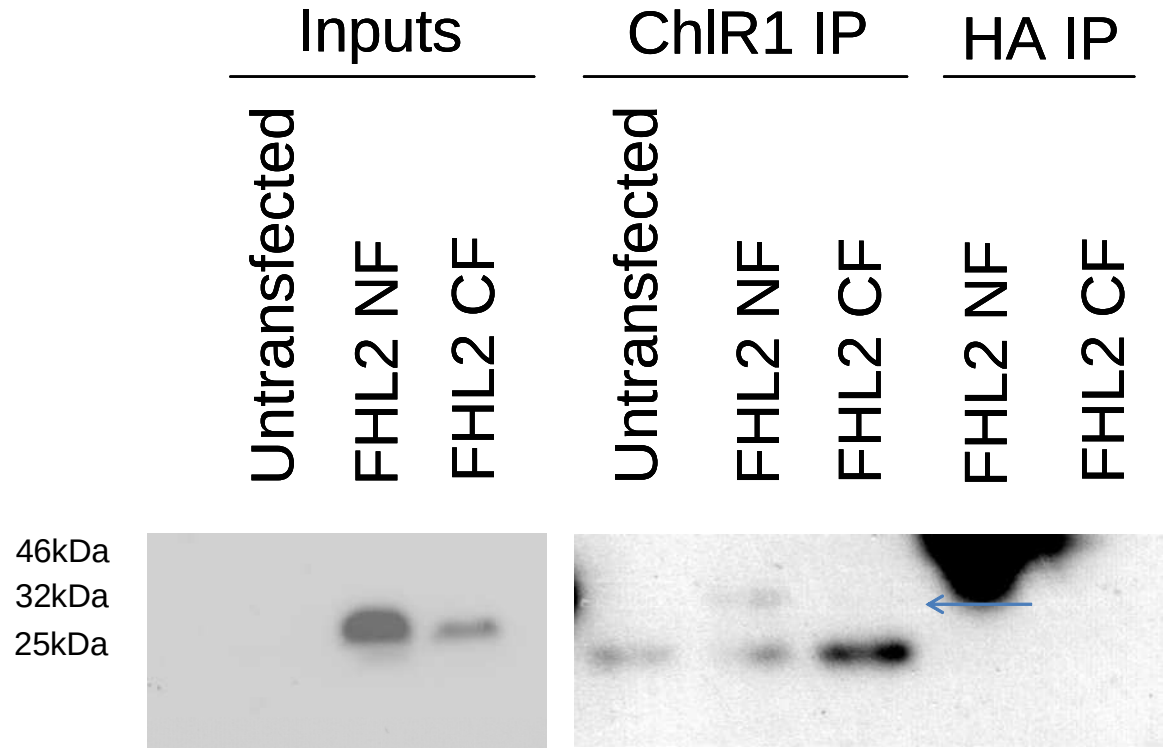

Figure 13: **Interaction between endogenous ChlR1 and FLAG FHL2.** *HEK 293 cells were transfected with FHL2-NF and -CF expression vectors and 10% input was loaded for each reaction. Whole cell lysates were immunoprecipitated with affinity purified rabbit anti-ChlR1 antibody and the presence of co-precipitating FHL2 detected by western blot using the M2 FLAG specific antibody. A band corresponding to the predicted molecular mass of FHL2 was co-immunoprecipitated from FHL2-NF transfected cell lysates suggesting an interaction between endogenous ChlR1 and N-terminally FLAG-tagged*

FHL2 (band indicated with arrow). An antibody specific for the HA epitope was used as a negative control

Immunoprecipitation of endogenous ChlR1 resulted in co-precipitation of N-terminally FLAG-tagged FHL2 providing evidence that ChlR1 interacts with FHL2 in mammalian cells. To confirm the interaction between ChlR1 and FHL2 in mammalian cells the reverse co-immunoprepipitation experiment was performed. This involved the immunoprecipitation of exogenously expressed FLAG tagged FHL2 and the detection of co-precipitating endogenous ChlR1.

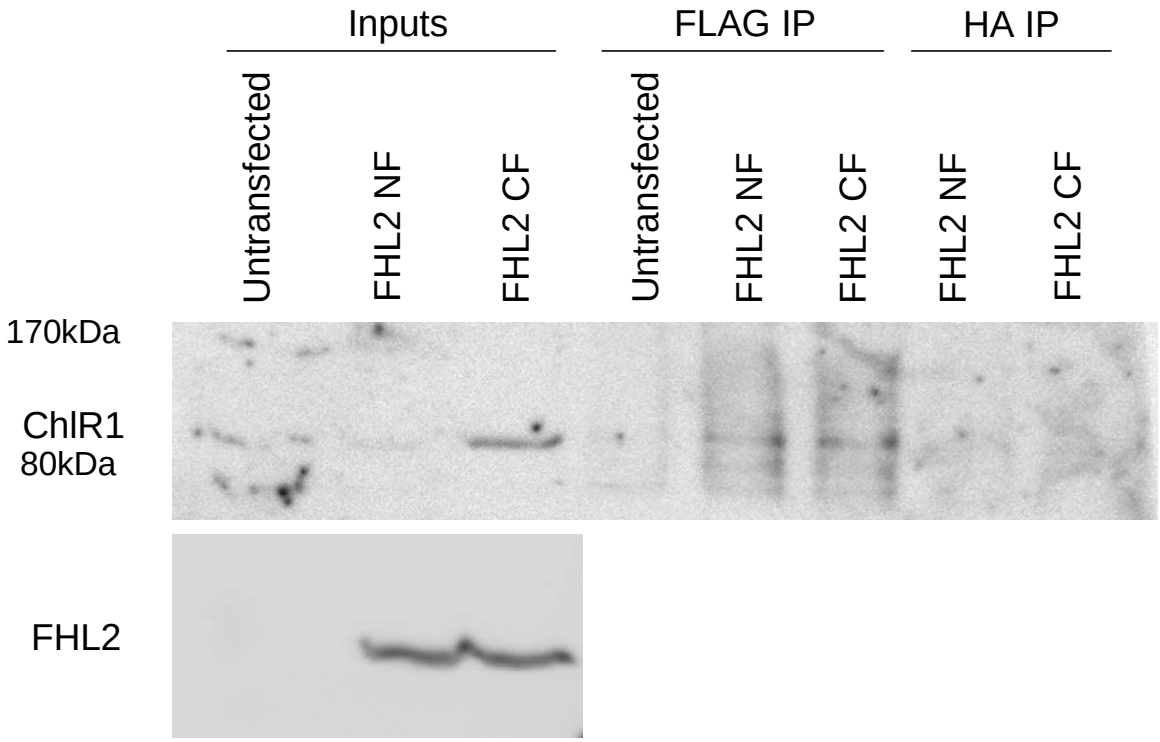

Figure 14: **Co-immunoprecipitation of endogenous ChlR1 with FLAG tagged FHL2.** *HEK 293 cells were transfected with FHL2-NF or -CF. 20% inputs were loaded for each reaction. Whole cell lysate was immunoprecipitated with FLAG antibody (M2). Co-precipitating ChlR1 was detected by western blot using affinity purified rabbit anti-peptide ChlR1 antibody. Bands corresponding to the predicted molecular mass of ChlR1 (108kDa) were detected in the FHL2-NF and -CF immunoprecipitated lanes suggesting an interaction between endogenous ChlR1 and N- and C- terminally FLAG- tagged FHL2. An antibody specific for the HA epitope was used as a negative control.*

As can been seen from the data in figure 14, immunoprecipitation of exogenously expressed, epitope tagged FHL2 resulted in co-precipitation of endogenous ChlR1, thus confirming the interaction in mammalian cells. Interestingly the immunoprecipitation of FHL2 and detection of ChlR1 shows that both the N-terminally tagged and C-terminally tagged FHL2 constructs interact with endogenous ChlR1. This was not the case in figure 13 where only the N-terminally tagged FHL2 was immunoprecipitated as an interacting partner. From figures 13 and 14 we can conclude that the interaction between ChlR1 and FHL2 first identified in the yeast two-hybrid screen is likely to be physiologically authentic in mammalian cells.

To further verify that ChlR1 and FHL2 interact *in vivo* and obtain more robust co-immunoprecipitation data, the co-immunoprecipitation of exogenously expressed epitope tagged FHL2 and ChlR1 was explored. The problem in performing this experiment was that the FHL2 and ChlR1 constructs available both had FLAG epitopes. Therefore, to perform an immunoprecipitation in co-transfected cells, I had to create an FHL2 construct with a different epitope. The FHL2 open reading frame was cloned into pCDNA in frame with an N terminally fused HA epitope as described in the materials and methods. Plasmids from individual clones were sequenced to verify correct insertion in the HA-FHL2 cDNA.

To confirm that the resulting HA-FHL2 was efficiently expressed in mammalian cells, HEK-293 cells were transiently transfected with HA-FHL2 by calcium phosphate precipitation and expression of HA-FHL2 clearly demonstrated by western blot (Figure 15). In order to verify the interaction between FLAG-ChlR1 and HA-FHL2, HEK 293 cells were co-transfected with both expression constructs. However although expression of each protein expressed alone was confirmed, co-expression of HA-FHL2 and FLAG-

ChlR1 was not successful in HEK 293, HeLa or hTERT-RPE1 cells using different transfection reagents and different amounts of plasmids. Therefore it was decided to further characterise this protein interaction *in vitro.*

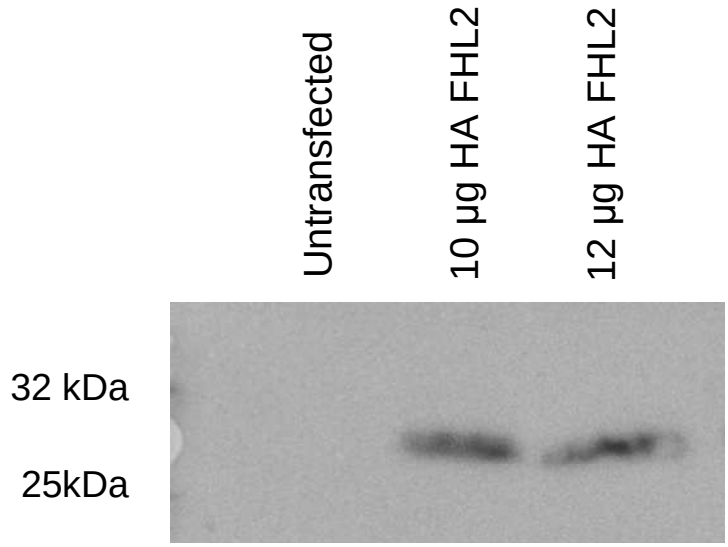

Figure 15: **Expression of HA-FHL2 in HEK 293 cells**. *HEK 293 cells were transfected with either 10 or 12 µg of pCDNA-HA-FHL2 by calcium phosphate precipitation. Whole cell lysates were separated by SDS PAGE and HA-FHL2 detected by western blot using mouse anti-HA (12CA5) diluted to 1:2000. A band of 30 kDa corresponding to the predicted molecular mass of FHL2 was expressed in both transfections but not in the untransfected cells.*

3.4 *In vitro* analysis of the interaction between ChlR1 and FHL2

For the *in vitro* analysis of the interaction between ChlR1 and FHL2, FHL2 was cloned into the bacterial protein expression pEHISTEV vector (obtained from Professor Jim Naismith, University of St Andrews) to create a hexahistidine-FHL2 fusion protein that can be expressed in *E.coli* as described in the materials and methods. Positive clones were verified by sequencing.

To express and purify His-FHL2, BL21 (DE3) *E.coli* were transformed with pEHISTEV-FHL2. This strain of *E.coli* has the T7 promoter expression system and after induction

with IPTG, should express hexa-histidine FHL2 from the pEHISTEV vector as the vector contains a T7 promoter. Following transformation, isolated colonies were picked and grown in liquid culture overnight. These overnight colonies were used to express the His-FHL2 protein upon induction with IPTG as described in the materials and methods.

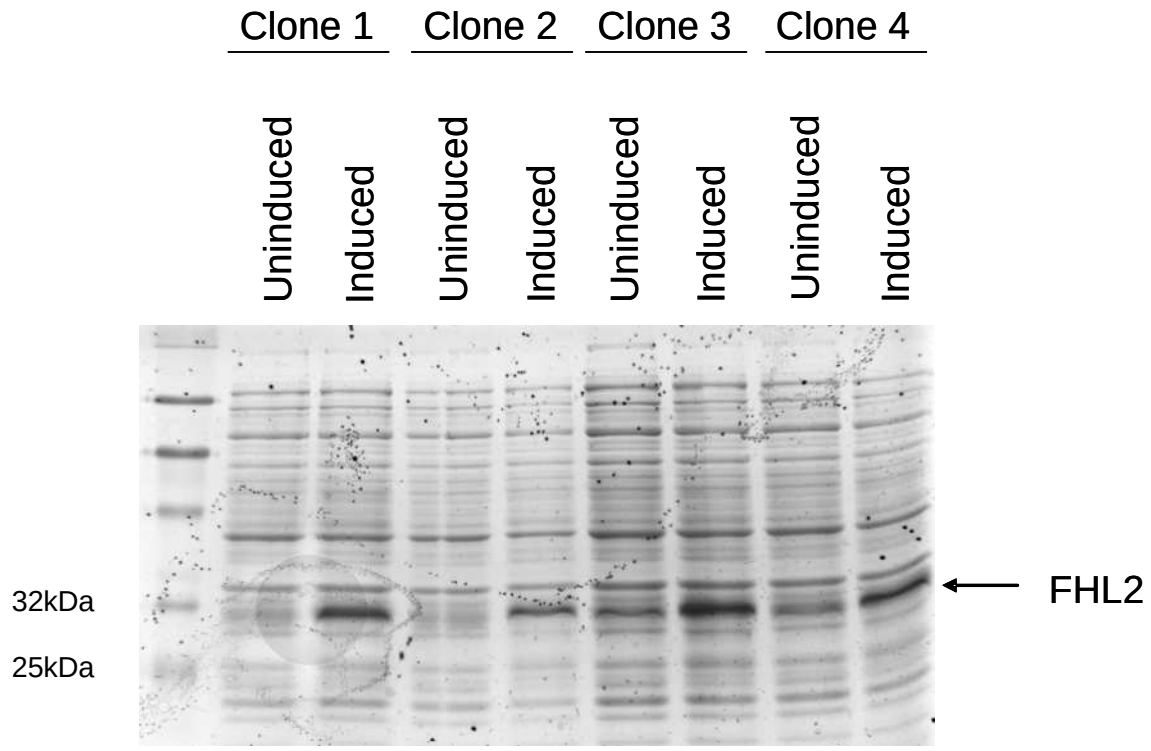

Figure 16: **Expression of His-FHL2 protein from the pEHISTEV expression vector in different clones of BL21 (DE3) *E.coli***. *BL21 (DE3) E.coli transformed with pEHISTEV-FHL2 were induced with 1mM IPTG for 4 hours at 37ºC. Bands of approximately 30 kDa in that correspond to the predicted mass of His-FHL2 are present in the induced lanes of all 4 clones analysed.*

All four BL21 clones tested express His-FHL2 upon induction with IPTG (figure 16). There is leaky expression of the protein in clones 3 and 4 as there is expression of the protein in the absence of IPTG. However clones 1 and 2 showed tight control of expression. Clone 1 has a higher level of expression than clone 2, therefore clone 1 was used to scale up the protein expression from 1 litre of bacterial culture. The His-FHL2

protein produced from this culture was purified using a nickel affinity resin as described in the materials and methods.

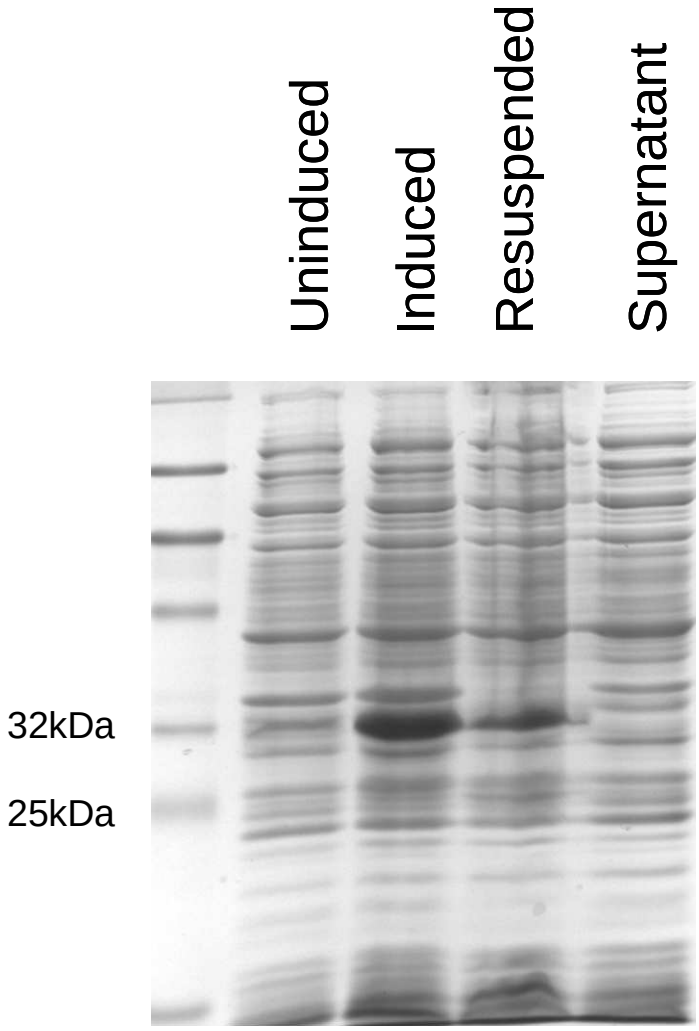

Figure 17: **Nickel affinity purification of Hexa-Histidine-FHL2**. *Protein expression in BL21 (DE3) transformed with pEHISTEV-FHL2 was induced with 1mM IPTG for 4 hours at 37ºC. Cells were lysed and samples separated on a SDS PAGE gel. A band of approximately 30 kDa corresponding to the predicted mass of His-FHL2 is present in the induced and solubilised pellet (resuspended) lanes but this was not present in the soluble supernatant lane.*

His-FHL2 was lost during purification when the cell debris was removed by centrifugation. Therefore it was believed that His-FHL2 is insoluble under the conditions used. Therefore the purification protocol was modified in an attempt to solve this problem.

The temperature at which the bacteria were induced was reduced to 30ºC and the concentration of IPTG was reduced to 0.5mM. However these modifications did not improve the solubility of the protein.

Therefore I created a GST tagged FHL2 construct, as GST has been shown to improve the solubility of some proteins. To this end, FHL2 was cloned into the pGEX-4T1 expression vector as described in the materials and methods.

Positive clones were verified by sequencing. The next step was too express GST-FHL2 from the pGEX-4T1 vector in BL21 (DE3) *E.coli.*

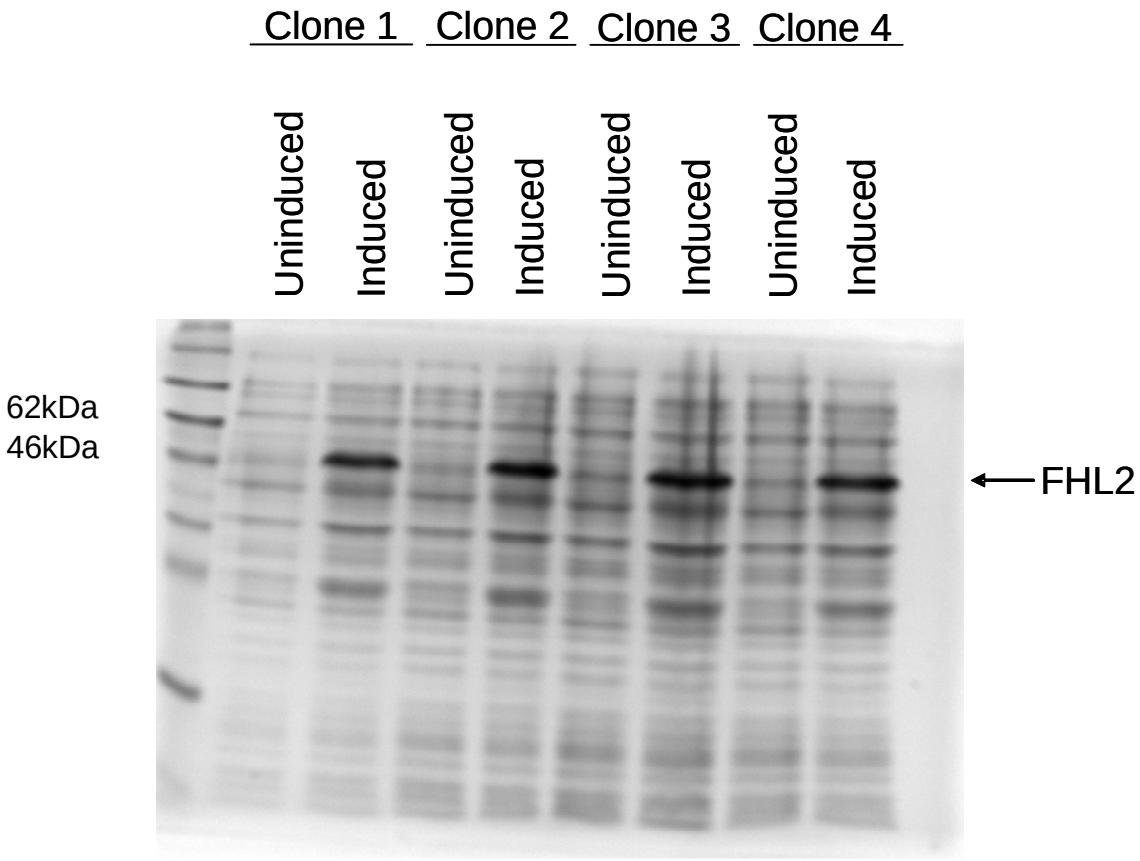

Figure 18: **Expression of GST-FHL2 from the pGEX-4T-2 expression vector in four clones of BL21 (DE3)**. *BL21 (DE3) E.coli transformed with pGEX-4T1-FHL2 were induced with 1mM IPTG for 4 hours at 30ºC. Bands of approximately 50 kDa in size can be seen in the induced bacteria lanes that correspond to the predicted mass of GST-FHL2.*

Induction of GST-FHL2 expression with IPTG all four BL21 clones resulted in high levels of expression of GST-FHL2. There was no detectable expression of the protein in the absence of IPTG. All four clones were deemed suitable for GST-FHL2 purification. Purification of GST-FHL2 was carried out as described in the materials and methods. An additional step in the protocol compared to the nickel purification, was the solubilisation of the pellet from the centrifugation of the lysed bacteria in 8M urea. It was believed that the insoluble protein was contained within this pellet. After the pellet was re-suspended in the urea, lysis buffer was added. The sample was then spun down and the supernatant collected. This supernatant was added to glutathione agarose beads (supernatant 2, Figure 19).

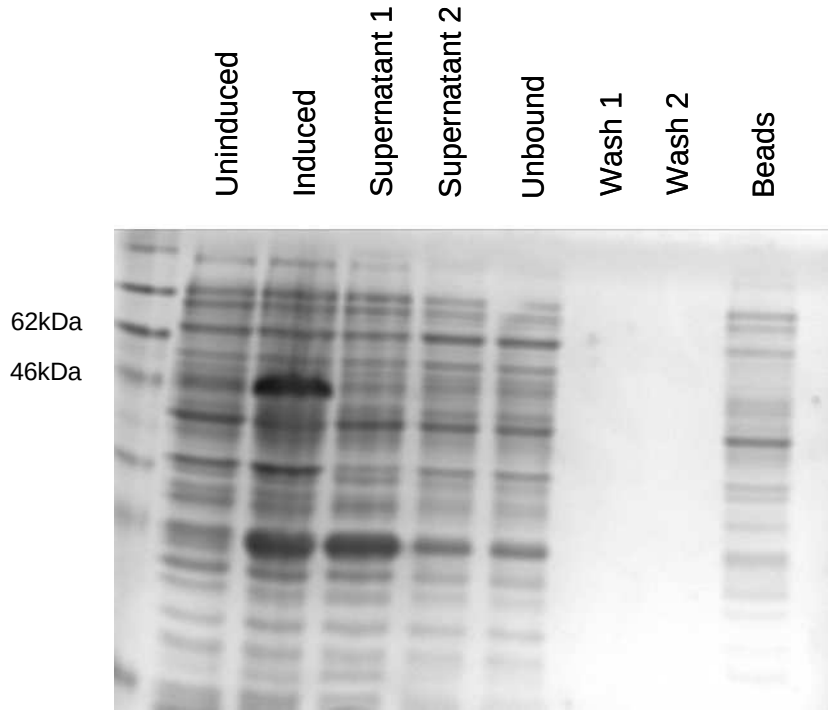

Figure 19: **Purification of GST-FHL2**. *BL21 (DE3) E.coli transformed with pGEX-4T1-FHL2 were induced with 1mM IPTG for 4 hours at 30ºC. Samples from the lysis (supernatant 1), urea solublisation step (supernatant 2) and a sample of protein bound beads after purification were collected and separated by SDS PAGE. A 50 kDa band corresponding to GST-FHL2 is seen in the induced lane but is not present in the lanes containing the samples taken from the supernatant after sonication and the resolublised pellet.*

GST-FHL2 was not recovered from the *E.coli* after lysis (Figure 19). The addition of the lysis buffer after the pellet was solubilised in urea may have caused the protein to re-fold incorrectly and precipitate. This would result in the protein being removed from the supernatant 2. To prevent this from happening the urea was removed gradually from the solution by serial dialysis. However, this did not improve the solubility of the protein.

The problem with the solubility of the protein may be due to a number of reasons. The *E.coli* may package the protein into inclusion bodies. Another possibility is the protein is still bound to DNA after lysis. Therefore a double lysis purification protocol described in the materials and methods was tested. It was thought that the double lysis of the bacteria may help to extract the protein from the inclusion bodies or remove it from the DNA.

In addition to these modifications, the expression of GST-FHL2 in a different bacterial strain was tested. FHL2 contains a number of rare codons. The BL21 (DE3) *E.coli* are unable to efficiently translate these codons as they do not contain the appropriate tRNA molecules in high abundance. The presence of rare codons can cause premature termination of the protein synthesis or mis-incorporation of amino acids. To remove the possibility that the rare codons were causing the protein solubility problem, the *E.coli* strain used for the purification was changed to the Rosetta *E.coli* (Novagen) for expression of GST-FHL2. This strain of *E.coli* contains a plasmid called pRARE that encodes the additional tRNA for the rare codons.

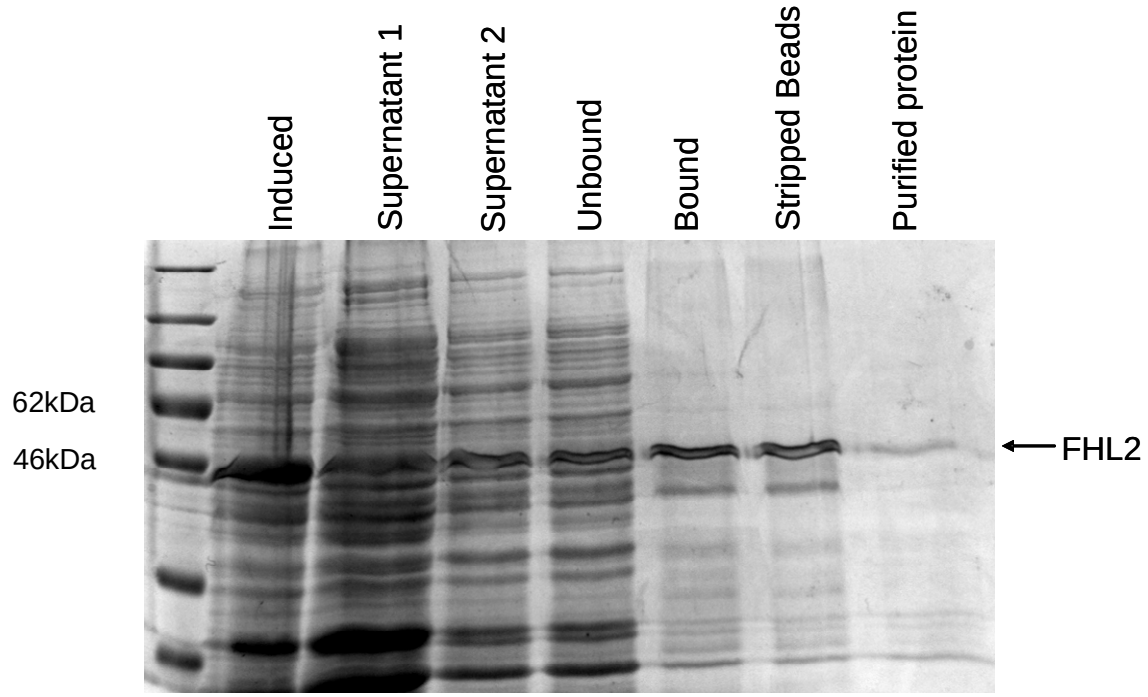

Figure 20: **Purification of GST-FHL2 protein from Rosetta *E.coli* following double lysis**. *Rosetta E.coli transformed with pGEX-4T1-FHL2 were induced with 1mM IPTG for 4 hours at 30ºC. Samples from the two lysis steps, the supernatant from the stripped beads along with a sample of beads before and after stripping, were collected and separated by SDS PAGE. A Band of approximately 50 kDa that corresponds to the predicted mass of GST-FHL2 can be seen in the induced, supernatant 2, bound and purified protein lanes. This suggests that FHL2 can be recovered from lysed bacteria and purified using glutathione agarose beads.*

GST-FHL2 can be recovered and purified from glutathione agarose beads when expressed in Rosetta *E.coli* and the cells lysed using the double lysis method (Figure 20). However, following elution of the protein with glutathione, a large amount of the protein remains in the bead pellet suggesting that the protein precipitates after elution from the beads. To confirm that the band in the purified lane was GST-FHL2, intact mass spectrometry analysis should be performed. However, the small amount of protein purified was not stable. A sample of the purified protein was run on an SDS gel 24 hours after purification and the band was no longer visible. This suggests that the protein degrades or precipitates quickly after purification.

Due to the problems highlighted above with FHL2 purification, I was not able to analyse the *in vitro* interaction between ChlR1 and FHL2.

3.5 The Role of FHL2 in Cohesin Establishment

To test the hypothesis that FHL2 has a role in cohesion establishment, FHL2 was depleted in HEK 293 by RNA interference. Sister chromatid cohesion in FHL2 depleted cells was analysed in metaphase spreads (described in the materials and methods). Using this assay, the structure of the chromatid and the distance between the chromatids pairs was analysed.

To deplete FHL2 in HEK 293 cells, an FHL2 specific siRNA oligonucleotide was designed using the siDESIGN siRNA design programme (Thermo). Cells were then transfected with increasing concentrations of FHL2 siRNA and a scrambled control using Dharmafect 1 transfection reagent as described in the materials and methods. The efficiency of FHL2 depletion was then assessed by western blot. As can be seen from the data in figure 17, FHL2 specific siRNA effectively depletes endogenous FHL2 protein by 55% at 70nM and 85% at 100nM. The knockdown of around 85% was thought sufficient for the analysis of FHL2 function on sister chromatid cohesion. Therefore metaphase spreads of HEK 293 cells transfected with 100nM of either FHL2 or scrambled siRNA were prepared.

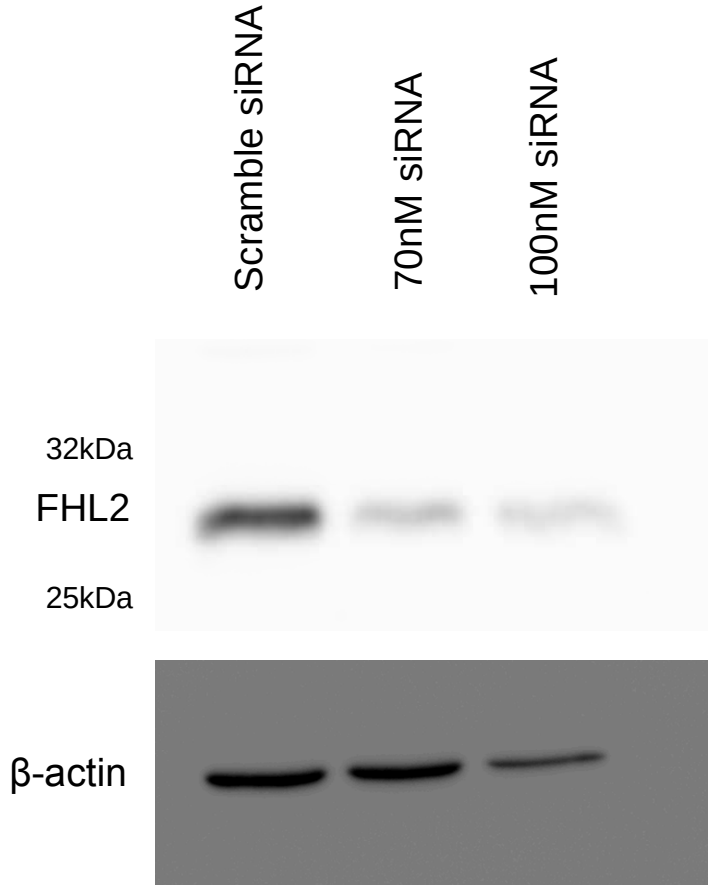

Figure 21: **Transfection of HEK 293 cells with varying amounts of siRNA specific for endogenous FHL2**. *HEK 293 cells were transfected with increasing amounts of FHL2 specific siRNA. The cells were harvested 24 hours after transfection. Rabbit derived FHL2 antibody was used to detect endogenous FHL2 by western blot. Bands of 32 kDa corresponding to the predicted mass of FHL2 are seen in all three lanes. The intensity of the bands decreases as the amount of siRNA increases. Mouse derived β-actin antibody was used as a loading control.*

(a)

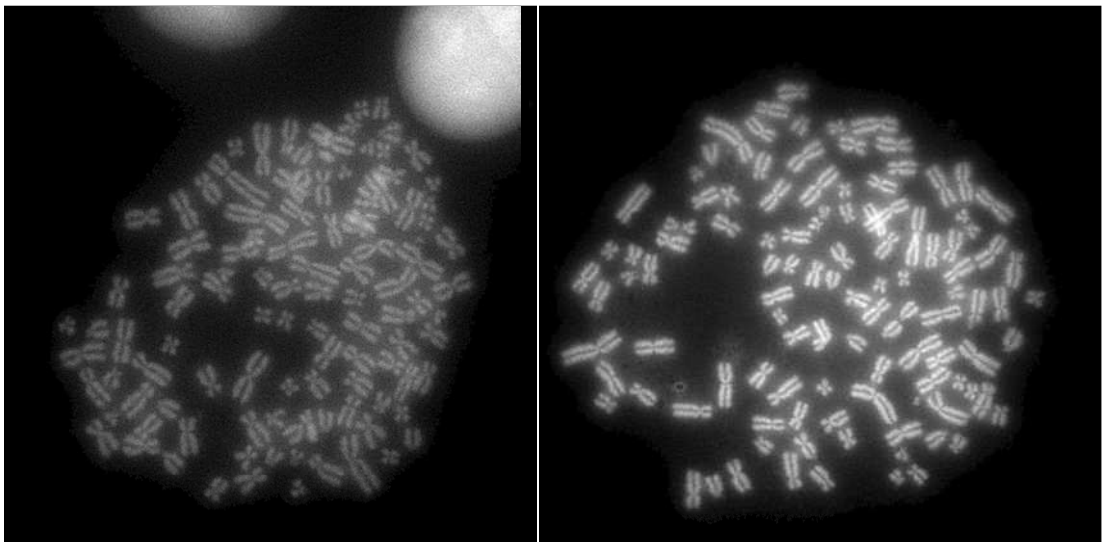

(b)

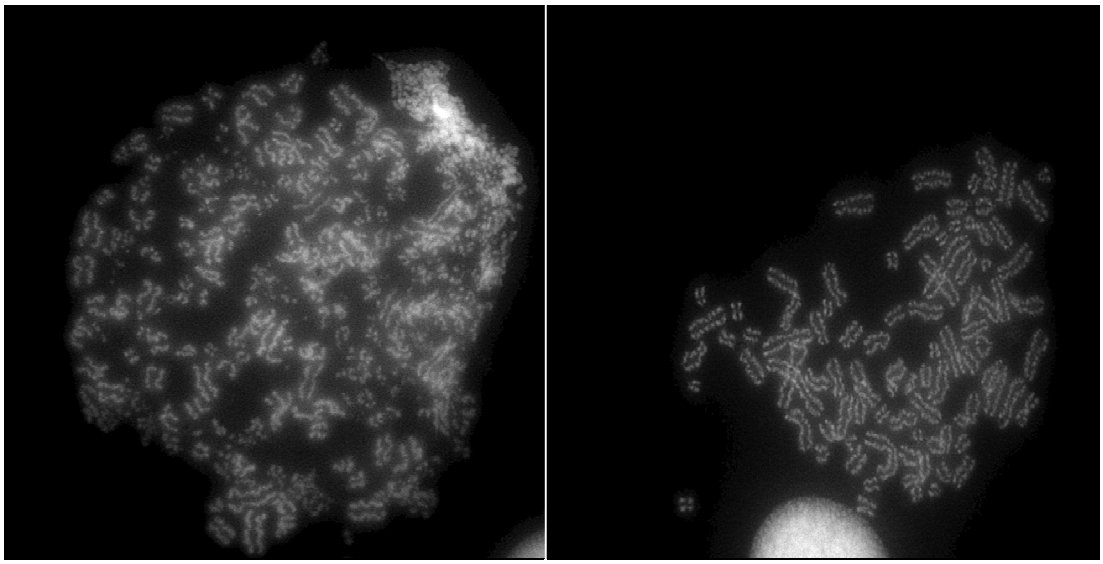

(c)

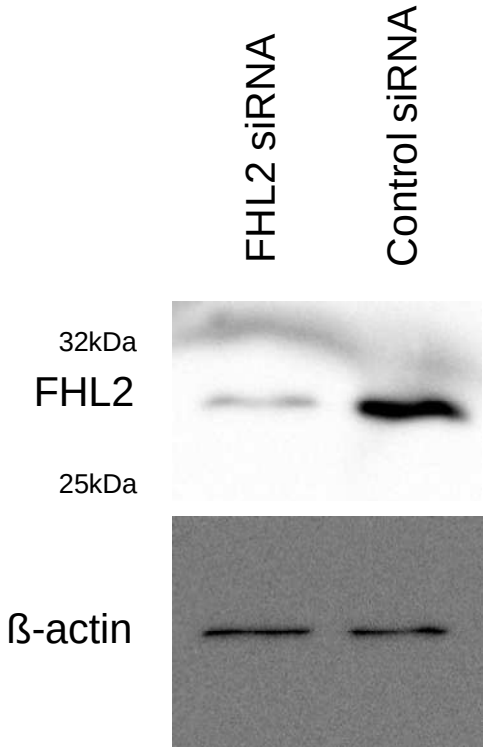

(d)

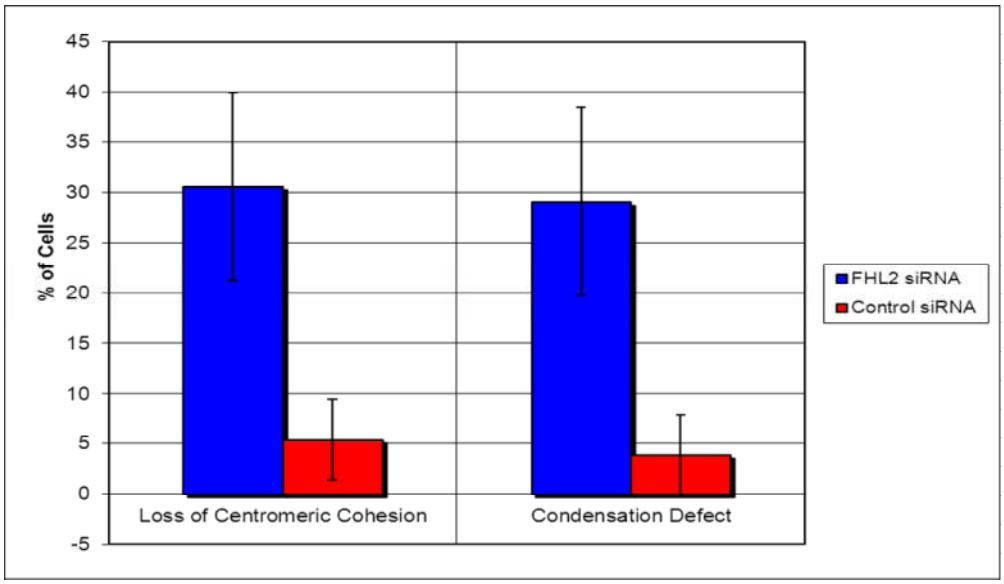

Figure 22: **Analysis of cohesion defects in FHL2 knockdown cells.** *HEK 293 cells were transfected with 100nM of FHL2 specific or scrambled siRNA. After 24 hours the cells were treated with 100ng/ml colcemid for 2 hours and harvested. The cells were swelled and fixed. After which they were spread on slides and stained with propidium iodide. Chromosome spreads were imaged using an epiflourescence microscope fitted with a TRITC filter set and a 63x objective. (a) Shows metaphase spreads from cells transfected with control siRNA. (b) Shows metaphase spreads from cells transfected with FHL2 siRNA. (c) Western blot showing knockdown of FHL2 in the cells used for the metaphase spreads. (d) Shows a quantification of the percentage of abnormal cells in each spread.*

The data represents the mean and standard deviation of 50 cells counted in each variable. The experiment was repeated twice.

In analysing the metaphase spreads, abnormal chromosomes were classed as chromosomes without centromeric cohesion, 'wavy' chromatids (which is believed to be abnormal condensation of the chromatids) and prematurely separated chromatids.

Figure 22 suggests that FHL2 has a role in sister chromatid cohesion as there is a highly significant increase in abnormal sister chromatid cohesion in FHL2 depleted cells compared to control cells ($p<0.0000000002$). Figure 22 also suggests that FHL2 has a role in the condensation of of the chromatids as there is a highly significant increase in wavy chromatids in FHL2 depleted cells compared to control cells ($p<0.0000000005$)

The apparent function of FHL2 in sister chromatid cohesion establishment and maintenance may be a result of its association with ChlR1. However, FHL2 may also interact with other proteins involved in the process sister chromatid cohesion including the cohesin complex. To test this theory a co-immunoprecipitation was performed to see if the Smc1 subunit of the cohesin complex was co-immunoprecipitated in a complex with FHL2. HEK 293 cells were transfected with FLAG-FHL2 and the whole cell lysates were immunoprecipitated with Smc1 specific antibody. The presence of co-precipitating FLAG-FHL2 was detected by western blot with FLAG antibody.

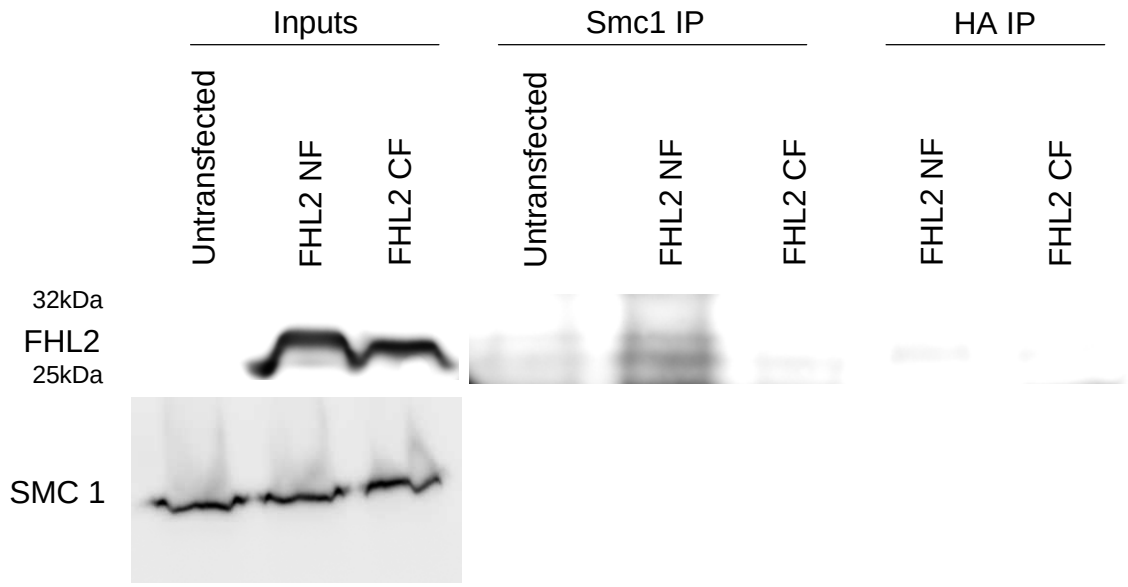

Figure 23: **Interaction between endogenous Smc1 and FLAG-FHL2.** *HEK 293 cells were transfected with FHL2-NF and -CF expression vectors and 10% input from whole cell lysate was loaded for each reaction. Whole cell lysates were immunoprecipitated with Smc1 specific antibody with a specific interaction between endogenous Smc1 and exogenous expressed FLAG-FHL2 detected by western blot using FLAG antibodies. A band corresponding to the predicted molecular mass of FLAG-FHL2 was detected in the FHL2-NF IP lane suggesting endogenous Smc1 may interact with N terminally FLAG-tagged FHL2. An antibody specific for the HA epitope was used as a negative control.*

The immunoprecipitation experiment shown in figure 23 suggests that FHL2 may interact with Smc1, a member of the cohesin complex. The cohesion defects seen in FHL2 knockdown cells along with the co-immunoprecipitation data suggests that FHL2 may have a central role in the establishment of sister chromatid cohesion.

The metaphase spreads of FHL2 depleted cells suggest that there is a reduction in centromeric cohesion, which would disrupt kinetochore tension and result in spindle checkpoint activation. To determine whether the sister chromatid cohesion defects seen in FHL2 knockdown cells results in an accumulation of cells at G_2/M, cells were harvested fixed in ethanol and stained with propidium iodide. The cell cycle distribution of FHL2 depleted cells compared to those transfected with scrambled siRNA control was determined by flow cytometry. In this assay activation of cell cycle checkpoints due to the cohesion defects would result an increased percentage of cells in the G_2 or M phases of the

cell cycle. The assay would be performed with hTERT-RPE1 cells as they have a robust checkpoint activation and cell cycle arrest compared to the HEK 293 cells used for the previous assays.

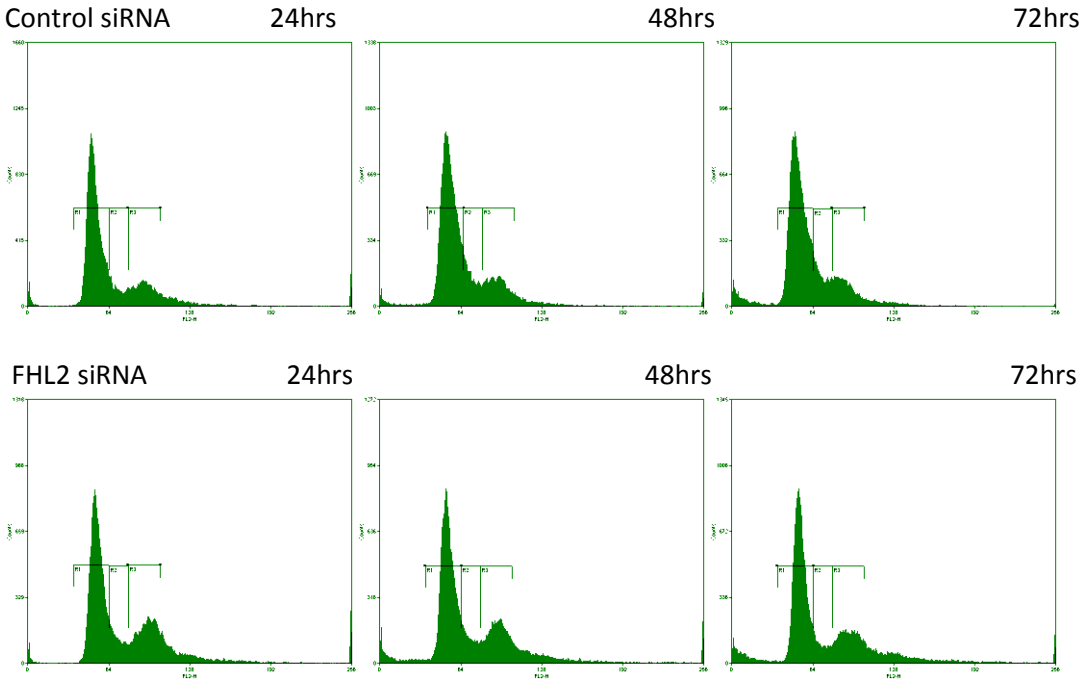

	Control siRNA			FHL2 siRNA		
	G_1	S	G_2/M	G_1	S	G_2/M
24hrs	61.82	11.08	16.30	54.40	9.05	23.20
48hrs	62.32	14.53	15.63	53.75	9.07	20.25
72hrs	62.76	14.60	14.33	50.52	8.54	18.83

Figure 24: **Cell cycle analysis of FHL2 knockdown cells by flow cytometry**. *hTERT-RPE1 cells were transfected with 100nM FHL2 or scrambled siRNA. Cells were harvested 24, 48 or 72 hours post transfection and fixed and stained with propidium iodide. (a) Cell cycle profiles plotting maximum fluorescence emission (FL2-H) against cell counts were obtained for each time point using BD systems FACS scan. Region 1 represents cells in G_1 phase, region 2 represents cells in S phase and region 3 represents cells in G_2/M phase (b) Shows the percentage of cells counted within each phase of the cell cycle for control and FHL2 knockdown cells. The percentage of cells in G_2/M is higher for FHL2 siRNA treated cells that control siRNA treated cells. There is also a decrease in the percentage of cells in S phase for FHL2 siRNA treated cells compared to control siRNA treated cells.*

Depletion of FHL2 from hTERT-RPE1 cells results in an accumulation of cells in the G_2/M phase of the cell cycle and a decrease in the number of cells in S phase (Figure 24). This suggests that there is a defect in progression through DNA replication and into or through mitosis. The defect in mitosis is likely to be due to a disruption of sister chromatid cohesion after depletion of FHL2 (Figure 22).

The evidence above corroborates with the hypothesis that the sister chromatid cohesion defects seen in FHL2 knockdown cells results in checkpoint activation resulting in abnormal progression through mitosis. The activation of the checkpoint is possibly due to disruption in kinetochore tension. The metaphase spreads of FHL2 depleted cells show a lack of centromeric cohesion, which would result in a disruption of kinetochore tension.

In summary I have shown that FHL2 interacts with ChlR1 in mammalian cells. This confirms the yeast two-hybrid screen data. I have shown that depletion of FHL2 results in sister chromatid cohesion defects and a G_2/M delay. These results suggest a novel function of FHL2 in mitosis.

Chapter 4: The Role of ChlR1 in DNA Damage Repair

4.1 Introduction

As discussed in the introduction to this thesis, the cohesin complex has a functional role in the repair of cellular DNA damage. A number of cohesin establishment factors have been shown to function in DNA damage repair pathway. It is believed that cohesin is recruited to sites of DNA damage to aid in the process of HR and stabilise the regions of DNA around the break. It is thought that cohesin establishment factors are actively recruit cohesin to these sites. ChlR1 is a cohesin establishment factor and the yeast homologue Chl1p is implicated in the cellular DNA damage repair response. Therefore, I hypothesise that ChlR1 functions in the recruitment and establishment of cohesin at sites of DNA damage.

Chl1p was initially discovered to function in the repair of DNA damage in *S.cerevisiae. CHL1* deleted cells were shown to be more sensitive to the DNA damage reagents methyl methanesulfonate (MMS), hydroxyurea (HU) and UV radiation [304, 305]. This led to the hypothesis that Chl1p is involved in the DNA damage sensing checkpoint or directly in the repair of DNA lesions. However *CHL1* null yeast have been shown to have functional DNA damage checkpoint activation as Rad53 was phosphorylated when DNA damage was induced, although this yeast strain did show signs of DNA repair defects [304]. Similar effects were seen in *CTF4* null *S.cerevisiae* [304]. Chl1p and Ctf4 were shown to associate with damaged chromatin during G_2/M phase even though sister chromatid cohesion is established in S phase [304]. NHEJ was shown not to be defective *CHL1* and *CTF4* deleted yeast but these cells had a defective HR pathway. Furthermore the frequency of unequal sister chromatid recombination in wild type cells increased with increasing doses of MMS. Conversely, this was not observed in the *CHL1* and *CTF4* deleted cells

suggesting that Chl1p and Ctf4 are involved in the recombination between sister chromatids [304].

An interaction between ChlR1 and TopBP1 has been shown through co-immunoprecipitation experiments (Parish and Feeney, unpublished). TopBP1, as discussed in the introduction, is involved in the repair of double strand breaks that occur during DNA replication [70]. An interaction between ChlR1 and DNA-PKcs has also been isolated (Parish and Feeney, unpublished). This protein interaction was isolated using tandem affinity purification (TAP) and confirmed by co-immunoprecipitation experiments in hTERT-RPE1 cells. The interaction between ChlR1 and DNA-PKcs increased 6-fold in response to DNA damage caused by ionising radiation. DNA-PKcs as discussed in the introduction is involved in the NHEJ repair process and recruits components involved in the process through phosphorylation. Recently ChlR1 was shown to be phosphorylated during G_1/S phase at a serine residue at amino acid 204 [306].

A number of other helicases related to ChlR1 have a functional role in the repair of DNA damage. The XPB and XPD helicases are members of the XPD family of helicases of which ChlR1 is closely related. This family of helicases contain iron sulphur cluster domains with XPD having a 5'-3' directionality and XPB the opposite polarity [222]. These helicases are part of the transcriptional factor IIH complex (TFIIH) that functions in transcriptional initiation and nucleotide excision repair [222]. This process removes bulky adducts from DNA such as cisplatin lesions and photoproducts generated from UV light. The TFIIH complex opens the DNA around the promoter or damage site. It is believed that the helicase activity of XPB and XPD is important for this function. Mutations in either helicase results in the DNA repair syndrome xeroderma pigmentosum (XP) [307].

The FANCJ helicase that has been associated with the genetic disorder Fanconi anemia is also highly related to ChlR1. This helicase also has an iron sulphur cluster and is a member

of the DEAH family [308]. It was initially shown to have a role in DNA damage repair when it was shown to interact with BRCA1 [309]. FANCJ unwinds homologous recombination intermediates, which suggests it is involved in the HR pathway of double strand break repair [310]. Indeed FANCJ knockout cells have HR defect and are sensitive to ionising radiation [310]. Interestingly FANCJ has been shown to play a role in the response to replication stress. Depletion of FANCJ in *Xenopus* oocytes resulted in replication fork restart defects following treatment with camptothecin that causes DSB during DNA replication [311].

4.2 Hypotheses and Aims

Hypothesis

ChlR1 is involved in DNA damage repair by recruiting cohesin to sites of DNA double strand breaks.

Aims

To confirm this hypothesis I aimed to

1) Confirm ChlR1 has a role in the repair of DNA damage using the DNA comet assay.

2) Confirm ChlR1 localises at sites of DNA double strand breaks by immunofluorescence.

3) Assay the effect of ChlR1 depletion on the recruitment of cohesin to DNA double strand breaks by ChIP assay.

4.3 The knockdown of ChlR1 Results in Inefficient Repair of DNA Damage

The evidence above suggests that ChlR1 may have a role in DNA damage repair. To confirm this hypothesis, cells were depleted of ChlR1 protein by RNA interference and the repair of DNA damage following ionising radiation assessed. The technique used to quantify the DNA damage in cells with ChlR1 knocked down was the comet assay. In this assay HeLa cells were transfected with either ChlR1 siRNA or scrambled siRNA as a non-specific control. Cells were then damaged with an appropriate dose of gamma radiation and allowed to repair for set time points before analysis. HeLa cells were used in this assay because I could efficiently knockdown ChlR1 in this cell line.

Initially, efficient knockdown of ChlR1 using RNA interference was optimised. A number of different siRNA oligonucleotides were tested, each of which targeted different regions of the ChlR1 mRNA. The first siRNA tested was ChlR1 212, which targets the ChlR1 open reading frame at nucleotide 212. The analysis of the knockdown is shown in figure 1. Efficient knockdown of ChlR1 protein using siRNA ChlR1 212 was achieved when the siRNA was transfected into cells at a concentration of 100nM.

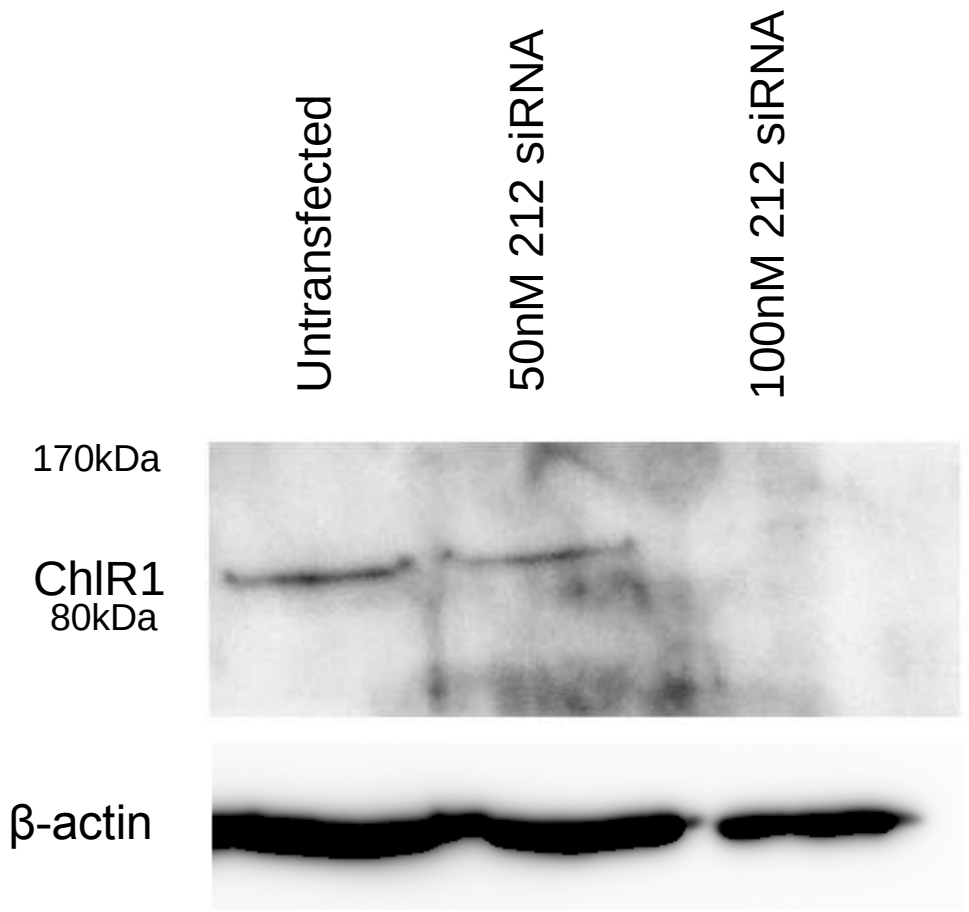

Figure 25: **Transfection of HeLa cells with siRNA specific for endogenous ChlR1**. *HeLa cells were transfected with increasing amounts of ChlR1 212 siRNA for 24 hours. Rabbit ChlR1 antiserum was used to detect endogenous ChlR1. Bands of approximately 100 kDa corresponding to the predicted mass of ChlR1 were present in the untransfected and 50nM siRNA lanes. This band was not present in the 100nM siRNA lane. Mouse anti-β-actin antibody was used as a loading control (lower panel).*

siRNA oligonucleotides were also designed that target the 5' and 3' UTRs of ChlR1 mRNA in order that endogenous ChlR1 could be depleted and exogenous ChlR1 (wild type or mutant) expressed from a construct that does not encode the UTRs of endogenous ChlR1, as will be discussed later. The siRNAs targeting the UTRs were tested for their efficiency to knockdown ChlR1. The analysis of the knock down was performed by RT-PCR using primers detailed in the materials and methods. RT-PCR analysis was performed because the efficiency of the antibody to detect endogenous ChlR1 is poor. Efficient

knockdown of ChlR1 mRNA using the siRNA targeting the 5' and 3' UTR was achieved when each siRNA was transfected at a concentration of 100nM (Figure 26).

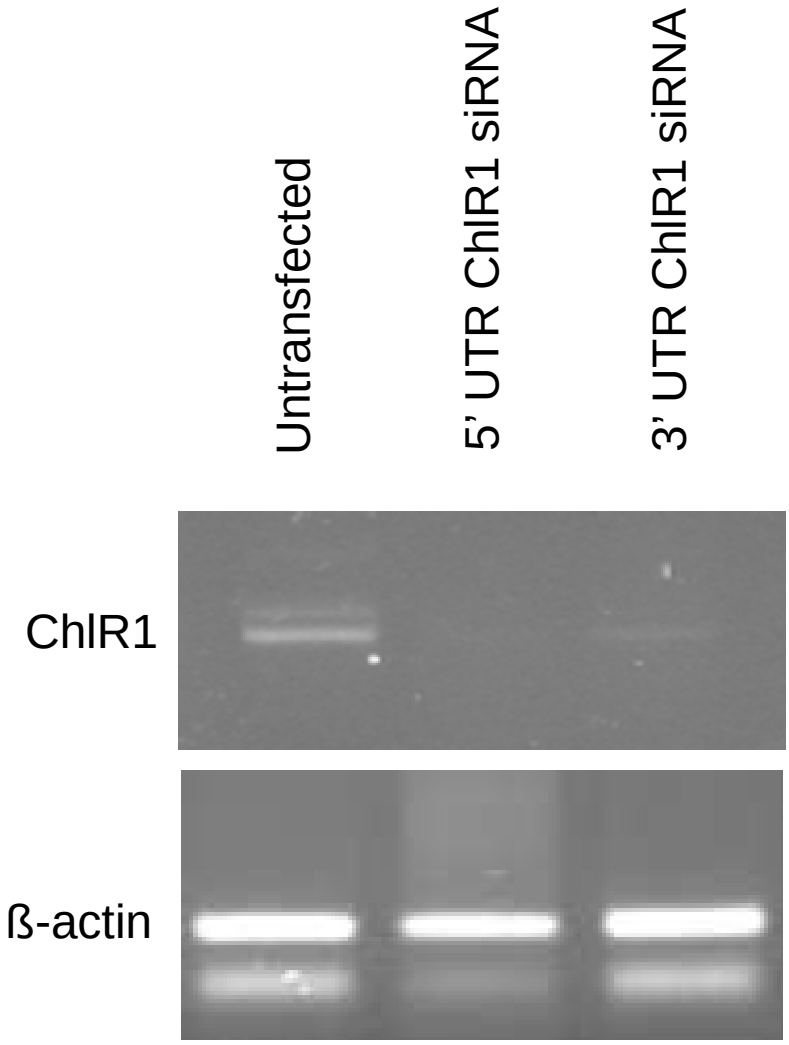

Figure 26: **Transfection of HeLa cells with siRNAs targeting either the 5' and 3' UTR of ChlR1**. *HeLa cells were transfected with 100nM of the siRNA targeting the 5' and 3' UTR regions of ChlR1, for 24 hours. RT-PCR was used to show the level of ChlR1 mRNA (700bp product) in treated cells with primers designed to anneal within the coding sequence of ChlR1 in alternative exons so that contaminating genomic DNA could be ruled out. β- actin (300bp product) was used as a control for input of DNA to each reaction. The RT-PCR data show that ChlR1 mRNA is depleted in the cells transfected with 100nM of siRNA specific to the 5' and 3' UTR of ChlR1 compared to untransfected cells.*

Next the assay used to detect DNA damage was optimised. The comet assay is used to detect fragmented DNA in individual cells. The comet assay involves the embedding of

cells in low melting point agarose on slides. The slides are then irradiated and the cells are allowed to repair by placing the slides in warm medium. After an appropriate time in medium the cells are lysed and subjected to electrophoresis to draw fragmented DNA out of the cells. Therefore the more damaged the DNA, the higher the percentage of DNA in the tails of the comets. The comets are stained, imaged and analysed using Comet Assay IV scoring software (Perceptive Instruments). This software is able to identify the head and tail of the comet and measure the percentage of DNA in each section.

The alkaline comet assay is used to detect single strand breaks as it involves the use of an alkaline electrophoresis buffer, which unwinds DNA allowing DNA single and double strand breaks to be drawn from the cell during electrophoresis. The neutral comet assay is used to examine DNA double strand breaks only and uses a neutral electrophoresis buffer. Therefore the DNA is not unwound and only double stranded breaks are drawn from the cells during electrophoresis.

Therefore I planned to use these assays on ChlR1 depleted HeLa cells to determine whether there was a defect in either single strand or double strand break repair, or both. The cells were irradiated to damage the DNA and allowed to repair. The levels of DNA damage was measured and compared to cells transfected with a scrambled siRNA oligonucleotide. This assay allowed me to test the hypothesis that ChlR1 has a functional role in the repair of DNA damage.

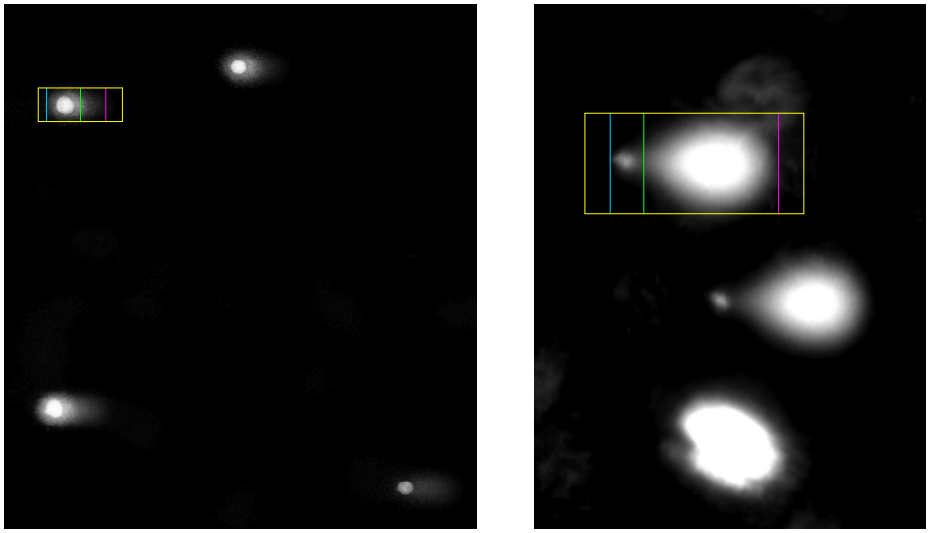

Figure 27: **Detection of DNA damage in HeLa cells using the alkaline comet assay**. *Shows cells undamaged (0 Gy) or irradiated with 10 Gy of gamma radiation and subjected to the alkaline comet assay. Comets were imaged using a Zeiss epifluorescent microscope fitted with a TRITC filter set and a 10x objective. The images were analysed using the Comet Assay IV scoring programme. Comets were selected and the programme gates the head (area between blue and green lines) and tail (area between green and purple lines) regions and calculates the intensity of each region.*

DNA damage was clearly detected in HeLa cells exposed to 10 Gy ionising radiation using the alkaline comet assay (Figure 27). The undamaged cells have a smaller comet tail compared to the cells that have been irradiated. The first step in optimising the alkaline comet assay was to determine a suitable dose of ionising radiation to use in the repair assay. Therefore I performed a dose response curve in which the cells were damaged with a variety of doses ranging from 1 to 10 Gy.

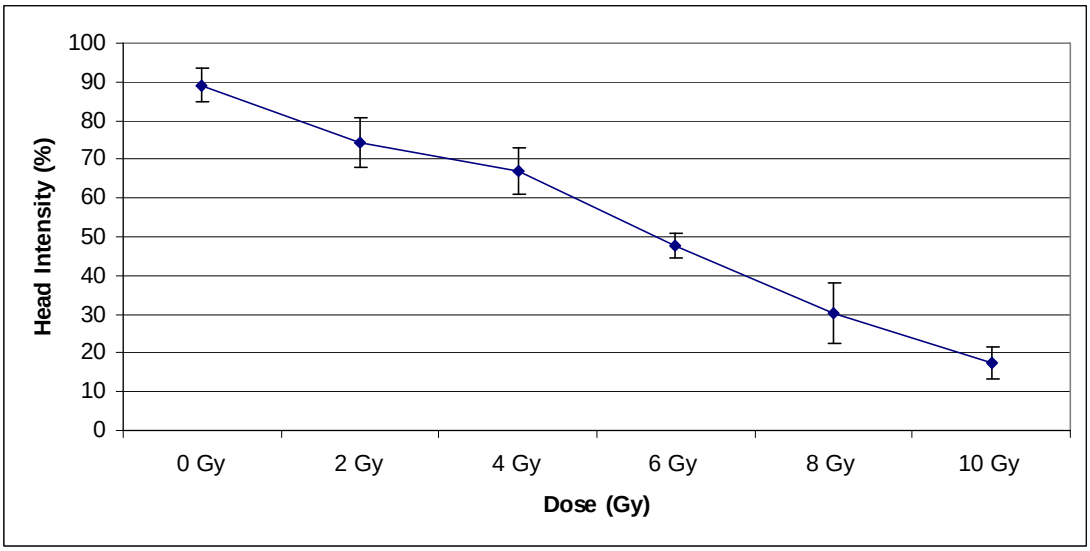

Figure 28: **Alkaline comet assay dose response curve**. *HeLa cells were damaged with different doses of gamma radiation and DNA damage detected using the alkaline comet assay. The graph shows the average head intensity and standard deviation of 30 cells collected for each dose. The experiment was repeated twice.*

As shown in figure 28 the percentage of DNA in the comet tails increases in a linear relationship with increasing doses of radiation which was expected since an increase in dose would create more fragmented DNA. The target percentage of DNA in the tail was 50%. This was decided as it would large enough to show repair over time. A larger percentage may cause apoptosis of the cells. The data in figure 4 shows that the dose required to create 50% tail intensity was 5 Gy of gamma radiation.

The length of time required for the cells to repair DNA lesions caused by the exposure to 5Gy was next examined. Cells were irradiated with a dose of 5Gy and incubated in medium at 37ºC for a range of time points. The head intensity of the undamaged cells was 85% and following irradiation, the head intensity decreased to 40%. Cells were also collected at 1 and 2 hours following damage. The data in figure 29 shows that cells were able to repair DNA damage by 2 hours post irradiation. Using the optimised alkaline comet assay I next performed a repair assay on cells transfected with ChlR1 and control siRNA oligonucleotides. Cells were transfected with ChlR1 specific or control scrambled siRNA

and incubated for 24 hours. The cells were then irradiated with a 5 Gy dose of ionising radiation and allowed to recover for 2 or 3 hours post irradiation (Figure 30).

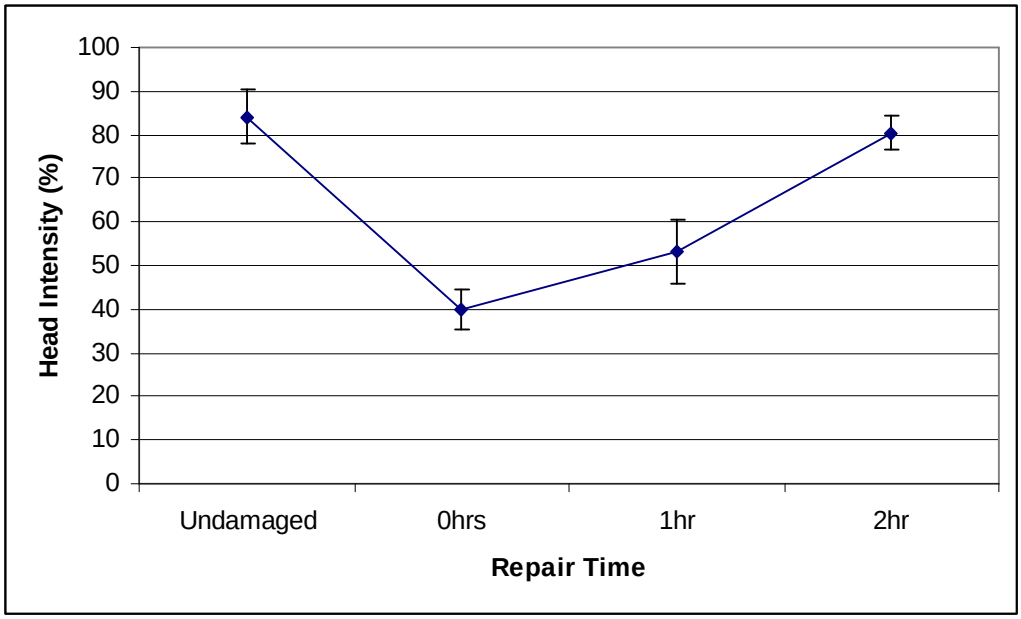

Figure 29: **Alkaline comet assay repair curve**. *HeLa cells were damaged with 5 Gy gamma radiation. Cells were collected at 0hrs, 2hrs and 3hrs after damage. The graph shows the average head intensity of 30 cells imaged at each time point. The data are presented as the mean and standard deviation of 30 cells analysed for each time point. The experiment was repeated twice.*

(A)

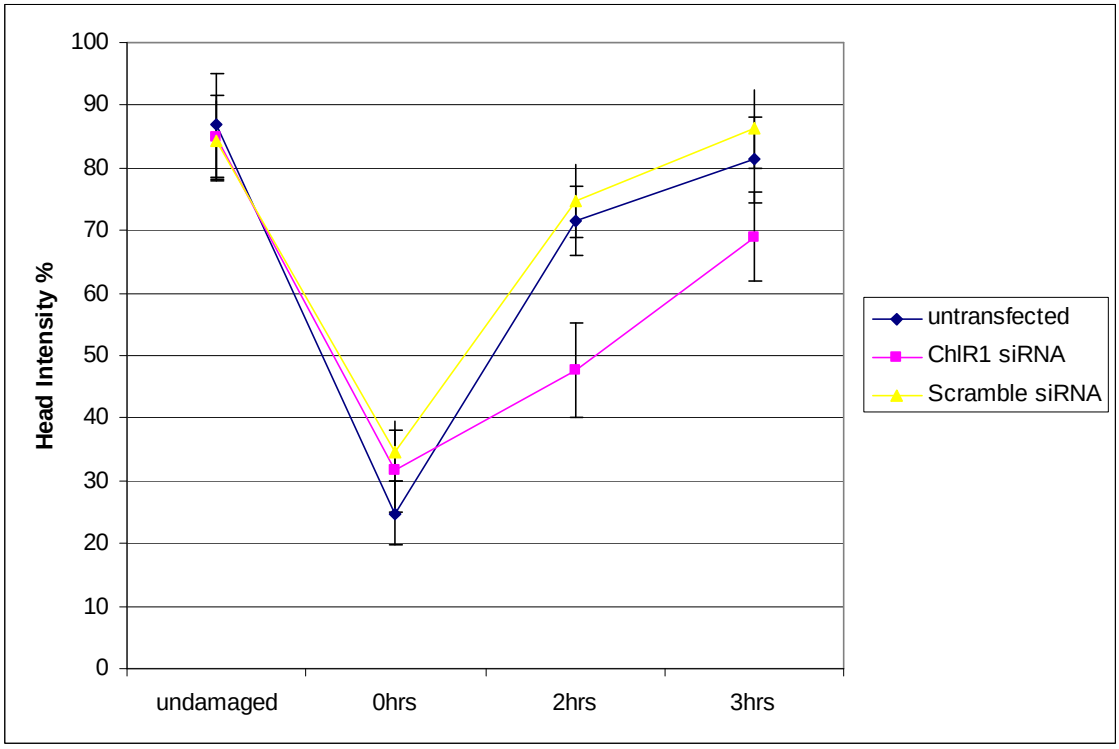

(B)

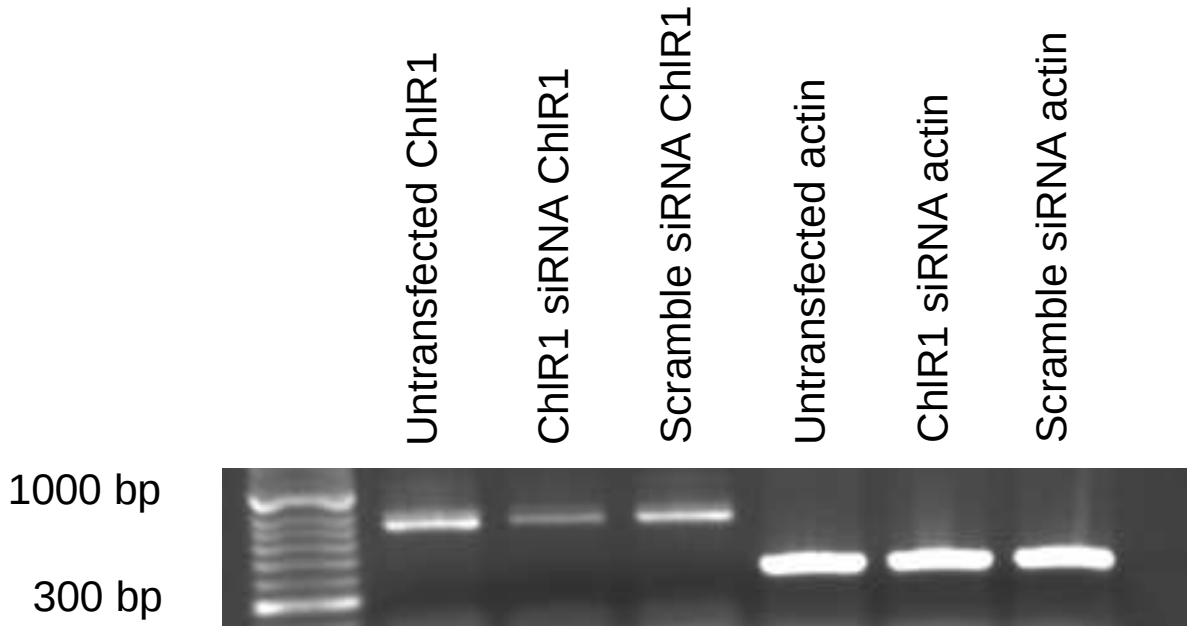

Figure 30: **Alkaline comet assay following ChlR1 depletion**. *HeLa cells were transfected with 100nM of ChlR1 or scrambled siRNA oligonucleotides and damaged with 5 Gy gamma radiation. The repair of the transfected cells was compared to untransfected cells. Cells were imaged at 0, 2 and 3 hours after damage. (A) Shows the average head intensity of 30 cells imaged at each time point for each control. The data represents the mean and*

standard deviation of the cells analysed for each time point in 3 experiments (B) RT-PCR was used to show the level of ChlR1 mRNA (700base pair product) in the cells used in this assay. Quantification of intensity of the RT-PCR products revealed that there was a 70% reduction in ChlR1 mRNA levels in the ChlR1 siRNA sample compared to the scrambled siRNA sample. β-actin (300base pair product) was used as a control for input of DNA to each reaction.

The data in Figure 30 show that there is a delay in the repair of the DNA damage in the ChlR1 siRNA transfected cells compared to the untransfected cells and control siRNA transfected cells. The control cells have repaired the DNA damage after 2 hours but the ChlR1 siRNA transfected cells require 3 hours to repair.

To determine whether ChlR1 specifically plays a role in the repair of double strand breaks, the neutral comet assay in cells depleted of ChlR1 and exposed to ionising radiation was used. The first step in optimising the neutral comet assay was to determine a suitable dose of radiation to use in the repair assay. The dose of radiation used in this assay is larger than the dose used in the alkaline comet assay. This is due to the fact that it measures only DNA double strand breaks. DNA double strand breaks occur at a ratio of approximately 1 to every 500 single strand breaks. Therefore the dose had to be increased to see an effect in the comet assay. Therefore we performed a dose response curve in which the cells were irradiated with a variety of doses ranging from 5 to 30 Gy.

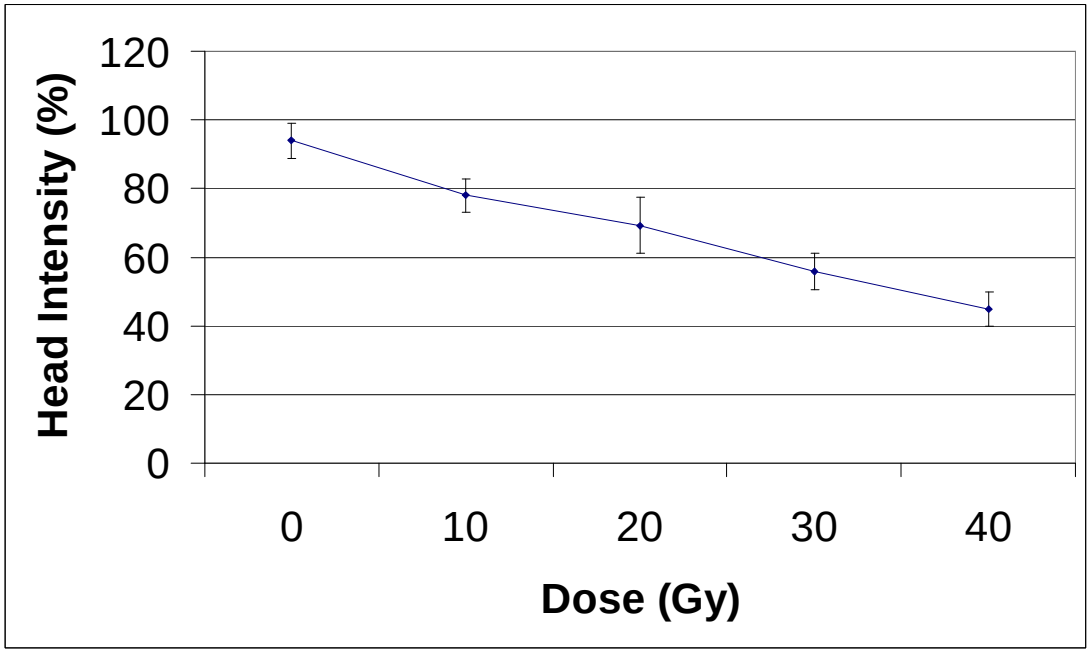

Figure 31: **Neutral comet assay dose response curve**. *HeLa cells were damaged with different doses of gamma radiation and subjected to the neutral comet assay. The graph shows the average head intensity and standard deviation of 30 cells imaged for each dose. The experiment was repeated twice.*

Figure 31 shows a linear relationship between the comet head intensity and the amount of ionising radiation used. The dose of 25 Gy resulted in a head intensity percentage of 60% deemed optimal for this assay because it was the percentage used in the alkaline comet assay.

I next examined the length of time required for the cells to recover from the dose of 25 Gy. Cells were irradiated with a dose of 25 Gy and incubated in medium at 37ºC for a range of time points.

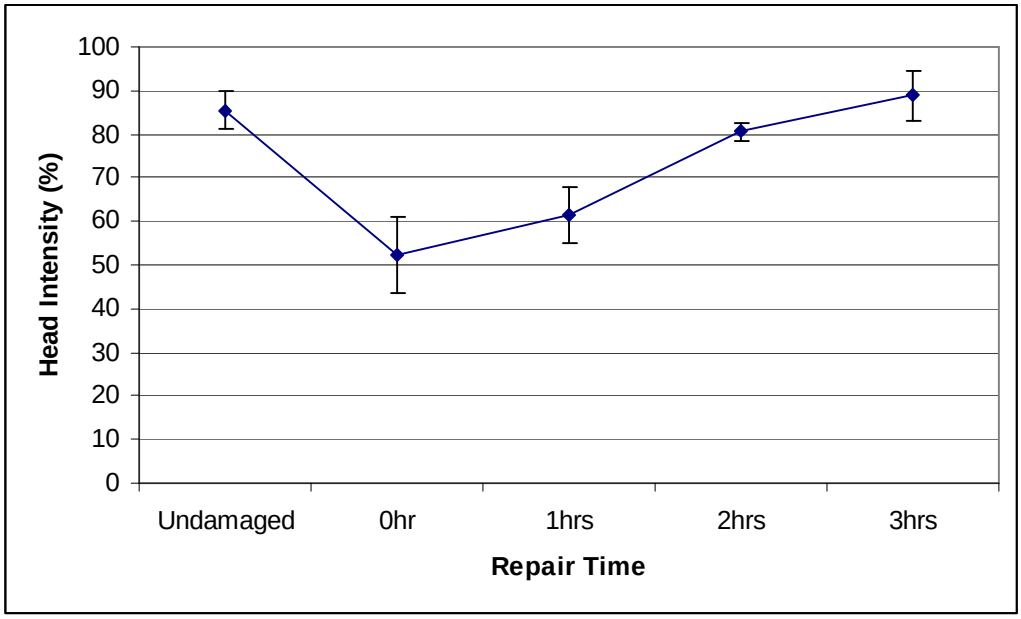

Figure 32: **Neutral comet assay repair curve**. *HeLa cells were damaged with 25 Gy gamma radiation. Cells were imaged 0, 2 and 3hrs after damage. The graph shows the average head intensity and standard deviation of 30 cells collected at each time point. The experiment was repeated twice.*

Figure 32 shows the head intensity of the undamaged cells is 85% and after irradiating the cells it takes three hours for the damage to repair to the same level as the undamaged cells. Having optimised the neutral comet assay, I performed repair assays on cells transfected with ChlR1 and control (scrambled) siRNA oligonucleotides. Cells were transfected and incubated for 24 hours. Then the cells were irradiated with 25 Gy ionising radiation dose and allowed to recover for 2 or 3 hours (Figure 33).

(A)

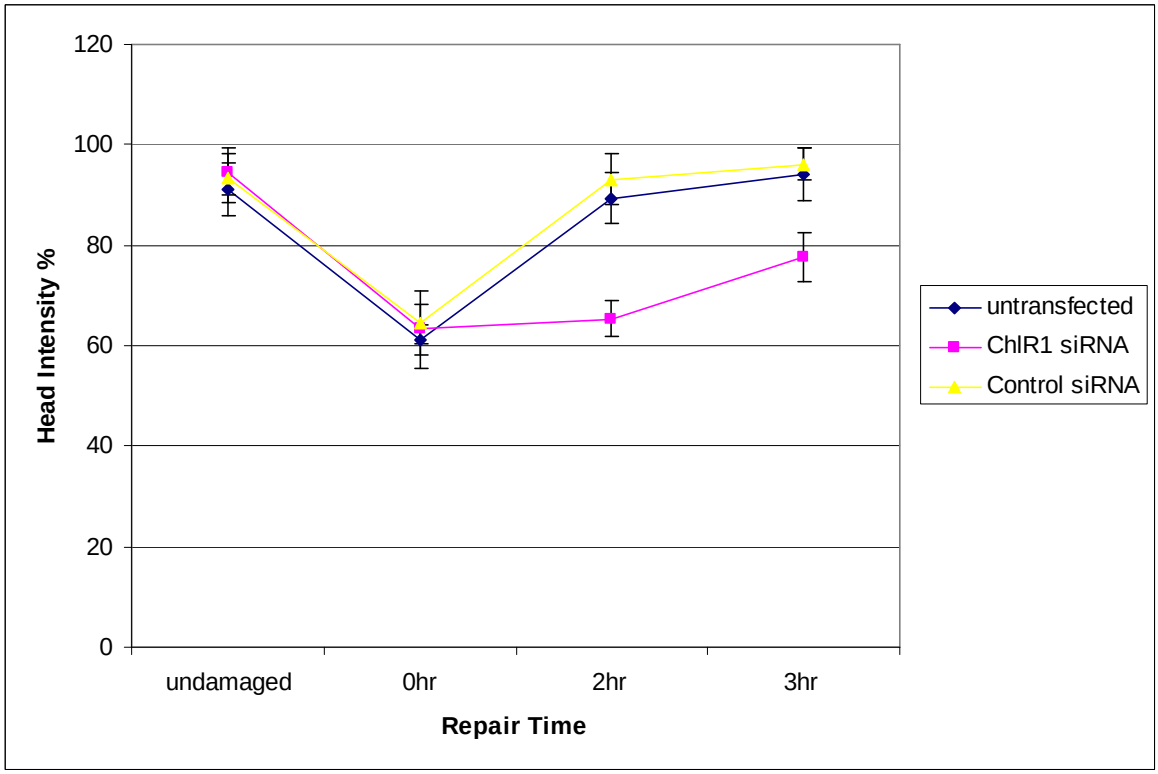

(B)

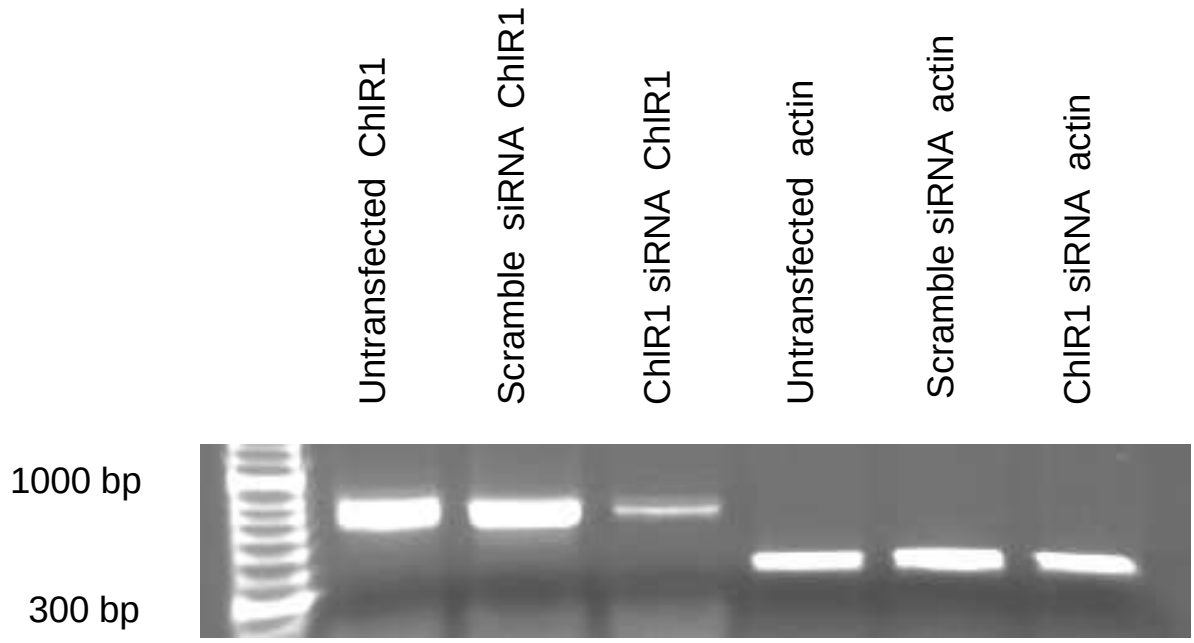

Figure 33: **Neutral comet assay following ChlR1 depletion**. *HeLa cells were transfected with 100nM of 5' UTR specific ChlR1 or scrambled siRNA oligonucleotide and damaged with 25 Gy gamma radiation. The repair of the transfected cells was compared to*

untransfected cells. Cells were collected 0, 2 and 3 hours after damage. (A) Shows the average head intensity and standard deviation of 30 cells collected at each time point for each control in 3 experiments. (B) RT-PCR was used to show the level of ChlR1 mRNA (700 base pair product) in the cells used in this assay. Quantification of intensity of the RT-PCR products revealed that there was an 85% reduction in ChlR1 mRNA levels in the ChlR1 siRNA sample compared to the scramble siRNA sample. β-actin (300base pair product) was used as a control for input of DNA to each reaction.

The data presented in Figure 33 show that there is a delay in the repair of the DNA double strand breaks in the ChlR1 siRNA transfected cells compared to the untransfected and control siRNA transfected cells. The control cells repair the DNA double strand breaks after 2 hours. However the DNA double strand breaks have not been fully repaired after 3 hours in the ChlR1 siRNA transfected cells. This suggests that ChlR1 has a function in the repair of DNA double strand breaks. The delay in single strand break repair seen in ChlR1 depleted cells is less significant that the delay seen in the repair of DNA double strand breaks suggesting that ChlR1 functions in the repair of DNA double strand breaks. The next step was to define the precise role of ChlR1 in the repair of DNA double strand breaks.

4.4 The Function of ChlR1 in DNA Damage Repair

The data in figure 33 shows that ChlR1 has a role in DNA double strand break repair but the function in this process is unclear. The hypothesis that ChlR1 is involved in the recruitment of the cohesin complex to DNA double strand breaks has been discussed above and would require that ChlR1 protein is also recruited to DNA double strand breaks. Therefore the first step in investigating a function for ChlR1 in DNA damage repair was to show that ChlR1 was recruited to DNA double strand breaks.

I planned to use immunofluorescence to investigate the theory that ChlR1 is recruited to sites of DNA double strand breaks. DNA double strand breaks can be visualised by immunofluorescence using an antibody that recognises the phosphorylated version of H2AX. The histone H2AX is phosphorylated in megabase regions around a DNA double strand break [312]. A serine at amino acid 139 is phosphorylated [312] by the PIKKs protein kinases ATM, ATR and DNA-PKcs [313]. $H2AX^{-/-}$ knockout mice are radiosensitive [314]. H2AX is believed to be phosphorylated around the breaks to recruit chromatin remodelling factors to the sites of double strand breaks [315]. These chromatin remodelling factors have been shown to convert double stranded DNA into single stranded overhangs at double strand break ends [316] which allows the repair enzymes involved in HR and NHEJ access to the DNA around breaks. Therefore using an antibody specific for the phosphorylated serine 139 residue, I can look at the number of DNA double strand breaks after DNA damage.

To optimise the antibody concentration required for the detection of gamma H2AX foci, the H2AX specific antibody was used at a concentration of 1 in 50 and the FITC conjugated anti-mouse secondary was used at a concentration of 1 in 150. The fixing and washing conditions for the assay are described in the Materials and Methods.

(a)

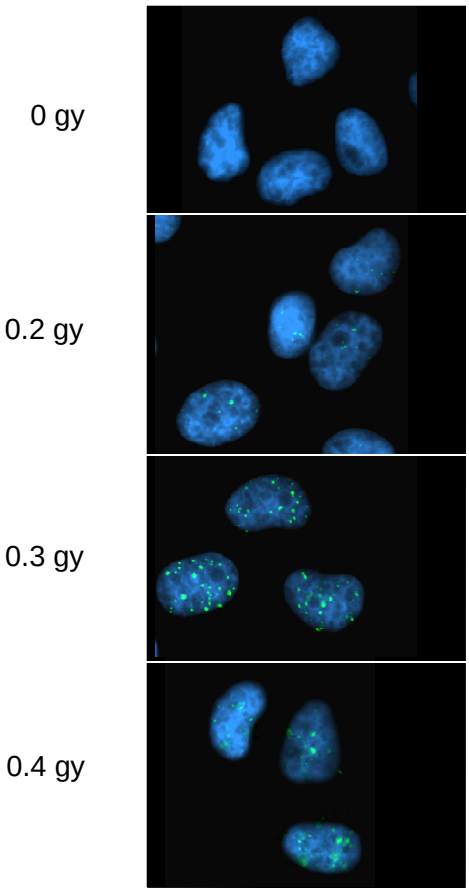

(b)

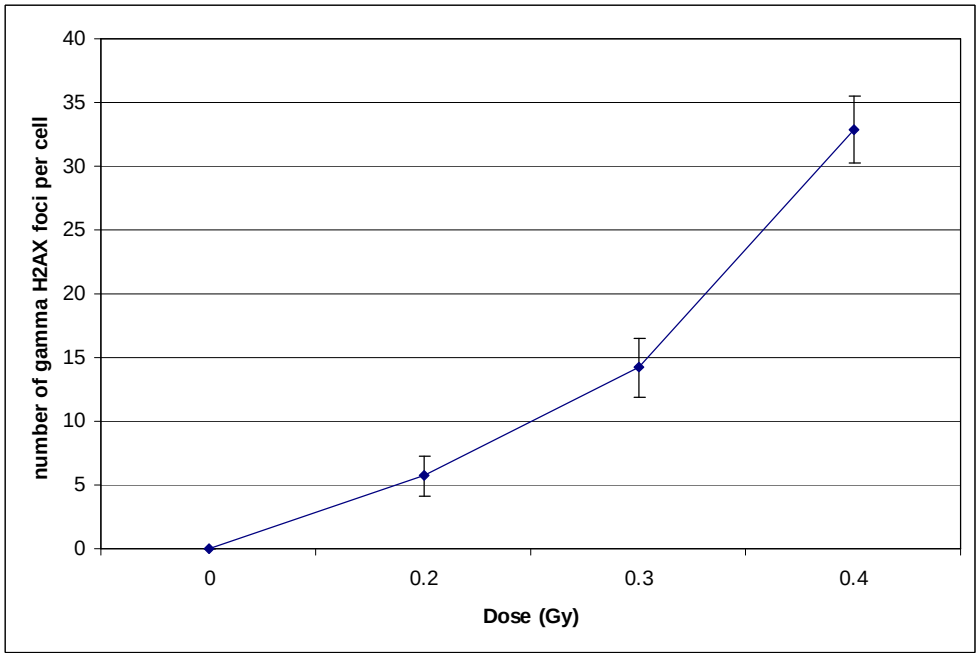

Figure 34: **HeLa cells damaged with increasing doses of gamma radiation and stained with gamma H2AX antibody by immunofluorescence**. (a) *DNA was stained with hoescht 33342 (blue). Gamma H2AX was visualised by immunofluorescence using gamma H2AX specific antibody and a FITC conjugated anti-mouse secondary antibody (green). Images were captured on a Zeiss epifluorescent microscope fitted with a FITC filter set and a 63x objective. As the dose increases there is an increase in the number of green foci. (b) Shows the average number of gamma H2AX foci per cell for each dose of radiation. The data are presented as the mean and standard deviation of 30 cells analysed for each data point.*

Figure 34 shows that the gamma H2AX antibody used was specific and that gamma H2AX foci were detectable with the concentrations of antibodies used. The number of foci increases as the dose of radiation increases. Conversely, no foci were visible in the undamaged cells. Therefore using these conditions I attempted to show the recruitment of ChlR1 to gamma H2AX foci by immunofluorescence. However the ChlR1-specific antibodies available are not suitable for immunofluorescence. Therefore I created a mCherry-ChlR1 expression construct that expresses ChlR1 with mCherry fused at the N terminus.

To confirm that the mCherry-ChlR1 expressed in mammalian cells, HeLa cells were transiently transfected with mCherry-ChlR1 using Fugene transfection reagent and expression of mCherry-ChlR1 is clearly demonstrated by epifluorescent microscopy (Figure 35).

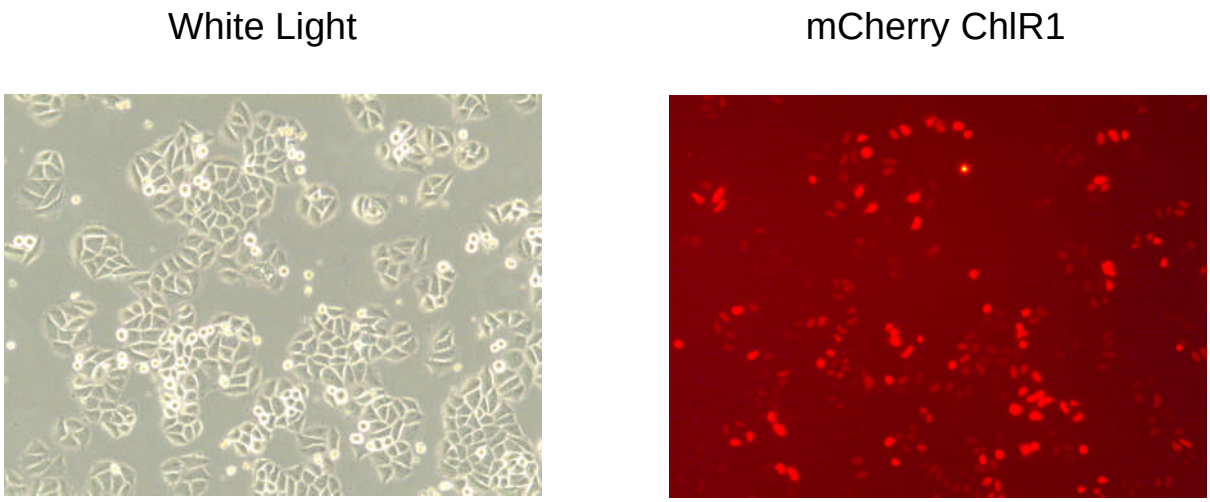

Figure 35: **Expression of HA-FHL2 in HeLa cells**. *HeLa cells were transfected with 7µg of pmCherry-N1-ChlR1. Images were captured after 24 hours on a Zeiss epifluorescence microscope fitted with a TRITC filter set and a 10x objective.*

Figure 35 shows robust expression of the mCherry-ChlR1 in HeLa cells. Therefore using this construct I could perform the experiment described above where HeLa cells transfected with the mCherry-ChlR1 construct would be damaged with 0.3 Gy of gamma radiation and stained with gamma-H2AX antibody.

Unfortunately, I was unable to show localisation of mCherry ChlR1 to gamma H2AX foci in asynchronously growing irradiated cells. Therefore, I attempted to damage cells that were synchronised in either S phase or G_2/M to determine whether the localisation of

ChlR1 to DNA double strand breaks was cell cycle specific. Again I was unsuccessful in showing the localisation of ChlR1 to gamma H2AX foci following these changes.

There are several potential reasons as to why I was unable to show ChlR1 localisation to gamma H2AX foci. Indeed ChlR1 may not localise to these repair foci. However, the negative results obtained above could also be explained by the possibility that the localisation of ChlR1 may be dynamic and occur only over a short period of time and therefore difficult to view. Another problem may be the sensitivity of the assay used as ChlR1 may be present at damage sites in very small quantities. Finally the mCherry tag may have affected the localisation of the ChlR1 fusion protein.

Therefore the experimental design was changed to look at whether ChlR1 depletion disrupted the localisation of Smc1 at sites of DNA damage. Smc1 has previously been shown to be localised to gamma H2AX by immunofluorescence [206]. The DNA damage was induced using laser microirradiation. This involves the tracking of a high intensity laser across cells. It results in a large dose of radiation across a small area of the cell. This requires an expensive stage and software for a confocal microscope. Therefore using an antibody specific for Smc1, I performed immunofluorescence on HeLa cells irradiated with 0.3 Gy to show localisation of the cohesin subunit to gamma H2AX foci. Unfortunately, I was unable to show localisation of Smc1 to gamma H2AX foci.

Interestingly, a second group using the laser microirradiation method described above, also failed to detect Smc1 at sites of DNA damage. Instead they reported the co-localisation of a phosphorylated Smc1 subunit with gamma H2AX by laser microirradiation [258]. As described in the introduction Smc1 and 3 are phosphorylated in an ATM dependent manner [262]. Smc1 is phosphorylated at serine 957 (one of ATM target sites) at gamma H2AX foci [258].

Therefore my experimental design was further changed to determine whether ChlR1 knockdown disrupted the phosphorylation of Smc1 at sites of DNA damage. Using the antibody specific for phosphorylated Smc1, I performed immunofluorescence on HeLa cells irradiated with 0.3 Gy to show localisation of the cohesin subunit to gamma H2AX foci. Again I was unable to show localisation of phosphorylated Smc1 to gamma H2AX foci. Therefore I then attempted to damage cells in synchronised in S or G_2/M phase to identify if the localisation of phosphorylated Smc1 to DSB was cell cycle specific. These changes were again unsuccessful in showing localisation of phosphorylated Smc1 to gamma H2AX foci.

Due to the problems with detecting either endogenous ChlR1 localisation by immunofluorescence or visualising the localisation of mCherry-ChlR1 to double strand breaks I attempted to use a ChIP assay to detect the presence of ChlR1 on the DNA surrounding a double strand break. A U20S derived cell line with the *E.coli* derived Tetrocyclin (Tet) operator inserted into the genome was used (shown in Figure 36). This cell line was created and provided by Dr Ciarian Morrison University of Galloway. The cell line also stably expresses the Tet repressor protein as a GFP fusion which enables the integrated operator sequence to be visualised. Located just upstream of the operator is a Sce-I endonucloease recognition sequence [260]. There are no Sce-I recognition sequences found in the human genome therefore the inserted recognition sequence is unique. This means that only one cut site is created in this assay.

The plasmid which expresses the Sce-I endonuclease fused to a glucocorticoid receptor (GR) is transfected into the cells, which are then treated with triamcinolone acetonide (TA) for 30 minutes to stimulate nuclear localisation of the endonuclease. This leads to the

creation of a DNA double strand break within the genome that can be visualised by confocal microscopy.

To perform the ChIP assay, primers were designed that anneal to the DNA upstream of the Sce-I restriction site. If this upstream region of DNA could be immunoprecipitated with a ChlR1 antibody, then ChlR1 associates with the regions around the cut sites. Primers were also designed that flank the Sce-I restriction site to confirm that the DNA was specifically restricted after treatment of the cells with TA. If the DNA is cut efficiently, there will be a break in the DNA between the primers used to amplify the DNA and therefore there should be no PCR product after TA treatment.

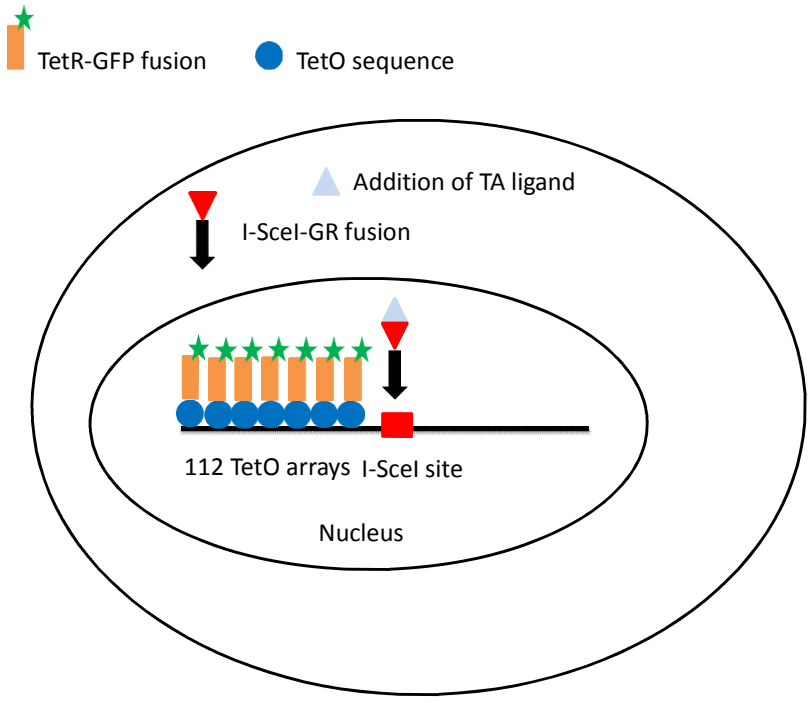

Figure 36: **Schematic representation of the integrated Tet Operator with the Sce-I restriction enzyme recognition sequence adjacent in U2OS cells**. *pBluescript vector was engineered to contain 112 repeated Tet operators upstream of the multiple cloning site (MCS) and the Sce-I restriction enzyme recognition sequence inserted into the MCS. This vector was linearised and inserted into the genome of a U2OS cell line. These cells were then transfected with a plasmid that expressed GFP tagged Tet repressor protein and transfected cells were selected. The inserted Tet operator can be visualised by GFP foci.*

The double strand break is created upon the addition of triamcinolone acetonide (TA; ligand). This results in the nuclear localisation of the Sce1 endonuclease and the creation of the cut [260].

We received 3 clones of the U2OS cell line with the integrated I-SceI and associated Tet array from the Morrison research group (University of Galloway) [260]. To confirm the Tet operator array was still integrated into the genomes of each of the clones, cells of all three clones were fixed and stained with Hoechst 33342 to stain the DNA. Cells were visualised by confocal microscopy to confirm that the expected number of GFP foci were present (Figure 37).

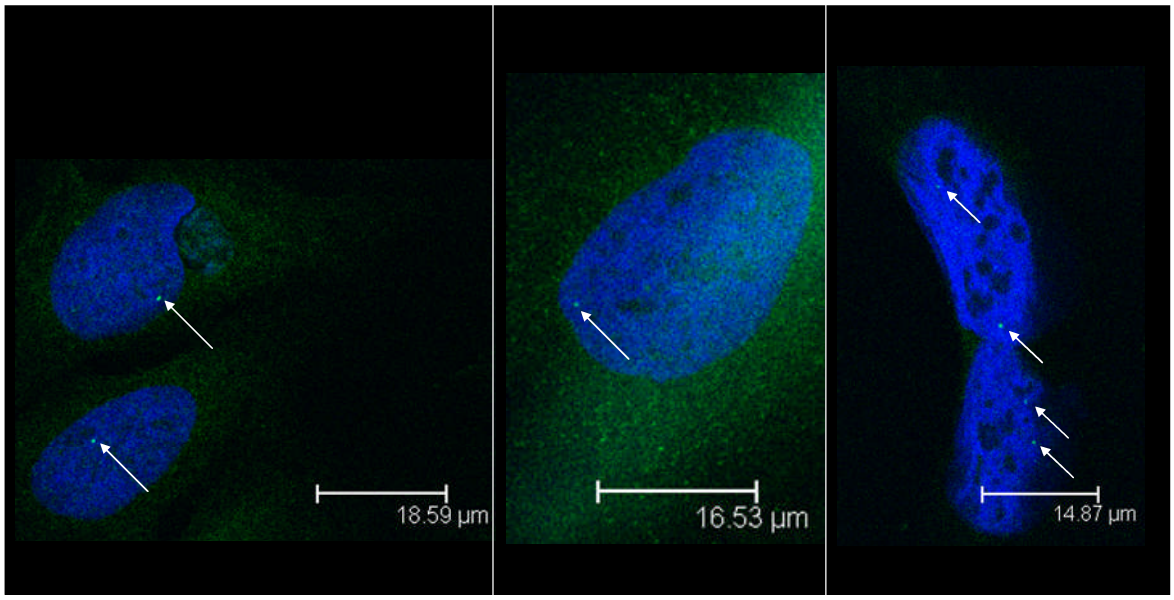

Figure 37: **Localisation of TetR-GFP foci in U2OS TetO/R I-Sce clones**. *The U2OS TetO/R integrated cells were subjected to 1 week selection with 0.4mg/ml G418. The cells were then fixed and stained with Hoechst 33342 (blue). GFP-TetR associates with the integrated Tet operator and the resulting GFP foci (green) were imaged using a Leica confocal microscope. The white arrows indicate the position of the foci.*

Figure 37 confirms the Tet operator arrays are still integrated into the three clones of U2OS TetO/R I-Sce cells and the integration sites can be visualised by confocal

microscopy. Clones 8 and 11 contained one integrated Tet O/R site, whereas clone 12 contained two integration sites. I decided to use clone 12 for the ChIP assays as there are two integration sites making it easier to ChIP, as there is more template compared to the clones with one integration sites.

To carry out the ChIP experiments, I had to confirm that the primers designed to amplify a region of DNA adjacent to the Sce-I restriction site yielded a PCR product of the correct size. The primer sequences are shown in the Materials and Methods. Genomic DNA was extracted from clone 12 of the U2OS Tet O/R I-SceI cells which had been grown 1 week in G418 selection and a PCR reaction performed using primers that were designed for the ChIP assay and primers that were designed to flank the cut site.

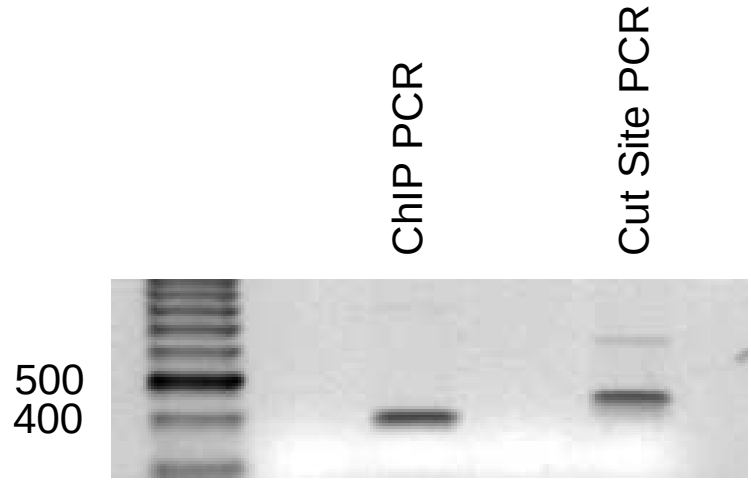

Figure 38: **PCR amplification of integrated sequence**. *U20S TetO/R I-sceI cells were subjected to selection in 0.4mg/ml G418 for 1 week. Genomic DNA was extracted from the selected cells. A product of approximately 400 base pairs is present in the reaction using primers that were designed for the ChIP experiment that anneal immediately upstream of the I-SceI restriction site. A PCR product of approximately 450bp is present in the reaction using the PCR primers that flank the I-SceI restriction site.*

Figure 38 shows that the primers that were designed for the ChIP assay and those that were designed to amplify the region containing the I-SceI restriction site worked on the genomic DNA extracted from the U2OS Tet O/R I-SceI cell line, yielding a product of the correct

size in the PCR reaction. Using clone 12 and the primers that amplify across the cut site, I subsequently showed that the endonuclease efficiently cuts the DNA. The G418 selected cells were incubated with 100nM TA for 1 hour and the genomic DNA was extracted and PCR performed with the primers that flank the I-SceI site (Figure 39).

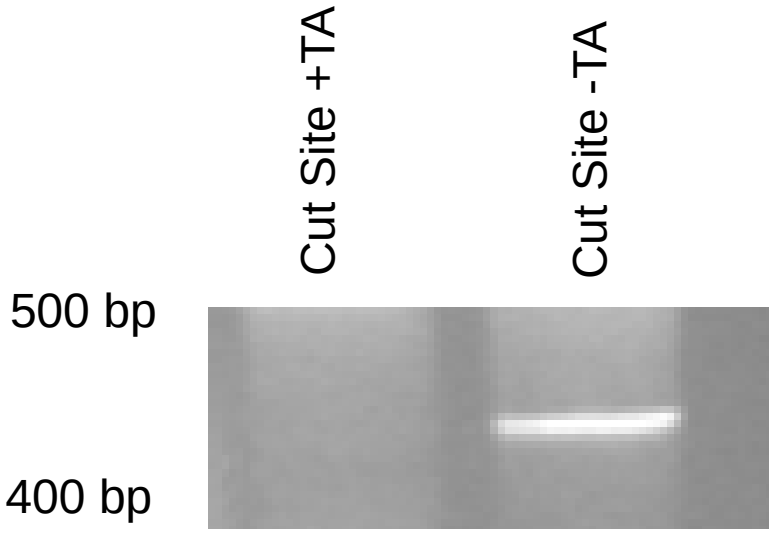

Figure 39: **PCR amplification of the Sce-I cut site on DNA extracted from U2OS TetO/R I-SceI cells with and without TA treatment**. *U2OS TetO/R I-SceI cells were subjected to selection with 0.4mg/ml G418 for 1 week and transfected with a plasmid expressing the Sce-I endonuclease fused to GR. Genomic DNA was extracted from the selected cells after treatment with 100nM triamcinolone acetonide (TA) for 1 hour, which promotes nuclear entry of the GR fused enzyme. PCR amplification was performed using the primers across the cut site. A PCR product of around 450 base pairs is present in the non-treated cells but absent in the TA treated cells.*

Figure 39 shows that after treatment of the cells with TA for 1 hour the PCR product is no longer present. This confirms that the endonuclease has been transported to the nucleus and restricts the DNA between the annealing sites of the two PCR primers. I next needed to confirm that the cut in the DNA created by the Sce-I endonuclease was recognised as a double strand break by the cell. To confirm this I transfected U2OS TetO/R I-SceI cells

with the I-SceI-GR expression plasmid and incubated these cells with TA for 1 hour. Cells were then fixed and stained with anti-gamma H2AX antibody and Alexa 647 conjugated anti-mouse secondary antibody too visualise H2AX phosphorylation at the cut site.

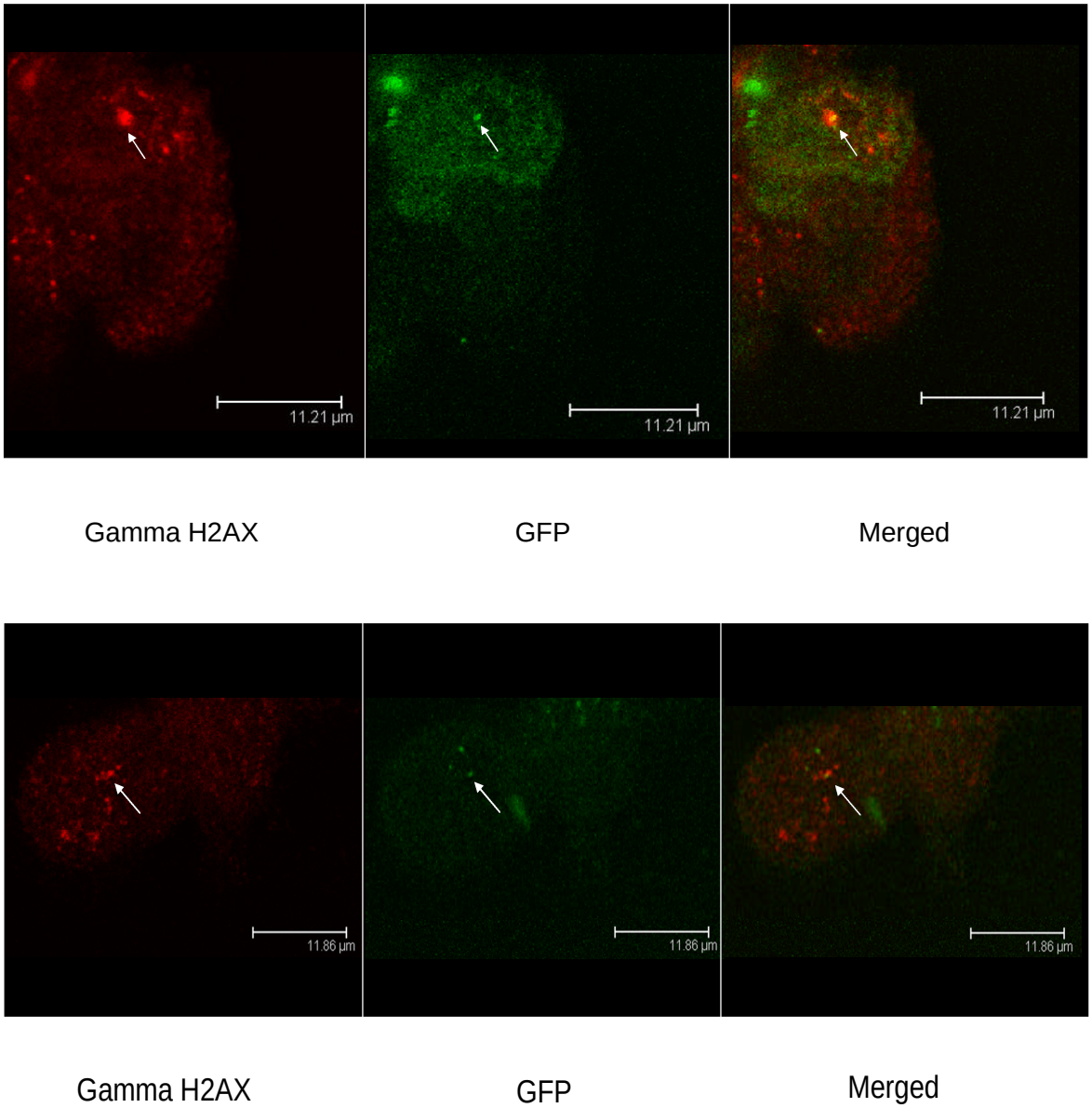

Figure 40: **The phosphorylation of H2AX to the TETO/R I-SceI GFP integration site after nuclear localisation of the SceI restriction enzyme**. *U2OS TET O/R cells were subjected to selection with 0.4mg/ml G418 for 1 week and transfected with the Sce1-GR endonuclease. The cells were treated with 100nM TA for 1 hour and then fixed. The cells were stained with a mouse anti- gamma H2AX antibody. Alexa 647 conjugated anti-mouse*

secondary antibody was used to visualize the phosphorylated H2AX. Phosphorylation of H2AX at the GFP foci is indicated by the white arrows.

The data in figure 40 show that H2AX is phosphorylated at the Sce-I restriction site. This suggests that the cell recognises the cut in the DNA as a DNA double strand break and processes it in the normal pathway of DNA double strand break repair. This confirms that the ChIP experiment planned is feasible. Therefore if ChlR1 is recruited to DNA double strand breaks then it will be recruited to this cut site. This result also confirms that gamma H2AX could be used as a positive control in the ChIP experiment.

With the conditions to create the cut and the PCR optimised, I performed the ChIP assay using quantitative PCR (qPCR) to amplify the immunoprecipitated DNA fragments. The chromatin preparations were prepared from G418 selected U2OS TetO/R I-SceI cells using the method described in the Materials and Methods. I attempted to precipitate the DNA around the Sce-I restriction site with ChlR1 specific antibodies, in addition to phosphorylated Smc1 and gamma H2AX antibodies which were used as positive controls, and a non-specific FLAG antibody as a negative control. The DNA in the immunoprecipitated samples was then de-proteinated and purified by phenol chloroform extraction and ethanol precipitation. qPCR reactions were then set up with the primers that anneal adjacent to the Sce-I restriction site.

Unfortunately, although the experiment was repeated several times with several modifications in an attempt to optimise the assay the ChIP experiment was unsuccessful and amplification of the DNA using the ChIP primers was not achieved. There was no amplification of the input DNA, which is taken from the chromatin preparation before immunoprecipitation and contains all the DNA in the cells. This suggests there was not enough PCR template in the genomic DNA for the PCR to amplify the ChIP specific region. The protocol was adjusted to include the use of more cells for the chromatin

preparation. Initial cells were harvested from one 10cm tissue culture dish. This was increased to three 10cm dishes in the hope that the input DNA could be amplified from this amount of DNA. Also the percentage of the input DNA used in the PCR reaction was increased from 5% to 30%.

These changes in the protocol had no effect on the amplification of the DNA around the Sce-I cut site and there was no amplification seen in the input samples. The plan to explore the hypothesis that ChlR1 is recruited to DSB by ChIP was therefore changed.

Using immunofluorscence I explored the use of the U2OS Tet O/R I-SceI cell line to show the recruitment of phosphorylated Smc1 to DNA double strand breaks. Immunofluorescence was performed on U2OS TetO/R I-SceI cells, which had been transfected with the plasmid expressing the GR fused Sce-I endonuclease and treated with TA, using an antibody specific for the phosphorylated form of Smc1. If detection of phosphorylated Smc1 at the Sce-I site using immunofluorescence was possible, this assay could then be used to examine if the depletion ChlR1 resulted in the disruption of the phosphorylation of Smc1 at DSBs.

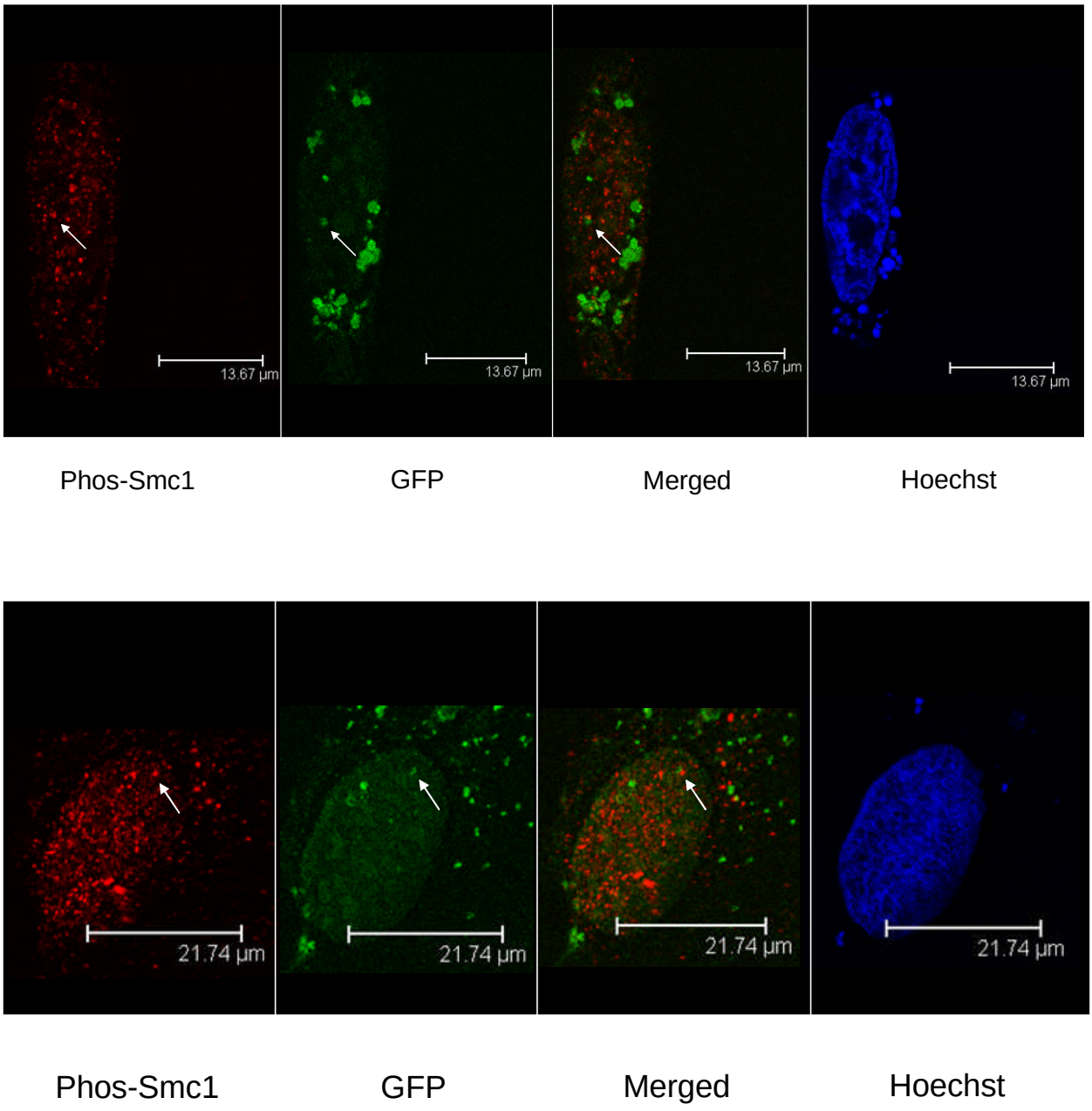

Figure 41: **The recruitment of phosphorylated Smc1 to the TetO/R I-SceI GFP integration site after nuclear localisation of the SceI enzyme**. *U2OS Tet O/R cells were transfected with the Sce1-GR endonuclease and subjected to selection with 0.4mg/ml G418 for 1 week. The cells were treated with 100nM triamcinolone acetonide (TA) for 1 hour and then fixed. The localisation of phosphorylated Smc1 was visualised by immunofluorescence. Alexa 647 conjugated rabbit secondary antibody was used to visualise the phosphorylated Smc1 (red) and localisation of phosphorylated of Smc1 at the GFP foci (green) is indicated by the white arrows. The DNA is stained with Hoescht 33342 (blue).*

Figure 41 shows that upon creation of the DSB, Smc1 is phosphorylated at the site of the Tet O/R I-SceI. Using this cell line I was therefore able to explore the hypothesis that ChlR1 is recruited to sites of DNA damage to facilitate the repair, as discussed in the introduction. The U2OS TetO/R I-SceI cell line was used to determine whether ChlR1 is recruited to DNA double strand breaks. Immunofluorescence was performed on U2OS TetO/R I-SceI cells, which had been transfected with the plasmid expressing the GR fused I-SceI endonuclease and treated with TA, using an antibody specific for the ChlR1 protein. The ChlR1 antibody was raised from rabbits inoculated with a purified fragment of the ChlR1 protein (amino acids 1-133).

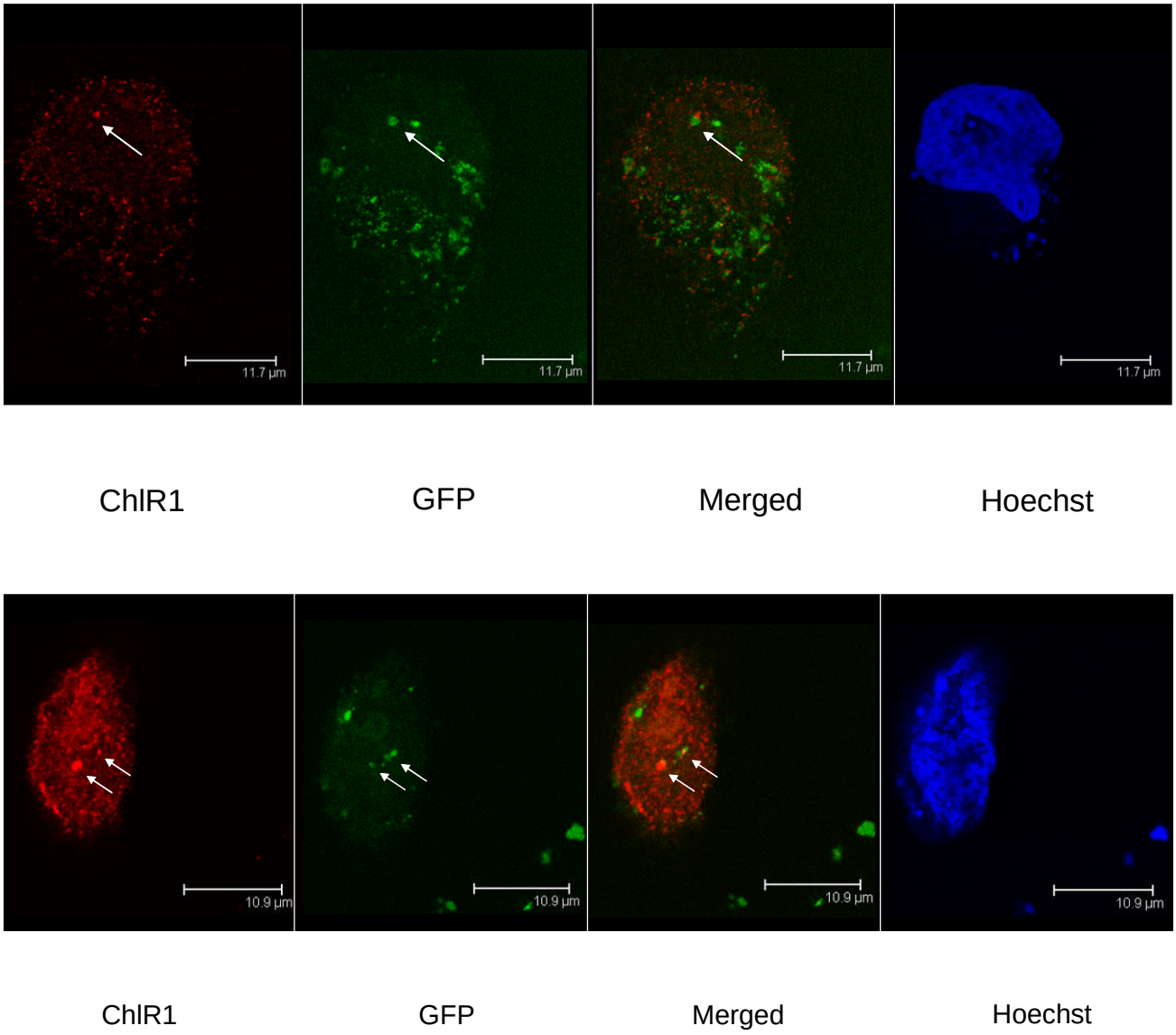

Figure 42: **The recruitment of ChlR1 to the TetO/R I-Sce GFP integration site after nuclear localisation of the Sce1 enzyme**. *U2OS TET O/R cells were transfected with the Sce1-GR endonuclease and subjected to selection with 0.4mg/ml G418 for 1 week. The cells were treated with 100nM triamcinolone acetonide (TA) for 1hour and then fixed and stained. The localisation of ChlR1 was visualised by immunofluorescence using rabbit ChlR1 130 antibody. An Alexa 647 conjugated rabbit secondary antibody was used to visualize the ChlR1 (red) and localisation of ChlR1 at the GFP foci (green) is indicated by the white arrows. The DNA is stained with Hoescht 33342 (blue).*

Figure 42 shows that upon creation of the DNA double strand break, ChlR1 was recruited to the site. Overall the U2OS TetO/R I-SceI cell line has been used to show that upon induction of the DNA double strand break by addition of Sce-I restriction enzyme, H2AX,

phosphorylated Smc1 and ChlR1 are recruited to the break. This indicates that the U2OS cell line can be used to examine if the phosphorylation of Smc1 at sites of double strand breaks is disrupted when ChlR1 is depleted. This would resolve the suggested hypothesis that ChlR1 has a role in recruiting the cohesin complex to DNA double strand breaks. ChlR1 interacts with DNA-PKcs (Feeney, unpublished), therefore ChlR1 may act as a linker between Smc1 and DNA-PKcs allowing DNA-PKcs to phosphorylate the cohesin subunit.

Chapter 5: The Role of ChlR1 in DNA Replication

5.1 Introduction

There is evidence to suggest that ChlR1 functions in DNA replication. Firstly, ChlR1 has been shown to interact with a number of proteins associated with the replication complex. These include Fen1, TopBP1, PCNA and the MCM complex, the functions of which are explained in the introduction. The interaction of ChlR1 with PCNA and the MCM complex was isolated during a TAP-ChlR1 purification experiment designed to isolate interacting partners of ChlR1 (Feeney and Parish, unpublished). The interaction of ChlR1 with Fen1 is discussed in the introduction. These interactions suggest a role for ChlR1 in DNA replication. An interaction with TopBP1 has been demonstrated by co-immunoprecipitation (Feeney and Parish, unpublished) and suggests that ChlR1 may have a role in restarting stalled replication forks because TopBP1 has a major role in the restarting of stalled replication as discussed earlier. This hypothesis is consistent with the results in Chapter 4 that suggest ChlR1 function is important in the DNA damage response since stalled replication forks account for a large percentage of DNA double strand breaks.

A number of related DNA helicases have a role in DNA replication. FANCJ has been shown to function in DNA replication checkpoint control. Like ChlR1, FANCJ interacts with TopBP1 [311] and FANCJ knockdown results in the inability of RPA to load onto the DNA. This is a prerequisite for ATR checkpoint activation. In fact FANCJ is involved in the phosphorylation of both Chk1 and RPA following replication stress [311]. Both TopBP1 and FANCJ have been shown to be involved in the early stages of replication stress checkpoint activation as ATR and RAD 9 (a member of the 9-1-1 complex discussed earlier) loading onto DNA [311].

Mutations in FANCJ are associated with the disorder Fanconi anaemia. Another protein associated with the disorder FANCM has been shown to have a role in replication restart after stalling [317]. In the absence of FANCM cells are unable to restart replication after stress. This is linked with the discovery that FANCM is crucial for the early stages of ATR checkpoint activation. It is involved in the chromatin retention of TopBP1 [317]. This suggests that replication does not restart because the damaged DNA that causes the stalling has not been repaired because the checkpoint is not appropriately activated.

RecF is a member of the recombination mediator proteins [318]. This family also includes BLM and WRN, both helicases that are related to ChlR1. RecF required for the maintenance of genome stability. The structure of RecF is similar to the DNA damage repair protein Rad50 [319]. Both these proteins contain a conserved ATP binding cassette ABC type ATPase. In *E.coli* when RecF is absent, replication fails to recover after UV damage [320]. Furthermore RecF is important in protecting the nascent DNA at stalled replication forks. In the absence of RecF in *E.coli* the nascent strand is degraded at these stalled replication forks [321]. It is believed that the ATP binding and ATP hydrolysis functions of the protein are required for fork stability and the resumption of replication. Point mutations within the ATP binding region of the protein results in the same effect seen in the absence of the protein [322]

The loading of cohesin onto DNA occurs after telophase. It has been shown that cohesin accumulates at sites approximately every 25kb in the human genome. In contrast to lower eukaryotes cohesin does not accumulate at sites of convergent transcripts in mammalian cells but accumulates at CTCF consensus binding sequences as discussed in the introduction [185]. This means the replication fork must pass through cohesin rings or that the ring has to transiently open to allow passage of the replication fork. Fork progression

through cohesin is also thought to be essential for generation of cohesion as trapping of nascent DNA strands within the cohesin ring generates functional cohesion [105]. Therefore a process must occur that allows for the replication fork to pass through the cohesin complex.

ChlR1 is a cohesin establishment factor and may have a role in the passage of the replication fork through the cohesin rings. A number of cohesion establishment factors have been shown to be associated with the replication fork complex and may also have a role in the progression of the replication fork through the cohesin complex.

Eco1 as discussed earlier is a cohesion establishment factor that is only required during S phase [106]. This suggests that Eco1 may have a role in the establishment of cohesion during DNA replication. This hypothesis is strengthened with the discovery of an interaction of Eco1 and PCNA. In addition mutations in Eco1 which are normally lethal in *S.cerevisiae* are viable when PCNA is overexpressed [323].

Another cohesion establishment factor that has links to the replication fork is Ctf4, a member of the replisome progression complex that associates with the GINS complex as well as the DNA polymerase α/primase [324]. Ctf18 is part of the replication factor C (RFC^{ctf18}) complex that is able to load PCNA onto DNA [325].

Eco1 Ctf4 and Ctf18 have been shown to localise to the replication forks in *S.cerevisiae* cells arrested in S phase with HU. In this assay, BrdU incorporated into newly synthesised DNA was immunoprecipitated with anti-BrdU antibodies. All three proteins were co-immunoprecipitated around the four early origins of replication on chromosome VI [105]. Interestingly Ctf4 was shown to promote Ctf18 recruitment. The co-immunoprecipitation of Ctf18 with newly synthesised DNA at replication origins was reduced in Ctf4 mutant cells [105]. Also the immunoprecipitation of newly replicated DNA with PCNA was

reduced in Ctf18 mutant cells, confirming that Ctf18 is involved in the recruitment of PCNA to the replication fork [105].

There are three theories as to how the replication fork passes through the cohesin complex. The first theory is that upon encountering the replication complex the cohesin complex disassociates with the DNA to allow for the replication complex to pass by. The cohesin complex then re-associates with the DNA after the replication complex passes. ChlR1 and other cohesin establishment factors are therefore thought to be present at the replication complex to allow for re-association of the cohesin complex.

The second theory is that the replication fork passes through the cohesin complex and the presence of the cohesin establishment factors prevents disruption of the association of cohesin and DNA as the replication complex passes through.

The final theory involves a conformational change in the cohesin complex to allow the replication complex through. Eco1 has been shown to acetylate Smc3. This is stimulated by Ctf18. Acetylated Smc3 does not associate with Wapl and Pds5A that are anti-establishment factors [10]. This may result in the conformation change in the cohesion ring that allows the passage of the replication complex through cohesin.

All three theories require the association of cohesin establishment factors with the replication complex. Current evidence suggests that ChlR1 associates with the replication complex and ChlR1 has a role in the passage of the replication complex through cohesin rich regions of the DNA.

5.2 Hypotheses and Aims

Hypothesis

ChlR1 has a role in DNA replication and the restarting of stalled replication forks.

Aims

To confirm this hypothesis I aimed to

1) Assay the effect of ChlR1 depletion on DNA replication using the DNA combing assay.

2) Assay the effect of ChlR1 depletion on restarting of stalled replication forks using the DNA combing assay on HU treated cells.

3) Confirm ChlR1 role in the repair of DNA damage is S phase specific using the DNA comet assay.

5.3 ChlR1 depleted cells display S phase DNA double strand break repair defects

The evidence from the literature above links ChlR1 to a role in DNA replication. ChlR1 function is important in the DNA damage responses (discussed in results chapter 2), and I hypothesised that this function of ChlR1 is DNA replication dependent. To test this hypothesis I performed the neutral comet assay on ChlR1 depleted HeLa cells synchronised in G_1 and S phase to investigate whether the deficient DNA double strand break repair responses in ChlR1 depleted cells was S phase dependent.

(a)

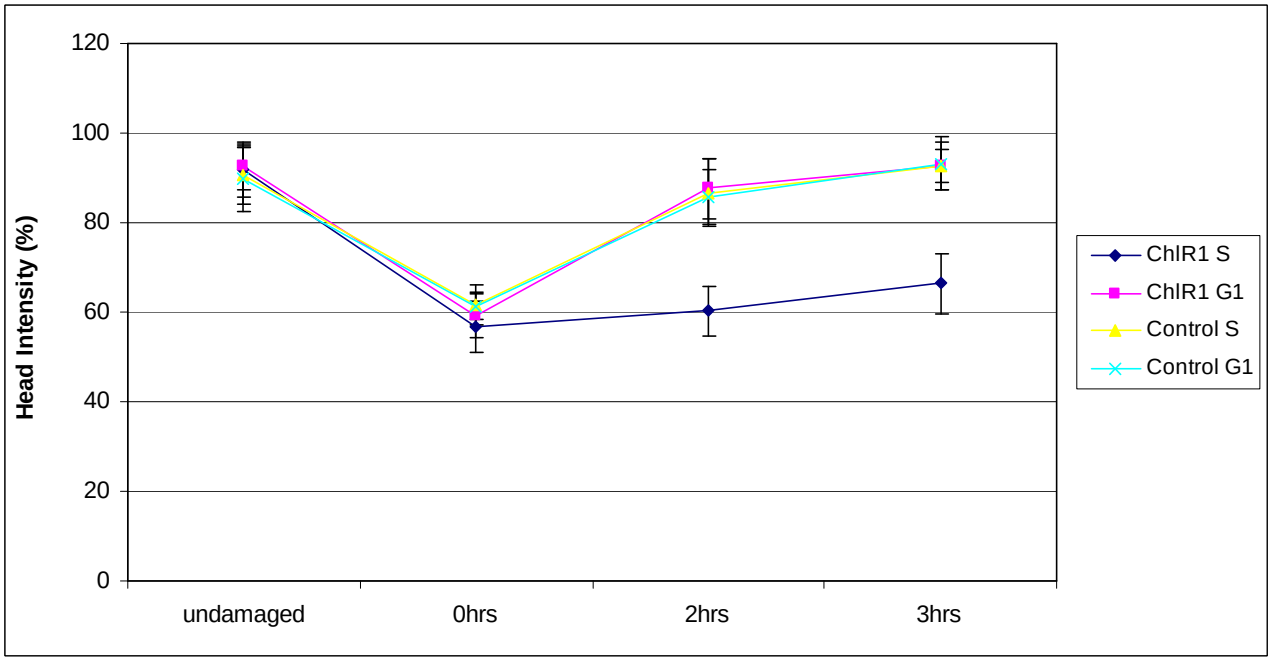

(b)

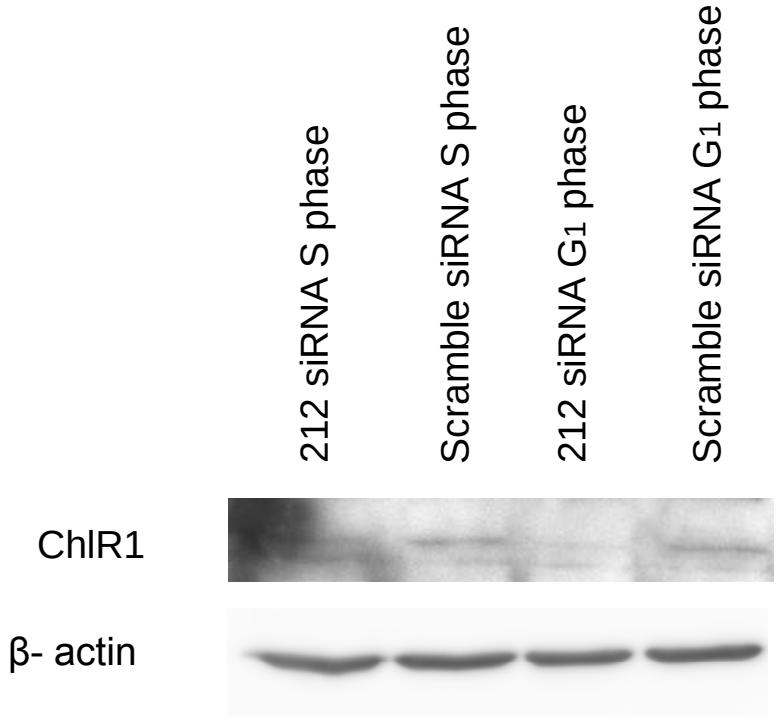

Figure 43: **Neutral comet assay following ChlR1 depletion**. *HeLa cells were transfected with 100 nM of 5' UTR specific ChlR1 or scrambled siRNA oligonucleotide and synchronised in either G_1 or S phase. The cells were damaged with 25Gy gamma radiation. The repair of the transfected cells was compared to untransfected cells. Cells*

were collected 0, 2 and 3 hours after damage. (A) Shows the average head intensity and standard deviation of 30 cells collected at each time point for each control. (b) Western blot showing the level of ChlR1 protein in the cells used in this assay. Rabbit specific ChlR1 antibody was used to detect endogenous ChlR1. A band of approximately 100 kDa is present in the control siRNA lane. This band is not present in the ChlR1 siRNA treated cells lane. This confirms ChlR1 protein is depleted in this assay.

Figure 43 shows there is a delay in the repair of DNA double strand breaks in the ChlR1 siRNA transfected cells synchronised in S phase compared to ChlR1 siRNA transfected cells synchronised in G_1 phase. Cells were synchronised in S phase by a double thymidine block and cells were synchronised in G_0 by serum starvation (both methods are described in the materials and methods). ChlR1 depleted cells, synchronised in G_1 repair the DNA double strand breaks after 2 hours. However the DNA double strand breaks have not yet been fully repaired after 3 hours in the ChlR1 siRNA transfected cells synchronised in S phase. This suggests that ChlR1 function in the repair of DNA double strand breaks is linked with DNA replication.

Therefore ChlR1 may have a function in restarting stalled replication forks which accounts for a large percentage of DNA double strand breaks in S phase. If there was a defect in the repair of double strand breaks and replication fork restarting in ChlR1 depleted cells then these cells would take longer to progress through S phase. This is shown in flow cytometry analysis of ChlR1 depleted hTERT-RPE1 cells (Parish, unpublished). hTERT-RPE1 cells were depleted of ChlR1 by RNA interference and the cell cycle distribution analysed by flow cytometry. The flow cytometry data shows that in ChlR1 depleted cells there is an accumulation of cells in S phase after 72 hours of RNA interference. This corroborates with the neutral comet assay data shown in figure 43, suggesting a defect in the repair of DNA double strand breaks during DNA replication. Therefore I planned to utilise a number of techniques to determine the role of ChlR1 during DNA replication. These included the DNA combing and reverse ChIP assay.

5.4 ChlR1 is required for efficient DNA replication

The delay in S phase seen in ChlR1 knockdown cells may be due to inefficient DNA replication. To examine the role that ChlR1 plays in DNA replication the DNA combing technique was employed which allows the examination of replication fork dynamics in ChlR1 depleted cells. The assay is described in Figure 45.

The DNA combing protocol obtained from the Jallepalli lab (Sloan-Kettering Institute) was optimised. The first step in optimising the protocol described in the materials and methods was to check if the DNA was spread correctly and to test the ability of the antibodies to recognise the synthetic nucleotides. The first experiment involved the pulsing of cells with halogenated nucleotides IdU and CldU and spreading the DNA from these cells onto slides and testing the antibodies that are specific for these halogenated nucleotides. Using an antibody that recognises DNA I also tested that the DNA was spread on the slides.

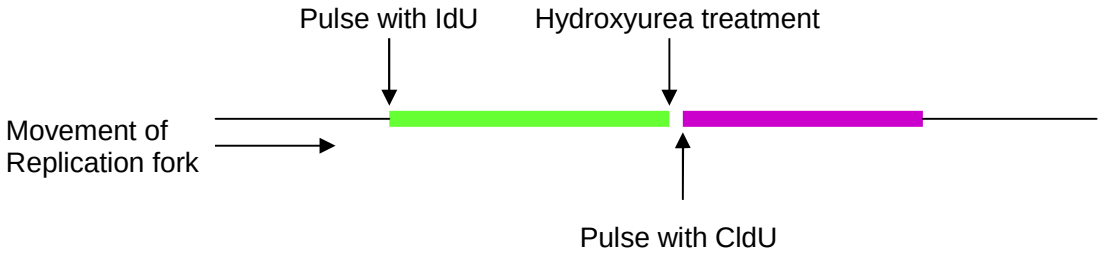

Figure 44: **Schematic representation of the DNA combing assay**.

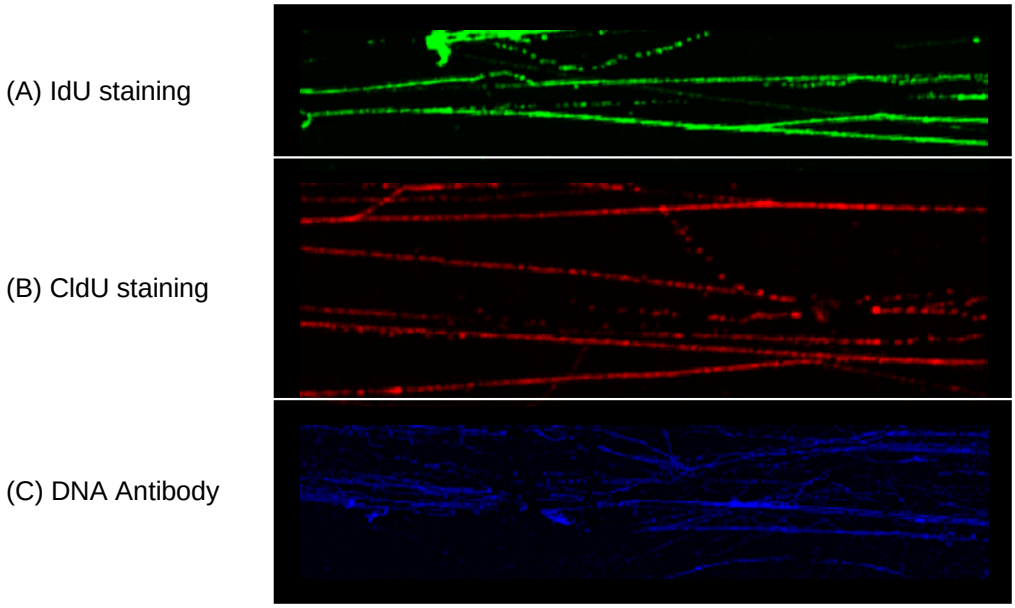

Figure 45: **Analysis of replicated DNA in hTERT-RPE1 cells**. *hTERT-RPE1 cells were (a) pulsed with halogenated nucleotide IdU and stained with an Alexa 547 secondary (green), (b) pulsed with halogenated nucleotide CldU and stained with an Alexa 594 secondary (red), (c) the DNA was stained with anti-DNA antibody with an Alexa 647 secondary (blue).*

Figure 45 shows that the spreading process works as the DNA is present on the slides and the strands separated well. Also both antibodies for the halogenated nucleotides work well at the concentrations stated in the materials and methods. The next step was to show that initiation of replication could be observed along with the restart of stalled replication forks using this assay. This involved the incubation of cells with IdU and then treatment the cells with HU to stall the replication forks. Following removal of HU, the replication forks can restart during which time the cells were incubated with CldU. The DNA was then spread onto glass slides and incubated with the appropriate antibodies. Using the confocal microscope tracks of DNA that were pulsed with IdU followed by CldU were imaged.

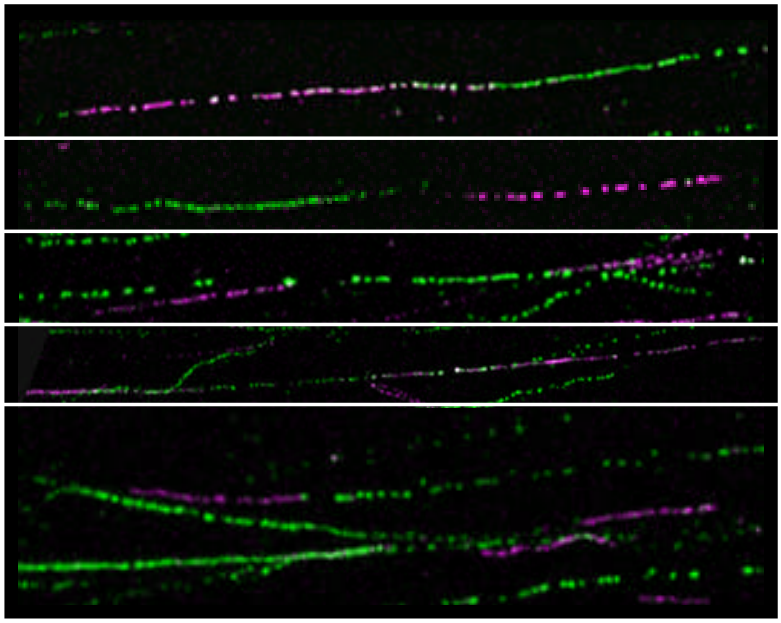

Figure 46: **Analysis of replication fork dynamics in hTERT-RPE1 cells**. *Cells were incubated with halogenated nucleotide IdU (pink), then treated with HU and incubated with a second halogenated nucleotide CldU (green). The halogenated nucleotides were detected using the secondary antibodies as described in Figure 45.*

Figure 46 shows the analysis of the replication fork dynamics after the treatment of the cells with HU. The DNA tracks were stained with IdU and following HU treatment, stained with CldU. The one problem with the assay was the staining with IdU was not as strong or consistent as the CldU staining and as such the IdU pulses are not continuous tracks in the DNA. I attempted to rectify this by increasing the amount of IdU analogue added to the cells and increasing the amount of antibody used to stain the IdU. Both these changes had no effect on the IdU pulsing. Therefore I planned to test the role of ChlR1 in initiation of replication and restarting stalled replication separately using only CldU staining. Firstly ChlR1 was depleted in hTERT-RPE1 cells and after 24 hours the cells were pulse with CldU. The length of the pulses was compared with control siRNA transfected cells. A reduction in length of the pulses in ChlR1 depleted cells would indicate a functional role of ChlR1 in DNA replication.

(A) Control siRNA

(B) ChlR1 siRNA

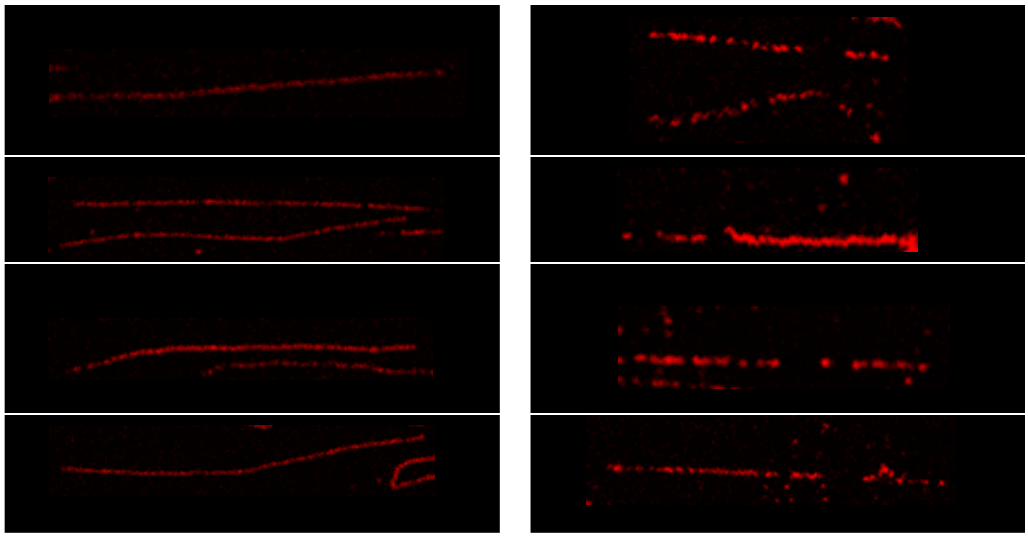

(C)

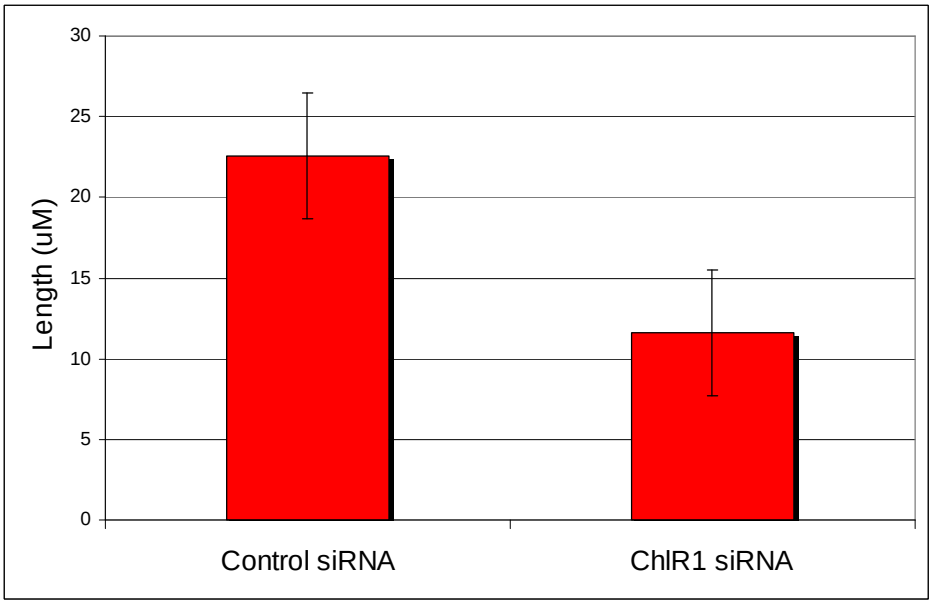

(D)

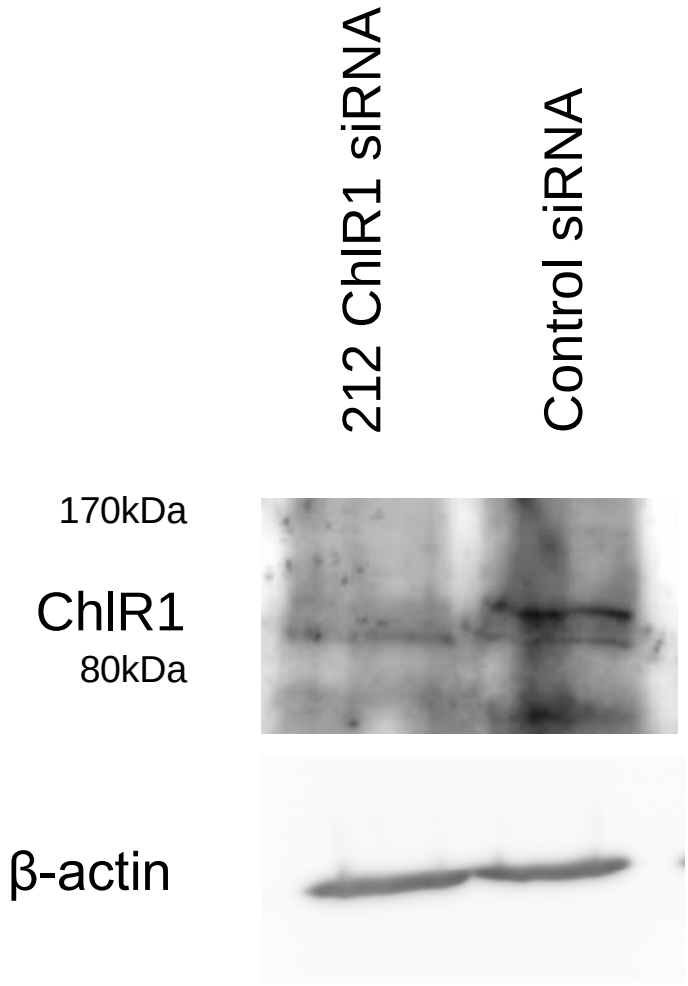

Figure 47: **Analysis of replication fork dynamics in ChlR1 siRNA and control siRNA transfected cells**. *hTERT-RPE1 cells were transfected with 100nM of ChlR1 and control siRNA for 24 hours. These cells were incubated with a halogenated nucleotide CldU to examine the effects on initiation of replication in ChlR1 knockdown cells. (a) Shows strands of DNA from cells transfected with control siRNA. (b) Shows strands of DNA from cells from cells transfected with ChlR1 siRNA. (c) Shows the average length of strands from cells transfected with both siRNA. Pulses were measured using Leica confocal software. The data represents the mean and standard deviation of 30 DNA strands analysed for each control in 2 experiments. (d) Western blot showing ChlR1 expression levels in the cells used for this assay.*

As shown in figure 47 there is a significant reduction in the length of CldU incorporated DNA strands in ChlR1 depleted cells compared to control siRNA transfected cells ($p < 0.0000005$). This is consistent with the flow cytometry data that suggests a defect in DNA replication upon ChlR1 depletion. Taken together, the data suggests that ChlR1 is

important in the replication of DNA possibily by assisting in initiation or in the progression of the replication fork via its DNA helicase activity.

5.5 ChlR1 is required for efficient DNA replication after hydroxyurea treatment

The data presented in chapter 4 shows that ChlR1 is involved in the repair of DNA double strand breaks. This role in DNA double strand break repair was shown to be S phase specific (Figure 44). Inefficient restarting of stalled replication forks accounts for the majority of DNA double strand breaks in S phase.

To examine the role ChlR1 plays in DNA replication after the stalling of DNA replication, the DNA combing technique was employed. ChlR1 depleted cells were treated with HU and pulsed with CldU to determine if there is a defect in DNA replication after HU treatment when ChlR1 is depleted. The ChlR1 depleted cells were compared to control siRNA transfected cells.

(a) Control siRNA

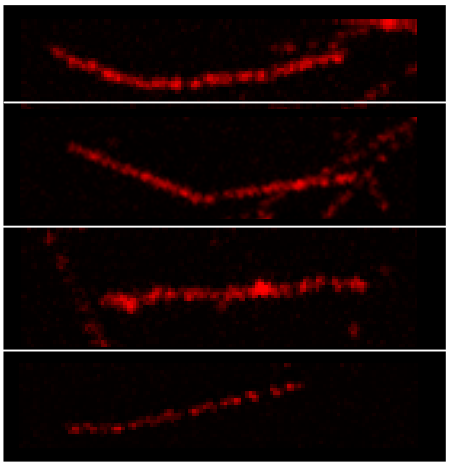

(b) ChlR1 siRNA

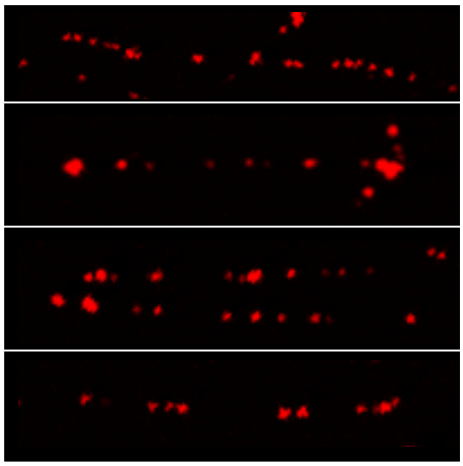

(c)

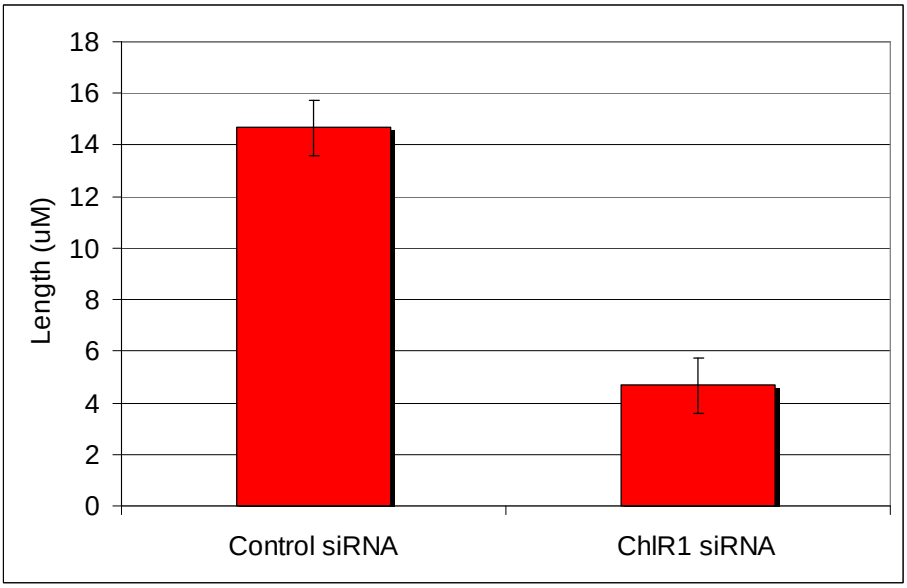

(d)

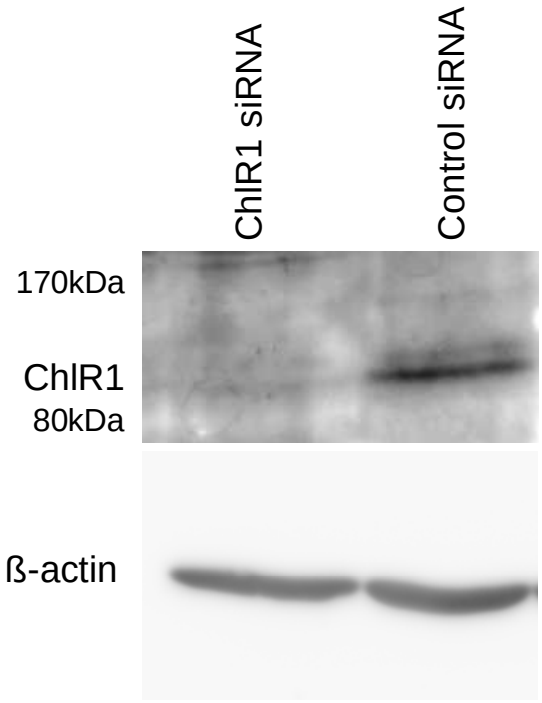

Figure 48: **Analysis of replication fork restart dynamics in ChlR1 siRNA and control siRNA transfected cells.** *hTERT-RPE1 cells were transfected with 100nM of ChlR1 and control siRNA for 24 hours. These cells were treated with HU and then incubated with a*

halogenated nucleotide CldU to examine the effects on restarting of stalled replication forks in ChlR1 knockdown cells. (a) Shows strands of replicated DNA from cells transfected with control siRNA, (b) Shows strands of replicated DNA from cells transfected with ChlR1 siRNA, (c) Shows the average length of strands from cells transfected with both siRNA. Pulses were measured using Leica confocal software. Data shown represents the mean and standard deviation of 30 DNA strands anaylsed for each control in 2 experiments, (d) Western blot showing ChlR1 expression levels in the cells used for this assay.

The data shown in figure 48 indicates that there is a defect in DNA replication in ChlR1 depleted cells following HU treatment, as shown by a reduction in the length of CldU incorporated DNA strands in ChlR1 knockdown cells compared to control siRNA cells ($p < 0.0000000005$). The images suggest that the replication forks are collapsing after treatment with HU as there are no visible pulses along the tracks.

5.6 Analysis of proteins that associate with newly replicating DNA

If ChlR1 is required for DNA replication then it must associate with newly replicated DNA. To confirm this theory I attempted to perform a reverse ChIP where hTERT-RPE1 cells were synchronised in G_1 and S phase and incubated with CldU which is then incorporated into newly replicated DNA. Cells synchronised in G_1 were used as a negative control as no replication takes place in this phase, so CldU should not be incorporated.

The cells were cross-linked and an antibody that recognises CldU was used to immunoprecipitate the newly synthesised DNA along with the associated proteins. After reversing the cross links and precipitating the proteins, the proteins were separated by SDS-PAGE and the presence of specific proteins detected by western blot. The first step was to confirm that the assay was working. PCNA was detected on CldU incorporated DNA as a positive control as this protein has been shown to specifically associate with newly replicated DNA [37].

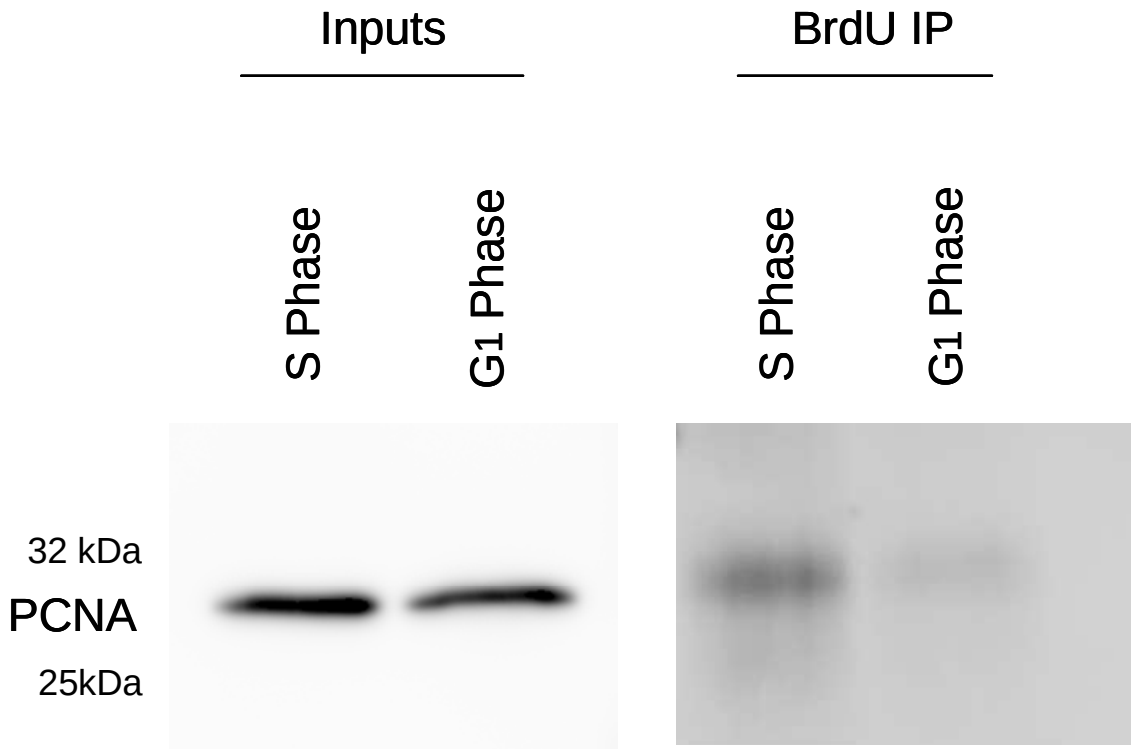

Figure 49: **BrdU incorporation and reverse ChIP for PCNA**. *hTERT-RPE1 cells were synchronised in S phase by double thymidine block or in G_1 by 16hr serum starvation. These cells were released and incubated with 50μM CldU for 1 hour. Chromatin preparations were prepared and CldU incorporated DNA was immunoprecipitated with rat BrdU antibody, which recognises CldU. Proteins associated with the immunoprecipitated DNA were precipitated and separated by SDS-PAGE. Mouse specific PCNA antibody was used at a 1:5000 dilution to detect PCNA. PCNA is specifically pulled down with the BrdU antibody in the cells synchronised in S phase but not in G_1 synchronised cells.*

The data shown in figure 49 confirm that PCNA associates with newly replicated DNA in cells synchronised in S phase. In addition the assay appears to be optimised for the detection of proteins that associate with replicating DNA. The next step was to repeat this experiment for ChlR1. PCNA is more abundant in the cell than ChlR1 and a major component of the replication complex. Therefore there would be a relatively large amount of the protein pulled down in the assay. In contrast ChlR1 is only present in a small amount at any time in the cell. Also although we believe ChlR1 functions in DNA

replication, it is not essential. Therefore there would be a smaller amount of the protein pulled down with replicating DNA compared to PCNA. With this in mind the amount of input was increased for the chromatin preparation from two 10cm dishes of cells to four 10cm dishes. This approach was unsuccessful at detecting precipitated ChlR1. Therefore the protocol was modified. A larger percentage of the chromatin preparation was included in the immunoprepitation reaction. The materials and methods states that 30% of the chromatin preparation was added to the immunoprecipitation. This was increased to 50% of the chromatin preparation. This was thought to increase the amount of ChlR1 that could be precipitated. Another modification to the reverse ChIP protocol was to treat the cells with hydroxyurea (HU) before harvesting. This would result in the stalling of replication forks. The data in this chapter shows ChlR1 that functions in the restarting of stalled replication forks. Therefore the induction of DNA damage during DNA replication from HU treatment may lead to an increase in the association of ChlR1 with the newly synthesised DNA. These modifications were unsuccessful in detecting precipitated ChlR1.

In summary I have shown that ChlR1 has a role in DNA replication and the restarting of stalled replication forks. Furthermore I have shown that the role of ChlR1 in DNA double strand break repair is link to DNA replication.

Discussion

6.1 The role of FHL2 in cohesion establishment

The hypothesis of this project was that ChlR1 interacts with FHL2 in mammalian cells and that FHL2 is important in the establishment of cohesion and subsequent progression through mitosis. ChlR1, as discussed in the introduction, has an important role in the establishment of cohesion. Therefore I hypothesised that FHL2 has a role in cohesion establishment through the interaction with ChlR1.

The results presented in Chapter 3 suggest that FHL2 has a role in sister chromatid cohesion. FHL2 co-immunoprecipitates with ChlR1 and the cohesin subunit Smc1 and both these proteins have important roles in sister chromatid cohesion. Furthermore the depletion of FHL2 in HEK293 cells results in abnormal metaphase chromosomes. The abnormalities include a lack of centromeric cohesion, loosely paired chromatids and chromatids that are wavy in appearance, which is hypothesised to be due to a chromosome condensation defect. Finally analysis of propidium iodide stained FHL2 depleted hTERT-RPE1 cells by flow cytometry showed an accumulation of cells in G_2/M phase of the cell cycle. This suggests that the cohesion defects results in checkpoint activation either at G_2 or during mitosis

To confirm the direct interaction between ChlR1 and FHL2, I attempted to purify FHL2 protein to perform *in vitro* binding assays with *in vitro* translated ChlR1 protein. However, the purification of FHL2 expressed from *E.coli* was a major problem. A number of strategies were employed to purify the protein. A Hexa-histidine- tagged and GST-tagged FHL2 proteins were created. Both these proteins were expressed in BL21 (DE3) *E.coli* but were not soluble. The addition of urea did not improve the solubility of the protein after

refolding. Changing the strain of *E.coli* to Rossetta blue *E.coli* which are able to transcribe rare codons, improved the solubility of the GST-FHL2 protein. FHL2 contains a number of rare codons that the BL21 strain of *E.coli* would have difficulty in transcribing. This may have resulted in truncation of the protein. Using the Rossetta blue *E.coli* strain a small amount of GST-FHL2 was purified but was not stable when stored in PBS. The binding of zinc to the LIM domains that forms FHL2 is important (as shown in Figure 50). Zinc precipitates at pH 7.2 and above. The lysis buffer used in the purification process was pH 7.4. Therefore it was possible that the majority of GST-FHL2 expressed in the *E.coli* precipitated. The small amount of GST-FHL2 that was purified was stored in PBS. The pH of PBS is 7.4 therefore the protein would have precipitated with the zinc. This would explain the results in figure 20 that shows as GST-FHL2 was stripped from the gluthonine beads the majority of the protein was collected with the stripped beads after centrifugation, presumable due to preciptitation.

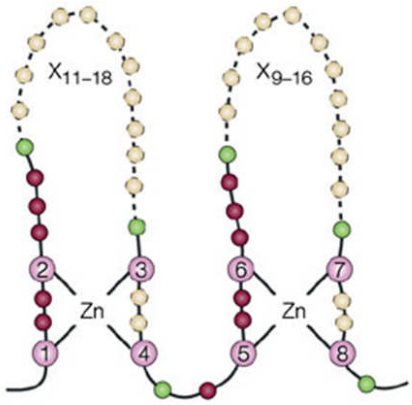

Figure 50: **The topology of the LIM domain.** *Two zinc ions associate with the LIM domain and create the zinc fingers that are essential for the function of LIM domain proteins. FHL2 contains four and a half LIM domains [326]. Image taken with permission from the Nature publishing group.*

The evidence in Chapter 3 suggests that depletion of FHL2 results in cohesion defects and G_2/M delay. Interestingly, a number of proteins including Cdc25, Wee1 and Orc6 that are

important in the progression of cells through mitosis were discovered to be down regulated when FHL2 is depleted [292]. The functions of these proteins will now be discussed in more detail below.

Cdc25 is a phosphatase that is involved in the progression of the cell cycle [327]. Cdc25a expression is down regulated when FHL2 is depleted [292]. In mammalian cells there are three isoforms of Cdc25; a, b and c [327]. Cdc25a is important in controlling the onset of mitosis and the initiation of S phase [328]. Its role in these processes is to dephosphorylate and activate cyclin dependent kinase 1 and 2 (cdk 1 and 2) [328]. Cdk1 and Cdk2 regulate the onset of mitosis and S phase respectively [329]. Down regulation of Cdc25a following FHL2 depletion could explain the accumulation of cells G_2/M shown here (Figure 24). Downregulation of Cdc25a would prevent the activation of Cdk1 and progression into mitosis resulting in an accumulation of cells in G_2. In conjunction with this, the tyrosine kinase that phosphorylates and inactivates Cdc2, called Wee1 [330] is also downregulated following depletion of FHL2. Cdc2 is the *S.pombe* homologue of Cdk1 and as discussed above Cdk1 is essential for the progression through mitosis. Therefore Wee1 is important in the G_2/M checkpoint ensuring the coordinated progression into mitosis [331]. In *S.pombe* Wee1 is a cell cycle regulator at the G_2 DNA damage checkpoint as it is phosphorylated by Chk1 [332]. These results were replicated in *Xenopus* egg extracts [331]. Wee1 phosphorylates Cdc2, which inactivates the Cdc2-cyclin B complex. In *Xenopus* egg extracts Wee1 is phosphorylated and activated by Chk1 [333]. Replacement of endogenous Wee1 with a mutant that Chk1 cannot phosphorylate results in an inability of Wee1 to phosphorylate Cdc2 [333]. Therefore down regulation of Wee1 would result in premature entry into mitosis. Premature entry into mitosis is likely to cause defects in chromosome separation and condensation, like those observed in FHL2 depleted cells.

Furthermore de-regulation of Wee1 has been shown to induce mitotic catastrophe in glioblastoma cells, which is an aggressive form of brain tumour. Inhibition of Wee1 resulted in the cells being pushed through the G_2 arrest phase which induced mitotic failure [334]. This confirms that Wee1 is important in the G_2/M checkpoint and depletion of Wee1 would result in mitotic defects as seen here FHL2 depleted cells (Figure 22).

The origin replication complex subunit 6 (Orc6) is another protein that is down regulated when FHL2 is depleted. Orc6 is the least conserved member of the recognition complex and is important for cell survival [335]. It has a role in the initiation of replication (as discussed in the introduction) and is also involved in chromosome segregation. In *drosophila* Orc6 was shown to accumulate along the length of the chromatids during anaphase. Deletion of Orc6 resulted in abnormal chromosome condensation and segregation [336]. This resulted in the arrest of the cells in the mitotic stages of the cycle [336]. In mammalian cells depletion of Orc6 resulted in multipolar spindles, aberrant mitosis and the formation of multinucleated cells [335]. These results suggest that Orc6 is important in the progression of cells through mitosis. The cohesion and condensation defects observed in FHL2 depleted cells maybe a result of Orc6 downregulation.

The defects in mitosis observed in FHL2 depleted cells may be a result of the downregulation of the proteins discussed above. Therefore the cohesion and condensation defects seen may be a downstream effect and not a direct function of FHL2. Conversely there is evidence to suggest that FHL2 has a direct role in sister chromatid cohesion. Evidence in this thesis suggests that FHL2 interacts with two key proteins involved in sister chromatid cohesion Smc1 and ChlR1. A future experiment to further explore the exact role of FHL2 in sister chromatid cohesion would be to look at the loading of cohesin onto chromosomes in FHL2 depleted cells. A ChIP assay examining the recruitment of cohesin to the H19 locus of the genome in FHL2 depleted cells could be used. The H19

locus is a cohesin rich region of the genome. This experiment would show if FHL2 has a role in the loading of cohesin onto chromosomes and would confirm whether the cohesion defects observed in FHL2 depleted cells is a direct function of FHL2 or a downstream effect.

The evidence above does not account for the distorted chromosome structure observed in FHL2 depleted cells. The distorted structure of the chromosomes may be due to the disruption of chromosome condensation when FHL2 is depleted. A future experiment to analyse whether FHL2 has a role in the condensation of chromosomes would be to stain metaphase spreads from FHL2 depleted cells with an antibody for CAP G (a condensin 1 subunit). This would show if there was a disruption of the CAP G subunit on the chromosomes in FHL2 depleted cells.

The distorted structure of the chromatids may be a result of the disruption of the heterochromatin regions of the chromosomes. As discussed in the introduction heterochromatin regions are transcriptionally silent loci with several functions, from gene regulation to the protection of the integrity of chromosomes [180]. FHL2 has previously been shown to have a function in transcriptional regulation. FHL2 acts as a transcriptional co activator for a number of transcriptional factors including the androgen receptor, CREB mediated transcription and β catenin/TCF mediated transcription pathways [337]. Depletion of FHL2 will result in the disruption of transcription. This in turn may disrupt the transcriptionally silent heterochromatin regions resulting in loss of chromosome integrity. This may account for the distorted structure of the chromatids. Also the ORC has a role in the maintenance of the heterochromatin regions [338]. The ORC subunit Orc6 is downregulated when FHL2 is depleted (as discussed above). The ORC subunits interact

with heterochromatin protein 1 (HP1) in mammalian cells [338]. Depletion of the Orc subunits causes a loss of HP1 association on the heterochromatin, which suggests the ORC facilitates the assembly of HP1 onto the chromatins. Cells with the ORC subunits depleted showed a loss of compaction at the satellite repeats which suggests that the ORC has a role in the organisation of heterochromatin regions [338]. Downregulation of the ORC subunit Orc6 in FHL2 depleted cells may account for the distorted chromatid structures as the heterochromatin regions are disrupted.

Finally, FHL2 interaction with the cohesin complex may be important in the ability of FHL2 to regulate gene expression. Cohesin has a role in the insulation of gene expression as discussed in the introduction [185]. In mammalian cells cohesion accumulates at CTCF consensus sequences and the major function of CTCF is in insulation of groups of genes that are transcriptionally co regulated by preventing communication between genes and enhancer elements of flanking genes [185]. Evidence in Chapter 3 suggests that FHL2 interacts with the cohesin complex subunit Smc1. Since the major function of FHL2 is in transcriptional regulation it is therefore possible that FHL2 interaction with the cohesin complex is important in this function. FHL2 may interact with cohesin at CTCF consensus sequences and disrupt the insulating function of cohesin that flank genes, which are co-regulated by FHL2. Disruption of insulation would allow for the transcription of genes co-regulated by FHL2. It is possible that is the method FHL2 deploys to regulate expression of genes. A future experiment to analyse whether cohesin is important in the regulation of FHL2-mediated transcription would be to analyse whether the expression of genes regulated by FHL2 changes in cells depleted of cohesin.

6.2 The role of ChlR1 in DNA damage responses

The hypothesis of this project was that ChlR1 has a role in the repair of DNA damage and ChlR1 is involved in the recruitment of the cohesion complex to sites of DNA double strand breaks. Previous studies have shown the *S.cerevisiae* homologue of ChlR1 (Chl1p) is involved in the repair of DNA damage (Discussed in Chapter 4)

The results presented in Chapter 4 suggest that ChlR1 has a role in the DNA damage repair pathway. Comet assays were used to show that ChlR1 is involved in DNA double strand break repair. The neutral comet assay, which uses an electrophoresis buffer that has a neutral pH, was used to detect double strand breaks. The DNA is unable to unwind and therefore only DNA with a double strand break is released during electrophoresis. Unlike the alkaline comet assay that uses an alkaline electrophoresis buffer. The alkaline pH causes DNA to unwind and therefore DNA with single strand breaks can be released during electrophoresis.

The alkaline comet assay data showed that there is no significant defect in repair after 3 hours in ChlR1-depleted cells compared to untransfected and scrambled siRNA transfected cells. The neutral comet assay data showed there was a significant defect in repair after 3 hours in ChlR1 depleted cells compared to untransfected and scrambled siRNA transfected cells. These results suggested that ChlR1 is involved in the repair of DNA double strand breaks.

These data provide evidence that ChlR1 has a role in the repair of DNA double strand breaks. Therefore it is possible that ChlR1 is recruited to DNA double strand breaks. To explore this theory a U2OS cell line with a unique restriction enzyme (SceI) recognition sequence inserted into the genome was used [260]. The restriction enzyme recognition sequence has a Tet operator upstream and the cells stably express GFP tagged Tet

repressor, which binds to sequences within the operator. Therefore the location of the inserted restriction enzyme sequence was indicated by GFP foci within the cells. I have confirmed that the addition of the restriction enzyme results in the formation of a DNA double strand break at the GFP foci and that the restriction enzyme-induced break is recognised as a DNA double strand break by the cell through the localisation of gamma H2AX to the break. Using immunofluorescent staining I have shown that ChlR1 is recruited to this DNA double strand break. In addition the cell line was used to investigate whether ChlR1 and phosphorylated Smc1 co-localised to the DNA double strand break. To this end, the evidence provided in this thesis suggests that both proteins were recruited to the DNA double strand break. Put together with the DNA repair assays described above that indicate a defect in the repair of DNA double strand breaks following ChlR1 depletion, these data suggest that ChlR1 may directly function in the repair of DNA double strand breaks.

To confirm the recruitment of ChlR1 to DNA double strand breaks, I also attempted a ChIP assay in which the U2OS-based double strand break induction system described above was used to immunoprecipitate DNA surrounding the break with ChlR1-specific antibodies. This involved designing primers specific for a sequence in the insert downstream of the restriction enzyme recognition site to produce a PCR product close to the break that could be used for ChIP assays. Unfortunately, this experiment could not be successfully optimised given the time restraints of my PhD. However, this assay still remains an attractive method to study the specific recruitment of ChlR1 to DNA double strand breaks and after sufficient optimisation should successfully resolve this hypothesis. This assay could also be used to confirm whether ChlR1 and phosphorylated Smc1 co-

localise to the regions around the DNA double strand break, as suggested by the immunofluorescent staining shown in this thesis.

Evidence suggests that Smc1 and 3 are phosphorylated at DNA double strand breaks [258] and this phosphorylation is ATM kinase dependent [262]. The phosphorylation of Smc1 and 3 may also require the kinase activity of DNA-PKcs. ChlR1 interacts with DNA-PKcs (Feeney and Parish, unpublished) and may recruit DNA-PKcs to the cohesin subunits. An experiment that could test this hypothesis would be to study the disruption of the phosphorylated Smc1 at DNA double strand breaks by immunoflourscence following ChlR1 depletion. This experiment would be performed using the U2OS TetO/R cell line used in the experiments described above.

It would be interesting to explore the possibility that the helicase activity of ChlR1 is important for its function in DNA damage repair. The helicase activity of a related helicase BLM is important in DNA damage repair [339]. BLM is mutated in Bloom syndrome (BS) patients [340]. BS is characterised by excessive chromosome breakage and increased rates of sister chromatid interchange in somatic cells [340]. BS cells also exhibit higher sensitivity to MMS and the homologous recombination repair pathway is defective [341]. BLM exhibits an ATP-dependent DNA helicase that unwinds DNA in a 3’-5’ direction [339]. Mutations in BLM that are found in BS patients abolish both the ATPase and helicase activity of the protein [339].

This suggests that the helicase activity of ChlR1 maybe important in DNA damage repair. I hypothesised that ChlR1 is important in the recruitment of the cohesin complex to DNA double strand breaks during the repair by the homologous recombination pathway. Disruption of the helicase activity of BLM results in defects in the homologous recombination repair pathway, which suggests that the helicase activity of ChlR1 is also

important in the recruitment of cohesin to DNA double strand breaks and the homologous recombination repair pathway.

To explore the possibility that the helicase activity of ChlR1 is important in the repair of DNA double strand breaks, a ChlR1 construct with a mutation within the ATPase domain that prevents ATP binding could be used. Using this construct, I could replace the endogenous ChlR1 with the mutant protein and perform the comet assays and gamma H2AX immunodetection on irradiated cells. This would allow the determination of whether the helicase activity of ChlR1 is important in DNA damage repair.

The data highlighting a role for ChlR1 in DNA damage repair described in this thesis corroborate with results from previous studies. In *S.cerevisiae*, Chl1p was initially discovered to function in the repair of DNA damage. Chl1p deleted cells were shown to be more sensitive to the DNA damage reagents methyl methanesulfonate (MMS), hydroxyurea (HU) and UV radiation [304, 305]. In addition to these studies, human ChlR1 interacts with TopBP1 and DNA-PKcs (Feeney and Parish, unpublished). These proteins are involved in DNA damage repair (as discussed earlier). These interactions have been confirmed by co-immunoprecipitation in mammalian cells. Furthermore the interaction between ChlR1 and DNA-PKcs increased 6-fold after exposure of the cells to ionising radiation (Feeney and Parish, unpublished). A number of related helicases are involved in the repair of DNA damage lesions. The XPB and XPD helicases are part of the transcriptional factor IIH complex (TFIIH) that functions in nucleotide excision repair [222]. This process removes bulky adducts from DNA generated from UV light exposure [222]. The TFIIH complex opens the DNA around the damage site through the helicase activity of XPD and XPB [222]. FANCJ is another related helicase involved in DNA damage repair [308]. FANCJ unwinds homologous recombination intermediates, which

suggests it is involved in the homologous recombination pathway of double strand break repair [310]. FANCJ knockout cells have a homologous recombination defect and are sensitive to ionising radiation [310].

The evidence above suggests that Chl1p functions in DNA damage repair. Now I have shown in this thesis that ChlR1 has a role in DNA damage repair. ChlR1 is required for the repair of DNA double strand breaks and ChlR1 was recruited to DNA double strand breaks.

6.3 The role of ChlR1 in DNA replication

The hypothesis of this project was that ChlR1 has a role in DNA replication and the restarting of stalled replication forks. ChlR1 is important in the progression of the replication machinery through cohesin rings. A number of other cohesion establishment proteins including Eco1, Ctf4 and Ctf18 are important for DNA replication. Therefore I believe the cohesion establishment function of ChlR1 is important in DNA replication.

The results presented in Chapter 5 suggest that ChlR1 has a role in DNA replication. The DNA combing technique was used to look at the replication fork dynamics in ChlR1 siRNA compared to scrambled siRNA transfected hTERT-RPE1 cells. The length of DNA strands labelled with the halogenated nucleotide CldU was smaller in ChlR1 siRNA transfected cells compared to scrambled siRNA transfected cells. These results suggest that ChlR1 has a role in DNA replication. ChlR1 interacts with proteins shown to be part of the replication fork. These include PCNA, Mcm7 (Feeney and Parish, unpublished) and Fen1 [50]. These results suggest that ChlR1 is a member of the replication fork complex and is involved in the progression of the replication fork.

Furthermore the results from this thesis suggest that ChlR1 has a role in the restarting of DNA replication after stalling. The DNA combing technique was used to look at DNA replication in ChlR1 and scramble siRNA transfected hTERT-RPE1 cells treated with hydroxyurea. The length of DNA strands labelled with the halogenated nucleotide CldU were smaller in ChlR1 siRNA transfected cells compared to scrambled siRNA transfected cells and in many cases no visible strands were seen in the ChlR1 siRNA transfected cells. These observations suggest that ChlR1 is required for the efficient DNA replication after stalling and when ChlR1 is depleted these replication forks collapse. ChlR1 was identified as an interacting partner of TopBP1 (Feeney and Parish, unpublished). TopBP1 is involved in the processing of stalled replication forks. It recruits the 9-1-1 complex to the stalled replication complex and this clamp acts to stabilise the replication fork [70]. This interaction between ChlR1 and TopBP1 corroborates with the DNA combing data and suggests that ChlR1 may bind to TopBP1 to facilitate efficient restarting of stalled replication forks in ChlR1 depleted cells.

The inefficient DNA replication after damage leads to an inefficient repair of DNA double strand breaks. The inefficient repair of DNA double strand breaks in ChlR1 depleted cells seen in Chapter 4 is S phase specific as seen in figure 44. The neutral comet assay was performed on ChlR1 depleted cells synchronised in either S phase or G_1 which showed inefficient repair of DNA double strand breaks in cells synchronised in S phase only. This suggests that ChlR1's role in DNA damage repair is linked to replication, specifically during the restarting of stalled replication forks. This result also suggests that ChlR1 is important in the homologous recombination repair pathway. Homologous recombination is important in the repair of DNA double strand breaks in S phase and mitosis, as a DNA template is available for recombination in these phases of the cell cycle.

ChlR1 interacts with proteins involved in replication fork progression and depletion of ChlR1 results in inefficient replication, I hypothesised that ChlR1 is a member of the replication machinery. If ChlR1 is a member of the replication machinery then it is possible ChlR1 associates with newly synthesised DNA. To explore this hypothesis, the reverse ChIP assay was used. hTERT-RPE1 cells were incubated with the halogenated nucleotide CldU and cross linked with formaldehyde. The whole cell lysate was prepared and the chromatin sheared before immunoprecipitation with an antibody specific for the halogenated nucleotide. Using this method, the CldU incorporated DNA only is precipitated along with any associated proteins. I attempted to detect co-precipitated ChlR1 and PCNA by western blot. PCNA was detected by western blot which suggested that the assay was working, however I was unable to detect ChlR1. ChlR1 protein levels in the cell are low compared to PCNA, and although ChlR1 is thought to be important in replication it is not essential, whereas PCNA is essential for replication. Therefore I except that more PCNA will associate with newly synthesised DNA compared to ChlR1. We increased the number of cells used in the assay by a factor of five to increase the amount of ChlR1 protein in the lysate. This alteration to the experiment was unsuccessful.

Future work in analysing whether ChlR1 associates with newly synthesised DNA would be to perform the reverse ChIP assay on hTERT-RPE1 cells transfected with FLAG-ChlR1. This would increase the levels of ChlR1 in the cells and the highly specific FLAG antibody would be used to detect ChlR1 by western blot, which is likely to have a higher affinity that the available endogenous ChlR1 antibody. The FLAG epitope is not likely to affect ChlR1 association with DNA because one of the co-immunoprecipitation experiments used to confirmed ChlR1's interaction with PCNA was performed using FLAG-ChlR1. Therefore the FLAG epitope does not disrupt the association of ChlR1 to

the replication fork protein complex, indicating it is unlikely to disrupt the possible association of ChlR1 with DNA.

One model to describe how the replication fork passes cohesin rich regions of DNA is that the cohesin complex has to dissociate from the DNA to allow for the progression of the replication fork then re-associate with the DNA after the replication fork has passed. My hypothesis is that ChlR1 is involved in the re-association of the cohesin complex after the replication fork has passed because ChlR1 is a cohesion establishment factor. This theory could be explored using the reverse ChIP assay. Following ChlR1 depletion, disruption of the association of the cohesin complex with newly synthesised DNA should be anaylsed. This would reveal whether ChlR1 is involved in the re-association of cohesin after the replication fork has passed. This assay should work as cohesin should co-immunoprecipitated with newly synthesised DNA because cohesin associates with the DNA during S phase as it is loaded onto the chromosomes in mammalian cells during telophase.

The helicase activity of ChlR1 may be important in DNA replication. In *in vitro* assays, the replicative helicase, the MCM complex has a preference to displace oligonucleotides annealed to single stranded DNA in a 3'-5' direction [16]. ChlR1 has a preference to unwind in the 5-3' direction on short single stranded DNA templates of 19 nucleotides in length [174]. Unlike other DNA helicases, ChlR1 can translocate along single stranded DNA in both directions when the substrates have a very long single stranded DNA region [174]. The MCM helicase and ChlR1 unwind DNA in opposite directions, suggesting they may work in tandem at the replication fork.

To explore the possibility that the helicase activity of ChlR1 is important in DNA replication, I would replace the endogenous ChlR1 with the ATP binding mutant protein

and perform the DNA combing assay. This would prove that the helicase activity of ChlR1 is important in DNA replication.

The results obtained in this thesis suggesting a role for ChlR1 in DNA replication, are in argeement with results from previous studies. ChlR1 interacts with a number of proteins involved in DNA replication including Mcm7, PCNA, TopBP1 (Feeney and Parish, unpublished) and Fen1 [50]. Furthermore ChlR1 stimulates the endonuclease *in vitro* activity of Fen1 three fold [50]. In addition, a number of other cohesion establishment factors associate with the replication fork, including Ctf18 and Esco1 and 2. A number of related helicases are involved in DNA replication. FANCJ has been shown to function in DNA replication checkpoint control [311]. FANCJ interacts with TopBP1 and FANCJ knockdown results in the inability of RPA to load onto the DNA [311]. This is a prerequisite for ATR checkpoint activation. FANCJ is involved in the phosphorylation of both Chk1 and RPA following replication stress [311]. These results suggest FANCJ has a role in the restarting of stalled replication forks after DNA damage. RecF is another related helicase involved in DNA replication. In *E.coli* depleted of RecF replication fails to recover after UV damage [320]. Furthermore RecF is important in protecting the nascent DNA at stalled replication forks [321]. In the absence of RecF in *E coli* the nascent strand is degraded at these stalled replication forks [321].

The evidence above suggests that ChlR1 functions in DNA replication. I have shown in this thesis that ChlR1 is important in DNA replication. Depletion of ChlR1 resulted in inefficient DNA replication. In addition depletion of ChlR1 resulted in inefficient restarting of stalled replication forks after Hydroxyurea treatment.

6.4 The role of ChlR1 in the maintenance of the papillomavirus genome

ChlR1 has been shown to have a role in the maintenance of papillomaviruses genomes [342]. Papillomaviruses are DNA viruses that are a causative agent of genital warts and cervical cancer [343]. The genome is maintained as a double stranded DNA plasmid. Segregation and maintenance of the episomal genome requires the virus to hijack the host cells mitotic pathway [343]. ChlR1 loads the papillomavirus genome onto the host cell chromosomes prior to mitosis to allow for the genome to transfer into the daughter cells [342]. The papillomavirus genome attaches to ChlR1 through an interaction with the papillomavirus E2 protein [342]. The papillomavirus E2 protein is involved in the replication of the viral genome. A mutation in E2 that prevents the interaction with ChlR1 prevents E2 from associating with the chromosomes and disrupts viral genome persistence [342]. Similar results occur when ChlR1 is depleted by RNA interference [342].

The interaction between ChlR1 and E2 may occur at stalled replication forks. Therefore the loading of the papillomavirus genome may occur at the stalled replication forks. With the replication fork stalled and ChlR1 stationary this would allow for easier loading of the viral genome onto the chromosomes. This theory requires that papillomaviruses can cause stalling of the replication fork. There is evidence that suggests E2 causes DNA damage in the host DNA. Expression of E2 causes increased phosphorylation of gamma H2AX and Chk2 [344]. Expression also results in growth arrest [344]. Therefore the papillomavirus may induce DNA damage which would result in stalled replication forks. The viral genome would then be loaded onto the chromosomes at the stalled replication forks. E2 also interacts with TopBP1, further evidence supporting this hypothesis [345]. As discussed earlier TopBP1 has a crucial role in the restarting of stalled replication forks. Finally the interaction between ChlR1 and E2 occurs in S phase of the cell cycle [346].

The results from this thesis shed light on the loading of the papillomavirus genome onto the host chromosome. The evidence in this thesis suggesting that ChlR1 is present at stalled replication forks and is involved in the restarting of stalled replication forks provides a mechanism for the loading of papillomavirus genomes onto host chromosomes.

6.5 Concluding Remarks

The data presented in this thesis sheds light on the phenotype found in Warsaw breakage syndrome, caused by a mutation in the DDX11 gene, which encodes ChlR1. The chromosome breaks observed in this syndrome are supported by the evidence provided here that highlight an involvement of ChlR1 with DNA damage repair and the restarting of stalled replication forks. Chromosome breaks result from the accumulation and inefficient repair of DNA double strand breaks. A related helicase, BLM, has been shown to be involved in the autosomal recessive disorder Bloom syndrome [347]. A feature of this syndrome is chromosome breaks [348]. The phenotype of the syndrome includes sensitivity to the sun, immunodeficiency and a pre-disposition to cancer [340]. Bloom syndrome cells display a high level of sister chromatid exchange, telomere association and chromosome breaks [348]. The high level of chromosome breaks suggests there is a defect in the repair of DNA damage in these cells. Furthermore, BLM depleted cells show a higher sensitivity to the DNA damaging reagent MMS [341]. Mutations in BLM found in bloom syndrome abolish the ATPase and DNA helicase activity of the BLM protein [339]. This suggests that the helicase activity of the protein is essential in its role in DNA damage repair. BLM also interacts with topoisomerase II α and topoisomerase II α stimulates the helicase activity of BLM [349]. Topoisomerase II α has been shown to be involved in the

processing of chromosome breaks [350]. The protein is involved in the unknotting and decatenation of the DNA by cleaving both strands of DNA to allow for the passage of other DNA duplexes [350]. Inhibition of topoisomerase II α causes high levels of chromosome breaks [351]. Interestingly, as discussed previously ChlR1 interacts with a topoisomerase binding protein 1 (TopBP1). This interaction may play a role in the processing of chromosome breaks. Therefore the results presented in this thesis suggest that the chromosome breaks present in Warsaw breakage syndrome cells are a result of inefficient DNA damage repair due to depleted levels of ChlR1.

ChlR1 has previously been shown to be a cohesion establishment factor. ChlR1 interacts with the subunits of the cohesin complex and depletion of ChlR1 results in premature chromosome segregation and chromosomes with reduced centromeric cohesion. It has been suggested that ChlR1 is involved in the loading of the cohesin complex onto the chromosomes but results in this thesis now lead to the hypothesis that ChlR1 is involved in cohesion establishment because cohesion establishment occurs during DNA replication and as shown in this thesis, ChlR1 plays a role in efficient DNA replication.

Work in this thesis has also shown that ChlR1 depleted cells repair DNA damage inefficiently. The data suggest that ChlR1 is involved in the repair of DNA double strand breaks during S phase. This supports the data highlighting that ChlR1 has an important role in the restarting of stalled replication forks. Stalled replication forks account for a large percentage of DNA damage in cells.

As discussed earlier defects in DNA damage repair pathways lead to increased cancer susceptibility. Therefore I believe ChlR1 is an important cancer research target in future. However, ChlR1 function is in need of further characterisation before this conclusion can be made. The crystal structure is still unknown and would reveal much about the function

of the protein in relation to other DNA helicases that are more extensively characterised. Nonetheless, my work has shown that ChlR1 is a helicase of emerging significance in the field of genomic integrity.

References

1. Bell, S.P. and B. Stillman, *ATP-dependent recognition of eukaryotic origins of DNA replication by a multiprotein complex.* Nature, 1992. **357**(6374): p. 128-134.
2. Xu, W., et al., *Genome-wide mapping of ORC and Mcm2p binding sites on tiling arrays and identification of essential ARS consensus sequences in S. cerevisiae.* BMC Genomics, 2006. **7**(1): p. 276.
3. Bell, S.P., et al., *The multidomain structure of Orc1 p reveals similarity to regulators of DNA replication and transcriptional silencing.* Cell, 1995. **83**(4): p. 563-568.
4. Marchler-Bauer, A., et al., *CDD: a conserved domain database for interactive domain family analysis.* Nucleic Acids Research, 2006. **35**(suppl 1): p. D237-D240.
5. Klemm, R.D., R.J. Austin, and S.P. Bell, *Coordinate Binding of ATP and Origin DNA Regulates the ATPase Activity of the Origin Recognition Complex.* Cell, 1997. **88**(4): p. 493-502.
6. Lee, J.-K., et al., *The Schizosaccharomyces pombe origin recognition complex interacts with multiple AT-rich regions of the replication origin DNA by means of the AT-hook domains of the spOrc4 protein.* Proceedings of the National Academy of Sciences of the United States of America, 2001. **98**(24): p. 13589-13594.
7. Thomae, A.W., et al., *Interaction between HMGA1a and the origin recognition complex creates site-specific replication origins.* Proceedings of the National Academy of Sciences, 2008. **105**(5): p. 1692-1697.
8. Randell, J.C.W., et al., *Sequential ATP Hydrolysis by Cdc6 and ORC Directs Loading of the Mcm2-7 Helicase.* Molecular Cell, 2006. **21**(1): p. 29-39.
9. Chen, S., M.A. de Vries, and S.P. Bell, *Orc6 is required for dynamic recruitment of Cdt1 during repeated Mcm2–7 loading.* Genes & Development, 2007. **21**(22): p. 2897-2907.
10. Terret, M.-E., et al., *Cohesin acetylation speeds the replication fork.* Nature, 2009. **462**(7270): p. 231-234.
11. Pape, T., et al., *Hexameric ring structure of the full-length archaeal MCM protein complex.* EMBO Rep, 2003. **4**(11): p. 1079 - 1083.
12. Maine, G.T., P. Sinha, and B.-K. Tye, *MUTANTS OF S. CEREVISIAE DEFECTIVE IN THE MAINTENANCE OF MINICHROMOSOMES.* Genetics, 1984. **106**(3): p. 365-385.
13. Tanaka, S. and J.F.X. Diffley, *Interdependent nuclear accumulation of budding yeast Cdt1 and Mcm2-7 during G1 phase.* Nat Cell Biol, 2002. **4**(3): p. 198-207.
14. Donovan, S., et al., *Cdc6p-dependent loading of Mcm proteins onto pre-replicative chromatin in budding yeast.* Proc Natl Acad Sci USA, 1997. **94**(11): p. 5611 - 5616.
15. Fletcher, R., et al., *The structure and function of MCM from archaeal M. Thermoautotrophicum.* Nat Struct Biol, 2003. **10**(3): p. 160 - 167.
16. Ishimi, Y., *A DNA Helicase Activity Is Associated with an MCM4, -6, and -7 Protein Complex.* Journal of Biological Chemistry, 1997. **272**(39): p. 24508-24513.

17. Ying, C.Y. and J. Gautier, *The ATPase activity of MCM2-7 is dispensable for pre-RC assembly but is required for DNA unwinding.* EMBO J, 2005. **24**(24): p. 4334-4344.
18. Moyer, S.E., P.W. Lewis, and M.R. Botchan, *Isolation of the Cdc45/Mcm2â€“7/GINS (CMG) complex, a candidate for the eukaryotic DNA replication fork helicase.* Proceedings of the National Academy of Sciences, 2006. **103**(27): p. 10236-10241.
19. Ilves, I., et al., *Activation of the MCM2-7 Helicase by Association with Cdc45 and GINS Proteins.* Molecular Cell, 2010. **37**(2): p. 247-258.
20. MacNeill, S.A., *Structure and function of the GINS complex, a key component of the eukaryotic replisome.* Biochem J, 2010. **425**(3): p. 489-500.
21. Bailis, J.M., et al., *Minichromosome Maintenance Proteins Interact with Checkpoint and Recombination Proteins To Promote S-Phase Genome Stability.* Mol. Cell. Biol., 2008. **28**(5): p. 1724-1738.
22. Nishiyama, A., L. Frappier, and M. Méchali, *MCM-BP regulates unloading of the MCM2–7 helicase in late S phase.* Genes & Development, 2011. **25**(2): p. 165-175.
23. Diffley, J.F.X., *Regulation of Early Events in Chromosome Replication.* Current Biology, 2004. **14**(18): p. R778-R786.
24. Noton, E. and J.F.X. Diffley, *CDK Inactivation Is the Only Essential Function of the APC/C and the Mitotic Exit Network Proteins for Origin Resetting during Mitosis.* Molecular Cell, 2000. **5**(1): p. 85-95.
25. Drury, L.S., G. Perkins, and J.F.X. Diffley, *The Cdc4/34/53 pathway targets Cdc6p for proteolysis in budding yeast.* EMBO J, 1997. **16**(19): p. 5966-5976.
26. Nguyen, V.Q., et al., *Clb/Cdc28 kinases promote nuclear export of the replication initiator proteins Mcm2-7.* Current Biology, 2000. **10**(4): p. 195-205.
27. Labib, K., J.F.X. Diffley, and S.E. Kearsey, *G1-phase and B-type cyclins exclude the DNA-replication factor Mcm4 from the nucleus.* Nature Cell Biology, 1999. **1**(7): p. 415-422.
28. Itzhaki, J.E., C.S. Gilbert, and A.C.G. Porter, *Construction by gene targeting in human cells of a /`conditional/' CDC2 mutant that rereplicates its DNA.* Nat Genet, 1997. **15**(3): p. 258-265.
29. Coverley, D., et al., *Protein Kinase Inhibition in G2 Causes Mammalian Mcm Proteins to Reassociate with Chromatin and Restores Ability to Replicate.* Experimental Cell Research, 1998. **238**(1): p. 63-69.
30. Coverley, D., et al., *Chromatin-bound Cdc6 persists in S and G2 phases in human cells, while soluble Cdc6 is destroyed in a cyclin A-cdk2 dependent process.* Journal of Cell Science, 2000. **113**(11): p. 1929-1938.
31. Liu, E., et al., *Cyclin-dependent Kinases Phosphorylate Human Cdt1 and Induce Its Degradation.* Journal of Biological Chemistry, 2004. **279**(17): p. 17283-17288.
32. Méndez, J., et al., *Human Origin Recognition Complex Large Subunit Is Degraded by Ubiquitin-Mediated Proteolysis after Initiation of DNA Replication.* Molecular Cell, 2002. **9**(3): p. 481-491.
33. McGarry, T.J. and M.W. Kirschner, *Geminin, an Inhibitor of DNA Replication, Is Degraded during Mitosis.* Cell, 1998. **93**(6): p. 1043-1053.
34. Wohlschlegel, J.A., et al., *Inhibition of Eukaryotic DNA Replication by Geminin Binding to Cdt1.* Science, 2000. **290**(5500): p. 2309-2312.
35. Geng, Y., et al., *Cyclin E ablation in the mouse.* Cell, 2003. **114**(4): p. 431-443.
36. Yan, Z., et al., *Cdc6 is regulated by E2F and is essential for DNA replication in mammalian cells.* Proceedings of the National Academy of Sciences of the United States of America, 1998. **95**(7): p. 3603-3608.

37. Krishna, T.S.R., et al., *Crystallization of Proliferating Cell Nuclear Antigen (PCNA) from Saccharomyces cerevisiae.* Journal of Molecular Biology, 1994. **241**(2): p. 265-268.
38. Majka, J., P.M.J. Burgers, and M. Kivie, *The PCNA-RFC Families of DNA Clamps and Clamp Loaders*, in *Progress in Nucleic Acid Research and Molecular Biology*. 2004, Academic Press. p. 227-260.
39. Gomes, X.V. and P.M.J. Burgers, *ATP Utilization by Yeast Replication Factor C.* Journal of Biological Chemistry, 2001. **276**(37): p. 34768-34775.
40. Dionne, I., et al., *On the mechanism of loading the PCNA sliding clamp by RFC.* Molecular Microbiology, 2008. **68**(1): p. 216-222.
41. Podust, V.N., et al., *Replication Factor C Disengages from Proliferating Cell Nuclear Antigen (PCNA) upon Sliding Clamp Formation, and PCNA Itself Tethers DNA Polymerase δ to DNA.* Journal of Biological Chemistry, 1998. **273**(48): p. 31992-31999.
42. Lee, S.H. and J. Hurwitz, *Mechanism of elongation of primed DNA by DNA polymerase delta, proliferating cell nuclear antigen, and activator 1.* Proceedings of the National Academy of Sciences, 1990. **87**(15): p. 5672-5676.
43. Ishino, Y., et al., *Functional interactions of an archaeal sliding clamp with mammalian clamp loader and DNA polymerase δ.* Genes to Cells, 2001. **6**(8): p. 699-706.
44. Li, X., et al., *Lagging Strand DNA Synthesis at the Eukaryotic Replication Fork Involves Binding and Stimulation of FEN-1 by Proliferating Cell Nuclear Antigen.* Journal of Biological Chemistry, 1995. **270**(38): p. 22109-22112.
45. Arias, E.E. and J.C. Walter, *PCNA functions as a molecular platform to trigger Cdt1 destruction and prevent re-replication.* Nat Cell Biol, 2006. **8**(1): p. 84-90.
46. Anderson, S. and M.L. DePamphilis, *Metabolism of Okazaki fragments during simian virus 40 DNA replication.* Journal of Biological Chemistry, 1979. **254**(22): p. 11495-11504.
47. Arezi, B. and R.D. Kuchta, *Eukaryotic DNA primase.* Trends in Biochemical Sciences, 2000. **25**(11): p. 572-576.
48. Murante, R.S., et al., *The calf 5'- to 3'-exonuclease is also an endonuclease with both activities dependent on primers annealed upstream of the point of cleavage.* Journal of Biological Chemistry, 1994. **269**(2): p. 1191-1196.
49. Harrington, J.J. and M.R. Lieber, *The characterization of a mammalian DNA structure-specific endonuclease.* EMBO J, 1994. **13**(5): p. 1235-46.
50. Farina, A., et al., *Studies with the Human Cohesin Establishment Factor, ChlR1.* Journal of Biological Chemistry, 2008. **283**(30): p. 20925-20936.
51. Rothwell, P.J., et al., *Structure and mechanism of DNA polymerases*, in *Advances in Protein Chemistry*. 2005, Academic Press. p. 401-440.
52. Bebenek, K., T.A. Kunkel, and Y. Wei, *Functions of DNA Polymerases*, in *Advances in Protein Chemistry*. 2004, Academic Press. p. 137-165.
53. Gambus, A., et al., *A key role for Ctf4 in coupling the MCM2-7 helicase to DNA polymerase [alpha] within the eukaryotic replisome.* EMBO J, 2009. **28**(19): p. 2992-3004.
54. Garg, P. and P.M.J. Burgers, *DNA Polymerases that Propagate the Eukaryotic DNA Replication Fork.* Critical Reviews in Biochemistry and Molecular Biology, 2005. **40**(2): p. 115-128.
55. Pursell, Z.F., et al., *Yeast DNA Polymerase Îµ Participates in Leading-Strand DNA Replication.* Science, 2007. **317**(5834): p. 127-130.

56. Kunkel, T.A. and P.M. Burgers, *Dividing the workload at a eukaryotic replication fork.* Trends in Cell Biology, 2008. **18**(11): p. 521-527.
57. Wold, M.S., *REPLICATION PROTEIN A:A Heterotrimeric, Single-Stranded DNA-Binding Protein Required for Eukaryotic DNA Metabolism.* Annual Review of Biochemistry, 1997. **66**(1): p. 61-92.
58. Wold, M.S. and T. Kelly, *Purification and characterization of replication protein A, a cellular protein required for in vitro replication of simian virus 40 DNA.* Proceedings of the National Academy of Sciences of the United States of America, 1988. **85**(8): p. 2523-2527.
59. Iftode, C., Y. Daniely, and J.A. Borowiec, *Replication Protein A (RPA): The Eukaryotic SSB.* Critical Reviews in Biochemistry and Molecular Biology, 1999. **34**(3): p. 141-180.
60. HÃ¼bscher, U., G. Maga, and S. Spadari, *EUKARYOTIC DNA POLYMERASES.* Annual Review of Biochemistry, 2002. **71**(1): p. 133-163.
61. Sancar, A., et al., *MOLECULAR MECHANISMS OF MAMMALIAN DNA REPAIR AND THE DNA DAMAGE CHECKPOINTS.* Annual Review of Biochemistry, 2004. **73**(1): p. 39-85.
62. Maga, G., et al., *DNA Elongation by the Human DNA Polymerase Î» Polymerase and Terminal Transferase Activities Are Differentially Coordinated by Proliferating Cell Nuclear Antigen and Replication Protein A.* Journal of Biological Chemistry, 2005. **280**(3): p. 1971-1981.
63. Wakasugi, M., J.T. Reardon, and A. Sancar, *The Non-catalytic Function of XPG Protein during Dual Incision in Human Nucleotide Excision Repair.* Journal of Biological Chemistry, 1997. **272**(25): p. 16030-16034.
64. MÃ¤kiniemi, M., et al., *BRCT Domain-containing Protein TopBP1 Functions in DNA Replication and Damage Response.* Journal of Biological Chemistry, 2001. **276**(32): p. 30399-30406.
65. Aparicio, O., D. Weinstein, and S. Bell, *Components and dynamics of DNA replication complexes in S. cerevisiae: redistribution of MCM proteins and Cdc45p during S phase.* Cell, 1997. **91**(1): p. 59 - 69.
66. Jeon, Y., et al., *Human TopBP1 Participates in Cyclin E/CDK2 Activation and Preinitiation Complex Assembly during G1/S Transition.* Journal of Biological Chemistry, 2007. **282**(20): p. 14882-14890.
67. Kelly, T.J. and G.W. Brown, *REGULATION OF CHROMOSOME REPLICATION.* Annual Review of Biochemistry, 2000. **69**(1): p. 829-880.
68. Dulic, V., et al., *p53-dependent inhibition of cyclin-dependent kinase activities in human fibroblasts during radiation-induced G1 arrest.* Cell, 1994. **76**(6): p. 1013-1023.
69. Muramatsu, S., et al., *CDK-dependent complex formation between replication proteins Dpb11, Sld2, Pol É›, and GINS in budding yeast.* Genes & Development. **24**(6): p. 602-612.
70. Yan, S. and W.M. Michael, *TopBP1 and DNA polymerase-Î± directly recruit the 9-1-1 complex to stalled DNA replication forks.* The Journal of Cell Biology, 2009. **184**(6): p. 793-804.
71. Venclovas, C. and M.P. Thelen, *Structure-based predictions of Rad1, Rad9, Hus1 and Rad17 participation in sliding clamp and clamp-loading complexes.* Nucleic Acids Research, 2000. **28**(13): p. 2481-2493.
72. Weiss, R.S., et al., *Hus1 Acts Upstream of Chk1 in a Mammalian DNA Damage Response Pathway.* Current Biology, 2002. **12**(1): p. 73-77.

73. Roos-Mattjus, P., et al., *Phosphorylation of Human Rad9 Is Required for Genotoxin-activated Checkpoint Signaling.* Journal of Biological Chemistry, 2003. **278**(27): p. 24428-24437.
74. Broomfield, S., T. Hryciw, and W. Xiao, *DNA postreplication repair and mutagenesis in Saccharomyces cerevisiae.* Mutation Research/DNA Repair, 2001. **486**(3): p. 167-184.
75. Friedberg, E.C., R. Wagner, and M. Radman, *Specialized DNA Polymerases, Cellular Survival, and the Genesis of Mutations.* Science, 2002. **296**(5573): p. 1627-1630.
76. Paciotti, V., et al., *Mec1p is essential for phosphorylation of the yeast DNA damage checkpoint protein Ddc1p, which physically interacts with Mec3p.* EMBO J, 1998. **17**(14): p. 4199-4209.
77. Nasmyth, K. and C.H. Haering, *THE STRUCTURE AND FUNCTION OF SMC AND KLEISIN COMPLEXES.* Annual Review of Biochemistry, 2005. **74**(1): p. 595-648.
78. Saitoh, N., et al., *ScII: an abundant chromosome scaffold protein is a member of a family of putative ATPases with an unusual predicted tertiary structure.* The Journal of Cell Biology, 1994. **127**(2): p. 303-318.
79. Melby, T.E., et al., *The Symmetrical Structure of Structural Maintenance of Chromosomes (SMC) and MukB Proteins: Long, Antiparallel Coiled Coils, Folded at a Flexible Hinge.* The Journal of Cell Biology, 1998. **142**(6): p. 1595-1604.
80. Haering, C.H., et al., *Molecular Architecture of SMC Proteins and the Yeast Cohesin Complex.* Molecular Cell, 2002. **9**(4): p. 773-788.
81. Hirano, M. and T. Hirano, *Hinge-mediated dimerization of SMC protein is essential for its dynamic interaction with DNA.* EMBO J, 2002. **21**(21): p. 5733-5744.
82. Hopfner, K.-P., et al., *Structural Biology of Rad50 ATPase: ATP-Driven Conformational Control in DNA Double-Strand Break Repair and the ABC-ATPase Superfamily.* Cell, 2000. **101**(7): p. 789-800.
83. Hirano, M., et al., *Bimodal activation of SMC ATPase by intra- and inter-molecular interactions.* EMBO J, 2001. **20**(12): p. 3238-3250.
84. Schleiffer, A., et al., *Kleisins: A Superfamily of Bacterial and Eukaryotic SMC Protein Partners.* Molecular Cell, 2003. **11**(3): p. 571-575.
85. Uhlmann, F., et al., *Cleavage of Cohesin by the CD Clan Protease Separin Triggers Anaphase in Yeast.* Cell, 2000. **103**(3): p. 375-386.
86. Arumugam, P., et al., *ATP Hydrolysis Is Required for Cohesin's Association with Chromosomes.* Current Biology, 2003. **13**(22): p. 1941-1953.
87. Weitzer, S., C. Lehane, and F. Uhlmann, *A Model for ATP Hydrolysis-Dependent Binding of Cohesin to DNA.* Current Biology, 2003. **13**(22): p. 1930-1940.
88. Haering, C.H., et al., *Structure and Stability of Cohesin's Smc1-Kleisin Interaction.* Molecular Cell, 2004. **15**(6): p. 951-964.
89. Gajiwala, K.S. and S.K. Burley, *Winged helix proteins.* Current Opinion in Structural Biology, 2000. **10**(1): p. 110-116.
90. Anderson, D.E., et al., *Condensin and cohesin display different arm conformations with characteristic hinge angles.* The Journal of Cell Biology, 2002. **156**(3): p. 419-424.
91. Losada, A., et al., *Identification and Characterization of Sa/Scc3p Subunits in the Xenopus and Human Cohesin Complexes.* The Journal of Cell Biology, 2000. **150**(3): p. 405-416.

92. Canudas, S. and S. Smith, *Differential regulation of telomere and centromere cohesion by the Scc3 homologues SA1 and SA2, respectively, in human cells.* The Journal of Cell Biology, 2009. **187**(2): p. 165-173.
93. Feeney, K.M., C.W. Wasson, and J.L. Parish, *Cohesin: a regulator of genome integrity and gene expression.* Biochemical Journal. **428**(2): p. 147-161.
94. Michaelis, C., R. Ciosk, and K. Nasmyth, *Cohesins: Chromosomal Proteins that Prevent Premature Separation of Sister Chromatids.* Cell, 1997. **91**(1): p. 35-45.
95. Darwiche, N., L.A. Freeman, and A. Strunnikov, *Characterization of the components of the putative mammalian sister chromatid cohesion complex.* Gene, 1999. **233**(1-2): p. 39-47.
96. Gerlich, D., et al., *Live-Cell Imaging Reveals a Stable Cohesin-Chromatin Interaction after but Not before DNA Replication.* Current Biology, 2006. **16**(15): p. 1571-1578.
97. Ciosk, R., et al., *Cohesin's Binding to Chromosomes Depends on a Separate Complex Consisting of Scc2 and Scc4 Proteins.* Molecular Cell, 2000. **5**(2): p. 243-254.
98. Losada, A. and T. Hirano, *Intermolecular DNA interactions stimulated by the cohesin complex in vitro: Implications for sister chromatid cohesion.* Current Biology, 2001. **11**(4): p. 268-272.
99. Gruber, S., C.H. Haering, and K. Nasmyth, *Chromosomal Cohesin Forms a Ring.* Cell, 2003. **112**(6): p. 765-777.
100. Ivanov, D. and K. Nasmyth, *A Physical Assay for Sister Chromatid Cohesion In Vitro.* Molecular Cell, 2007. **27**(2): p. 300-310.
101. Mc Intyre, J., et al., *In vivo analysis of cohesin architecture using FRET in the budding yeast Saccharomyces cerevisiae.* EMBO J, 2007. **26**(16): p. 3783-3793.
102. Haering, C.H., et al., *The cohesin ring concatenates sister DNA molecules.* Nature, 2008. **454**(7202): p. 297-301.
103. Zhang, N., et al., *A handcuff model for the cohesin complex.* The Journal of Cell Biology, 2008. **183**(6): p. 1019-1031.
104. Chang, C.-R., et al., *Targeting of cohesin by transcriptionally silent chromatin.* Genes & Development, 2005. **19**(24): p. 3031-3042.
105. Lengronne, A., et al., *Establishment of Sister Chromatid Cohesion at the S. cerevisiae Replication Fork.* Molecular Cell, 2006. **23**(6): p. 787-799.
106. TÃ³th, A., et al., *Yeast Cohesin complex requires a conserved protein, Eco1p(Ctf7), to establish cohesion between sister chromatids during DNA replication.* Genes & Development, 1999. **13**(3): p. 320-333.
107. Kenna, M.A. and R.V. Skibbens, *Mechanical Link between Cohesion Establishment and DNA Replication: Ctf7p/Eco1p, a Cohesion Establishment Factor, Associates with Three Different Replication Factor C Complexes.* Mol. Cell. Biol., 2003. **23**(8): p. 2999-3007.
108. Parnas, O., et al., *The Elg1 Clamp Loader Plays a Role in Sister Chromatid Cohesion.* PLoS ONE, 2009. **4**(5): p. e5497.
109. Moldovan, G.-L., B. Pfander, and S. Jentsch, *PCNA Controls Establishment of Sister Chromatid Cohesion during S Phase.* Molecular Cell, 2006. **23**(5): p. 723-732.
110. Ben-Shahar, T.R., et al., *Eco1-Dependent Cohesin Acetylation During Establishment of Sister Chromatid Cohesion.* Science, 2008. **321**(5888): p. 563-566.

111. Maradeo, M.E. and R.V. Skibbens, *Epitope tag-induced synthetic lethality between cohesin subunits and Ctf7/Eco1 acetyltransferase.* FEBS Letters, 2010. **584**(18): p. 4037-4040.
112. Gandhi, R., P.J. Gillespie, and T. Hirano, *Human Wapl Is a Cohesin-Binding Protein that Promotes Sister-Chromatid Resolution in Mitotic Prophase.* Current Biology, 2006. **16**(24): p. 2406-2417.
113. Kueng, S., et al., *Wapl Controls the Dynamic Association of Cohesin with Chromatin.* Cell, 2006. **127**(5): p. 955-967.
114. Rowland, B.D., et al., *Building Sister Chromatid Cohesion: Smc3 Acetylation Counteracts an Antiestablishment Activity.* Molecular Cell, 2009. **33**(6): p. 763-774.
115. Chan, G.K., S.-T. Liu, and T.J. Yen, *Kinetochore structure and function.* Trends in Cell Biology, 2005. **15**(11): p. 589-598.
116. Tanaka, T.U., M.J.R. Stark, and K. Tanaka, *Kinetochore capture and bi-orientation on the mitotic spindle.* Nat Rev Mol Cell Biol, 2005. **6**(12): p. 929-942.
117. Nogales, E., et al., *High-Resolution Model of the Microtubule.* Cell, 1999. **96**(1): p. 79-88.
118. Desai, A. and T.J. Mitchison, *MICROTUBULE POLYMERIZATION DYNAMICS.* Annual Review of Cell and Developmental Biology, 1997. **13**(1): p. 83-117.
119. Kirschner, M. and T. Mitchison, *Beyond self-assembly: From microtubules to morphogenesis.* Cell, 1986. **45**(3): p. 329-342.
120. Caudron, M., et al., *Spatial Coordination of Spindle Assembly by Chromosome-Mediated Signaling Gradients.* Science, 2005. **309**(5739): p. 1373-1376.
121. Khodjakov, A., et al., *Minus-end capture of preformed kinetochore fibers contributes to spindle morphogenesis.* The Journal of Cell Biology, 2003. **160**(5): p. 671-683.
122. Takaki, T., et al., *Polo-like kinase 1 reaches beyond mitosis--cytokinesis, DNA damage response, and development.* Current Opinion in Cell Biology, 2008. **20**(6): p. 650-660.
123. ÖStergren, G., *THE MECHANISM OF CO-ORIENTATION IN BIVALENTS AND MULTIVALENTS.* Hereditas, 1951. **37**(1-2): p. 85-156.
124. Hauf, S., et al., *The small molecule Hesperadin reveals a role for Aurora B in correcting kinetochore–microtubule attachment and in maintaining the spindle assembly checkpoint.* The Journal of Cell Biology, 2003. **161**(2): p. 281-294.
125. Tanaka, T.U., et al., *Evidence that the Ipl1-Sli15 (Aurora Kinase-INCENP) Complex Promotes Chromosome Bi-orientation by Altering Kinetochore-Spindle Pole Connections.* Cell, 2002. **108**(3): p. 317-329.
126. Cheeseman, I.M., et al., *Phospho-Regulation of Kinetochore-Microtubule Attachments by the Aurora Kinase Ipl1p.* Cell, 2002. **111**(2): p. 163-172.
127. Tien, J.F., et al., *Cooperation of the Dam1 and Ndc80 kinetochore complexes enhances microtubule coupling and is regulated by aurora B.* The Journal of Cell Biology, 2010. **189**(4): p. 713-723.
128. Keating, P., et al., *Ipl1-dependent phosphorylation of Dam1 is reduced by tension applied on kinetochores.* J Cell Sci, 2009. **122**(Pt 23): p. 4375-82.
129. Sun, Y., et al., *Separase Is Recruited to Mitotic Chromosomes to Dissolve Sister Chromatid Cohesion in a DNA-Dependent Manner.* Cell, 2009. **137**(1): p. 123-132.
130. Steuer, E.R., et al., *Localization of cytoplasmic dynein to mitotic spindles and kinetochores.* Nature, 1990. **345**(6272): p. 266-268.

131. Sharp, D.J., G.C. Rogers, and J.M. Scholey, *Cytoplasmic dyein is required for poleward chromosome movement during mitosis in Drosophila embryos.* Nature Cell Biology, 2000. **2**(12): p. 922-930.
132. Lombillo, V.A., R.J. Stewart, and J. Richard McIntosh, *Minus-end-directed motion of kinesin-coated microspheres driven by microtubule depolymerization.* Nature, 1995. **373**(6510): p. 161-164.
133. Rogers, G.C., et al., *Two mitotic kinesins cooperate to drive sister chromatid separation during anaphase.* Nature, 2004. **427**(6972): p. 364-370.
134. Hoyt, M.A., L. Totis, and B.T. Roberts, *S. cerevisiae genes required for cell cycle arrest in response to loss of microtubule function.* Cell, 1991. **66**(3): p. 507-517.
135. Musacchio, A. and K.G. Hardwick, *The spindle checkpoint: structural insights into dynamic signalling.* Nat Rev Mol Cell Biol, 2002. **3**(10): p. 731-741.
136. Hwang, L.H., et al., *Budding Yeast Cdc20: A Target of the Spindle Checkpoint.* Science, 1998. **279**(5353): p. 1041-1044.
137. Pangilinan, F. and F. Spencer, *Abnormal kinetochore structure activates the spindle assembly checkpoint in budding yeast.* Mol. Biol. Cell, 1996. **7**(8): p. 1195-1208.
138. Gorbsky, G. and W. Ricketts, *Differential expression of a phosphoepitope at the kinetochores of moving chromosomes.* The Journal of Cell Biology, 1993. **122**(6): p. 1311-1321.
139. Taylor, S.S., et al., *Kinetochore localisation and phosphorylation of the mitotic checkpoint components Bub1 and BubR1 are differentially regulated by spindle events in human cells.* J Cell Sci, 2001. **114**(24): p. 4385-4395.
140. Sharp-Baker, H. and R.-H. Chen, *Spindle Checkpoint Protein Bub1 Is Required for Kinetochore Localization of Mad1, Mad2, Bub3, and Cenp-E, Independently of Its Kinase Activity.* The Journal of Cell Biology, 2001. **153**(6): p. 1239-1250.
141. Tang, Z., et al., *Phosphorylation of Cdc20 by Bub1 Provides a Catalytic Mechanism for APC/C Inhibition by the Spindle Checkpoint.* Molecular Cell, 2004. **16**(3): p. 387-397.
142. Chan, G.K.T., et al., *Human Bubr1 Is a Mitotic Checkpoint Kinase That Monitors Cenp-E Functions at Kinetochores and Binds the Cyclosome/APC.* The Journal of Cell Biology, 1999. **146**(5): p. 941-954.
143. Abrieu, A., et al., *CENP-E as an Essential Component of the Mitotic Checkpoint In Vitro.* Cell, 2000. **102**(6): p. 817-826.
144. Weaver, B.A.A., et al., *Centromere-associated protein-E is essential for the mammalian mitotic checkpoint to prevent aneuploidy due to single chromosome loss.* The Journal of Cell Biology, 2003. **162**(4): p. 551-563.
145. Mao, Y., A. Abrieu, and D.W. Cleveland, *Activating and Silencing the Mitotic Checkpoint through CENP-E-Dependent Activation/Inactivation of BubR1.* Cell, 2003. **114**(1): p. 87-98.
146. Pinsky, B.A., et al., *The Ipl1-Aurora protein kinase activates the spindle checkpoint by creating unattached kinetochores.* Nat Cell Biol, 2006. **8**(1): p. 78-83.
147. Ditchfield, C., et al., *Aurora B couples chromosome alignment with anaphase by targeting BubR1, Mad2, and Cenp-E to kinetochores.* The Journal of Cell Biology, 2003. **161**(2): p. 267-280.
148. Howell, B.J., et al., *Cytoplasmic dynein/dynactin drives kinetochore protein transport to the spindle poles and has a role in mitotic spindle checkpoint inactivation.* The Journal of Cell Biology, 2001. **155**(7): p. 1159-1172.

149. Palframan, W.J., et al., *Anaphase Inactivation of the Spindle Checkpoint.* Science, 2006. **313**(5787): p. 680-684.
150. Stemmann, O., et al., *Dual Inhibition of Sister Chromatid Separation at Metaphase.* Cell, 2001. **107**(6): p. 715-726.
151. Lindon, C., *Control of mitotic exit and cytokinesis by the APC/C.* Biochemical Society Transactions, 2008. **036**(3): p. 405-410.
152. Peters, J.-M., *The anaphase promoting complex/cyclosome: a machine designed to destroy.* Nat Rev Mol Cell Biol, 2006. **7**(9): p. 644-656.
153. Zou, H., et al., *Identification of a Vertebrate Sister-Chromatid Separation Inhibitor Involved in Transformation and Tumorigenesis.* Science, 1999. **285**(5426): p. 418-422.
154. Mei, J., X. Huang, and P. Zhang, *Securin is not required for cellular viability, but is required for normal growth of mouse embryonic fibroblasts.* Current Biology, 2001. **11**(15): p. 1197-1201.
155. Losada, A., M. Hirano, and T. Hirano, *Cohesin release is required for sister chromatid resolution, but not for condensin-mediated compaction, at the onset of mitosis.* Genes & Development, 2002. **16**(23): p. 3004-3016.
156. Sumara, I., et al., *The Dissociation of Cohesin from Chromosomes in Prophase Is Regulated by Polo-like Kinase.* Molecular Cell, 2002. **9**(3): p. 515-525.
157. Alexandru, G., et al., *Phosphorylation of the Cohesin Subunit Scc1 by Polo/Cdc5 Kinase Regulates Sister Chromatid Separation in Yeast.* Cell, 2001. **105**(4): p. 459-472.
158. Hauf, S., et al., *Dissociation of cohesin from chromosome arms and loss of arm cohesion during early mitosis depends on phosphorylation of SA2.* PLoS Biol, 2005. **3**(3): p. e69.
159. Giménez-Abián, J.F., et al., *Regulation of Sister Chromatid Cohesion between Chromosome Arms.* Current Biology, 2004. **14**(13): p. 1187-1193.
160. McGuinness, B.E., et al., *Shugoshin Prevents Dissociation of Cohesin from Centromeres During Mitosis in Vertebrate Cells.* PLoS Biol, 2005. **3**(3): p. e86.
161. Salic, A., J.C. Waters, and T.J. Mitchison, *Vertebrate Shugoshin Links Sister Centromere Cohesion and Kinetochore Microtubule Stability in Mitosis.* Cell, 2004. **118**(5): p. 567-578.
162. Kitajima, T.S., S.A. Kawashima, and Y. Watanabe, *The conserved kinetochore protein shugoshin protects centromeric cohesion during meiosis.* Nature, 2004. **427**(6974): p. 510-517.
163. Indjeian, V.B., B.M. Stern, and A.W. Murray, *The Centromeric Protein Sgo1 Is Required to Sense Lack of Tension on Mitotic Chromosomes.* Science, 2005. **307**(5706): p. 130-133.
164. Tang, Z., et al., *PP2A Is Required for Centromeric Localization of Sgo1 and Proper Chromosome Segregation.* Developmental Cell, 2006. **10**(5): p. 575-585.
165. Riedel, C.G., et al., *Protein phosphatase 2A protects centromeric sister chromatid cohesion during meiosis I.* Nature, 2006. **441**(7089): p. 53-61.
166. Kitajima, T.S., et al., *Shugoshin collaborates with protein phosphatase 2A to protect cohesin.* Nature, 2006. **441**(7089): p. 46-52.
167. Tang, Z., et al., *Human Bub1 protects centromeric sister-chromatid cohesion through Shugoshin during mitosis.* Proceedings of the National Academy of Sciences of the United States of America, 2004. **101**(52): p. 18012-18017.
168. Kitajima, T.S., et al., *Human Bub1 Defines the Persistent Cohesion Site along the Mitotic Chromosome by Affecting Shugoshin Localization.* Current Biology, 2005. **15**(4): p. 353-359.

169. Spencer, F., et al., *Mitotic Chromosome Transmission Fidelity Mutants in Saccharomyces cerevisiae.* Genetics, 1990. **124**(2): p. 237-249.
170. Gerring, S.L., F. Spencer, and P. Hieter, *The CHL 1 (CTF 1) gene product of Saccharomyces cerevisiae is important for chromosome transmission and normal cell cycle progression in G2/M.* EMBO J, 1990. **9**(13): p. 4347-58.
171. Holloway, S.L., *CHL1 is a nuclear protein with an essential ATP binding site that exhibits a size-dependent effect on chromosome segregation.* Nucleic Acids Research, 2000. **28**(16): p. 3056-3064.
172. Amann, J., V.J. Kidd, and J.M. Lahti, *Characterization of Putative Human Homologues of the Yeast Chromosome Transmission Fidelity Gene, CHL1.* Journal of Biological Chemistry, 1997. **272**(6): p. 3823-3832.
173. Frank, S. and S. Werner, *The Human Homologue of the Yeast CHL1 Gene Is a Novel Keratinocyte Growth Factor-regulated Gene.* Journal of Biological Chemistry, 1996. **271**(40): p. 24337-24340.
174. Hirota, Y. and J.M. Lahti, *Characterization of the enzymatic activity of hChlR1, a novel human DNA helicase.* Nucleic Acids Research, 2000. **28**(4): p. 917-924.
175. Parish, J.L., et al., *The DNA helicase ChlR1 is required for sister chromatid cohesion in mammalian cells.* J Cell Sci, 2006. **119**(23): p. 4857-4865.
176. Gregson, H.C., et al., *A Potential Role for Human Cohesin in Mitotic Spindle Aster Assembly.* Journal of Biological Chemistry, 2001. **276**(50): p. 47575-47582.
177. Inoue, A., et al., *Loss of ChlR1 helicase in mouse causes lethality due to the accumulation of aneuploid cells generated by cohesion defects and placental malformation.* Cell Cycle, 2007. **6**(13): p. 1646-54.
178. Lengronne, A., et al., *Cohesin relocation from sites of chromosomal loading to places of convergent transcription.* Nature, 2004. **430**(6999): p. 573-578.
179. Gullerova, M. and N.J. Proudfoot, *Cohesin Complex Promotes Transcriptional Termination between Convergent Genes in S. pombe.* Cell, 2008. **132**(6): p. 983-995.
180. Laloraya, S., V. Guacci, and D. Koshland, *Chromosomal addresses of the cohesin component Mcd1p.* J Cell Biol, 2000. **151**(5): p. 1047-56.
181. Rine, J. and I. Herskowitz, *Four Genes Responsible for a Position Effect on Expression From HML and HMR in Saccharomyces cerevisiae.* Genetics, 1987. **116**(1): p. 9-22.
182. Kobayashi, T., et al., *SIR2 Regulates Recombination between Different rDNA Repeats, but Not Recombination within Individual rRNA Genes in Yeast.* Cell, 2004. **117**(4): p. 441-453.
183. Donze, D., et al., *The boundaries of the silenced HMR domain in Saccharomyces cerevisiae.* Genes & Development, 1999. **13**(6): p. 698-708.
184. Lau, A., H. Blitzblau, and S.P. Bell, *Cell-cycle control of the establishment of mating-type silencing in S. cerevisiae.* Genes & Development, 2002. **16**(22): p. 2935-2945.
185. Parelho, V., et al., *Cohesins Functionally Associate with CTCF on Mammalian Chromosome Arms.* Cell, 2008. **132**(3): p. 422-433.
186. Klenova, E.M., et al., *Characterization of the Chicken CTCF Genomic Locus, and Initial Study of the Cell Cycle-regulated Promoter of the Gene.* Journal of Biological Chemistry, 1998. **273**(41): p. 26571-26579.
187. Kim, T.H., et al., *Analysis of the Vertebrate Insulator Protein CTCF-Binding Sites in the Human Genome.* Cell, 2007. **128**(6): p. 1231-1245.
188. Wendt, K.S., et al., *Cohesin mediates transcriptional insulation by CCCTC-binding factor.* Nature, 2008. **451**(7180): p. 796-801.

189. Saitoh, N., et al., *Structural and functional conservation at the boundaries of the chicken [beta]-globin domain.* EMBO J, 2000. **19**(10): p. 2315-2322.
190. Splinter, E., et al., *CTCF mediates long-range chromatin looping and local histone modification in the Î²-globin locus.* Genes & Development, 2006. **20**(17): p. 2349-2354.
191. Rubio, E.D., et al., *CTCF physically links cohesin to chromatin.* Proceedings of the National Academy of Sciences, 2008. **105**(24): p. 8309-8314.
192. Hadjur, S., et al., *Cohesins form chromosomal cis-interactions at the developmentally regulated IFNG locus.* Nature, 2009. **460**(7253): p. 410-413.
193. Rothkamm, K., et al., *Pathways of DNA Double-Strand Break Repair during the Mammalian Cell Cycle.* Mol. Cell. Biol., 2003. **23**(16): p. 5706-5715.
194. Meek, K., et al., *The DNA-dependent protein kinase: the director at the end.* Immunological Reviews, 2004. **200**(1): p. 132-141.
195. Kim, J.-S., et al., *Independent and sequential recruitment of NHEJ and HR factors to DNA damage sites in mammalian cells.* J. Cell Biol., 2005. **170**(3): p. 341-347.
196. Cary, R.B., et al., *DNA looping by Ku and the DNA-dependent proteinâ€‰kinase.* Proceedings of the National Academy of Sciences of the United States of America, 1997. **94**(9): p. 4267-4272.
197. Uematsu, N., et al., *Autophosphorylation of DNA-PKCS regulates its dynamics at DNA double-strand breaks.* J. Cell Biol., 2007. **177**(2): p. 219-229.
198. Meek, K., et al., *trans Autophosphorylation at DNA-Dependent Protein Kinase's Two Major Autophosphorylation Site Clusters Facilitates End Processing but Not End Joining.* Mol. Cell. Biol., 2007. **27**(10): p. 3881-3890.
199. Ma, Y., et al., *Hairpin Opening and Overhang Processing by an Artemis/DNA-Dependent Protein Kinase Complex in Nonhomologous End Joining and V(D)J Recombination.* Cell, 2002. **108**(6): p. 781-794.
200. Ma, Y., et al., *The DNA-dependent Protein Kinase Catalytic Subunit Phosphorylation Sites in Human Artemis.* Journal of Biological Chemistry, 2005. **280**(40): p. 33839-33846.
201. Drouet, J.r.m., et al., *Interplay between Ku, Artemis, and the DNA-dependent Protein Kinase Catalytic Subunit at DNA Ends.* Journal of Biological Chemistry, 2006. **281**(38): p. 27784-27793.
202. Paull, T.T., *Saving the Ends for Last: The Role of Pol [mu] in DNA End Joining.* Molecular Cell, 2005. **19**(3): p. 294-296.
203. Grawunder, U., et al., *Activity of DNA ligase IV stimulated by complex formation with XRCC4 protein in mammalian cells.* Nature, 1997. **388**(6641): p. 492-495.
204. Drouet, J.r.m., et al., *DNA-dependent Protein Kinase and XRCC4-DNA Ligase IV Mobilization in the Cell in Response to DNA Double Strand Breaks.* Journal of Biological Chemistry, 2005. **280**(8): p. 7060-7069.
205. Downs, J.A., M.C. Nussenzweig, and A. Nussenzweig, *Chromatin dynamics and the preservation of genetic information.* Nature, 2007. **447**(7147): p. 951-958.
206. Kim, J.-S., et al., *Specific Recruitment of Human Cohesin to Laser-induced DNA Damage.* Journal of Biological Chemistry, 2002. **277**(47): p. 45149-45153.
207. Lee, J.-H. and T.T. Paull, *ATM Activation by DNA Double-Strand Breaks Through the Mre11-Rad50-Nbs1 Complex.* Science, 2005. **308**(5721): p. 551-554.
208. Ivanov, E.L., et al., *Mutations in XRS2 and RAD50 delay but do not prevent mating-type switching in Saccharomyces cerevisiae.* Mol. Cell. Biol., 1994. **14**(5): p. 3414-3425.

209. Lengsfeld, B.M., et al., *Sae2 Is an Endonuclease that Processes Hairpin DNA Cooperatively with the Mre11/Rad50/Xrs2 Complex.* Molecular Cell, 2007. **28**(4): p. 638-651.
210. Mimitou, E.P. and L.S. Symington, *Sae2, Exo1 and Sgs1 collaborate in DNA double-strand break processing.* Nature, 2008. **455**(7214): p. 770-774.
211. Sung, P. and H. Klein, *Mechanism of homologous recombination: mediators and helicases take on regulatory functions.* Nat Rev Mol Cell Biol, 2006. **7**(10): p. 739-750.
212. Song, B. and P. Sung, *Functional Interactions among Yeast Rad51 Recombinase, Rad52 Mediator, and Replication Protein A in DNA Strand Exchange.* Journal of Biological Chemistry, 2000. **275**(21): p. 15895-15904.
213. Ristic, D., et al., *Human Rad51 filaments on double- and single-stranded DNA: correlating regular and irregular forms with recombination function.* Nucleic Acids Research. **33**(10): p. 3292-3302.
214. Ira, G. and J.E. Haber, *Characterization of RAD51-Independent Break-Induced Replication That Acts Preferentially with Short Homologous Sequences.* Mol. Cell. Biol., 2002. **22**(18): p. 6384-6392.
215. Amitani, I., R.J. Baskin, and S.C. Kowalczykowski, *Visualization of Rad54, a Chromatin Remodeling Protein, Translocating on Single DNA Molecules.* Molecular Cell, 2006. **23**(1): p. 143-148.
216. Szostak, J.W., et al., *The double-strand-break repair model for recombination.* Cell, 1983. **33**(1): p. 25-35.
217. McIlwraith, M.J., et al., *Human DNA Polymerase [eta] Promotes DNA Synthesis from Strand Invasion Intermediates of Homologous Recombination.* Molecular Cell, 2005. **20**(5): p. 783-792.
218. Batty, D., et al., *Stable binding of human XPC complex to irradiated DNA confers strong discrimination for damaged sites.* Journal of Molecular Biology, 2000. **300**(2): p. 275-290.
219. Sugasawa, K., et al., *A multistep damage recognition mechanism for global genomic nucleotide excision repair.* Genes & Development, 2001. **15**(5): p. 507-521.
220. Min, J.-H. and N.P. Pavletich, *Recognition of DNA damage by the Rad4 nucleotide excision repair protein.* Nature, 2007. **449**(7162): p. 570-575.
221. Zurita, M. and C. Merino, *The transcriptional complexity of the TFIIH complex.* Trends in Genetics, 2003. **19**(10): p. 578-584.
222. Dip, R., U. Camenisch, and H. Naegeli, *Mechanisms of DNA damage recognition and strand discrimination in human nucleotide excision repair.* DNA Repair, 2004. **3**(11): p. 1409-1423.
223. Nakatsu, Y., et al., *XAB2, a Novel Tetratricopeptide Repeat Protein Involved in Transcription-coupled DNA Repair and Transcription.* Journal of Biological Chemistry, 2000. **275**(45): p. 34931-34937.
224. Stigger, E., R. Drissi, and S.-H. Lee, *Functional Analysis of Human Replication Protein A in Nucleotide Excision Repair.* Journal of Biological Chemistry, 1998. **273**(15): p. 9337-9343.
225. Camenisch, U., et al., *Recognition of helical kinks by xeroderma pigmentosum group A protein triggers DNA excision repair.* Nat Struct Mol Biol, 2006. **13**(3): p. 278-284.
226. Kolpashchikov, D.M., et al., *Polarity of human replication protein A binding to DNA.* Nucl. Acids Res., 2001. **29**(2): p. 373-379.

227. Staresincic, L., et al., *Coordination of dual incision and repair synthesis in human nucleotide excision repair.* EMBO J, 2009. **28**(8): p. 1111-1120.
228. Volker, M., et al., *Sequential Assembly of the Nucleotide Excision Repair Factors In Vivo.* Molecular Cell, 2001. **8**(1): p. 213-224.
229. Saijo, M., et al., *Sequential Binding of DNA Repair Proteins RPA and ERCC1 to XPA in vitro.* Nucl. Acids Res., 1996. **24**(23): p. 4719-4724.
230. Evans, E., et al., *Mechanism of open complex and dual incision formation by human nucleotide excision repair factors.* EMBO J, 1997. **16**(21): p. 6559-6573.
231. Costa, R.M.A., et al., *The eukaryotic nucleotide excision repair pathway.* Biochimie, 2003. **85**(11): p. 1083-1099.
232. Gordienko, I. and W.D. Rupp, *The limited strand-separating activity of the UvrAB protein complex and its role in the recognition of DNA damage.* EMBO J, 1997. **16**(4): p. 889-895.
233. Truglio, J.J., et al., *Prokaryotic Nucleotide Excision Repair:â€‰ The UvrABC System.* Chemical Reviews, 2006. **106**(2): p. 233-252.
234. Wood, R.D., *Nucleotide Excision Repair in Mammalian Cells.* Journal of Biological Chemistry, 1997. **272**(38): p. 23465-23468.
235. Ogawa, H., et al., *Functions of the yeast meiotic recombination genes, MRE11 and MRE2.* Advances in Biophysics, 1995. **31**: p. 67-76.
236. Dolganov, G.M., et al., *Human RAD50 is physically associated with human Mre11: Identification of a conserved multiprotein complex implicated in recombinational DNA repair.* Molecular and Cellular Biology, 1996. **16**(9): p. 4832-4841.
237. Hopkins, B.B. and T.T. Paull, *The P. furiosus Mre11/Rad50 Complex Promotes 5' Strand Resection at a DNA Double-Strand Break.* Cell, 2008. **135**(2): p. 250-260.
238. Williams, R.S., J.S. Williams, and J.A. Tainer, *Mre11-Rad50-Nbs1 is a keystone complex connecting DNA repair machinery, double-strand break signaling, and the chromatin template.* Biochemistry and Cell Biology, 2007. **85**(4): p. 509-520.
239. Williams, R.S., et al., *Mre11 Dimers Coordinate DNA End Bridging and Nuclease Processing in Double-Strand-Break Repair.* Cell, 2008. **135**(1): p. 97-109.
240. Paull, T.T. and M. Gellert, *The 3' to 5' Exonuclease Activity of Mre11 Facilitates Repair of DNA Double-Strand Breaks.* Molecular Cell, 1998. **1**(7): p. 969-979.
241. de Jager, M., et al., *Human Rad50/Mre11 Is a Flexible Complex that Can Tether DNA Ends.* Molecular Cell, 2001. **8**(5): p. 1129-1135.
242. Wiltzius, J.J.W., et al., *The Rad50 hook domain is a critical determinant of Mre11 complex functions.* Nat Struct Mol Biol, 2005. **12**(5): p. 403-407.
243. Lloyd, J., et al., *A Supramodular FHA/BRCT-Repeat Architecture Mediates Nbs1 Adaptor Function in Response to DNA Damage.* Cell, 2009. **139**(1): p. 100-111.
244. Williams, R.S., et al., *Nbs1 Flexibly Tethers Ctp1 and Mre11-Rad50 to Coordinate DNA Double-Strand Break Processing and Repair.* Cell, 2009. **139**(1): p. 87-99.
245. Desai-Mehta, A., K.M. Cerosaletti, and P. Concannon, *Distinct Functional Domains of Nibrin Mediate Mre11 Binding, Focus Formation, and Nuclear Localization.* Mol. Cell. Biol., 2001. **21**(6): p. 2184-2191.
246. Stewart, G.S., et al., *The DNA Double-Strand Break Repair Gene hMRE11 Is Mutated in Individuals with an Ataxia-Telangiectasia-like Disorder.* Cell, 1999. **99**(6): p. 577-587.
247. Uziel, T., et al., *Requirement of the MRN complex for ATM activation by DNA damage.* EMBO J, 2003. **22**(20): p. 5612-5621.
248. You, Z., et al., *ATM Activation and Its Recruitment to Damaged DNA Require Binding to the C Terminus of Nbs1.* Mol. Cell. Biol., 2005. **25**(13): p. 5363-5379.

249. Buis, J., et al., *Mre11 Nuclease Activity Has Essential Roles in DNA Repair and Genomic Stability Distinct from ATM Activation.* Cell, 2008. **135**(1): p. 85-96.
250. Carson, C.T., et al., *Mislocalization of the MRN complex prevents ATR signaling during adenovirus infection.* EMBO J, 2009. **28**(6): p. 652-662.
251. Hopfner, K.-P., et al., *The Rad50 zinc-hook is a structure joining Mre11 complexes in DNA recombination and repair.* Nature, 2002. **418**(6897): p. 562-566.
252. Sjögren, C. and K. Nasmyth, *Sister chromatid cohesion is required for postreplicative double-strand break repair in Saccharomyces cerevisiae.* Current Biology, 2001. **11**(12): p. 991-995.
253. Sonoda, E., et al., *Scc1/Rad21/Mcd1 Is Required for Sister Chromatid Cohesion and Kinetochore Function in Vertebrate Cells.* Developmental Cell, 2001. **1**(6): p. 759-770.
254. Takata, M., et al., *Homologous recombination and non-homologous end-joining pathways of DNA double-strand break repair have overlapping roles in the maintenance of chromosomal integrity in vertebrate cells.* EMBO J, 1998. **17**(18): p. 5497-508.
255. Hartsuiker, E., et al., *Fission yeast Rad50 stimulates sister chromatid recombination and links cohesion with repair.* EMBO J, 2001. **20**(23): p. 6660-6671.
256. Ström, L., et al., *Postreplicative Recruitment of Cohesin to Double-Strand Breaks Is Required for DNA Repair.* Molecular Cell, 2004. **16**(6): p. 1003-1015.
257. Ünal, E., et al., *DNA Damage Response Pathway Uses Histone Modification to Assemble a Double-Strand Break-Specific Cohesin Domain.* Molecular Cell, 2004. **16**(6): p. 991-1002.
258. Bekker-Jensen, S., et al., *Spatial organization of the mammalian genome surveillance machinery in response to DNA strand breaks.* J. Cell Biol., 2006. **173**(2): p. 195-206.
259. Ström, L. and C. Sjögren, *Chromosome segregation and double-strand break repair -- a complex connection.* Current Opinion in Cell Biology, 2007. **19**(3): p. 344-349.
260. Dodson, H. and C.G. Morrison, *Increased sister chromatid cohesion and DNA damage response factor localization at an enzyme-induced DNA double-strand break in vertebrate cells.* Nucl. Acids Res., 2009. **37**(18): p. 6054-6063.
261. Kim, S.-T., B. Xu, and M.B. Kastan, *Involvement of the cohesin protein, Smc1, in Atm-dependent and independent responses to DNA damage.* Genes & Development, 2002. **16**(5): p. 560-570.
262. Yazdi, P.T., et al., *SMC1 is a downstream effector in the ATM/NBS1 branch of the human S-phase checkpoint.* Genes & Development, 2002. **16**(5): p. 571-582.
263. Lans, H., et al., *Involvement of Global Genome Repair, Transcription Coupled Repair, and Chromatin Remodeling in UV DNA Damage Response Changes during Development.* PLoS Genet. **6**(5): p. e1000941.
264. Hakimi, M.-A., et al., *A chromatin remodelling complex that loads cohesin onto human chromosomes.* Nature, 2002. **418**(6901): p. 994-998.
265. Hara, R. and A. Sancar, *The SWI/SNF Chromatin-Remodeling Factor Stimulates Repair by Human Excision Nuclease in the Mononucleosome Core Particle.* Mol. Cell. Biol., 2002. **22**(19): p. 6779-6787.
266. Gong, F., D. Fahy, and M.J. Smerdon, *Rad4-Rad23 interaction with SWI/SNF links ATP-dependent chromatin remodeling with nucleotide excision repair.* Nat Struct Mol Biol, 2006. **13**(10): p. 902-907.

267. Andersen, E.C., X. Lu, and H.R. Horvitz, *C. elegans ISWI and NURF301 antagonize an Rb-like pathway in the determination of multiple cell fates.* Development, 2006. **133**(14): p. 2695-2704.
268. Ura, K., et al., *ATP-dependent chromatin remodeling facilitates nucleotide excision repair of UV-induced DNA lesions in synthetic dinucleosomes.* EMBO J, 2001. **20**(8): p. 2004-2014.
269. Liu, J. and I. Krantz, *Cornelia de Lange syndrome, cohesin, and beyond.* Clinical Genetics, 2009. **76**(4): p. 303-314.
270. Hirano, T., *At the heart of the chromosome: SMC proteins in action.* Nat Rev Mol Cell Biol, 2006. **7**(5): p. 311-322.
271. Rollins, R.A., et al., *Drosophila Nipped-B Protein Supports Sister Chromatid Cohesion and Opposes the Stromalin/Scc3 Cohesion Factor To Facilitate Long-Range Activation of the cut Gene.* Mol. Cell. Biol., 2004. **24**(8): p. 3100-3111.
272. Liu, J., et al., *Transcriptional Dysregulation in <italic>NIPBL</italic> and Cohesin Mutant Human Cells.* PLoS Biol, 2009. **7**(5): p. e1000119.
273. Krantz, I.D., et al., *Cornelia de Lange syndrome is caused by mutations in NIPBL, the human homolog of Drosophila melanogaster Nipped-B.* Nat Genet, 2004. **36**(6): p. 631-635.
274. Liu, J. and I.D. Krantz, *Cohesin and Human Disease.* Annual Review of Genomics and Human Genetics, 2008. **9**(1): p. 303-320.
275. Schüle, B., et al., *Inactivating Mutations in ESCO2 Cause SC Phocomelia and Roberts Syndrome: No Phenotype-Genotype Correlation.* The American Journal of Human Genetics, 2005. **77**(6): p. 1117-1128.
276. Gordillo, M., et al., *The molecular mechanism underlying Roberts syndrome involves loss of ESCO2 acetyltransferase activity.* Human Molecular Genetics, 2008. **17**(14): p. 2172-2180.
277. Gard, S., et al., *Cohesinopathy mutations disrupt the subnuclear organization of chromatin.* The Journal of Cell Biology, 2009. **187**(4): p. 455-462.
278. van der Lelij, P., et al., *Warsaw Breakage Syndrome, a Cohesinopathy Associated with Mutations in the XPD Helicase Family Member DDX11/ChlR1*. The American Journal of Human Genetics. **86**(2): p. 262-266.
279. KLEIBER, K., K. STREBHARDT, and B.T. MARTIN, *The Biological Relevance of FHL2 in Tumour Cells and its Role as a Putative Cancer Target.* Anticancer Research, 2007. **27**(1A): p. 55-61.
280. Labalette, C., et al., *Interaction and Functional Cooperation between the LIM Protein FHL2, CBP/p300, and {beta}-Catenin.* Mol. Cell. Biol., 2004. **24**(24): p. 10689-10702.
281. Behrens, J., et al., *Functional interaction of [beta]-catenin with the transcription factor LEF-1.* Nature, 1996. **382**(6592): p. 638-642.
282. Brantjes, H., et al., *TCF: Lady Justice Casting the Final Verdict on the Outcome of Wnt Signalling.* Biological Chemistry, 2005. **383**(2): p. 255-261.
283. Chan, H.M. and N.B. La Thangue, *p300/CBP proteins: HATs for transcriptional bridges and scaffolds.* J Cell Sci, 2001. **114**(13): p. 2363-2373.
284. Levy, L., et al., *Acetylation of {beta}-Catenin by p300 Regulates {beta}-Catenin-Tcf4 Interaction.* Mol. Cell. Biol., 2004. **24**(8): p. 3404-3414.
285. Tetsu, O. and F. McCormick, *[beta]-Catenin regulates expression of cyclin D1 in colon carcinoma cells.* Nature, 1999. **398**(6726): p. 422-426.
286. Wei, Y., et al., *Identification of the LIM Protein FHL2 as a Coactivator of Î²-Catenin.* Journal of Biological Chemistry, 2003. **278**(7): p. 5188-5194.

287. Shaywitz, A.J. and M.E. Greenberg, *CREB: A Stimulus-Induced Transcription Factor Activated by A Diverse Array of Extracellular Signals.* Annual Review of Biochemistry, 1999. **68**(1): p. 821-861.
288. Mayr, B. and M. Montminy, *Transcriptional regulation by the phosphorylation-dependent factor CREB.* Nat Rev Mol Cell Biol, 2001. **2**(8): p. 599-609.
289. White, P.C., et al., *Regulation of cyclin D2 and the cyclin D2 promoter by protein kinase A and CREB in lymphocytes.* Oncogene, 2005. **25**(15): p. 2170-2180.
290. Desdouets, C., et al., *Cell cycle regulation of cyclin A gene expression by the cyclic AMP- responsive transcription factors CREB and CREM.* Mol. Cell. Biol., 1995. **15**(6): p. 3301-3309.
291. Fimia, G.M., D. De Cesare, and P. Sassone-Corsi, *A Family of LIM-Only Transcriptional Coactivators: Tissue-Specific Expression and Selective Activation of CREB and CREM.* Mol. Cell. Biol., 2000. **20**(22): p. 8613-8622.
292. Labalette, C., et al., *The LIM-only Protein FHL2 Regulates Cyclin D1 Expression and Cell Proliferation.* Journal of Biological Chemistry, 2008. **283**(22): p. 15201-15208.
293. Chan, K.K., et al., *Protein-protein interaction of FHL2, a LIM domain protein preferentially expressed in human heart, with hCDC47.* Journal of Cellular Biochemistry, 2000. **76**(3): p. 499-508.
294. Kang, C.M., et al., *Possible biomarkers for ionizing radiation exposure in human peripheral blood lymphocytes.* Radiat Res, 2003. **159**(3): p. 312-9.
295. Scholl, F.A., et al., *DRAL is a p53-responsive gene whose four and a half LIM domain protein product induces apoptosis.* J Cell Biol, 2000. **151**(3): p. 495-506.
296. Paul, C., et al., *The LIM-only protein FHL2 is a negative regulator of E4F1.* Oncogene, 2006. **25**(40): p. 5475-5484.
297. Le Cam, L., et al., *E4F1 Is an Atypical Ubiquitin Ligase that Modulates p53 Effector Functions Independently of Degradation.* Cell, 2006. **127**(4): p. 775-788.
298. Yan, J., et al., *BRCA1 interacts with FHL2 and enhances FHL2 transactivation function.* FEBS Letters, 2003. **553**(1-2): p. 183-189.
299. Rahman, N. and M.R. Stratton, *THE GENETICS OF BREAST CANCER SUSCEPTIBILITY.* Annual Review of Genetics, 2003. **32**(1): p. 95-121.
300. Moynahan, M.E., et al., *Brca1 Controls Homology-Directed DNA Repair.* Molecular Cell, 1999. **4**(4): p. 511-518.
301. Scully, R., et al., *Association of BRCA1 with Rad51 in Mitotic and Meiotic Cells.* Cell, 1997. **88**(2): p. 265-275.
302. Zhong, Q., et al., *Association of BRCA1 with the hRad50-hMre11-p95 Complex and the DNA Damage Response.* Science, 1999. **285**(5428): p. 747-750.
303. Cortez, D., et al., *Requirement of ATM-Dependent Phosphorylation of Brca1 in the DNA Damage Response to Double-Strand Breaks.* Science, 1999. **286**(5442): p. 1162-1166.
304. Ogiwara, H., et al., *Chl1 and Ctf4 are required for damage-induced recombinations.* Biochemical and Biophysical Research Communications, 2007. **354**(1): p. 222-226.
305. Laha, S., et al., *The budding yeast protein Chl1p is required to preserve genome integrity upon DNA damage in S-phase.* Nucl. Acids Res., 2006. **34**(20): p. 5880-5891.
306. Dephoure, N., et al., *A quantitative atlas of mitotic phosphorylation.* Proceedings of the National Academy of Sciences, 2008. **105**(31): p. 10762-10767.

307. Lehmann, A.R., *DNA repair-deficient diseases, xeroderma pigmentosum, Cockayne syndrome and trichothiodystrophy.* Biochimie, 2003. **85**(11): p. 1101-1111.
308. Levitus, M., et al., *The DNA helicase BRIP1 is defective in Fanconi anemia complementation group J.* Nat Genet, 2005. **37**(9): p. 934-935.
309. Peng, M., et al., *BACH1 is a DNA repair protein supporting BRCA1 damage response.* Oncogene, 2006. **25**(15): p. 2245-2253.
310. Litman, R., et al., *BACH1 is critical for homologous recombination and appears to be the Fanconi anemia gene product FANCJ.* Cancer Cell, 2005. **8**(3): p. 255-265.
311. Gong, Z., et al., *BACH1/FANCJ Acts with TopBP1 and Participates Early in DNA Replication Checkpoint Control.* Molecular Cell. **37**(3): p. 438-446.
312. Rogakou, E.P., et al., *DNA Double-stranded Breaks Induce Histone H2AX Phosphorylation on Serine 139.* Journal of Biological Chemistry, 1998. **273**(10): p. 5858-5868.
313. Wang, H., et al., *Complex H2AX phosphorylation patterns by multiple kinases including ATM and DNA-PK in human cells exposed to ionizing radiation and treated with kinase inhibitors.* Journal of Cellular Physiology, 2005. **202**(2): p. 492-502.
314. Celeste, A., et al., *Genomic Instability in Mice Lacking Histone H2AX.* Science, 2002. **296**(5569): p. 922-927.
315. Downs, J.A., et al., *Binding of Chromatin-Modifying Activities to Phosphorylated Histone H2A at DNA Damage Sites.* Molecular Cell, 2004. **16**(6): p. 979-990.
316. Shroff, R., et al., *Distribution and Dynamics of Chromatin Modification Induced by a Defined DNA Double-Strand Break.* Current Biology, 2004. **14**(19): p. 1703-1711.
317. Schwab, R.A., A.N. Blackford, and W. Niedzwiedz, *ATR activation and replication fork restart are defective in FANCM-deficient cells.* EMBO J. **29**(4): p. 806-818.
318. Kuzminov, A., *Recombinational Repair of DNA Damage in Escherichia coli and Bacteriophage lambda.* Microbiol. Mol. Biol. Rev., 1999. **63**(4): p. 751-813.
319. Koroleva, O., et al., *Structural conservation of RecF and Rad50: implications for DNA recognition and RecF function.* EMBO J, 2007. **26**(3): p. 867-877.
320. Chow, K.-H. and J. Courcelle, *RecO Acts with RecF and RecR to Protect and Maintain Replication Forks Blocked by UV-induced DNA Damage in Escherichia coli.* Journal of Biological Chemistry, 2004. **279**(5): p. 3492-3496.
321. Morimatsu, K. and S.C. Kowalczykowski, *RecFOR Proteins Load RecA Protein onto Gapped DNA to Accelerate DNA Strand Exchange: A Universal Step of Recombinational Repair.* Molecular Cell, 2003. **11**(5): p. 1337-1347.
322. Michel-Marks, E., et al., *ATP Binding, ATP Hydrolysis, and Protein Dimerization Are Required for RecF to Catalyze an Early Step in the Processing and Recovery of Replication Forks Disrupted by DNA Damage.* Journal of Molecular Biology. **401**(4): p. 579-589.
323. Skibbens, R.V., et al., *Ctf7p is essential for sister chromatid cohesion and links mitotic chromosome structure to the DNA replication machinery.* Genes & Development, 1999. **13**(3): p. 307-319.
324. Wittmeyer, J. and T. Formosa, *The Saccharomyces cerevisiae DNA polymerase alpha catalytic subunit interacts with Cdc68/Spt16 and with Pob3, a protein similar to an HMG1-like protein.* Mol Cell Biol, 1997. **17**(7): p. 4178-90.
325. Bermudez, V.P., et al., *The alternative Ctf18-Dcc1-Ctf8-replication factor C complex required for sister chromatid cohesion loads proliferating cell nuclear*

antigen onto DNA. Proceedings of the National Academy of Sciences of the United States of America, 2003. **100**(18): p. 10237-10242.
326. Kadrmas, J.L. and M.C. Beckerle, *The LIM domain: from the cytoskeleton to the nucleus.* Nat Rev Mol Cell Biol, 2004. **5**(11): p. 920-931.
327. Karlsson-Rosenthal, C. and J.B.A. Millar, *Cdc25: mechanisms of checkpoint inhibition and recovery.* Trends in Cell Biology, 2006. **16**(6): p. 285-292.
328. Busino, L., et al., *Cdc25A phosphatase: combinatorial phosphorylation, ubiquitylation and proteolysis.* Oncogene. **23**(11): p. 2050-2056.
329. Murray, A.W., *Recycling the Cell Cycle: Cyclins Revisited.* Cell, 2004. **116**(2): p. 221-234.
330. Parker, L. and H. Piwnica-Worms, *Inactivation of the p34cdc2-cyclin B complex by the human WEE1 tyrosine kinase.* Science, 1992. **257**(5078): p. 1955-1957.
331. Kellogg, D.R., *Wee1-dependent mechanisms required for coordination of cell growth and cell division.* J Cell Sci, 2003. **116**(24): p. 4883-4890.
332. Smith, J.J., et al., *Apoptotic Regulation by the Crk Adapter Protein Mediated by Interactions with Wee1 and Crm1/Exportin.* Mol. Cell. Biol., 2002. **22**(5): p. 1412-1423.
333. Lee, J., A. Kumagai, and W.G. Dunphy, *Positive Regulation of Wee1 by Chk1 and 14-3-3 Proteins.* Mol. Biol. Cell, 2001. **12**(3): p. 551-563.
334. Mir, S.E., et al., *In Silico Analysis of Kinase Expression Identifies WEE1 as a Gatekeeper against Mitotic Catastrophe in Glioblastoma.* Cancer Cell. **18**(3): p. 244-257.
335. Prasanth, S.G., K.V. Prasanth, and B. Stillman, *Orc6 Involved in DNA Replication, Chromosome Segregation, and Cytokinesis.* Science, 2002. **297**(5583): p. 1026-1031.
336. Balasov, M., R.P. Huijbregts, and I. Chesnokov, *Functional analysis of an Orc6 mutant in Drosophila.* Proc Natl Acad Sci U S A, 2009. **106**(26): p. 10672-7.
337. Johannessen, M., et al., *The multifunctional roles of the four-and-a-half-LIM only protein FHL2.* Cellular and Molecular Life Sciences, 2006. **63**(3): p. 268-284.
338. Prasanth, S.G., et al., *Human origin recognition complex is essential for HP1 binding to chromatin and heterochromatin organization.* Proceedings of the National Academy of Sciences, 2010. **107**(34): p. 15093-15098.
339. Bahr, A., et al., *Point mutations causing Bloom's syndrome abolish ATPase and DNA helicase activities of the BLM protein.* Oncogene, 1998. **17**(20): p. 2565-71.
340. German, J., *Bloom syndrome: a mendelian prototype of somatic mutational disease.* Medicine (Baltimore), 1993. **72**(6): p. 393-406.
341. Wang, W., et al., *Possible association of BLM in decreasing DNA double strand breaks during DNA replication.* EMBO J, 2000. **19**(13): p. 3428-3435.
342. Parish, J.L., et al., *ChlR1 Is Required for Loading Papillomavirus E2 onto Mitotic Chromosomes and Viral Genome Maintenance.* Molecular Cell, 2006. **24**(6): p. 867-876.
343. Doorbar, J., *The papillomavirus life cycle.* Journal of Clinical Virology, 2005. **32**(Supplement 1): p. 7-15.
344. Sakakibara, N., *The HPV replication proteins induce the DNA damage response pathway.* molecular biology of DNA tumour viruses conference, 2010.
345. Boner, W., et al., *A Functional Interaction between the Human Papillomavirus 16 Transcription/Replication Factor E2 and the DNA Damage Response Protein TopBP1.* Journal of Biological Chemistry, 2002. **277**(25): p. 22297-22303.
346. Feeney, K.M., et al., *In vivo analysis of the cell cycle dependent association of the bovine papillomavirus E2 protein and ChlR1.* Virology, 2011. **414**(1): p. 1-9.

347. Hanada, K. and I. Hickson, *Molecular genetics of RecQ helicase disorders.* Cellular and Molecular Life Sciences, 2007. **64**(17): p. 2306-2322.
348. Chaganti, R.S.K., S. Schonberg, and J. German, *A Manyfold Increase in Sister Chromatid Exchanges in Bloom's Syndrome Lymphocytes.* Proceedings of the National Academy of Sciences of the United States of America, 1974. **71**(11): p. 4508-4512.
349. Russell, B., et al., *Chromosome Breakage Is Regulated by the Interaction of the BLM Helicase and Topoisomerase IIÎ±.* Cancer Research. **71**(2): p. 561-571.
350. Watt, P.M. and I.D. Hickson, *Structure and function of type II DNA topoisomerases.* Biochem J, 1994. **303 (Pt 3)**: p. 681-95.
351. Holm, C., T. Stearns, and D. Botstein, *DNA topoisomerase II must act at mitosis to prevent nondisjunction and chromosome breakage.* Mol. Cell. Biol., 1989. **9**(1): p. 159-168.